Functional Analysis of Conserved Motifs within Herpes Simplex Virus Regulatory Protein ICP0

Kathleen Pheasant

A thesis presented for the degree of Doctor of Philosophy in the College of Medical, Veterinary and Life Sciences

MRC-University of Glasgow Centre for Virus Research
Institute of Infection Immunity and Inflammation
University of Glasgow

2015

Abstract

Herpes simplex virus type 1 (HSV-1) Immediate-early protein ICP0 is important for regulating the balance between lytic and latent infections. The RING finger domain of ICP0 acts as an E3 ubiquitin ligase, binding to E2-ubiquitin conjugating enzymes and target proteins, promoting their polyubiquitination and subsequent degradation. ICP0 localises to cellular nuclear sub-structures known as ND10 at early stages of infection, and the RING finger domain induces the degradation and dispersal of ND10 proteins, which form part of the cell's intrinsic antiviral defence mechanism. The RING finger domain of ICP0 consists of an alpha-helix, and this and the loop regions are involved in interactions with the E2 ubiquitin-conjugating enzymes UBE2D1 and UBE2E1. Previous work using an ICP0-inducible cell line system found a mutation (N151D) in ICP0's alpha-helix, which allowed complementation of an ICP0-null mutant virus plaque formation but caused a substantial defect in the induction of reactivation of quiescent HSV-1. This raised the possibility that the mechanisms controlling lytic infection and reactivation may be separable. The main focus of this study was to investigate the N151D mutation and other mutations located within the alpha-helix (including K144E and K144E/N151D) using an inducible ICP0 expression cell system and virus infection studies. The phenotypes of these alpha-helix mutants were characterised to investigate if complementation/lytic infection and reactivation involve differential activities of ICP0. Additionally, these alpha-helix mutants were analysed for their *in vitro* E3 ligase ability and ability to interact with components of the ubiquitin pathway, focusing on E2 ubiquitin-conjugating enzymes.

The results from this study using the inducible ICP0 cell system confirmed previous results. The alpha-helix mutants had a greater defect during reactivation than complementing the plaque forming defect of an ICP0-null mutant virus, and this was more noticeable for the K144E mutant. The virus infection studies showed a greater correlation between the effects of the mutations on the degradation of ND10 proteins, plaque formation and replication at low multiplicity of infection. The defect of the K144E mutation was more profound than N151D in all the assays, and the activity of a double mutant including mutations at both K144 and N151 (KE/ND) was reduced to levels comparable with the RING finger deletion mutant. Infection with mutants K144E and KE/ND greatly reduced the efficiency of reactivation of quiescent HSV-1 even at multiplicities of infection where their lytic infection was not severely affected, whereas N151D showed an intermediate phenotype.

Furthermore, this study showed that ICP0 has the potential to interact with multiple E2 ubiquitin-conjugating enzymes, and the alpha-helix mutations may affect these interactions. Further investigation will be required to examine the roles that these E2 ubiquitin-conjugating enzymes play during HSV-1 infection. The data in this study indicate that there is no strong evidence to suggest that ICP0 utilises differential activities of its RING finger to mediate reactivation and the stimulation of lytic infection, despite the likely dissimilar nature of the viral chromatin structure in the two situations. These findings, however, provide an insight into the biological importance of the RING finger alpha-helix of ICP0 during the course HSV-1 infection and especially during reactivation from quiescence.

In addition, motifs present within ICP0 that may be involved in interactions with other cellular proteins were analysed. These included the PPEYPTAP motif present within retroviral Gag proteins, the SIAH-1 interaction motif and residue T67 (which are all involved in interactions with cellular E3 ubiquitin ligases), and the CoREST binding region. Furthermore, a region of homology between alphaherpesvirus ICP0 proteins downstream of the RING finger domain, which had not previously been investigated in detail, was studied. These studies indicated that the region downstream of the RING finger domain (residues 211-222) may contribute to ICP0's activity, but no major role was detected for the other motifs studied.

Table of Contents

List of Tables

List of Figures

Acknowledgements

Firstly and most importantly, I would like to thank my supervisor Professor Roger Everett for allowing me to do my MRes and PhD in his laboratory. For providing enormous support and guidance during my PhD (and MRes), and in particular for always being encouraging and motivating. I have been extremely lucky to have had such a great mentor through my PhD.

I thank Dr Chris Boutell for the collaboration on the ubiquitin pathway part of this thesis and for the helpful discussions throughout my PhD, and Steven McFarlane for all the technical help and expertise during the collaboration especially with the Y2H experiments.

I owe great thanks to past and present members of the Everett group who it has been great to work with. They provided a productive and friendly working environment that made my time in the lab so enjoyable; Anne Orr (help on experimental techniques), Delphine Cuchet-Lourenço (being so welcoming), and Mandy Glass (technical advice and list of places to visit in Scotland). My special thanks go to Liz Sloan for being an excellent flatmate and friend (for all her positivity and always being willing to listen, proof-reading chapters of this thesis and widening my film knowledge), and YongXu Lu for sharing the PhD experience with me (the company at the IHW in Japan and late nights/weekends in the lab, and motivating me to train and complete the half marathon twice). Thanks also to the current and former members of the Boutell group who have given advice and helped me over the course of my PhD.

I am very grateful to all my friends and fellow PhD students at the CVR, especially those in the old Church Street office. Thanks for keeping me sane during the stressful times (of which luckily there were not too many), the laughs and Friday night drinks. Thanks for the many great memories throughout my time in Glasgow.

Finally I would like to thank my family and friends for their constant love and support; especially my mum who has always believed in and encouraged me and was at the end of the phone to talk to, my sisters Clare and Ann-Marie, for all the encouragement, laughs, phone calls, visits and trips to the rugby, and my Auntie for the support and sightseeing trips. I really could not have done any of this without you all. I would also like to remember my dad; I wish he were here to see this.

Author’s Declaration

All the results presented in this thesis were obtained by the author’s own efforts, unless stated otherwise.

Abbreviations

3-AT	3-amino-1,2,4-triazole
µ	Micro (10^{-6})
aa	Amino acid
ACV	Acyclovir
AD	*GAL4* DNA-activating domain
AIDS	Acquired immune deficiency syndrome
Amp	Ampicillin
APOBEC	Apolipoprotein B mRNA-editing enzyme catalytic polypeptide
ATP	Adenosine triphosphate
ATRX	Alpha-thallasaemia mental retardation X-linked
bp	Base pair
BHK	Baby hamster kidney
BK	*GAL4* DNA-binding domain
C-	Carboxy
ºC	Degrees Celsius
CoREST	Corepressor of REST
c.p.e	Cytopathic effect
Da	Dalton
dH_20	Distilled water
DNA	Deoxyribonucleic acid
DNA-PK	DNA-dependent protein kinase
DMEM	Dulbecco's modified Eagle's medium
DMSO	Dimethyl sulphoxide
EBV	Epstein-Barr virus
ECL	Enhanced chemiluminescence
EGFP	Enhanced green fluorescent protein
FBS	Foetal calf serum
FITC	Fluorescein isothiocyanate
g	gram
GST	Glutathione S-transferase
HCF	Host cell factor
HCMV	Human cytomegalovirus
HDAC	Histone deacetylase

hDaxx	Human death-domain associated protein
HECT	Homologous to E6-associated protein C-terminus
HF	Human fibroblast
HHV	Human herpesvirus
HIV	Human immunodeficiency virus
HSV	Herpes simplex virus
ICP	Infected cell protein
IE	Immediate-early
IFN	Interferon
Ig	Immunoglobulin
IPTG	Isopropylthio-β-D-galactoside
IRF3	Interferon regulatory factor 3
ISRE	IFN-stimulated response element
ISG	IFN-stimulated gene
K	Kilo (10^3)
KSHV	Kaposi's sarcoma-associated herpesvirus
l	Litre
LAT	Latency associated transcript
LB	Luria-Bertani medium (L-Broth)
m	Milli (10^{-3})
M	Molar
mA	Milliamps
MHC	Major histocompatibility complex
MI	Mock infected
MOI	Multiplicity of infection
mRNA	Messenger RNA
n	Nano (10^{-9})
N-	Amino (terminal region of a protein)
NBCS	New-born calf serum
ND	Nuclear domain
NEDD	Neuronal precursor cell-expressed developmentally downregulated
NF-κB	Nuclear factor – kappa B
NLS	Nuclear localisation signal
NP40	Nonidet-P 40
OAS	2'5' oligoadenylate synthetase

OCT-1	Octamer-binding protein 1
ORF	Open reading frame
Ori	Origin of replication
PBS	Phosphate-buffered saline
PCR	Polymerase chain reaction
PFE	Plaque forming efficiency
PKR	Protein kinase R
PML	Promyelocytic leukaemia protein
RBCC	RING, B-box(es), coiled coil motif
RING	Really interesting new gene
RNA	Ribonucleic acid
RNase	Ribonuclease
rpm	Revolutions per minute
SDS	Sodium dodecyl sulphate
shRNA	Short hairpin RNA
siRNA	Small inhibitory RNA
SIM	SUMO interaction motif
SLS	SIM-like sequence
Sp100	Speckled protein of 100 kDa
STAT	Signal transducers and activators of transcription
SUMO	Small ubiquitin-like modifier
TAP	Transporter for antigen processing
TE	Tris/EDTA buffer
TEMED	Tetramethylethylene diamine
tk	Thymidine kinase
TLR	Toll-like receptor
Tmtc	Too many plaques to count
TRIM	Tripartite motif
U_L	Unique long
U_S	Unique short
UBE2	E2 ubiquitin-conjugating enzyme
USP7	Ubiquitin specific protease 7
UV	Ultraviolet
V	Volts
v/v	Volume to volume ratio

w/v	Weight to volume ratio
Vhs	Virion host shut off
VP	Virion protein
VZV	Varicella-zoster virus
wt	Wild type
YPD	Yeast extract peptone-dextrose
X-gal	5-bromo-4-chloro-3-indolyl-β-D-galactoside

1 Introduction

1.1 Family *Herpesviridae*

1.1.1 Overview

Herpesviruses are pathogens that have evolved with their hosts for millions of years, infecting a wide range of vertebrate and invertebrate hosts. The order *Herpesvirales* is composed of three families; the *Herpesviridae* (infecting mammals, birds and reptiles), the *Alloherpesviridae* (infecting fish and frogs), and the most recently discovered *Malacoherpesviridae* family that consists of the ostreid herpesvirus 1 that infects oysters (Davison *et al.*, 2009; Davison *et al.*, 2005). The *Herpesviridae* family is based on virion morphology and is divided into three subfamilies; the *Alpha-*, *Beta-*, and *Gamma-herpesvirinae* (Davison *et al.*, 2005).

There are eight herpesviruses that are known to infect humans; herpes simplex virus type 1 (HSV-1), HSV-2, varicella-zoster virus (VZV), human cytomegalovirus (HCMV), Epstein-Barr virus (EBV), human herpesvirus 6 (HHV6, which is the collective name for the two closely related viruses, HHV6A and HHV6B) and HHV7 and HHV-8 (Kaposi's sarcoma-associated herpesvirus, KSHV) (Davison *et al.*, 2005). A common feature of all herpesviruses is their ability to establish a life-long latent infection following primary infection.

1.1.2 Subfamilies

The *Herpesviridae* family is divided into three subfamilies and the characteristics of each family will be discussed briefly below (Roizman & Pellett, 2001).

The subfamily *Alphaherpesvirinae* (alphaherpesviruses) contains the genera *Simplexvirus* (HSV-1, HSV-2) and *Varicellovirus* (VZV). These viruses have a variable host range and can infect a variety of cells including epithelial cells and mucous membranes, making them easy to study in a laboratory setting. They also have a short replication cycle, cause the destruction of infected cells, and establish latency in sensory ganglia.

The subfamily *Betaherpesvirinae* (betaherpesviruses) contains the genera *Cytomegalovirus* (HCMV) and *Roseolovirus* (HHV-6 and HHV-7). The betaherpesviruses are characterised

by a restricted host range and a long reproductive cycle making them difficult to study as they replicate slowly in cell culture.

The subfamily *Gammaherpesvirinae* (gammaherpesviruses) is divided into two genera, *Lymphocryptovirus* (EBV) and *Rhadinovirus* (KSHV). EBV and KSHV replicate in lymphoblastoid cells and latency is established in lymphoid tissue. Gammaherpesviruses have the narrowest host range compared to the other herpesviruses and spread slowly in cell culture. Infections with gammaherpesviruses have been associated with the development of lymphomas, carcinomas and sarcomas.

1.2 Pathogenesis of herpesvirus infections

1.2.1 HSV infections (HSV-1 and HSV-2)

HSV-1 and HSV-2 are transmitted by personal contact with infected individuals. The virus infects mucosal surfaces or abraded skin producing vesicular lesions. However, infection maybe asymptomatic in healthy individuals. It has been traditionally thought that HSV-1 is transmitted via oral contact and primary infection usually occurs in the oral mucosa, whereas HSV-2 infection is transmitted sexually and infects the genital areas causing genital herpes. However, there is increasing overlap between these two viruses, with HSV-1 commonly detected from genital herpes (Whitley *et al.*, 2007). This was highlighted by a study of samples collected over a 14 year period (1986-2000), which found that 49% of genital herpes in the West of Scotland were typed as HSV-1 and 51% as HSV-2 (Scoular *et al.*, 2002).

HSV infections can also infect other areas of the skin and mucosal membranes. Gingivostomatitis, an HSV infection of the mouth and gums, leads to sores and swelling, and HSV can also infect the skin on fingertips (herpetic whitlow). HSV-1 infection of the eye can cause keratoconjunctivitis, which can led to scarring of the cornea and progressive vision loss and blindness from frequent reactivation and the host response. Close contact sports such as rugby and wrestling can also spread HSV, leading to scrum pox and herpes gladiatorum respectively (reviewed in Whitley *et al.*, 2007). HSV can also be transmitted from infected mothers to newborns during delivery (or less commonly in utero), and this can lead to a localised or disseminated infection with over 1500 infections of newborns each year in the United States (Kimberlin, 2004). The risk of transmission to newborns is higher with primary infection of genital herpes than recurrent episodes. However the risk

can be prevented or minimised by caesarean delivery and the use of antivirals such as acyclovir (ACV) (see **section 1.2.7**) (Kimberlin, 2004). In severe cases, HSV can invade and replicate in the central nervous system, leading to encephalitis. In immunocompromised individuals, reactivation of HSV can be problematic, with many episodes of infection over the year (reviewed in Whitley *et al.*, 2007).

1.2.2 VZV

VZV is the causative agent of varicella (chickenpox), which primarily infects musocal epithelial cells of the upper respiratory tract. VZV infection commonly occurs in childhood, and the disease is characterised by a rash with vesicular cutaneous lesions. Chickenpox is a highly contagious disease that is spread by the respiratory route through infected air droplets or by contact with infected vesicle fluid from skin lesions. Chickenpox is usually self-limiting and can be controlled by an effective immune response. However, it can lead to bacterial infections of the skin and in severe cases pneumonia. VZV establishes latency in the sensory nerve ganglia, and the virus can reactivate and replicate to cause zoster (shingles). Shingles is characterised by a vesicular rash and severe pain to an area of the skin that is served by the infected nerve ganglia. Shingles mainly affects immunocompromised or older patients with a weaker immune system. Chickenpox and shingles can both transmit VZV to susceptible individuals, leading to chickenpox (Gershon & Gershon, 2013).

There is a live attenuated vaccine available against VZV, which is derived from the Oka strain of the virus that was attenuated by serial passage in cell culture. The vaccine has been licenced for use in the US since 1995 and is part of the childhood immunisation programme. The vaccine is used routinely in many other countries, but in the UK is given only to at risk groups. The vaccine induces immunity to VZV, but the virus enters latency and can reactivate to produce shingles. There is also a vaccine against shingles, the zoster vaccine that was licensed for use in the US in 2006. The zoster vaccine uses the same Oka strain as the VZV vaccine but contains a greater dose. The vaccine is targeted at individuals usually over 60 or 70 years of age that have already had primary VZV infection in order to reduce the frequency or severity of shingles. However the vaccine does not fully prevent VZV reactivation leading to shingles (Oxman, 2010).

1.2.3 HCMV

HCMV is ubiquitous and is transmitted through bodily fluids including saliva, breast milk, semen, blood products and urine. HCMV replicates in a variety of differentiated cell types and latency is maintained in CD34+ haematopoietic stem cells. Primary infection with HCMV is usually asymptomatic and only causes problems in individuals that are immunocompromised (for example HIV-infected individuals or transplant recipients) or in congenital infections. In immunocompromised individuals, reactivation of latent HCMV or primary infection with a different stain can cause retinitis which can lead to blindness, gastritis, encephalitis, pneumonitis or hepatitis. In severe cases, HCMV can cause a systemic infection that can be life threatening. The severity of the disease often depends on the degree of immunosuppression and the viral load (Reddenhase, 2013).

HCMV can also be transmitted transplacentally during pregnancy, during childbirth or via breastfeeding. Transplacental infection can be due to primary infection or recurrent infection of the mother. The risk of transmission to the foetus is higher with primary infection, where this leads to a 30-40% chance of transplacental transmission to the foetus, whereas with reactivation the risk is about 1-3%. Congenital HCMV infection can lead to a number of health problems for the newborns, including mental retardation, cerebral palsy, hearing loss, impaired vision and damage to the central nervous system, with more severe consequences associated with infection early in pregnancy (Malm & Engman, 2007).

1.2.4 HHV-6 and HHV-7

HHV-6 and HHV-7 infect a variety of cell types, including T lymphocytes. HHV-6 establishes latency in macrophages and CD34+ haematopoietic stem cells, whereas HHV-7 causes a persistent infection in the salivary glands and establishes latency in CD4+ cells. Infection with HHV-6B and HHV-7 usually occurs during childhood and causes exanthema subitum (roseola). Roseola is characterised by a sudden fever that lasts several days and the appearance of a rash once the fever subsides. HHV-6 infection is also associated with encephalitis, pneumonitis and hepatitis in immunocompromised individuals (Mori & Yamanishi, 2007).

1.2.5 EBV

EBV infects over 90% of the world's population. Primary infection is usually asymptomatic and generally occurs in early childhood, however if delayed until adolescence it can lead to the development of infectious mononucleosis (glandular fever). Infectious mononucleosis is characterised by the acute onset of fever, sore throat, enlarged lymph glands and severe fatigue. Following primary infection, EBV establishes latency in B lymphocytes, where it persists for the life of the host with intermittent low level excretion of virus in the saliva, which is the main transmission route. Under certain conditions such as immunodeficiency, latent EBV genes can moderate B-cell proliferation and are implicated in the development of several EBV-associated malignancies, including Hodgkin's lymphoma, Burkitt's lymphoma and nasopharyngeal carcinoma. Burkitt's lymphoma is typically associated with tumours of the jaw in children and shows a high incidence in equatorial Africa where malaria is present. Hodgkin's lymphoma arises in young adults and is characterised by the presence of large multinucleate Reed-Sternberg cells, while nasopharyngeal carcinoma affects middle aged infected individuals and is a tumour of the squamous epithelium (reviewed in Crawford, 2001).

1.2.6 KSHV

The KSHV (or HHV-8) DNA sequence was first identified in 1994 in Kaposi's sarcoma tissue from an AIDS patient (Chang *et al.*, 1994). Since then, HHV-8 has been shown to be a causative agent of Kaposi's sarcoma and is associated with Castleman's disease and primary effusion lymphoma, all of which are proliferative disorders. HHV-8 establishes latency in lymphoid tissue, and latent gene expression promotes cell cycle progression, cellular proliferation and inhibits apoptosis. Kaposi's sarcoma is the most common cancer of untreated HIV-1 patients, and is characterised by formation of spindle-shaped cells (reviewed in Ganem, 2007; Kaplan, 2013).

1.2.7 Treatments

ACV and penciclovir and their prodrugs valacyclovir and famciclovir are used to treat herpesvirus infections. ACV and penciclovir are guanosine analogues that are phosphorylated by the viral thymidine kinase and then subsequently by the cellular kinases GMP kinase and nucleoside diphosphate kinase. The triphosphate form of ACV is a competitive substrate of the viral DNA polymerase, and is incorporated into newly

synthesised DNA, resulting in chain termination as it lacks a hydroxyl group in the 3' position. ACV is effective and has low toxicity, and is used to treat HSV, VZV and EBV infections, but is not sufficient for the treatment of HCMV (Piret & Boivin, 2011).
Ganciclovir (a nucleoside analogue) was the first line drug used for prophylaxis and treatment of HCMV. Ganciclovir is phosphorylated by the HCMV gene UL97 (Sullivan *et al.*, 1992), a protein kinase, and this phosphorylated ganciclovir is incorporated into newly synthesised DNA where it slows and eventually stops chain elongation. Second line drugs for the treatment of HCMV include foscarnet, an inhibitor of the viral DNA polymerase, and cidofovir, a nucleoside analogue similar to ACV but that does not require initial activation by viral thymidine kinase (Piret & Boivin, 2014).

Long term treatment or prophylaxis with ACV and its derivatives can lead to the development of viral resistance mutations within the viral thymidine kinase or viral DNA polymerase, which can be a problem in immunocompromised patients. Therefore, there is a need for anti-virals with different modes of action, or preventative vaccines (reviewed in Piret & Boivin, 2011; 2014). At present, a live attenuated VZV vaccine is the only human herpesvirus vaccine licenced for use (see **section 1.2.2**).

1.3 Virion structure and organisation of HSV-1 genome

The HSV-1 virion (**Figure 1.1**) is approximately 185 nm in diameter and consists of double-stranded DNA genome encased within an icosahedral capsid. A protein layer termed the tegument surrounds the capsid and is enclosed within a lipid envelope derived from the host cell with viral glycoproteins embedded on the surface. The main features of each component are described below.

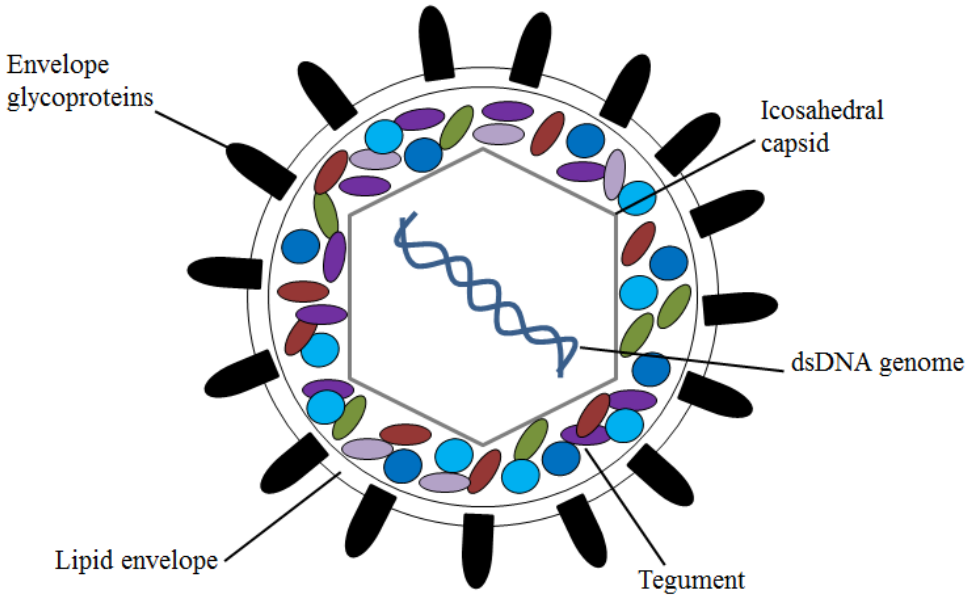

Figure 1.1 HSV-1 virion structure.
The main components of the HSV-1 virion are the nucleocapsid containing the double-stranded DNA genome, the protein tegument layer and lipid envelope containing embedded glycoproteins.

1.3.1 Double-stranded DNA core

The core consists of a single copy of linear, double-stranded DNA, which circularises on release from the viral capsids. The HSV-1 genome is 152 kbp and has a G+C content of 68% (McGeoch *et al.*, 1988). The genome consists of two unique coding regions termed unique long (U_L) and unique short (U_S) (**Figure 1.2)**. U_L and U_S are both flanked by inverted repeat sequences termed 'b' for U_L and 'c' flanking U_S. 'a' repeat sequences are present at both ends of the genome and an inverted copy is present between U_L and U_S. U_L and U_S can invert producing four possible sequence orientations. Three origins of replication are present within the genome, one within U_L region (oriL) and two within the c repeat region flanking U_S (oriS). The origins of replication are composed of A+T-rich sequences flanked by binding sites for the viral origin-binding protein UL9 that is important for viral DNA replication (**section 1.4.1.3**) (Ward & Weller, 2011).

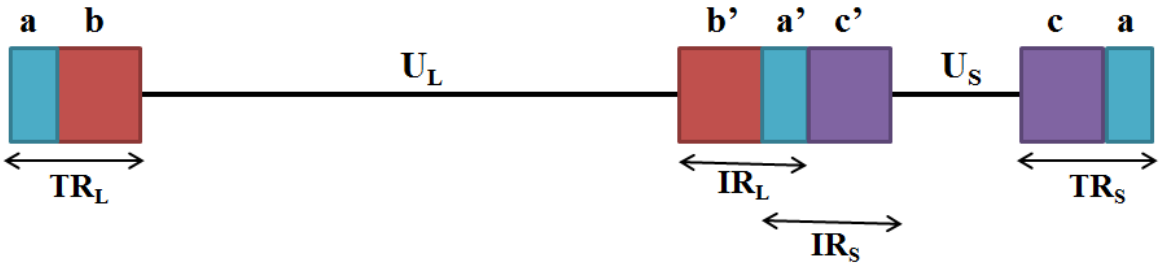

Figure 1.2 Organisation of the HSV-1 genome.
The unique coding regions U_L and U_S are flanked by inverted repeat sequences. The repeats flanking U_L are TR_L (ab) and IR_L (b'a'), and those flanking U_S are IR_L (a'c') and TR_S (ca).

1.3.2 Nucleocapsid

The HSV-1 nucleocapsid structure has been resolved by cryo-electron microscopy to 8.5 Å (Zhou *et al.*, 2000). The nucleocapsid is composed of 150 hexons and 11 pentons and one portal and is arranged in T=16 icosahedral symmetry. The outer capsid is composed of the viral proteins UL19 (VP5), UL35 (VP26), UL18 (VP23) and UL38 (VP19C). The major capsid protein UL19 is present in five or six copies in each penton or hexon, and six copies of UL35 form a ring on top of the UL19 subunits of each hexon. One UL38 protein and two copies of UL18 form the triplexes (Zhou *et al.*, 2000). The capsid also contains the UL6 protein which forms a 12 subunit ring structure, which forms a pore known as the portal through which the viral DNA is packaged (**section 1.4.1.4**) (Chang *et al.*, 2007; Newcomb *et al.*, 2001).

1.3.3 Tegument layer

The tegument layer occupies the space in between the capsid and lipid envelope. The tegument layer is composed of proteins that are transported into the newly infected cell and play roles in affecting host protein synthesis and inhibiting cellular defences, and many are important for efficient infection (Kelly *et al.*, 2009). Analysis of the proteins present in the tegument layer by mass spectrometry found 23 potential tegument proteins (Loret *et al.*, 2008).

Tegument proteins include VP16, which stimulates viral immediate-early (IE) gene expression and plays a role in particle assembly, UL31, UL34, multifunctional VP22, IE proteins ICP0 and ICP4, the virion host shut off protein UL42 (vhs), which regulates

host/viral translation, and UL36, which plays roles in release of viral DNA into the nucleus and capsid envelopment (Kelly *et al.*, 2009).

1.3.4 Envelope

The envelope is composed of a lipid bilayer containing up to 13 viral envelope glycoproteins, including gB, gC, gD, gE, gG, gH, gI, gL and gM (Loret *et al.*, 2008). Cryo-electron tomography showed that each HSV-1 virion has between 600 to 750 glycoprotein spikes embedded in the lipid envelope, and these range in length from 10-25 nm (Grünewald *et al.*, 2003). Five of the viral envelope proteins (gB, gC, gD, gH and gL) are involved in virus attachment to host cells and entry, and their roles are discussed in **section 1.4.1.1**.

1.4 HSV-1 life cycle

1.4.1 Lytic infection

The HSV-1 life cycle is characterised by two distinct phases: primary infection, which can result in a lytic infection, and long periods of latency, during which the virus can periodically reactivate to create a lytic infection. The virus life cycle during lytic infection and the latent state are discussed below.

1.4.1.1 Recognition and entry into cell

HSV-1 entry into host cells involves fusion of the viral envelope with the host cell plasma membrane, and requires multiple viral proteins in a multi-step process. Firstly, the virus attaches to the host cell by the interaction of gC and/or gB with heparan sulphate proteoglycans on the cell surface (Herold *et al.*, 1991). This attachment step is not essential but enhances virus infectivity by concentrating virus on the cell surface. This binding step does not lead to changes in the cell membrane that are required for membrane fusion. After attachment, gD interacts with cellular receptors called nectins, herpesvirus entry mediator (HVEM) or O-sulphated moieties on heparan sulphate, and these interactions, together with the interactions of the fusion proteins gB and gH/gL heterodimer, trigger fusion with the plasma membrane (reviewed in Campadelli-Fiume *et al.*, 2007; Heldwein & Krummenacher, 2008).

After membrane fusion, the viral capsid and tegument proteins are released into the cytoplasm. The capsids are transported to the nuclear pore along microtubules, through interaction with the cellular microtubule dynein/dynactin complex (Dohner *et al.*, 2002). The viral proteins that are responsible for interacting with the dynein/dynactin complex include the tegument proteins UL36 and UL37 (Wolfstein *et al.*, 2006). UL36 has also been implicated in localisation of the nucleocapsid to the nuclear membrane and interacting with the nuclear pore to allow the release of viral DNA into the cell nucleus (reviewed in Kelly *et al.*, 2009).

1.4.1.2 Viral gene expression

HSV-1 gene expression is a temporally regulated cascade that can be divided into three phases; IE (or α), early (β) and late (γ) genes. IE genes are the first viral genes to be transcribed during infection and the proteins encoded by them play a crucial role in the regulation of gene expression. The IE genes encode five proteins ICP0, ICP4, ICP22, ICP27 and ICP47, which are described in **section 1.5**. The promoter region of the IE genes contains a TAATGARAT sequence motif (where R indicates a purine), and downstream of this is a TATA box and transcription factor-binding sites. Transcription of IE genes involves the viral tegument protein VP16, which forms a complex with the cellular proteins host cell factor (HCF) and Oct-1 that binds to the consensus TAATGARAT sequence present in all IE promoters, allowing the C-terminal activation domain of VP16 to activate transcription (reviewed in Wysocka & Herr, 2003).

IE gene products are involved in activating expression of the early and late genes. The early genes encode enzymes and DNA-binding proteins that promote viral DNA replication, and include viral thymidine kinase. Expression of early genes requires the presence of ICP4. The early gene promoter regions contain cellular transcription factor binding sites upstream of a TATA box, and generally do not have distinctive virus-specific elements. Following DNA replication, increased viral template numbers enhance late gene expression to produce large amounts of structural proteins that are involved in the assembly of the progeny virions. Late genes can be further classified into two classes, leaky late genes of which expression is enhanced by viral DNA synthesis, and true late genes that are transcribed only after viral DNA synthesis has taken place. Late gene promoters are the simplest, containing only an initiator region downstream of the TATA box (Rajčáni *et al.*, 2004; Weir, 2001).

1.4.1.3 The replication of viral DNA

Replication of HSV-1 DNA takes place in the nucleus and requires seven essential viral proteins; the origin binding protein UL9, the single-stranded DNA-binding protein UL29 (ICP8), the DNA helicase/primase complex composed of UL5, UL52 and UL8, and a two-subunit DNA polymerase composed of the catalytic subunit UL30 and the DNA polymerase processivity factor UL42 (Ward & Weller, 2011).

DNA replication initiates at the origin of replication sequences ori_S or ori_L with the binding of UL9. ICP8 acts together with UL9 to distort and destabilise this region. The helicase/primase complex is then recruited to the replication fork, where it further acts to unwind the DNA and synthesises short RNA primers for the initiation of DNA replication. The viral DNA polymerase is recruited to the replication fork to catalyse leading and lagging strand DNA synthesis, which then continues in a rolling circle model to generate linear concatemers (reviewed in Weller & Coen, 2012).

1.4.1.4 Capsid assembly and packaging

Capsid formation requires essential viral proteins, including the major capsid protein UL19, the triplex proteins UL18 and UL38, and the maturational protease UL26. Capsid assembly takes place in the nucleus, where the interaction of UL19 and UL6 (which forms the portal) with scaffolding protein UL26.5 leads to autocatalytic assembly of a procapsid (Mettenleiter *et al.*, 2006; 2009).

Replication of the viral genome produces linear concatemers of DNA, which are cleaved during packaging into unit length monomers by the terminase complex composed of UL15, UL28 and UL33. The terminase complex is located at the portal complex (UL6) positioned at a single capsid vertex. The DNA is packaged and enters the capsid at this portal complex (Conway & Homa, 2011).

1.4.1.5 Maturation and egress

The widely accepted model of maturation and egress of HSV involves envelopment, de-envelopment, and re-envelopment. After assembly in the nucleus, mature nucleocapsids undergo primary envelopment through the inner nuclear membrane to the perinuclear space, and viral proteins UL31 and UL34 play a role in this process. The UL31/UL34 complex is required for efficient budding of the nucleocapsids through the inner nuclear

membrane, and is involved in disrupting the nuclear lamina and recruitment of viral proteins to the inner nuclear membrane. The UL31/UL34 complex recruits cellular protein kinase C and interacts with tegument protein kinase US3, which are both involved in phosphorylation of nuclear lamins, thereby disrupting the integrity of inner nuclear membrane. The immature enveloped nucleocapsids then fuse with the outer nuclear membrane, resulting in the loss of their primary envelope (de-envelopment). In the cytoplasm, inner tegument viral proteins are acquired by the capsid. The addition of the outer tegument proteins and secondary envelopment by membranes including the viral glycoproteins occurs at the Golgi. Virions are released from the cell by exocytosis (reviewed in Kelly *et al.*, 2009; Mettenleiter *et al.*, 2009).

1.4.2 Latency

All herpesviruses, including HSV-1, establish a life-long latent infection in the host. After primary infection of epithelial cells in the oral mucosa, the virus enters the sensory neurones and then undergoes retrograde axonal transport along the microtubules to the neuronal cell bodies in the trigeminal ganglion, where the virus establishes latency. Latency is characterised by an absence of gene expression, which is believed to be a consequence of failure of IE gene expression. During latency, the genomes exist in a non-replicating state in a circular episome configuration that associate with non-acetylated histones, and transcription is restricted to the latency associated transcripts (LATs, see **section 1.4.2.2**). Through latency, HSV-1 limits recognition by the immune system, and this is likely to be a major factor in establishing life-long persistence. The virus can reactivate in response to stimuli such as stress, fever, ultraviolet (UV) light and immune suppression, resulting in productive viral replication. The virus then travels down the axon by anterograde transport to create a lytic infection at the original primary infection site. This may be an asymptomatic infection or can appear as epithelial lesions, thereby facilitating viral transmission (reviewed in Efstathiou & Preston, 2005; Nicoll *et al.*, 2012).

1.4.2.1 Establishment, maintenance and reactivation from latency

Latency may result from a failure of IE gene expression. As described in detail in **section 1.4.1.2**, the transcription of IE genes involves viral protein VP16 forming a complex with the cellular proteins HCF and Oct-1 to activate transcription (Wysocka & Herr, 2003). However, in neurones, VP16, HCF and Oct-1 expression and localisation are altered. In sensory neurones, HCF is detected in the cytoplasm rather than its normal nuclear

localisation (Kristie *et al.*, 1999) and this may affect the nuclear localisation of VP16, which lacks a nuclear localisation signal and is dependent on HCF for its nuclear import (Boissière *et al.*, 1999). Oct-1 has been shown to be down regulated in neurones (Lakin *et al.*, 1995). The availability and localisation of VP16, Oct-1 and HCF may impair viral gene transcription in sensory neurones (reviewed in Nicoll *et al.*, 2012).

Latently infected mouse neurones contain a variable number of HSV genomes per cell, ranging from less than 10 to more than 1000 (Sawtell, 1997). A study by the Efstathiou group investigated whether the variable number of genomes in latently infected neurones was due to gene expression prior to the establishment of latency. Using Cre reporter mice containing a *Lac*Z gene and infected with Cre-expressing HSV-1 mutants, it was determined that viral gene expression can occur before the establishment of latency (Proença *et al.*, 2008). IE gene expression was detected in around a third of latently infected neurones, and in a small number of neurones there was activation of early and late gene promoters (Proença *et al.*, 2011). The number of latent viral genomes per cell may influence the likelihood of reactivation, with cells infected with high number of latent genomes showing a higher probability of reactivation (Sawtell, 1998). Reactivation is a response to cellular or external signals that bring about the activation of viral gene expression and lytic infection. However, the mechanisms controlling the balance between lytic and latent infections and factors that affect the establishment, maintenance and reactivation from latency remain poorly understood despite extensive research (reviewed in Efstathiou & Preston, 2005; Nicoll *et al.*, 2012).

1.4.2.2 Transcript expression during latency

During lytic infection, the whole viral genome is actively transcribed, whereas viral genomes are repressed during latency and transcription is restricted to the LATs. LATs are non-coding RNA transcripts that are produced from the repeat regions flanking the U_L region of the viral genome (IR_L/TR_L) (Stevens *et al.*, 1987). Their transcription produces an 8.3 kb primary transcript, which undergoes splicing to produce a 2.0 kb LAT that is further spliced to yield a 1.5 kb LAT. The LATs are transcribed antisense to the IE gene encoding ICP0 (Farrell *et al.*, 1991). The major LAT shows a nuclear distribution and accumulates to high levels in the nucleus of latently infected neurones (Thomas *et al.*, 2002). The LATs have been proposed to have many roles, including enhancing the establishment of latency, reactivation and promoting neuronal survival. The main phenotype of LAT deletion mutants is reduced efficiency of reactivation, which may be

related to fewer viruses establishing latency. However, the general consensus is that LATs are not essential for the establishment of latency, maintenance or reactivation (reviewed in Efstathiou & Preston, 2005; Nicoll *et al.*, 2012).

1.4.2.3 Models of HSV-1 latency and quiescent infections

Latency is an important part of the HSV-1 life cycle and is central to the survival strategy of the virus. It is important to research this stage of the virus life cycle, as the virus is not visible to the immune system so remains undetected. The broad host range of HSV-1 has allowed experimental models to be developed for studying viral latency. The models do not recreate all aspects of the human disease, as this is not possible. Animal models such as inoculation of the footpad/eye of mice or the eye of rabbits produces a local infection, and the virus is then transported to the trigeminal ganglia or dorsal root ganglia (depending on the site of inoculation), where latency is established. In very few cases using these animal models, the virus sporadically reactivates. However, reactivation can be induced by addition of epinephrine to the eye of rabbits, induction of hyperthermia in mice or explanting the mouse ganglia that are then grown in culture to test for reactivation. *In vitro* systems using neuronal and non-neuronal cells for studying latency have also been developed. In some aspects, these cell-based systems in some aspects are advantageous to animal models as they are easier, cheaper and more controllable. These systems rely on replication-deficient viruses or the use of drugs such as ACV to prevent replication and IE gene expression and to enable the virus to establish quiescence, and the virus can be reactivated or de-repressed under specific conditions. These models have provided an insight into the mechanisms of latency and reactivation (reviewed in Nicoll *et al.*, 2012; Wagner & Bloom, 1997).

1.5 Immediate-early gene expression

The IE genes are the first viral genes to be transcribed during infection and they can be expressed in the absence of *de novo* viral protein synthesis. The IE genes encode five proteins ICP4, ICP22, ICP27 and ICP47, which are described in detail below, and ICP0 in **section 1.6.**

1.5.1 ICP4

ICP4 a protein of 175 kDa apparent molecular weight is encoded by the RS1 gene within the IR_S/TR_S region of the genome therefore is present as two copies. ICP4 is essential for viral infection and functions as a transcriptional activator of early and late genes (Watson & Clements, 1980). Viral gene expression does not proceed past the IE stage in cells infected with an ICP4 mutant virus, and there is an accumulation of IE gene products (Preston, 1979). ICP4 contains a DNA-binding domain that enables it to bind to locations within the viral genome, including specific sequences on some IE, early and late promoter sites (Kuddus & DeLuca, 2007; Sampath & DeLuca, 2008). However, it is the general DNA-binding ability of ICP4, rather than the presence of specific binding sequences, that is important for its activity. ICP4 binds to viral DNA and forms a tripartite complex with the cellular transcription factors TATA-binding protein and transcription factor 11B (TF11B), which are required for transcription by RNA polymerase II (Smith *et al.*, 1993).

1.5.2 ICP27

ICP27 (UL54 gene) is also essential for viral replication and functions at multiple post-transcriptional levels, including mRNA splicing, nuclear export of viral transcripts and increasing late gene expression (extensively reviewed in Sandri-Goldin, 2011). ICP27 binds to and recruits RNA polymerase II to viral replication sites, thus increasing the transcription of early and late genes (Dai-Ju *et al.*, 2006). Early in infection, ICP27 also inhibits pre-mRNA splicing by interacting with cellular proteins, thereby reducing host cell protein synthesis (Hardy & Sandri-Goldin, 1994). This is believed to be advantageous to the virus, as only four of the viral transcripts contain introns. ICP27 additionally binds to RNA and plays a role in viral mRNA export from the nucleus by interacting with nuclear export adaptor proteins and with the cellular mRNA export receptor (reviewed in Sandri-Goldin, 2011). Furthermore, ICP27 stimulates the translation of viral mRNAs, including VP16, by the recruitment of translation initiation factors to these mRNAs (Ellison *et al.*, 2005).

ICP27 may also play a role in HSV-1 evading the immune response. ICP27 expression induces the expression of type I IFN antagonising protein and down regulates the phosphorylation of STAT1, both of which prevent the accumulation of STAT1 in the nucleus (Johnson & Knipe, 2010; Johnson *et al.*, 2008).

1.5.3 ICP22

ICP22 (US1 gene) is not required for viral replication in all cell types, but in some cells it is required for efficient viral replication and the expression of some late genes (reviewed in Weir, 2001). ICP22 is phosphorylated by the protein kinase UL13, and can alter the phosphorylation status of the large subunit of RNA polymerase II, thereby promoting viral transcription (Long *et al.*, 1999; Rice *et al.*, 1995).

1.5.4 ICP47

ICP47 (US12 gene) is involved in evading the immune response by disrupting antigen presentation. ICP47 achieves this by binding to the transporter associated with antigen processing protein (TAP). TAP transports antigenic peptides into the endoplasmic reticulum for presentation at the cell surface to activate the T cell response. The binding of ICP47 to TAP inhibits presentation of viral peptides by major histocompatibility complex (MHC) class I, enabling the virus to evade the cytotoxic T cell response (Fruh *et al.*, 1995; Hill *et al.*, 1995).

1.6 ICP0

ICP0, the product of the IE1 gene, contains 775 amino acids. The gene is located with the long repeat element (IR_L/TR_L), and is therefore present as two copies within the genome (Perry *et al.*, 1986). The ICP0 gene contains three exons, divided by two introns of 767 and 136 bases, and thus ICP0 is translated from one of the few HSV-1 mRNAs that undergo splicing (Perry *et al.*, 1986). The coding region of ICP0 has a high G+C composition of 75.4% (Perry *et al.*, 1986).

ICP0 is a multi-functional protein that acts to relieve cell-mediated transcriptional repression, and therefore it stimulates viral gene expression in general. ICP0 contains several functional domains and has been implicated in many diverse cellular pathways that are discussed below.

1.6.1 Overview of ICP0 protein structure

ICP0 contains several domains and motifs (**Figure 1.3**) that have been studied extensively and have functions assigned to them. Some of these will be explained in more detail in

subsequent sections of this chapter. The N-terminal third of ICP0 (residues 116-156) contains a zinc-binding RING finger domain that shows sequence homology to the related proteins expressed by other alphaherpesviruses (Barlow *et al.*, 1994). The regions downstream of the RING finger contain three distinct sequences at residues 224-234, 365-371 and 508-518 that are phosphorylation sites (Davido *et al.*, 2005), but in general this region of the protein has been poorly characterised. The third phosphorylation site is in proximity to the nuclear localisation signal (NLS) located at residues 500-509 (Everett, 1988; Mullen *et al.*, 1994). The C-terminal third of ICP0 contains a cellular ubiquitin specific protease (USP7) interaction motif between residues 618-634 (Meredith *et al.*, 1995). This region also contains a domain required for ICP0 self-interaction or dimerisation (Ciufo *et al.*, 1994) and sequences between residues 634-719 that are required for ICP0's localisation to ND10 (Maul & Everett 1994).

Figure 1.3 Domains and motifs present within ICP0.
The N-terminal third of ICP0 contains a RING finger domain. The C-terminal third contains a nuclear localisation signal (NLS), a USP7-binding motif, and sequences required for localisation at ND10.

1.6.2 ICP0-null mutant phenotype

The phenotype of an ICP0-null HSV-1 mutant has been shown to be highly dependent on cell type. Stow and Stow generated an ICP0-null mutant *dl*1403, which contains a 2 kb deletion within both copies of the gene (Stow & Stow, 1986). Although *dl*1403 was able to replicate and produce plaques in baby hamster kidney (BHK) cells, the yield of infectious virus compared to wild-type (wt) was 20- to 100-fold lower (Stow & Stow, 1986). Subsequent experiments have shown that human fibroblasts (HFs) are one of the most restrictive cell types for an ICP0-null mutant virus, having a 1000-fold defect (Everett *et al.*, 2004a), whereas in HepaRG cells the defect is around 500-fold (Everett, 2010; Everett *et al.*, 2009), and in other cells such as Vero, HeLa and BHK the defect is between 30- to 100-fold (Chen & Silverstein, 1992; Everett *et al.*, 2004a). In some cells, such as

the osteosarcoma cell line U2OS, the ICP0-null mutant virus replicates as efficiently as wild-type (wt) virus, meaning that ICP0 is not required for HSV-1 replication in this cell type (Yao & Schaffer, 1995). The reasons for lack of requirement of ICP0 in U2OS cells is not known, but may be due to the cells lacking an antiviral mechanism that is targeted by ICP0 (Yao & Schaffer, 1995), including lower levels of PML and lack of ATRX expression (Lukashchuk & Everett, 2010). Alternatively, U2OS cells may lack signalling or chromatin assembly pathways that are present in restrictive cell types (Hancock *et al.*, 2010; Hancock *et al.*, 2006). Due to the lack of requirement of ICP0, U2OS cells are used to calculate viral titres of wt and ICP0 mutant virus stocks in a truly comparative manner.

Plaque formation efficiency (PFE) of an ICP0-null mutant virus and apparent phenotype is also dependent on the input multiplicity of infection (MOI), as well as the cell type. In non-permissive cells, infection with an ICP0-null mutant virus can cause a reduction in PFE. However, above a certain input multiplicity ICP0-null mutant viruses replicate as efficiently as wt (Everett *et al.*, 2004a; Stow & Stow, 1986). Therefore, compared to wt virus, the ICP0-null mutant virus has a high virus particle to plaque forming unit ratio. In restrictive cell types, the virus also has a high probability of entering a non-productive infection leading to quiescence (Everett *et al.*, 2004a).

1.6.3 The RING finger of ICP0

The N-terminal third of ICP0 between residues 116 to 156 contains a C_3HC_4 RING finger domain (Barlow *et al.*, 1994; Everett *et al.*, 1993a). At present, there is no solved crystal structure of ICP0 in HSV-1. The closest related structure is the RING finger domain of the homologous equine herpesvirus 1 IE protein (EHV-63) determined by H-NMR (**Figure 1.4**). The tertiary structure of the RING finger domain showed it consists of an amphipathic alpha-helix that lies between the second and third strands of triple-stranded antiparallel beta-sheets. A hydrophobic core is formed from conserved residues within the alpha-helix, beta-sheets and loop regions (Barlow *et al.*, 1994). The RING finger domain is important for ICP0's activity, as deletion of the RING finger domain causes a defect in replication and PFE as severe as complete deletion of the ICP0 gene (Everett, 1989; Everett *et al.*, 2004a; Lium & Silverstein, 1997).

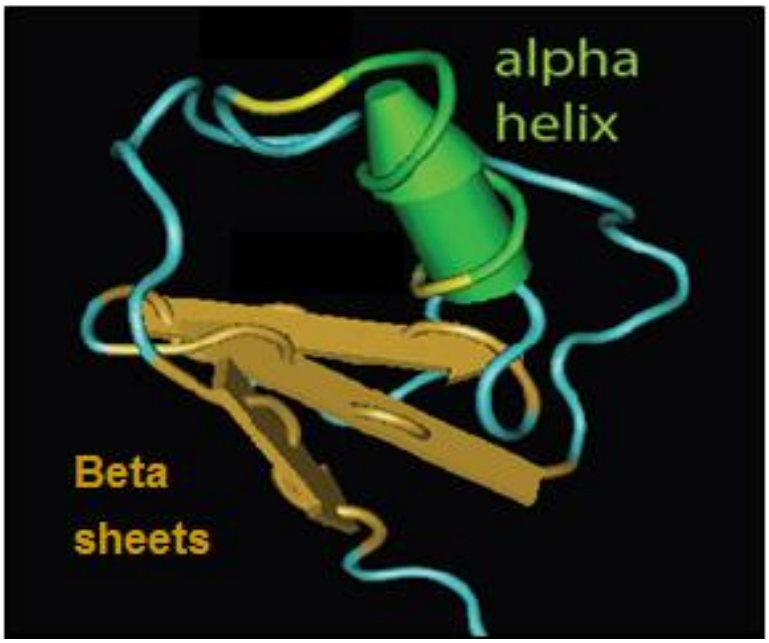

Figure 1.4 The RING finger domain of EHV EICP0.
The RING finger domain of EICP0 consists of an amphipathic alpha-helix (green) that lies between the second and third strands of the triple-stranded anti-parallel beta-sheets (brown). Conserved cysteine and histidine residues within the RING finger domain coordinate the binding of two zinc atoms (**Figure 1.5**). The residues in yellow are the positions of the K144E and N151D residues that are the focus of this study.

Conserved cysteine residues at position 116, 119, 139, 142, 143, 153 and 156, and a histidine residue at position 136, coordinate the binding of two zinc atoms in a tetrahedral geometry (**Figure 1.5**). The first and third pairs of residues bind one zinc atom, while the second and fourth pair of residues bind the other zinc molecule (Barlow *et al.*, 1994; Everett *et al.*, 1993a; Lium & Silverstein, 1997). Mutations in these conserved cysteine and histidine residues show they are essential for the transactivation properties of ICP0, whereas the non-conserved cysteine 129 and histidine 126 residues are not involved in zinc binding but may play a role in the layout of the RING finger domain (Lium & Silverstein, 1997).

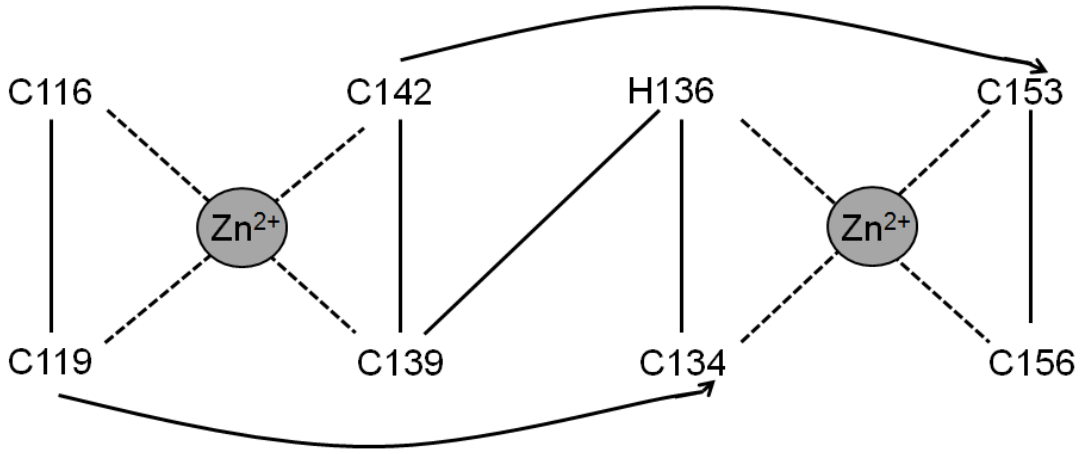

Figure 1.5 Zinc coordinating residues within the RING finger domain of ICP0. Conserved cysteine and histidine residues coordinate the binding of two zinc (Zn^{2+}) atoms within the RING finger domain of ICP0. The first and third pairs of residues bind one zinc atom, while the second and fourth pair of residues bind the other zinc molecule.

Between the third and fourth pair of zinc coordinating residues lies the alpha-helix, from which several polar and charged side chains extend from the RING finger domain. By site-directed mutagenesis, it has been shown that these side chains are involved in ICP0 activity (Barlow *et al.*, 1994; Everett *et al.*, 1995; Vanni *et al.*, 2012). Mutations K144E and N151D, which are located in the charged side chains that are exposed on the surface of the alpha-helix, will be one of the focuses of this thesis. It was found that these mutations affected ICP0's activity in gene expression reporter assays and also the limited number of virus infection assays that were available at the time (Barlow *et al.*, 1994; Everett *et al.*, 1995). More recently, using an inducible ICP0 expression system, mutation N151D was shown to have a slight defect in complementing the plaque formation ability of an ICP0-null mutant HSV-1 but was defective in inducing reactivation of quiescent HSV-1 (Vanni *et al.*, 2012). Therefore, as these residues are exposed on the surface of the alpha-helix, they may have a role in forming an interface with ICP0 interaction partners.

Proteins containing RING finger domains were shown to be involved in the ubiquitination of substrates, and it was suggested that RING finger proteins act as E3 ubiquitin ligases that mediated the transfer of ubiquitin onto target proteins (Joazeiro & Weissman, 2000). The RING finger domain of ICP0 was shown to function as an E3 ubiquitin ligase, inducing the formation of polyubiquitination chains and the subsequent proteasome-dependent degradation of selected cellular proteins (Boutell *et al.*, 2002). The E3 ubiquitin

ligase activity of ICP0, its cellular substrates and the ubiquitin pathway are discussed in more detail in **section 1.8**.

1.6.4 Association with ND10

At early stages of infection, ICP0 localises to cellular nuclear structures known as nuclear domains 10 (ND10, otherwise known as PML nuclear bodies or PML oncogenic domains) (Maul *et al.*, 1993), and this requires the C-terminal region of ICP0 (Maul & Everett, 1994). ND10 are dynamic, macromolecular structures that appear as distinct punctate foci within the nucleus by immunofluorescence. They range from 0.2-1 μm in size, with anything from 2-30 present in each cell, depending on the cell type and status (Ascoli & Maul, 1991). ND10 are composed of PML, Sp100, hDaxx and small ubiquitin-like modifier 1 protein (SUMO-1), as well as several other regulatory proteins (reviewed in Tavalai & Stamminger, 2008). PML can be covalently modified with the SUMO family of proteins, and this SUMO-modification is required for ND10 formation, in which PML acts as a scaffold protein and recruits other proteins to ND10 (Ishov *et al.*, 1999; Zhong *et al.*, 2000).

As the infection progresses, ICP0 causes the disruption of ND10 (Maul *et al.*, 1993), and the RING finger of ICP0 is essential for this disruption (Everett & Maul, 1994). ICP0 induces the proteasome-mediated degradation of PML and Sp100, particularly their SUMO-modified isoforms (Chelbi-Alix & de The, 1999; Everett *et al.*, 1998a; Parkinson & Everett, 2000), and this process also requires the RING finger of ICP0 (Everett *et al.*, 1998a) due to its E3 ligase ability (discussed in **section 1.8**). The degradation of PML and Sp100 leads to the dispersal of other ND10 proteins.

Additionally, after the HSV-1 genome enters the nucleus, ND10 proteins including PML, Sp100, hDaxx and ATRX become associated with the viral genomes and early replication compartments (Everett & Murray, 2005). This recruitment of ND10 proteins to viral genomes occurs very rapidly (Everett & Chelbi-Alix, 2007), but, due to ICP0 inhibiting the recruitment, it is difficult to detect in wt infections (Everett & Murray, 2005). This recruitment can be visualised in ICP0-null mutant infected cells at the edges of developing plaques, as ICP4 is recruited to replicating viral genomes at the early stages of infection and forms discrete foci, most of which become associated with ND10 proteins (Everett *et al.*, 2003). Unlike the formation of ND10, the recruitment of ND10 proteins to viral genomes is not dependent on PML (Everett *et al.*, 2007; Everett *et al.*, 2008; Everett *et al.*,

2006), but the recruitment of ATRX is dependent on hDaxx (Lukashchuk & Everett, 2010). The recruitment of ND10 proteins to incoming viral genomes is involved in the host response to HSV-1. PML and Sp100 are IFN-stimulated genes (ISGs), and so are upregulated in response to IFN (Grotzinger *et al.*, 1996; Guldner *et al.*, 1992; Lavau *et al.*, 1995) and play a role in the cellular restriction of viral infection, as explained in **section 1.7.3**.

1.6.5 Association and interaction of ICP0 with other cellular proteins

As well as its association with ND10, ICP0 has been implicated in many diverse cellular pathways, including the DNA damage response, transcriptional regulation, influencing chromatin assembly and modification, and immune signalling pathways. Therefore, ICP0 associates or interacts with many diverse cellular proteins involved in these pathways, some of which will be described below. The interactions of ICP0 with components of the innate immune response (particularly the IFN response) will be discussed in **section 1.7.1**.

1.6.5.1 ICP0 and interactions with chromatin assembly and modification components

Within cells, free DNA normally becomes associated with histones to form chromatin. During lytic infection, HSV-1 DNA is not extensively associated with histones, and viral proteins may play a role in preventing the addition of histones to viral DNA. In latently infected cells however, the viral DNA is in a heterochromatin structure tightly associated with histones leading to the silencing of viral gene expression. A potential way that ICP0 may promote gene expression and influence the switch from lytic to latent infections is through association with chromatin and its related modifying complexes (reviewed in Knipe & Cliffe, 2008).

The structure of chromatin plays a role in gene regulation, and can be influenced by post-translational modification of the core histones, including acetylation, methylation, ubiquitination and phosphorylation. Acetylation of histones by histone acetyltransferases forms less condensed active euchromatin, which is associated with active gene expression (reviewed in Knipe & Cliffe, 2008). The removal of the acetyl group from the lysine of the acetylated histone protein by histone deacetylases (HDACs) forms highly condensed heterochromatin that is transcriptionally inactive and is associated with repression of gene

expression (reviewed in de Ruijter *et al.*, 2003). In transfected cells, ICP0 interacts with class II HDACs 4, 5 and 7 and leads to the redistribution of HDAC 4 to colocalise with ICP0 (Lomonte *et al.*, 2004). HDAC inhibitors can induce gene expression in trigeminal ganglia latently infected with ICP0-null mutants (Arthur *et al.*, 2001; Terry-Allison *et al.*, 2007). However, inhibitors of HDACs cannot complement the defects of an ICP0-null mutant virus in restrictive cell lines (Everett *et al.*, 2008).

ICP0 has also been shown to displace HDAC1 from the REST/CoREST/HDAC transcriptional repressor complex, which has a role in chromatin modification. ICP0 achieves this by binding to CoREST, a corepressor for the cellular protein REST (Gu *et al.*, 2005), through residues (671 and 673) located in the C-terminal third of ICP0 (Gu *et al.*, 2005; Gu & Roizman, 2009). Therefore, the presence of ICP0 and its displacement of HDAC1 from this complex may have a role in reactivation/derepression of viral gene expression (Gu & Roizman, 2007). However, depletion of CoREST did not improve the PFE or replication efficiency of an ICP0-null mutant virus (Everett, 2010).

1.6.5.2 ICP0 interactions with components of the DNA damage response

HSV-1 infection activates the DNA damage response (Lilley *et al.*, 2005; Mohni *et al.*, 2010; Weller, 2010; Wilkinson & Weller, 2006), and ICP0 interacts with some components of this response. The DNA damage response pathway consists of a variety of cellular proteins and signalling pathways for sensing and repairing DNA damage within cells. DNA damage sensor proteins detect DNA damage and activate protein kinases, including ATM kinase and DNA-dependent protein kinase (DNA-PK), which are involved in responses to double-stranded DNA breaks, and ATR kinase, which responds to single strand DNA damage. These protein kinases activate downstream signalling components to mediate repair of the damaged site (reviewed in Ciccia & Elledge, 2010).

ICP0 induces the degradation of components of the DNA damage response, including DNA-PK and the cellular ubiquitin ligase RNF8 (Chaurushiya *et al.*, 2012; Lilley *et al.*, 2010; Parkinson *et al.*, 1999; Wilkinson & Weller, 2006). DNA-PK is composed of a large catalytic subunit and DNA-binding protein Ku, which targets DNA-PK to DNA. DNA-PK is involved in DNA double-strand break repair and V(D)J recombination (reviewed in Lees-Miller, 1996). The RING finger of ICP0 induces the degradation of the catalytic subunit of DNA-PK in a proteasome-dependent manner (Parkinson *et al.*, 1999).

RNF8 is also degraded by ICP0 (Lilley *et al.*, 2010). RNF8 is recruited to double-strand breaks by binding to phosphorylated Mdc1, and ubiquitinates histones H2A and H2AX (Huen *et al.*, 2007; Mailand *et al.*, 2007). RNF168 binds to ubiquitinated histone H2A and acts to further ubiquitinate histones to enhance the recruitment of repair proteins involved in the damage response, including 53BP1 and BRCA1 (Doil *et al.*, 2009; Stewart *et al.*, 2009). ICP0 is phosphorylated by the cellular kinase CK1 at residue T67, which mimics phosphorylated Mdc1, allowing ICP0 to bind to RNF8 and induce its degradation (Chaurushiya *et al.*, 2012). By inducing the degradation of this cellular ligase, ICP0 prevents histone ubiquitination and the recruitment of cellular repair factors to sites of DNA damage.

ICP0 additionally affects the DNA damage response by disrupting the ATR signalling pathway. ICP0 causes the redistribution of the ATR recruitment protein ATRIP, preventing the colocalisation with ATR and the recruitment of ATR to sites of DNA damage (Wilkinson & Weller, 2006). Therefore, ICP0 has multiple mechanisms to disrupt the DNA damage response by targeting proteins for degradation and preventing downstream signalling events involved in DNA repair.

1.6.6 ICP0 in reactivation from latency

Although ICP0 is not essential for HSV-1 replication, the virus is more likely to enter a non-productive infection and enter a quiescent state in cells infected at a low MOI if ICP0 is not present (Everett *et al.*, 2004a; Stow & Stow, 1989). However the requirement of ICP0 initiating reactivation from latency or quiescent infections and during reactivation remains controversial. ICP0-null mutant viruses reactivate inefficiently from latency following explant of infected mouse trigeminal ganglion cells, indicating ICP0 may induce efficient reactivation (Cai *et al.*, 1993; Halford & Schaffer, 2001). Additionally, ICP0 has been shown to have the ability to reactivate gene expression in quiescently infected non-neuronal *in vitro* models (Everett *et al.*, 2009; Harris *et al.*, 1989; Samaniego *et al.*, 1998), and this was dependent on the RING finger region of ICP0 (Everett *et al.*, 2009; Ferenczy *et al.*, 2011; Harris *et al.*, 1989). Furthermore, the expression of ICP0 in latently infected mouse trigeminal ganglion cells resulted in active replication of viral genomes (Halford & Schaffer, 2001; Terry-Allison *et al.*, 2007).

Reactivation of gene expression and viral replication in quiescently infected non-neuronal cells, however, can also be induced, albeit to a less marked degree, by cellular stress in the

absence of ICP0 (Preston & Nicholl, 2008). *In vivo* mouse studies using hyperthermic stress found that ICP0 was not required for the initiation of reactivation. However, ICP0 was important for productive replication and gene expression following the exit from latency (Thompson & Sawtell, 2006). Other viral proteins, such as VP16, may additionally play a role in initiating reactivation (Thompson *et al.*, 2009). Therefore, despite extensive research into the requirements for reactivation from latency, whether ICP0 plays a role still remains unclear. Other viral or cellular factors may also be important and play a role, and the conclusions gained may depend on the experimental system used.

1.7 Host defences against viruses

The host response to viral infection and viral evasion strategies determine the outcome of the infection. The immune response has traditionally been divided into two groups, the innate and the adaptive immune responses. However, a recently emerged third aspect of the immune response, termed intrinsic antiviral resistance, acts immediately against invading viruses and involves pre-existing cellular proteins. Each aspect of the immune response and the effects on HSV-1, and the interactions of viral and cellular immune response proteins, are discussed below.

1.7.1 Innate immunity to HSV-1

The innate immune response is a non-specific response that aims to resist microbial infection. The consequences of activated innate immunity include the induction cell lysis, the priming of neighbouring cells to induce an antiviral state, and also the shaping of the adaptive immune response. Natural killer cells, the complement system and IFN-mediated defences are all components of the innate immune response.

Pattern recognition receptors such as Toll-like receptors detect 'pathogen-associated molecular patterns', which activate a signalling cascade leading to the activation of IRF3 and NF-κB transcription factors. These proteins enter the nucleus and activate the transcription of chemokine and cytokine genes including those of type I IFNs (IFN α/β). Type I IFNs bind to cellular receptors, leading to the activation of Janus kinase (JAK) and phosphorylation of signal transducer and activator of transcription (STAT) molecules (STAT1 and STAT2), initiating the JAK/STAT signalling pathways. Phosphorylated of STAT1 and STAT2 allows the formation of a heterodimer that is then translocated into the

nucleus, where it binds to IFN-stimulated response elements (ISRE) within the promoters of IFN stimulated genes (ISGs) in order to activate their transcription. The activation of type I IFNs induces an antiviral state in both the initially stimulated and neighbouring cells, thereby limiting viral replication and spread, and it leads to the transcription of further ISGs. ISGs include dsRNA-dependent protein kinase R (PKR) and 2'-5' oligoadenylate synthetase (OAS), which both recognise double-stranded RNA. PKR is activated after binding double-stranded RNA, and phosphorylates eukaryotic initiation factor 2α (eIF-2α), which inhibits protein synthesis. OAS binding of double-stranded RNA activates RNase L, which leads to the degradation of viral (as well as cellular) mRNA within the cell (reviewed in Randall & Goodbourn, 2008).

HSV-1 is sensitive to both type 1 IFN (IFN-α/-β) and type II IFN (IFNγ), which together inhibit virus replication both *in vivo* and *in vitro* (Halford *et al.*, 2005; Leib *et al.*, 1999; Mittnacht *et al.*, 1988; Sainz & Halford, 2002). Three Toll-like receptors (TLR) have been shown to recognise HSV; TLR2, which recognises extracellular ligands (Kurt-Jones *et al.*, 2004), TLR3, which binds to double-stranded RNA (Zhang *et al.*, 2007), and TLR9, which recognises unmethylated CpG motifs (Lund *et al.*, 2003). However, HSV-1 proteins have been shown to act on multiple levels to evade and inhibit the innate immune response (reviewed in Paladino & Mossman, 2009; Vandevenne *et al.*, 2010). Some of the strategies used by the different viral proteins are described below.

ICP0 inhibits the TLR2 activation of NF-κB in a RING-dependent manner, possibly through the degradation of TLR adaptor proteins, therefore blocking the production of inflammatory chemokines and cytokines (van Lint *et al.*, 2010). ICP0 also acts to prevent TLR signalling and NF-κB activation through its association with USP7, which de-ubiquitinates key components in this signalling pathway (Daubeuf *et al.*, 2009). ICP0 has also been shown to block ISG expression by inhibiting transcriptional activator IRF3 (Lin *et al.*, 2004; Melroe *et al.*, 2004). ICP0 interferes with the activation of STAT-1 (Halford *et al.*, 2006) and also induces the degradation of key ISGs including PML and Sp100 (see **section 1.7.3**).

Other viral proteins also play a role in evading the immune response including the IE protein ICP27 and several late proteins. In addition to the roles described in **section 1.5.2,** ICP27 causes a decrease in cytokine production in infected cells, probably through down regulating IRF3 activation (Melchjorsen *et al.*, 2006), and also decreases STAT-1

phosphorylation, thereby preventing the accumulation of STAT-1 in the nucleus and inhibiting the JAK/STAT pathway (Johnson *et al.*, 2008). Late viral protein ICP34.5 blocks the inhibition of protein synthesis mediated by PKR, by inducing the desphosphorylation of eIF-2α (He *et al.*, 1997) and inhibiting the activation of IRF3, thereby preventing induction of IFN and ISGs in infected cells (Verpooten *et al.*, 2009). US11 protein also inhibits PKR activation by binding to PKR, therefore preventing the phosphorylation of eIF-2α (Cassady *et al.*, 1998), and also blocks 2'-5' OAS activation (Sànchez & Mohr, 2007). The late proteins US3 and vhs have also been implicated in antagonising the innate immune response (reviewed in Paladino & Mossman, 2009).

HSV-1 has evolved multiple mechanisms to prevent IRF3 and NF-κB signalling, therefore inhibiting IFN production. However, a study found that depletion of IRF3 or STAT-1 in HFs did not improve the PFE of an ICP0-null mutant virus (Everett *et al.*, 2008). ICP0-null mutant viruses though were sensitive to IFN pre-treatment of cells both at high and low MOIs, indicating that the phenotype of an ICP0-null mutant virus is not due to repression through IFN pathways alone (Everett *et al.*, 2008).

HSV-1 also evades the complement component of the innate immune response. Viral glycoprotein gC binds to complement protein C3b, therefore inhibiting the complement pathway and preventing neutralisation and cell lysis (Friedman *et al.*, 1984; Harris *et al.*, 1990). Therefore, HSV-1 encodes multiple proteins that can antagonise the host innate immune response at different points in multiple pathways.

1.7.2 Adaptive immunity to HSV-1

The adaptive or acquired immune response is pathogen-specific and exhibits memory against re-infecting pathogens. The key components of the adaptive immune system are B lymphocytes, which are involved in the humoral response and the production of antibodies, and T lymphocytes, which initiate the cell mediated response. B lymphocytes recognise viral antigens via their B-cell receptors, which leads to the production of antibodies directed against the invading virus. T lymphocytes are able to recognise infected cells through MHC complexes presenting viral peptides, and act either to destroy the infected cell or to assist B-cells with antibody production. T lymphocytes are divided into two classes: CD4+ and CD8+ cells. CD4+ cells recognise peptides presented on MHC class II, and their role is to activate other effector cells and provide co-stimulation to B lymphocytes to enable them to produce antibodies. Cytotoxic CD8+ cells recognise

peptides presented via MHC class I and, when activated, kill virus-infected cells (Janeway, 2001).

The adaptive immune response is important for the control of HSV infections. Individuals with a compromised immune system, such as those with HIV and transplant recipients, are more likely to suffer many episodes of reactivation, and primary infection in newborns whose immune system is yet to develop is associated with more severe disease (reviewed in Whitley *et al.*, 2007).

Infection with HSV-1 leads to the production of antibodies directed against a number of viral proteins, including glycoproteins and a nucleocapsid protein (Zweerink & Stanton, 1981). However, HSV-1 employs multiple mechanisms to evade recognition by the adaptive immune response by inhibiting antigen presentation. As described in **section 1.5.4**, ICP47 disrupts antigen presentation by MHC class I by binding to TAP, enabling the virus to prevent cell lysis by cytotoxic T lymphocytes (Fruh *et al.*, 1995; Hill *et al.*, 1995). Glycoprotein gB targets the MHC class II pathway by interacting with HLA-DR (MHC class II cell surface receptor), preventing its cell surface expression and causing release of HLA-DR into the exosome pathway (Neumann *et al.*, 2003; Temme *et al.*, 2010). HSV infection of B lymphocytes has additionally been shown to inhibit their ability to activate CD4+ T cells (Barcy & Corey, 2001).

Furthermore, viral glycoproteins gE and gI play a role in evading the immunoglobulin G (IgG)-mediated response, which act to neutralises viruses, targeting them for phagocytosis and activating the complement system. gE and gI form a heterodimeric transmembrane complex gE-gI that binds the Fc domain of IgG (Johnson *et al.*, 1988). The antigen-binding fragment of the IgG can still bind viral antigens, but the activation of downstream signalling pathways is prevented, and these are then targeted for degradation within lysosomes (Ndjamen *et al.*, 2014).

1.7.3 Intrinsic antiviral resistance

Intrinsic antiviral resistance is a relatively recently discovered part of the immune response, and is mediated by pre-existing cellular factors that are constitutively expressed. Intrinsic resistance is the first line of defence against virus infection, acting on a cellular level to suppress or prevent viral infections. Unlike innate immunity, proteins involved in intrinsic resistance are not upregulated in response to infection and do not require

intracellular signalling, but some of these factors can further be induced by IFN during viral infection (reviewed in Bieniasz, 2004).

Intrinsic resistance was first recognised as a response to retroviruses, with cellular proteins TRIM5α and APOBEC3G. TRIM5α, which is present in the cytoplasm, recognises and binds to incoming HIV capsids, and although the mechanisms of restriction are not fully understood, it occurs in a species specific manner (Stremlau *et al.*, 2004). APOBEC3G is a cytidine deaminase that catalyses the hydrolysis of cytidines to uridines. APOBEC3G affects HIV replication, leading to guanine to adenine hypermutation on the positive-sense DNA, which therefore may lead to the encoding of defective viral proteins (Mangeat *et al.*, 2003). Tetherin also restricts HIV-1 infection by binding to and retaining retrovirus particles on the cell surface, therefore inhibiting their release (Neil *et al.*, 2008).

In many instances, viruses express regulatory proteins that counteract the effects of intrinsic resistance factors. Therefore, proteins involved in intrinsic resistance are most easily studied in the context of infections with mutant viruses that fail to express these regulatory proteins, as the restriction effect can then be observed. For example, tetherin is counteracted by the HIV protein vpu, which facilitates virus spread (Neil *et al.*, 2008), and the HIV viral infectivity factor (vif), which binds to APOBEC3G, promoting its polyubiquitination and degradation by the proteasome (Sheehy *et al.*, 2003). Intrinsic resistance also has the potential to be overcome by the infecting virus, especially when present in large amounts, thereby swamping the inhibitory effects.

The proteins within ND10, including PML, Sp100 and hDaxx, are involved in intrinsic resistance to virus infection. Therefore, different herpesviruses have evolved ways to target these ND10 components to prevent viral gene repression and promote viral replication. These include ICP0 (Everett & Maul, 1994), IE1 protein of HCMV (Ahn & Hayward, 1997), EBV proteins BLZF1 and BNRF1 (Adamson & Kenney, 2001; Tsai *et al.*, 2011) and KSHV proteins LANA2 and ORF75 (Full *et al.*, 2014; Marcos-Villar *et al.*, 2009). The restrictive effects of some of the individual components of ND10 (PML, Sp100, hDaxx and ATRX) and their intrinsic resistance to herpesviruses are explored in more detail below, focussing on HSV-1.

1.7.3.1 PML

PML is a major component of ND10, and is required for ND10 assembly (Ishov *et al.*, 1999; Zhong *et al.*, 2000). There are six major isoforms of PML produced by alternative splicing. These isoforms differ in their C-terminal region, but the N-terminal region composed of a RING finger, two B-boxes and a coiled-coil domain is conserved and forms the tri-partite motif (TRIM) that is found in a large family of proteins (Jensen *et al.*, 2001). PML is covalently modified by members of the SUMO family of small ubiquitin-like proteins (Sternsdorf *et al.*, 1997) at one of three SUMO modification sites at lysine 65 within the RING finger domain, at residue 160 located in the B1-box and one within the nuclear localisation signal at residue 490 (Kamitani *et al.*, 1998).

PML plays a role in restricting the replication of ICP0-null mutant HSV-1. In HFs depleted of PML by shRNA, ICP0-null mutant virus PFE was increased by five- to ten-fold and gene expression also increased, but no effect was seen with the wt virus. The increase in PFE of an ICP0-null mutant virus, however, did not restore it to wt levels (Everett *et al.*, 2008; Everett *et al.*, 2006). The depletion of PML in HFs also increased the replication and PFE of wt HCMV at low MOIs, and increased the IE gene expression of IE1 deletion HCMV mutant in both low and high MOI infections (Tavalai *et al.*, 2006). PML depletion furthermore improved the replication of VZV (Kyratsous & Silverstein, 2009). Additionally, in differentiated human neural and skin cells infected with VZV *in vivo*, PML isoform IV (PML.IV) sequestered newly synthesised VZV nucleocapsids in the nucleus. This is thought to occur by PML.IV binding to VZV capsid surface protein ORF23, preventing nuclear egress and the formation of infectious particles (Reichelt *et al.*, 2011).

1.7.3.2 Sp100

Sp100 is another permanent ND10-associated protein, and, like PML, undergoes alternative splicing to produce different isoforms designated Sp100-A, Sp100-B, Sp100-C and Sp100-HMG (Guldner *et al.*, 1999). Sp100-B, Sp100-C and Sp100–HMG all contain a SAND domain required for DNA binding in other proteins (Bottomley *et al.*, 2001). Sp100 can be covalently modified by SUMO family members (Sternsdorf *et al.*, 1997), and during infection ICP0 induces the degradation of SUMO-modified but not unmodified forms of Sp100 (Parkinson & Everett, 2000; Sternsdorf *et al.*, 1997). SUMO modification of Sp100 is not required for its localisation to ND10 (Sternsdorf *et al.*, 1997), but this

localisation is dependent on PML (Ishov *et al.*, 1999). However, in the absence of PML, Sp100 and hDaxx are still recruited to HSV-1 genomes (Everett *et al.*, 2008), and therefore these proteins as well as PML are likely to play a role in viral restriction. Depletion of Sp100 in HFs increased ICP0-null mutant gene expression by about five-fold, and simultaneous depletion of PML and Sp100 gave an 15-fold rise in PFE of an ICP0-null mutant in HFs (Everett *et al.*, 2008).

1.7.3.3 ATRX and hDaxx

The Swi/SNF protein ATRX and the transcriptional repressor protein hDaxx, which that plays a role in chromatin remodelling, are constitutive components of ND10. hDaxx is recruited to ND10 by a SUMO interaction motif located at its C-terminal domain binding to SUMO-modified PML (Ishov *et al.*, 1999; Li *et al.*, 2000), whereas ATRX localisation at ND10 is dependent on interaction with the PAH1 domain of hDaxx located near its N-terminus (Ishov *et al.*, 2004; Lukashchuk & Everett, 2010). hDaxx functions as a transcriptional repressor by interactions with chromatin-related proteins, including HDACs (Hollenbach *et al.*, 2002). ATRX and hDaxx are recruited to viral genomes, but the recruitment of ATRX, as in the case of ND10 recruitment, requires hDaxx (Lukashchuk & Everett, 2010).

Overexpression of hDaxx repressed HCMV IE gene expression, but this restriction was multiplicity-dependent (Cantrell & Bresnahan, 2006; Woodhall *et al.*, 2006). In cells depleted of hDaxx by siRNA, HCMV showed an increase in IE protein expression (Woodhall *et al.*, 2006), and this was also seen in pp71-null HCMV mutant infected cells (Cantrell & Bresnahan, 2006; Preston & Nicholl, 2006). Transcriptional activator pp71 of HCMV lifts the restriction mediated by ATRX by interacting with hDaxx, leading to the displacement of ATRX from the complex and its relocation from ND10 to the nucleoplasm. Cells depleted of ATRX showed an increase in IE gene expression and viral replication of an pp71-null HCMV mutant (Lukashchuk *et al.*, 2008). In cells depleted of hDaxx or ATRX, an ICP0-null mutant virus has been shown to have an increase in PFE and gene expression, but no effect was observed with the wt virus (Lukashchuk & Everett, 2010).

Depletion of PML, Sp100 and hDaxx simultaneously increased the PFE of an ICP0-null mutant virus by around 50-fold, which was greater than the increase achieved by the addition of individual protein depletions (Glass & Everett, 2013). However, depletion of

these ND10 factors did not restore the phenotype of ICP0-null mutant virus to wt, and therefore other restriction factors must play a role in the intrinsic immunity against HSV-1 infection that are antagonised by ICP0 (Glass & Everett, 2013).

1.8 E3 ligase activity of ICP0 and its interactions with the ubiquitin pathway

The RING finger domain of ICP0 functions as an E3 ubiquitin ligase, inducing the formation of polyubiquitin chains and the subsequent proteasome-dependent degradation of a range of cellular proteins (see **section 1.8.5**) (Boutell *et al.*, 2002). Ubiquitin, a small, highly conserved 76 amino acid protein is attached to protein substrates by an enzymatic cascade involving an E1 ubiquitin activating enzyme, an E2 ubiquitin-conjugating enzyme and one of many substrate specific E3 ubiquitin ligase enzymes, in a process known as ubiquitination. Ubiquitination of proteins controls a variety of cellular processes, including the DNA damage response, apoptosis, cell cycle progression and differentiation, and is involved in protein degradation, signal transduction and cellular localisation (reviewed in Deshaies & Joazeiro, 2009).

1.8.1 Overview of the ubiquitin pathway

The ubiquitin pathway consists of the sequential activities of an E1 activating enzyme, an E2 ubiquitin-conjugating enzyme and an E3 ubiquitin ligase, and is summarised in **Figure 1.6**. The E1 enzyme activates ubiquitin, using ATP to adenylate the C-terminal carboxyl group of ubiquitin. The E1 enzyme binds to adenylated ubiquitin through its cysteine active-site, forming a covalent thioester bond between the E1 enzyme and ubiquitin. The ubiquitin is then transferred from the E1 enzyme to the cysteine active-site of an E2 ubiquitin-conjugating enzyme. The C-terminus of ubiquitin is then conjugated to the ε-amino group of a lysine in the substrate protein through a covalent isopeptide bond, using an E3 ubiquitin ligase, which provides the substrate specificity. Subsequently, further ubiquitin molecules can be conjugated to the first via an analogous process that involves lysine residues within ubiquitin. Multiple rounds of ubiquitination lead to the formation of a polyubiquitin chain, which can regulate cellular processes such as DNA repair, proteasome mediated degradation, cell cycle regulation and inflammation (reviewed in Deshaies & Joazeiro, 2009).

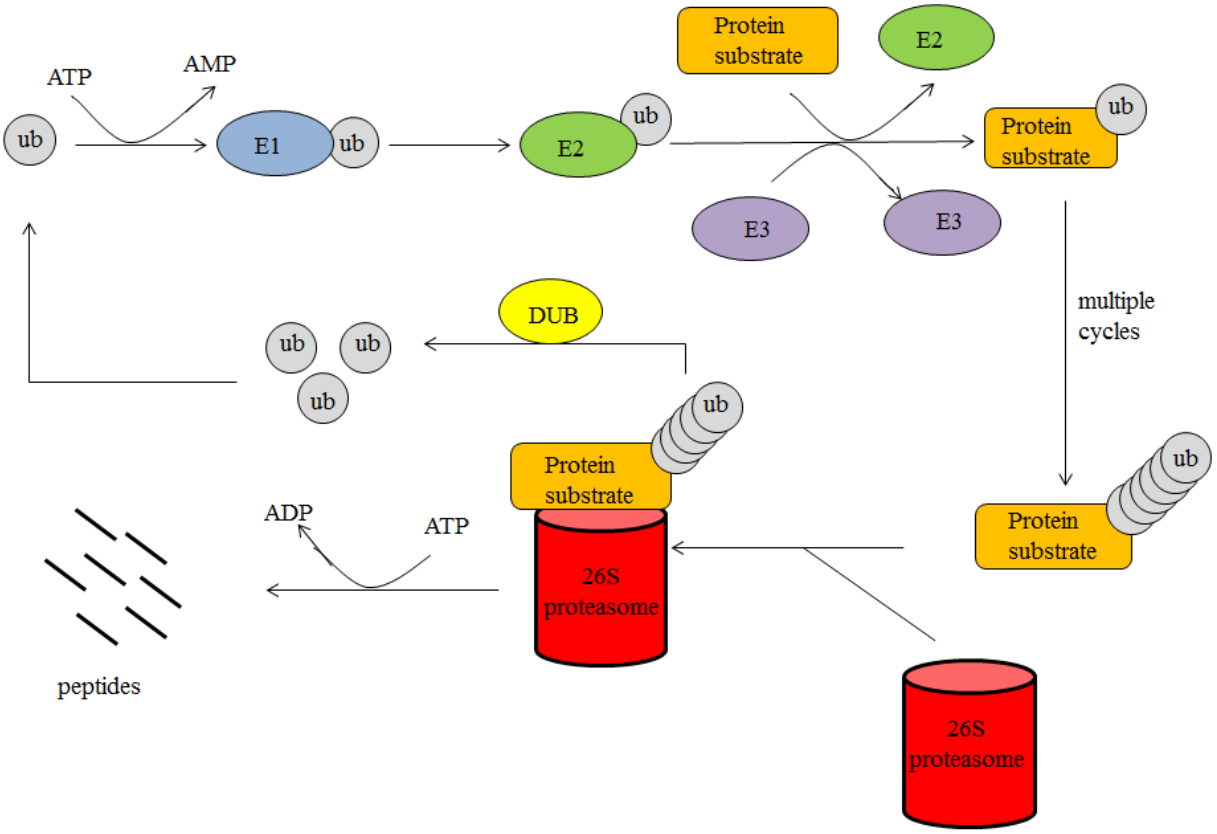

Figure 1.6 Overview of the ubiquitin pathway.
Ubiquitination of a given substrate requires an E1 ubiquitin activating enzyme, an E2 ubiquitin-conjugating enzyme and one of many substrate-specific E3 ubiquitin ligases. The E1 enzyme activates ubiquitin (ub), and the adenylated ubiquitin forms a covalent thioester bond with the cysteine active-site residue of the E1 enzyme. Ubiquitin is transferred to the active site of the E2 ubiquitin-conjugating enzyme. The E3 ubiquitin ligase binds to the E2-ubiquitin and the substrate protein to mediate the transfer of ubiquitin onto the target protein. These steps can occur multiple times to create a polypeptide chain that acts as a proteosomal degradation marker if the chain contains at least four ubiquitin molecules linked via K48 residues. The ubiquitin molecules are removed by the action of deubiquitinating enzymes (DUBs), so the ubiquitin can be used in subsequent ubiquitination reactions (adapted from Deshaies & Joazeiro, 2009).

1.8.2 Components of the ubiquitin pathway and processes

The main components of the ubiquitin pathway are E1 ubiquitin activating enzymes, E2 ubiquitin-conjugating enzymes and the E3 ubiquitin ligases. There are two known E1 ubiquitin activating enzymes in humans, UBA1 and UBA6, that activate and form thioester bonds with ubiquitin (Jin *et al.*, 2007; Pelzer *et al.*, 2007). There are at least 32 E2 ubiquitin-conjugating enzymes in humans, which all contain a highly conserved ubiquitin conjugating domain of about 150 residues composed of the catalytic cysteine residue, anti-

parallel beta-sheet and four alpha-helices (Huang *et al.*, 1999; VanDemark *et al.*, 2001; Zheng *et al.*, 2000).

The E3 ubiquitin ligases, of which there are hundreds, are the determinants of substrate specificity. E3 ligases can be classed into two main groups, those that contain a RING domain and those that contain a HECT domain. The RING finger E3 ubiquitin ligases, of which ICP0 is one, bind to the E2 enzyme-ubiquitin and the target protein simultaneously (sometimes with the aid of adaptor proteins). This simultaneous binding enables close proximity between the substrate and ubiquitin, allowing the direct transfer of ubiquitin from the E2 enzyme to the substrate protein. With HECT E3 ligases, the transfer of ubiquitin from the E2 ubiquitin conjugating enzyme to the substrate is a two-step process. The ubiquitin is first transferred from the E2 enzyme to an active site cysteine within the HECT domain, and the ubiquitin is then transferred to the substrate protein (reviewed in Kerscher *et al.*, 2006).

Ubiquitinated proteins containing a chain of at least four ubiquitin molecules linked by Lys48 residues are targeted for degradation via the 26S proteasome (Thrower *et al.*, 2000). The proteasome is composed of two 19S regulatory subunits and a 20S catalytic core subunit. Ubiquitinated substrates bind to ubiquitin receptors located on the 19S complex, and the substrate is then unfolded, translocated to the catalytic core, and degraded into small peptide fragments in a process that is dependent upon ATP (reviewed in Finley, 2009). The ubiquitin molecules do not get degraded and are removed by the action of deubiquitinating enzymes (DUBs), so the ubiquitin is recycled and can be used in subsequent ubiquitination reactions.

1.8.3 Chain linkage

The addition of one ubiquitin protein to a substrate protein is termed monoubiquitination. This mainly functions for signalling and transcriptional regulatory control, and does not function as a degradation signal. Ubiquitin contains seven lysine residues; Lys6, Lys11, Lys27, Lys29, Lys33, Lys48 and Lys63. These lysine residues can act as acceptor sites for further rounds of ubiquitin addition, leading to the formation of a chain of ubiquitin molecules on the substrate protein, termed polyubiquitination. The linkage between ubiquitin molecules can determine their signal and function. Polyubiquitin chains linked through Lys48 residues act to target substrates for degradation via the 26S proteasome (Chau *et al.*, 1989; Finley *et al.*, 1994; Thrower *et al.*, 2000), whereas Lys63 polyubiquitin

chains are involved in the DNA damage response (Hoege *et al.*, 2002; Hofmann & Pickart, 1999; Spence *et al.*, 1995) and NF-κB signalling (Deng *et al.*, 2000). Lys11-linked polyubiquitin chains may also play a role in proteasomal degradation of proteins involved in cell cycle control (Jin *et al.*, 2008; Matsumoto *et al.*, 2010). The functions of the other chain linkages remains poorly characterised and understood. Polyubiquitin chains can also contain mixed lysine linkages to form branched chains, although the functions of these are not clear.

1.8.4 ICP0 and its interactions with components of the ubiquitin pathway

The RING finger domain of ICP0 has been shown to interact with the highly homologous E2 ubiquitin-conjugating enzymes UBE2D1 and UBE2E1, and can catalyse the formation of unanchored polyubiquitin chains *in vitro* (Boutell *et al.*, 2002; Vanni *et al.*, 2012). The alpha-helix and loop regions of the RING finger domain of ICP0 are important for the interaction with UBE2D1 (Vanni *et al.*, 2012). ICP0 has also been shown to interact with UBE2R1 (cdc34) via its RING finger domain (Van Sant *et al.*, 2001). However, this interaction was not verified in a yeast-two-hybrid study that detected an interaction with UBE2D1 and UBE2E1 (Vanni *et al.*, 2012), and ICP0 does not produce polyubiquitin chains in the presence of UBE2R1 *in vitro* (Boutell *et al.*, 2002).

ICP0 undergoes auto-ubiquitination *in vitro* in the presence of UBE2D1 and UBE2E1, therefore targeting itself for degradation (Boutell *et al.*, 2002; Canning *et al.*, 2004; Vanni *et al.*, 2012). To prevent its own degradation, ICP0 interacts with a deubiquitylating enzyme (USP7) through a motif located in the C-terminal third of ICP0 (Everett *et al.*, 1997; Meredith *et al.*, 1995; Meredith *et al.*, 1994). This interaction with USP7 increases the stability of ICP0 by the removal of ubiquitin molecules from ICP0, thereby preventing its degradation (Boutell *et al.*, 2005; Canning *et al.*, 2004). Mutations of residues within the USP7-binding motif of ICP0 caused the protein to be highly unstable during viral infection and resulted in significantly reduced viral replication and ability to stimulate gene expression (Everett *et al.*, 1999b; Everett *et al.*, 1997). It is likely that the cellular function of USP7 is to prevent degradation of cellular proteins that are still required by the cell. However, USP7 binding contributes to the ability of ICP0 to transactivate gene expression and stimulate viral lytic infection (Canning *et al.*, 2004). ICP0 also induces the ubiquitination and degradation of USP7, which is surprising given that the interaction with USP7 stabilises ICP0. The significance of these two opposing functions is not fully

understood, but it is thought that the stabilisation of ICP0 by USP7 is more relevant *in vivo*, especially when there are low levels of ICP0 (Boutell *et al.*, 2005).

It has been shown that E3 ubiquitin ligases have the ability to interact with other E3 ligases (Weissman *et al.*, 2011). This is also the case for ICP0, which interacts with cellular RING finger E3 ubiquitin ligases RNF8 (see **section 1.6.5.2**) and SIAH-1 (Chaurushiya *et al.*, 2012; Lilley *et al.*, 2010; Nagel *et al.*, 2011). SIAH-1 is involved in the cellular stress response, cell signalling pathways and the degradation of a number of substrates (reviewed in Qi *et al.*, 2013), including PML (Fanelli *et al.*, 2004). Most substrates of SIAH-1 contain a PXAXVXP motif for interaction with a conserved substrate-binding domain within SIAH-1 (House *et al.*, 2003). ICP0 contains the PXAXVXP interaction motif at residues 401-407, and was shown to interact with SIAH-1 and be targeted for proteasomal degradation (Nagel *et al.*, 2011). Overexpression of ICP0 resulted in the stabilisation of SIAH-1, whereas silencing of SIAH-1 increased ICP0 stability during infection (Nagel *et al.*, 2011). Therefore, it is possible that SIAH-1 and ICP0 act together to regulate their functions.

1.8.5 Cellular proteins targeted for proteasome-mediated degradation by ICP0 in a RING finger-dependent manner

The RING finger domain of ICP0 possesses E3 ubiquitin ligase activity and induces the proteasome-mediated degradation of a range of cellular proteins. A screen for SUMO-conjugated proteins that were destabilised during HSV-1 infection identified over 100 proteins that showed a three-fold or greater decrease in levels of their sumoylated species, some of which have later been identified as potential substrates of ICP0 (E. Sloan unpublished data).

The catalytic subunit of DNA-PK, RNF8 (**section 1.6.5.2**), and USP7 (**section 1.8.4**), are substrates of ICP0 that are degraded in a RING finger and proteasome-dependent manner (Boutell *et al.*, 2005; Canning *et al.*, 2004; Chaurushiya *et al.*, 2012; Lilley *et al.*, 2010; Parkinson *et al.*, 1999). Substrates of ICP0 also include high molecular weight SUMO-1 and SUMO-2/3 conjugated proteins (Boutell *et al.*, 2011; Everett *et al.*, 1998a), and SUMO-modified isoforms of PML and Sp100 (Chelbi-Alix & de The, 1999; Everett *et al.*, 1998a; Muller & Dejean, 1999). The ability of ICP0 to degrade proteins conjugated to SUMO is influenced by its SUMO interaction motif-like sequences (SLS), especially SLS4 (Boutell *et al.*, 2011; Everett *et al.*, 2014). The E2 ubiquitin conjugating enzyme UBE2D1

and its association with ICP0 have also been shown to be important for the degradation of PML and Sp100 (Gu & Roizman, 2003). ICP0 also degrades PML.I, which is not modified by SUMO in a SUMO-independent manner, and this occurs more rapidly than the degradation of the majority of proteins conjugated to SUMO (Boutell *et al.*, 2011; Cuchet-Lourenço *et al.*, 2012). The N-terminal third of ICP0 and the C-terminal region of PML.I are important for the interaction between ICP0 and PML.I (Cuchet-Lourenço *et al.*, 2012).

At early stages of infection, ICP0 associates with centromeres of condensed chromosomes in cells in mitosis and also during interphase, which is dependent on the RING finger domain of ICP0 (Everett *et al.*, 1999a). ICP0 induces the proteasome-dependent degradation of the centromeric proteins A (CENP-A), CENP-B, CENP-C, CENP-H, CENP-I and CENP-N, which are involved in centromere assembly. The degradation of these proteins results in the stalling or arrest of mitosis and defects in chromosomal alignment with condensed chromosomes in a prometaphase alignment (Everett *et al.*, 1999a; Gross *et al.*, 2012; Lomonte & Everett, 1999; Lomonte & Morency, 2007; Lomonte *et al.*, 2001).

The transcription factor E2FBP1 is also a substrate of ICP0. During HSV-1 infection, high expression levels of E2FBP1 caused a decrease in ICP0 transcripts. Therefore, ICP0 may induce the ubiquitination of E2FBP1 to lift the restrictive effect of this protein on viral transcription and promote replication (Fukuyo *et al.*, 2011). Another substrate of ICP0 is IκBα. IκBα binds to the NF-κB transcription factor in the cytoplasm, preventing its translocation into the nucleus until the pathway is activated, and IκBα is ubiquitinated and degraded. ICP0 interacts with IκBα and induces its ubiquitination, causing the activation of NF-κB leading to relocation to the nucleus and the transcription of its target genes. The significance of ICP0 targeting IκBα for degradation is unknown (Diao *et al.*, 2005).

1.9 Aims and objectives of this study

ICP0 is a multifunctional protein that is involved in interactions with a number of diverse cellular pathways, and plays a role in regulating the balance between lytic and latent infections. The N-terminal third of ICP0 contains a RING finger domain, which acts as an E3 ubiquitin ligase targeting cellular proteins for degradation, including PML and Sp100, which are involved in intrinsic immunity.

This study was separated into two distinct parts. Part I investigated the RING finger alpha-helix of ICP0, and part II investigated regions of ICP0 that have high similarity to related proteins of other alphaherpesviruses or contained motifs that were believed to interact with cellular proteins but whose functions had not, in most cases, been investigated in detail.

1.9.1 Investigations of the RING finger alpha-helix of ICP0

This section of the study was stimulated by an observation in Vanni et al. (2012) that a mutation in the alpha-helix region of the RING finger of ICP0 (N151D) had differential effects on complementation of an ICP0 null mutant virus and reactivation of quiescent HSV-1 in experiments using an inducible ICP0 expression system. This raised the possibility that complementation and reactivation involve differential activities of ICP0.

Therefore, one of the aims of this section of the study was to investigate in greater detail the N151D mutation. The nearby mutation K144E was also included in the study, as it is located in the alpha-helix along with N151, and has previously been analysed in limited transfection and virus-based assays and had phenotypes similar to the N151D mutation. These alpha-helix mutants were initially characterised using the inducible ICP0 expression system to further investigate the findings of Vanni et al. (2012). The mutations were then analysed in the context of viral infection to investigate if these mutations differentially affect the stimulation of lytic infection and reactivation from quiescence.

Vanni et al. (2012) additionally showed that the alpha-helix of the RING finger region of ICP0 is involved in interactions with E2 ubiquitin-conjugating enzyme UBE2D1, and that ICP0 has the potential to interact with different E2 enzymes. As the N151 and K144 residues are located in the charged side chains that are exposed on the surface of the alpha-helix, they may play a role in the interactions of ICP0 with cellular components, including E2 ubiquitin-conjugating enzymes. Therefore, these mutants were also analysed for their ability to interact with components of the ubiquitin pathway, particularly focusing on interactions with E2 ubiquitin-conjugating enzymes, to investigate if interactions with E2 ubiquitin-conjugating enzymes affect the stimulation of lytic infection and reactivation from quiescence.

1.9.2 Regions of ICP0 that have high sequence similarity between alphaherpesviruses or contained motifs that were believed to interact with cellular proteins

The second part of this study investigated regions throughout ICP0 that contain sequences with similarity to other alphaherpesviruses (other than the RING finger). Furthermore, sequences or motifs within ICP0 that are related to those present within other viral proteins, and which are thought to interact with cellular proteins and have not previously been studied in detail, were also characterised.

1.9.2.1 High sequence similarity downstream of the RING finger domain

Areas of high sequence similarity between alphaherpesvirus proteins have been shown to have conserved functions. One of the highest regions of similarity within the ICP0 family of proteins is the RING finger domain, which acts as an E3 ligase (Boutell *et al.*, 2002), and deletion of this region causes a defect as severe as deletion of the whole ICP0 gene (Everett, 1989; Everett *et al.*, 2004a; Lium & Silverstein, 1997). When examining other regions of high sequence conservation between alphaherpesvirueses HSV-1, HSV-2 and herpesvirus B of macaque monkeys (HVB), the C-terminal third shows sections of high sequence similarity. This region contains the USP7 binding motif, SLS 5/6/7, the ND10 localisation domain and the nuclear localisation sequence (Everett *et al.*, 2014).

A region that additionally shows high sequence similarity is downstream of the RING finger domain. The effect of deletion of the region immediately downstream of the RING finger domain (Δ162-188) has been investigated, and has been shown to render ICP0 E3 ligase negative (Boutell *et al.*, 2002). Further downstream from this region there is an additional region (residues 193-224) that also shows high sequence similarity, but has not been studied in detailed (**Figure 1.7)**. Although this region (Δ197-222) is not required for E3 ligase activity *in vitro*, its deletion causes ICP0 to be defective in the ability to form intracellular conjugated ubiquitin chains (Everett, 2000). Therefore, this region may affect either the E3 ligase function of ICP0 or its ability to interact with E2 ubiquitin-conjugating enzymes.

This region located downstream of the RING finger and E3 ligase negative region was investigated by constructing viruses containing deletions within the area of sequence similarity from amino acids 188-224. Two separate deletion mutants were constructed

from residues 197-211 and 211-222. These deletions were studied in the context of viral infection to investigate if these sequences play a role in HSV-1 infection and whether they affect the E3 ligase ability of ICP0.

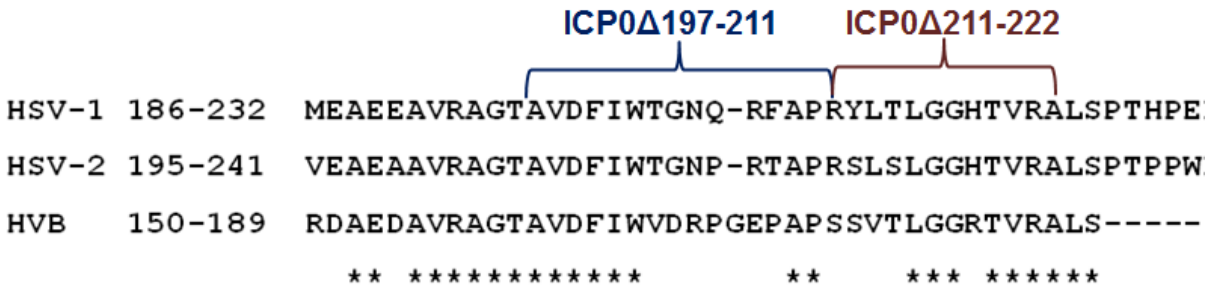

Figure 1.7 The region downstream of the RING finger domain shows high sequence similarity in HSV-1, HSV-2 and herpesvirus B (HVB).
The asterisks denote completely conserved residues from the three alphaherpesviruses. Labelled are the deletion mutants ICP0Δ197-211 and ICP0Δ211-222 that were analysed in this study.

1.9.2.2 Sequences within ICP0 that are reported to interact with cellular proteins, including E3 ubiquitin ligases

Region of ICP0 that has been implicated in binding to CoREST

A region within the C-terminal third of ICP0 contains a sequence of amino acids (537-613 aa) that show some sequence homology to the N-terminal part of the cellular protein CoREST (Gu *et al.*, 2005). Outside of this region, two residues of ICP0 (aa 671 and 673), have been reported to be required for the binding of ICP0 to CoREST (Gu & Roizman, 2009), and that this binding leads to the displacement of HDAC1 from the REST/CoREST/HDAC transcriptional repressor complex (Gu *et al.*, 2005). In cells infected with virus containing mutations in the CoREST-binding region (R8507-D671A/E673A), PML was not fully degraded and viral replication was delayed (Gu & Roizman, 2009). It has been suggested that the REST/CoREST/HDAC complex may repress viral gene expression in the absence of ICP0, and therefore may have a role in the reactivation/derepression of viral gene expression (Gu & Roizman, 2009). The role of these residues on derepression of viral gene expression from quiescent genomes was investigated using the ICP0 inducible cell line system.

1.9.2.3 A residue that has been shown to be required for binding to RNF8

Residue T67 of ICP0 is involved in interacting with and inducing the degradation of cellular E3 ubiquitin ligase RNF8. RNF8 is involved in the DNA damage response, leading to the loss of ubiquitinated forms of histones H2A and H2AX (Chaurushiya *et al.*, 2012; Lilley *et al.*, 2010). The T67 RNF8-binding residue within ICP0 was investigated to analyse whether ICP0 promotes transcription and prevents histone mediated transcriptional repression by inducing the degradation of RNF8. As stimuli such as UV light can induce both the DNA damage response and HSV-1 reactivation, it is possible that these two pathways are linked through the T67 residue. The effect of this residue on the ability of ICP0 to reactivate quiescent HSV-1 to initiate gene expression was also investigated.

1.9.2.4 The PPEYPTAP motif

The sequence PPEYPTAP is present within ICP0 at residues 717-724. The sequence is highly related to PTAP and PPXY motifs present in other viral proteins, including retroviral Gag proteins that have been shown to be involved in interactions with cellular E3 ubiquitin ligases, including HECT and Nedd4. These motifs play a role in retroviral budding (reviewed in Bieniasz, 2006; Freed, 2002). This PPEYPTAP motif was investigated within ICP0, to analyse if it played a role during HSV-1 infection.

1.9.2.5 SIAH-1 binding motif

ICP0 contains the cellular E3 ubiquitin ligase SIAH-1 interaction motif PXAXVXP at residues 401-407, and was shown to interact with SIAH-1 and be targeted for proteasomal degradation (Nagel *et al.*, 2011). The SIAH-1 interaction motif within ICP0 was mutated and studied within the context of the inducible cell line system and virus infection.

2 Materials and Methods

2.1 Bacterial and nucleic acid techniques

2.1.1 Solutions and buffers

STET	8% sucrose (Sigma-Aldrich), 5% Triton-X 100 (Sigma-Aldrich), 50 mM EDTA (VWR International Ltd), 50 mM Tris-HCl (VWR International Ltd) pH 8.0
40x TAE buffer	96.8 g Tris (Roche), 8.2 g sodium acetate (Sigma-Aldrich), 7.4 g EDTA, pH to 7.6 with glacial acetic acid (VWR International Ltd), dH_2O added to 500 ml
1x TE	1 mM EDTA, 10 mM Tris-HCl pH 8.0

2.1.2 Transformation

Transformation of bacteria with plasmid DNA was carried out using 50 µl aliquots of competent *Escherichia coli* DH5α cells (Invitrogen). Transformation after ligation used 5 µl of the precipitated ligation mixture (**section 2.1.7**), and re-transformation of a plasmid was carried out using 100 ng DNA. The DNA was added to the competent cells and mixed gently, after which the cells were incubated on ice for 30 minutes. The cells were heat-shocked for 40 seconds at 42 °C and incubated on ice for 2 minutes to recover, after which 300 µl pre-warmed Luria-Bertani medium (LB broth) (E&O Laboratories Ltd) was added to the cells, which were then placed at 37 °C for 30 minutes with constant agitation. The cells were plated onto agar (E&O laboratories Ltd) plates with the appropriate antibiotic selection, usually ampicillin (Amp) (Melford laboratories Ltd), and incubated at 37 °C overnight for colonies to grow. Amp was added to liquid media and molten agar (once cooled to 50 °C) at a concentration of 100 µg/ml, but this was increased to 150 µg/ml for lentiviral vector plasmids in order to prevent satellite colonies.

2.1.3 Plasmid DNA extractions

2.1.3.1 Small scale (miniprep) plasmid DNA extraction

A single colony selected from freshly transformed bacteria on an agar plate was grown overnight at 37 °C in 5 ml LB broth with horizontal agitation. The following day, 1.3 ml of the culture was transferred to an Eppendorf tube and centrifuged at 13000 rpm for 20 seconds in a bench top centrifuge (MSE Micro Centaur). The bacterial pellet was resuspended in 200 µl STET buffer, and the bacteria were lysed by adding 5 µl 10 mg/ml lysozyme (Sigma-Aldrich) and boiled in a boiling water bath for 50 seconds. To remove the cellular debris, the lysed bacterial cells were centrifuged at 13000 rpm for 30 minutes, and 180 µl of supernatant was transferred to a fresh Eppendorf tube. The supernatant was vortexed with 165 µl isopropanol (VWR International Ltd) and centrifuged at 13000 rpm for 2 minutes to pellet the DNA. The supernatant was discarded, and 200 µl 80% EtOH (Fisher Scientific UK Ltd) was added to wash the pellet and was removed after a short 13000 rpm spin. The pellet containing the DNA was air dried at room temperature and resuspended in 30 µl dH_2O.

2.1.3.2 Large scale (midiprep) plasmid DNA extraction

A single colony was selected from freshly transformed bacteria on an agar plate, which was grown for 8 hours in 10 ml LB broth with the appropriate antibiotic selection at 37 °C with horizontal agitation. The culture was transferred into 350 ml LB broth with antibiotic selection and grown overnight at 37 °C with horizontal agitation. The following day the DNA was extracted using the NucleoBond® Xtra Midi kit (Macherey-Nagel), following the NucleoBond Xtra plasmid purification, high-copy plasmid purification (midi) protocol as described by the manufacturer.

2.1.4 Restriction endonuclease digestions

All restriction endonucleases and associated buffers were sourced from New England Biolabs. Standard restriction digest reactions were carried out in a total volume of 20 µl. The reaction consisted of 2 µl of the appropriate 10x buffer supplied with the enzymes, plasmid DNA (10 µg for fragment preparations, 0.5 µg for analytical digestions) and 10 units (1 µl) of restriction enzymes and dH_2O to make up the final volume to 20 µl. Reactions were incubated at 37 °C for 2 hours. Digestions were analysed by agarose gel electrophoresis and, when necessary, fragments were purified as described in **section 2.1.6**.

2.1.5 Annealing and cloning of complementary oligonucleotides

Oligonucleotides were dissolved in the recommended volume of dH_2O to give concentrations of 100 µM. A reaction mix containing 50 µl of each oligonucleotide, 2 µl 50x TE and 1 µl 5 M NaCl (10 mM Tris-HCl pH 8.0, 50 mM NaCl) was prepared. Reactions were incubated in a PCR thermal cycler (Techne Endurance TC-312) with the following temperature change conditions:

Heated lid	105 °C		
Initial denaturation step	95 °C		2 minutes
Oligonucleotide annealing	72 °C		2 minutes 30 seconds
	65 °C		2 minutes 30 seconds
	60 °C		2 minutes 30 seconds
	Sequential 5 °C decreases,	each	2 minutes 30 seconds
	15 °C		2 minutes 30 seconds
Hold	4 °C		∞

The annealed oligonucleotide mix was diluted 1 in 100, and 5 µl of this diluted annealed mix was used per ligation (**section 2.1.7**).

2.1.6 Gel electrophoresis

1.5% agarose (Sigma-Aldrich) gels prepared in 1x TAE buffer were used for DNA restriction digest analysis and DNA fragment purification on the basis of fragment size. The gels were run in 1x TAE buffer at 100 volts, with samples mixed with 5 µl of 6x loading dye (Thermo Scientific) and run alongside 1 kb and 100 bp marker ladders (Thermo Scientific) of known fragment sizes. The gels were stained with 1 µg/ml ethidium bromide (Sigma-Aldrich) in 1x TAE buffer for 15 minutes with constant agitation, and washed in dH_2O, and the DNA bands were visualised on a UV transilluminator (long wave for fragment isolations, short wave for analytical gels). DNA fragments requiring purification were excised from the agarose gel using a scalpel and purified using the Biomega-Dundee Cell Products Gel Purification kit, according to the manufacturer's instructions. The purified fragments were eluted from the purification columns in 30 µl of the elution buffer provided.

2.1.7 Ligation of DNA fragments

Ligation of DNA fragments extracted and purified from agarose gels or from PCR was carried out using 5 µl of each purified DNA fragment, 2.5 µl 10x T4 DNA ligase buffer (New England Biolabs) and 1 µl T4 DNA ligase (New England Biolabs) in a total reaction volume of 20 µl. Reactions were incubated at room temperature overnight. The ligated DNA was precipitated by the addition of 10 µl 3 M sodium acetate (Merck Millipore), 65 µl of 1x TE, 1-2 µl pellet paint (Merck Millipore) to allow visualisation of the pellet, and 250 µl 100% EtOH. After incubation at -20 °C for 10 minutes, the sample was centrifuged at 13000 rpm (MSE Micro Centaur) for 5 minutes to pellet the DNA. The supernatant was removed and the visible pellet was washed in 80% EtOH and resuspended in 20 µl dH_2O. The DNA was then transformed into DH5α cells using 5 µl of precipitated DNA (**Section 2.1.2**).

2.1.8 DNA sequencing

The overall structure of newly constructed plasmids was confirmed by the appropriate restriction enzyme digestions prior to DNA sequencing. Selected plasmid DNA prepared on a small scale (**Section 2.1.3**) were purified by removing RNA by digestion with 1 µg/µl RNase A for 30 minutes at 37°C, and then purifying the DNA using the Biomega- Dundee Cell Products Gel Purification kit, as outlined above (**Section 2.1.6**). The sequencing reactions containing 500 ng DNA in 30 µl dH_2O and 2 µl primer at 3.2 µM were submitted to the DNA sequencing service at the University of Dundee. Sequencing data was analysed using VectorNTI (Life Technologies) software.

2.2 Specific cloning strategies used in this study

2.2.1 Plasmids

The plasmids used in the study are described in **Table 2.1**, with their main characteristics described. The cloning strategies for the construction of all other plasmids containing mutations generated throughout this study are described in **section 2.2.3**. All plasmids used throughout this study were Amp resistant unless otherwise stated.

Table 2.1 Plasmids provided for use in this study

Plasmid	Characteristics	Source
pUCDT.cICP0	The ICP0 cDNA coding region linked to a truncated HCMV promoter/enhancer under tetracycline inducible control in pUC9	R.D. Everett, unpublished.
pLKO.DCMV.TetO.cICP0 (pLDT.cICP0)	Expresses ICP0 from a tetracycline inducible promoter in a lentiviral vector plasmid	Everett *et al.*, 2009
p110	Expresses ICP0 under the control of the genomic IE1 transcription unit	Perry *et al.*, 1986
p111	Same as p110 but elimination of the EcoRI site in the pUC9 multi-cloning sequence.	Everett, 1987
p110 JA1 (K144E)	Contains the ICP0 K144E mutation	Barlow *et al.*, 1994
p110 JD (N151D)	Contains the ICP0 N151D mutation	
p110 JE (KE/ND)	Contains the ICP0 K144E/N151D double mutation	
T67A	Contains the ICP0 T67A mutation	Chaurushiya *et al.*, 2012
p110-E32-1	12-mer EcoRI linker 5'-CCCGAATTCGGG-3' inserted in codon 222 of ICP0 in plasmid p111	Everett, 1987
p110 R3	12-mer EcoRI linker 5'-CCCGAATTCGGG-3' inserted in codon 212 of ICP0 in plasmid p111	
p110 E13	12-mer EcoRI linker 5'-CCCGAATTCGGG-3' inserted in codon 197 of ICP0 in plasmid p111	
p110 D13/32	In-frame deletion of codons 197-222 of ICP0 in plasmid p111	Everett, 1988

2.2.2 Oligonucleotides

All oligonucleotides used in this study were synthesised by Sigma-Aldrich. The oligonucleotides were dissolved in dH_2O to a final concentration of 100 µM by adding the volume specified by the manufacturer. The sequences of the oligonucleotides and their purpose of use are described in **Table 2.2** below. The positions of the oligonucleotides within the ICP0 cDNA sequence are illustrated in **Figure 2.1**.

Table 2.2 Oligonucleotides used in this study

Name	Sequence 5'-3'	Purpose of use
PTAP1 F	GTAACCACGTGATGGCCGCCGAGTACG CGACGGCCGCCGCGTCGGAGTGGAACA	Mutation of the PPEYPTAP motif of ICP0 to AAEYATAA
PTAP2 F	GCCTCTGGATGACCCCCGTGGGGAACAT GCTGTTCGACCAGGGCACCCTAGTGGGC GCC	
PTAP3 F	CTGGACTTCCGCAGCCTGCGGTCTCGGC ACCCGTGGTCCGGGGAGCAGGGGGCG	
PTAP4 R	GTGCACTACCGGCGGCTCATGCGCTGCC GGCGGCGCAGCCTCACCTTGTCGGAGA CCTACTG	
PTAP2 R	GGGGCACCCCTTGTACGACGGGCTGGTC CCGTGGGATCACCCGCGGGACCTGAAG GCGTCG	
PTAP3 R	GACGCCAGAGCCGTGGGCACCAGGCCC CTCGTCCCCCGCAGCT	
R8507 F	CTGCCCATCCTGGCCATGGCCACGGGGA ACATC	Mutation of the LPILDMETGNI motif of ICP0 to LPILAMATGNI
R8507 R	GATGTTCCCCGTGGCCATGGCCAGGATG GGCAG	
SIAH F	CGTGCAGCAGGTGCCGGATGCGTACGA GCGCCGCCTCCG	Mutation of the SIAH1 binding motif of ICP0 RPRAAVAPCVR to RPRAAGAGCVR
SIAH R	TCCGGCACCTGCTGCACGTGGGCGCGCG GGTCCCGA	
110seq2 R	CTTGTTCACGTAAGGCGACAG	Used as PCR and sequencing primers in SIAH mutagenesis
ICP0-24 F	GCCCCCCTTGCAAACAACAG	
ICP0-4 R	GACACGGATTGGCTGGTGTA	Used as PCR and sequencing primers in PTAP and R8507 mutagenesis
ICP0-15 F	GTCGGGCCAGGAAAACCCCT	
ICP0-17 F	CGTGTGCACGGATGAGATCG	Sequencing of viral DNA
ICP0-18 R	CTGCTGCAAGAGACAACGGG	
X110 F	CTCGAGAGGACGGGGGGA	Sequencing of the RING finger region of ICP0

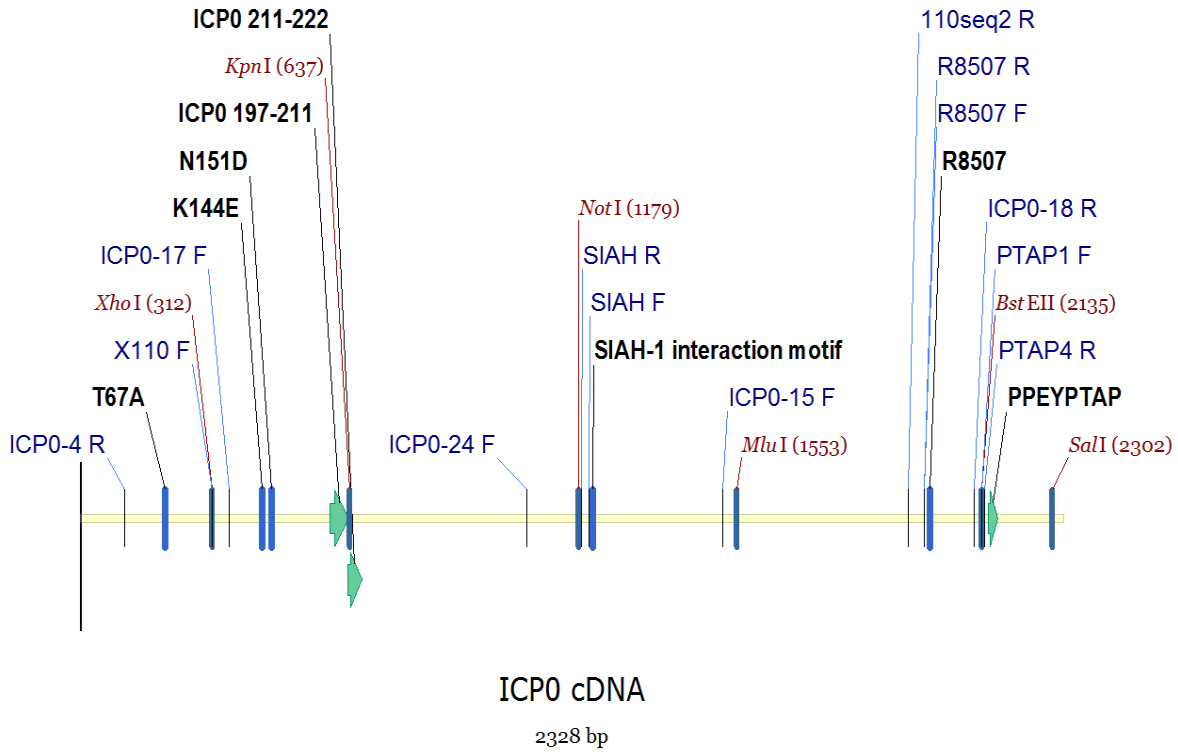

Figure 2.1 The position of the mutations, restriction sites and primer binding locations used in this study relative to the ICP0 cDNA.
The locations of the mutations within ICP0 investigated in this study are illustrated. The primer binding positions and restriction sites used in the cloning strategies and construction of these mutants described within this section are also annotated.

2.2.3 Construction of lentiviral vector plasmids expressing ICP0 mutants

The overall cloning strategy was to transfer fragments containing existing plasmid mutations to, or create novel mutations within, the simple vector plasmid pUCDT.cICP0 prior to transfer of the required complete ICP0 cDNA sequence into the plasmid pLKO.DCMV.TetO.cICP0 (**Figure 2.2)** (Everett *et al.*, 2009). Lentiviral vector plasmid pLKO.DCMV.TetO.cICP0 expresses ICP0 from a tetracycline-inducible promoter and was used for the production of lentiviruses to generate inducible cell lines that expressed wt or mutant ICP0. The production of the mutants used in this study and the strategies used to sub-clone the mutants into the pUCDT.cICP0 and then into the pLKO.DCMV.TetO.cICP0 vector plasmid are detailed below. All intermediates in the pUCDT.cICP0 plasmid backbone and pLKO.DCMV.TetO.cICP0 derivate plasmids were confirmed by DNA sequencing (University of Dundee).

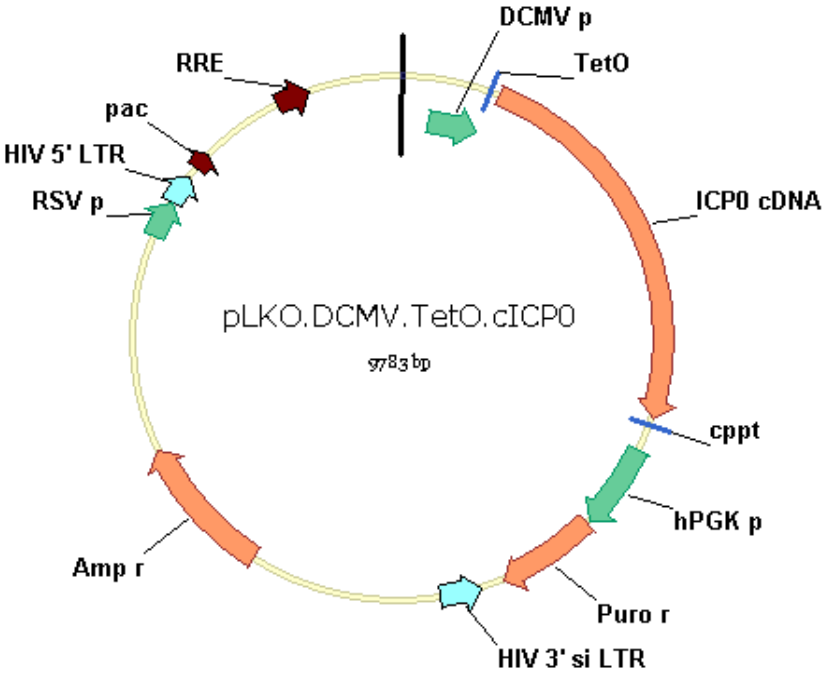

Figure 2.2 Map of the pLKO.DCMV.TetO.cICP0 (pLDT.cICP0) plasmid vector.
The lentivirus vector contains an HCMV promoter/enhancer (DCMVp) with a tetracycline-dependent operator (TetO) located downstream. This system is tetracycline-inducible to induce the expression of ICP0. The vector encodes puromycin resistance (Puro r), which was used for selection of cell lines. This ICP0 inducible cell line system induces ICP0 expression in the majority of induced cells to levels that are comparable to the very early stages of HSV-1 infection. This system is advantageous as long term ICP0 expression is detrimental for long-term cell survival (Everett *et al.*, 2009).

2.2.3.1 ICP0 RING finger mutants N151D and K144E

Plasmids p110-JA1, p110-JD and p110-JE containing the K144E, N151D and K144E/N151D (KE/ND) mutations respectively were digested with *Xho*I and *Kpn*I and the 320 bp fragment isolated. The pUCDT.cICP0 plasmid was digested with *Kpn*I and *BstE*II and the 1.5 kb fragment isolated, and pUCDT.cICP0 was also digested with *Xho*I and *BstE*II and the 4 kb fragment isolated. The 320 bp fragment containing the alpha-helix mutations was ligated together with pUCT.cICP0 1.5 kb *Kpn*I-*BstE*II fragment and 4 kb pUCDT.cICP0 *Xho*I-*BstE*II.

2.2.3.2 PCR-driven overlap extension for site-directed mutagenesis of the PPEYPTAP, R8507 and SIAH-1 interaction motif sequences

Site-directed mutagenesis was carried out using PCR-driven overlap extension and splicing, in order to create the desired mutations R8507 and those within the PPEYPTAP and SIAH-1 interaction motifs. This technique, described in Heckman & Pease, 2007 and summarised in **Figure 2.3**, uses mutagenic primers and flanking primers to amplify selected regions creating overlapping fragments of the sequence containing the mutations. These overlapping fragments act as the template for the amplification of the whole DNA fragment with the desired mutations using the flanking primers. The DNA fragment was inserted into vector plasmids by restriction digestion using sites present in the flanking primers, or that exist within the whole amplified fragment.

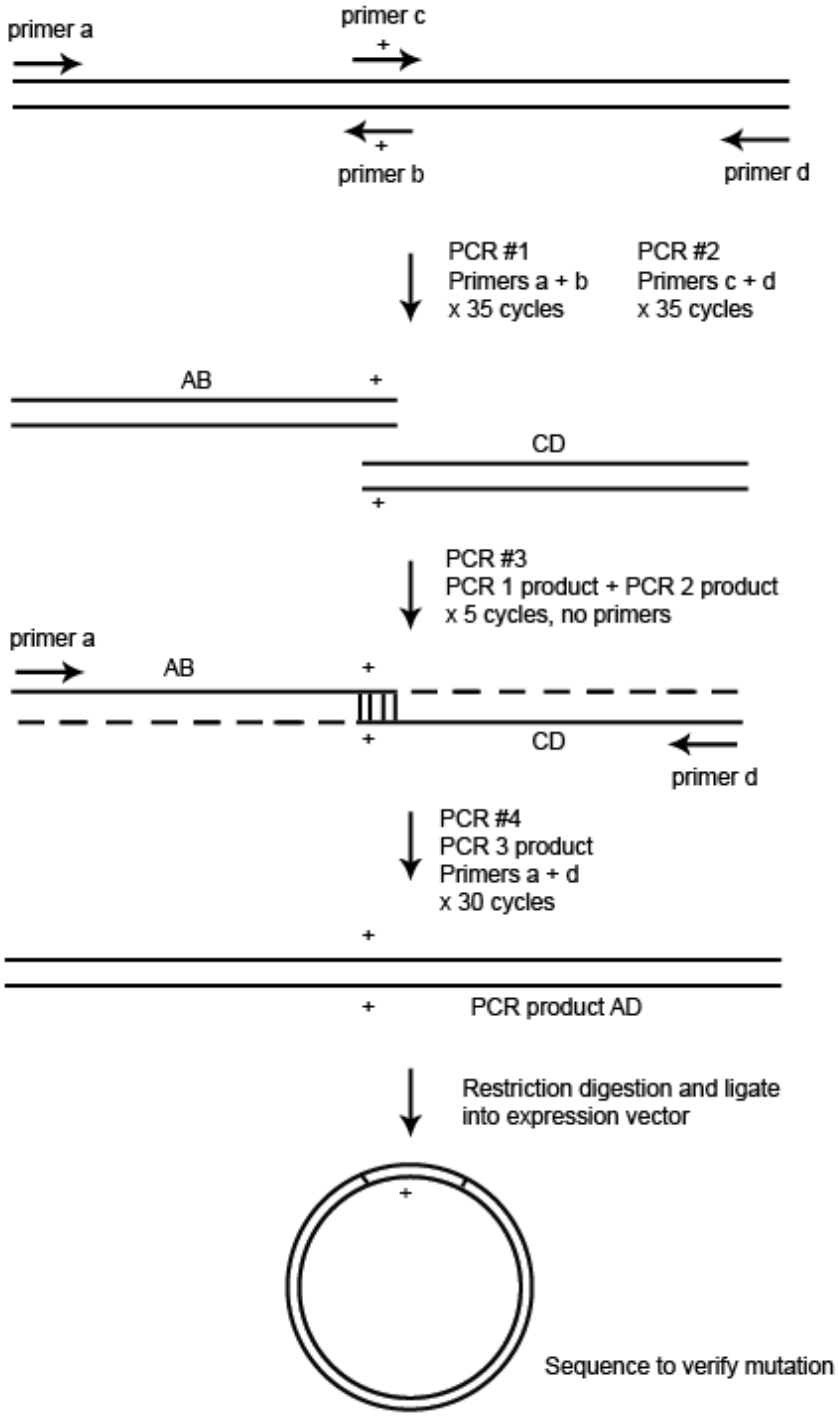

Figure 2.3 PCR splicing strategy for site-directed mutagenesis.
Flanking primers a and d amplify the sequence of interest, and mutagenic primers b and c contain the mutation of interest (denoted by +). During the first rounds of PCR (PCR#1 and #2), the flanking primers (a/d) and mutagenic primers (b/c) amplify selected regions, producing PCR fragments that overlap in the region containing the mutation(s). The PCR products from PCR#1 (AB) and PCR#2 (CD) are annealed in PCR#3 in a reaction that contains no primers. The amplification of the whole DNA fragment containing the mutation is carried out in PCR#4 in a reaction containing the flanking primers. The DNA fragment can be inserted into vector plasmids by restriction digests (Heckman & Pease, 2007).

For site-directed mutagenesis to generate the PPEYPTAP, R8507 and SIAH-1 interaction motif mutations, the initial PCR reaction consisted of 50 ng template DNA, 10x Pfu buffer, 10 mM dNTPs, 10 µM forward primer, 10 µM reverse primer, 1 µl Pfu phusion enzyme and dH_2O to 50 µl. The PCR cycling conditions (Techne Endurance TC-312) are detailed below:

PCR cycling conditions

98 °C	30 seconds	
98 °C	30 seconds	x 35 cycles
60 °C	30 seconds	
72 °C	30 seconds	
72 °C	5 minutes	
4 °C	Hold	

The PCR products from the initial reactions were separated on a 1.5% agarose gel and the DNA products purified (**section 2.1.6)**. The two overlapping PCR fragments were annealed together by a second round of PCR performed using 2 µl of each of the PCR products, 10 x Pfu buffer, 10 mM dNTPs, 1 µl Pfu phusion enzyme and dH_2O to 50 µl. The PCR cycling conditions were the same as above but carried out for 5 cycles and without primers to allow the fragments to anneal. After 5 cycles, 10 µM of each of the outside flanking primers were added to the reaction and the PCR continued for another 30 cycles. The PCR product was run on an agarose gel and the DNA extracted and purified. The extracted PCR product was digested with the relevant restriction enzymes and could then be ligated into the pUCDT.cICP0 plasmid.

Plasmid p111, which expresses wt ICP0, was used a template for site-directed mutagenesis by PCR splicing for construction of the PPEYPTAP and R8507 mutants. The wt PPEYPTAP motif was mutated to AAEYATAA using mutagenic primers PTAP-4 and PTAP-1. Substitution mutations in the R8507 sequence mutated the wt amino acid sequence from LPILDMETGNI to LPILAMATGNI using mutagenic primers R8507-F and R8507-R. The flanking primers for both mutants PPEYPTAP and R8507 were ICP0-4 and ICP0-15, and the resulting PCR fragments were digested with *Mlu*I and *Sal*I and ligated individually with the 4.8 kb *Mlu*I-*Sal*I pUCDT.cICP0 fragment.

Plasmid pUCDT.cICP0 was used as a template for site-directed mutagenesis by PCR splicing using mutagenic primers SIAH1-F and SIAH1-R, and flanking primers 110seq2 and ICP0-24 to change the wt SIAH-1 interaction motif sequence from RPRAAVAPCVR to RPRAAGAGCVR. The PCR products were spliced together by a second round of PCR using flanking primers ICP0-24 and 110seq2. The *Not*I-*Mlu*I PCR fragment was then ligated with the 4.5 kb *Not*I-*Sal*I and 0.7 kb *Mlu*I-*Sal*I fragments of pUCDT.cICP0.

2.2.3.3 Transfer of ICP0 mutations from pUCT.cICP0 intermediate plasmids into the pLKO.DCMV.TetO.cICP0 lentiviral vector plasmids

The pUCDT-based intermediate vectors were restriction digested with *Nde*I/*Sal*I/*Sca*I and the 2.7 kb band containing the promoter, the tetracycline operator sequences and all but the last 7 codons of the ICP0 cDNA sequence was isolated (the other bands were 2.2 kb and 0.7 kb). Plasmid pLKO.DCMV.TetO.cICP0 was restriction digested with *Nde*I and *Sal*I and the 7.1 kb vector band isolated (this includes the last 7 codons of the ICP0 cDNA sequence). The 2.7 kb band from the pUCDT-intermediate and the 7.1 kb vector band from pLKO.DCMV.TetO.cICP0 were ligated together. Once all the mutations were in the pLKO.DCMV.TetO.cICP0 plasmids, restriction digests were carried out to check the overall structures of the plasmids, and the desired mutations were confirmed by DNA sequencing.

2.2.4 Construction of deletion mutants downstream of the RING finger (197-222) in the p110 backbone to enable construction of viral deletion mutants

Plasmids containing deletions of regions downstream of the RING finger domain ICP0Δ197-211 and ICP0Δ211-222 were constructed using plasmids that are derivates of p111 backbone. These plasmids were used for the construction of viruses containing these deletions (**section 2.6**).

2.2.4.1 Deletion mutant ICP0Δ197-211

Plasmid p110-E13 was digested with *EcoR*I and *Sal*I and the 5.4 kb fragment isolated. Plasmid p110-R3 was also digested with *EcoR*I and *Sal*I and the 1.8 kb fragment isolated. These 5.4 kb and 1.8 kb fragments were then ligated together to produce the ICP0Δ197-211 plasmid, which contains a deletion of codons 197-211 of ICP0.

2.2.4.2 Deletion ICP0Δ211-222

The 5.4 kb fragment isolated from the digestion of p110-R3 with *EcoR*I and *Sal*I was ligated together with the 1.8 kb fragment isolated from the *EcoR*I and *Sal*I digestion of p110-E32-1. This produced the ICP0Δ211-222 plasmid, which contains a deletion of codons 211-222 of ICP0.

2.3 Protein methods

2.3.1 Antibodies

Primary and secondary antibodies used throughout this study are listed in **Tables 2.3 and 2.4**, respectively. The tables detail their dilutions used for Western blot (WB) and immunofluorescence (IF), and the suppliers.

Table 2.3 Primary antibodies used in this study

Antibody	Type	Target	Dilution in WB	Dilution in IF	Source
AC-40	Mouse monoclonal	Actin	1/10000	N/A	Sigma-Aldrich
Z378A	Mouse monoclonal	β-galactosidase	N/A	1/500	Promega
M2	Mouse monoclonal	FLAG tag	N/A	1/1000	Stratagene
27-4577-01	Goat polyclonal	GST	1/2000	N/A	Amersham Pharmacia Biotech
07-471	Rabbit polyclonal	hDaxx	N/A	1/200	Upstate
11060	Mouse monoclonal	ICP0	1/2000	1/1000	Everett *et al.*, 1993b
R190	Rabbit polyclonal	ICP0	N/A	1/200	Everett *et al.*, 1998b
58S	Mouse monoclonal	ICP4	1/1000	1/500	Showalter *et al.*, 1981
ABD-030	Rabbit polyclonal	PML	N/A	1/2000	Jena Bioscience
5E10	Mouse monoclonal	PML	1/100	1/20	Stuurman *et al.*, 1992
SpGH	Rabbit serum	Sp100	1/2000	1/2000	Sternsdorf *et al.*, 1995
T4026	Mouse monoclonal	Tubulin	1/5000	N/A	Sigma-Aldrich
P4D1	Mouse monoclonal	Ubiquitin	1/1000	N/A	Santa Cruz
FK2	Mouse monoclonal	Mono- and poly-conjugated ubiquitin	N/A	1/2000	International Bioscience Inc
ZIF11	Mouse monoclonal	UL42	1/1000	N/A	Schenck *et al.*, 1988
DM165	Mouse monoclonal	VP5	1/1000	N/A	McClelland *et al.*, 2002
A303-257A	Rabbit polyclonal	ZBTB10	1/2000	N/A	Bethyl Laboratories

Table 2.4 Secondary antibodies used in this study

	Antibody	Raised in	Dilution	Source
Anti-mouse	Anti-mouse IgG horseradish peroxidase conjugate	Sheep	1/1000	Sigma-Aldrich A4416
	Anti-mouse IgG-FITC	Sheep	1/100	Sigma-Aldrich F3008
	Alexa Fluor 555	Donkey	1/5000	Invitrogen Molecular Probes A31570
Anti-rabbit	Anti-rabbit IgG horseradish peroxidase conjugate	Sheep	1/20000	Sigma-Aldrich A4914
	Alexa Fluor 555	Donkey	1/5000	Invitrogen Molecular Probes A31570
	Alexa Fluor 633	Goat	1/1000	Invitrogen Molecular Probes A21071
Anti-goat	Anti-goat IgG horseradish peroxidase conjugate	Rabbit	1/80000	Sigma-Aldrich A5420

2.3.2 Western blot solutions and buffers

Resolving gel buffer (RGB) — 1.5 M Tris-HCl (Roche), 0.4% sodium dodecyl sulphate (SDS) (VWR International Ltd) pH 8.8

Stacking gel buffer (SGB) — 0.5 M Tris-HCl, 0.4% SDS pH 6.8

3x sample boiling mix — 1 ml SGB, 1 ml 20% SDS, 1 ml glycerol (VWR International Ltd), 0.5 ml β-mercaptoethanol (VWR International Ltd), bromophenol blue (Sigma-Aldrich)

Resolving gel (7.5% gels) — 5 ml dH_2O, 2.5 ml RGB, 2.5 ml 30% acrylamide/bis-acrylamide (30:1) (National Diagnostics), 80 µl 10% ammonium persulphate (APS, Biorad), 8 µl TEMED (Sigma-Aldrich)

Stacking gel	1.4 ml dH_2O, 0.6 ml SGB, 0.4 ml 30% acrylamide/bis-acrylamide (30:1), 20 µl 10% APS, 3 µl TEMED
Running buffer	0.05 M Tris-base, 0.05 M glycine (VWR International Ltd), 0.1% SDS
Towbin buffer	25 mM Tris-base, 192 mM glycine, 20% methanol (VWR International Ltd)
PBST	1x PBS (Sigma-Aldrich, made from 10% stock solution), 0.05% Tween-20 (VWR International Ltd)
Blocking buffer	5% dried milk powder (Marvel) in PBST
Stripping buffer	2% SDS, 62.5 mM Tris-HCl, 100 mM β-mercaptoethanol pH 6.7

2.3.3 Western blotting for the detection of protein expression

Cells were seeded at 1 x 10^5 in 24 well plates (**section 2.5.3**) and infected or induced as required. The cells were incubated at 37 °C for the required length of time and harvested in 70 µl of 1x boiling mix, boiled for 2 minutes, and placed immediately on ice. The samples were stored at -20 °C until ready for analysis by Western blot. Samples were resolved on 7.5% polyacrylamide gels consisting of a lower resolving gel and upper stacking gel. Polymerisation of the gels was initiated by the addition of TEMED and APS immediately prior to pouring. The samples were boiled for 2 minutes prior to loading 25-30 µl per well, and were analysed alongside 10 µl of Spectra^{TM} Multicolor broad range protein ladder (Thermo Scientific) in running buffer and run at 100 volts until the dye front reached the bottom of the gel.

2.3.4 Transfer of proteins to a nitrocellulose membrane

Resolved proteins were transferred to a Hybond-ECL nitrocellulose membrane (Amersham Biosciences) in a cassette submerged in Towbin buffer and consisting of a fibre pad, a 3

mm filter paper, the polyacrylamide gel, a nitrocellulose membrane, a second layer of filter paper and another fibre pad. The cassette was orientated to allow the transfer of proteins from the gel to the membrane. An ice pack was added to the gel tank, which was filled with Towbin buffer, and the transfer occurred at 250 mA for 2.5 hours at room temperature. Membranes were incubated in blocking buffer for 10 minutes with constant agitation, and stored in the blocking buffer at 4 °C overnight.

2.3.5 Immunodetection of proteins

Primary antibodies (**Table 2.3**) were diluted in blocking buffer and incubated with the membrane for 2 hours at room temperature with constant agitation. After incubation with the primary antibody, the membrane was washed six times in PBST with each wash lasting 5 minutes. Secondary antibodies (**Table 2.4**) were diluted in 1% dried milk powder/PBST and the membrane incubated for 2 hours at room temperature with constant agitation. Following this the membrane was washed six times as described before. The secondary antibody was conjugated to horse radish peroxidase, which could be detected using Western Lightning ECL reagent (Perkin Elmer Inc), or in the case of the 5E10 antibody, Amersham™ ECL Prime Western Blotting Detection Reagent (GE Healthcare) was used due to increased sensitivity. The membrane was incubated for 3 minutes in equal volumes of ECL reagent one and reagent two and then exposed to UV X-Omat film (Kodak) for variable lengths of time as determined by protein band intensity. The film sheets were developed using a Konica Minolta SRX-101-A film processor.

2.3.6 Stripping of nitrocellulose membranes

To allow sequential re-probing to detect proteins with different antibodies, the nitrocellulose membranes were incubated in stripping buffer (with the β-mercaptoethanol added just before use) for 45 minutes at 50 °C with occasional agitation. The membranes were washed three times for 5 minutes in PBST, and incubated for 1 hour in blocking buffer at room temperature with constant agitation. The membranes were then ready for re-probing with antibody dilutions as described above.

2.4 Production of GST-tagged proteins from bacteria

2.4.1 Solutions and buffers for purification of GST-tagged proteins from bacteria

Buffer A	50 mM Tris-HCl (pH 7.5), 250 mM NaCl, 5% glycerol, 0.1% NP40, 1 mM DTT, 2.5 mM $MgCl_2$ (VWR International Ltd), protease inhibitor (Roche, 1 pellet for every 200 ml of buffer)
Buffer B	50 mM Tris-HCl (pH 8.0), 150 mM NaCl, 2.5 mM $MgCl_2$, 1 mM DTT, 2.5% glycerol.

2.4.2 Transformation of plasmid DNA for protein purification

The transformation of pGEX GST fusion protein expression plasmids into BL21(DE3) pLysS bacterial cells (Merck) was performed using a similar method to transformation into DH5α cells described in **section 2.1.2**, using 50 µl of the BL21 cells and 100 ng of plasmid DNA. The only difference was that 250 µl S.O.C medium (Invitrogen) was added to the cells instead of LB broth.

2.4.3 Growth of bacterial cultures for protein purification

Individual colonies were picked from the agar plates and added to 10 ml LB broth containing the appropriate antibiotic selection and incubated at 37 °C with horizontal agitation overnight. The following day, 4 ml overnight starter culture was added to 200 ml of pre-warmed LB broth (with antibiotic selection) and incubated for 3 hours at 37 °C with horizontal agitation until the culture was in mid-log phase. Protein expression was induced by addition of IPTG (Sigma-Aldrich) (final concentration 0.1 mM) to the culture, which was then incubated at 37 °C with horizontal agitation for 4 hours. The culture was harvested and centrifuged at 4000 rpm (Sorvall Evolution RC, FIBERLite F10S rotor) for 20 minutes at room temperature. The bacterial pellets were frozen on dry ice and stored at -20 °C.

2.4.4 Purification of GST-tagged proteins from bacterial extracts

Bacterial pellets were resuspended in 30 ml buffer A and probe sonicated to lyse the cells. The cellular debris was removed by centrifugation at 13000 rpm (Sorvall Evolution RC, FIBERLite F10S rotor) for 15 minutes. Approximately 50-100 µl of glutathione agarose beads (Sigma-Aldrich) were hydrated in 5 ml PBS, tumbling end-over-end at room temperature for 1 hour. The beads were spin washed in 10 ml PBS and then washed three further times in 1 ml PBS. The glutathione agarose beads were finally resuspended in 400 µl PBS (giving an approximate 50% v/v mixture). The bacterial supernatant was incubated with the beads for 90 minutes to allow protein binding, tumbling end-over-end at room temperature. The beads were centrifuged at 1000 rpm (MSE Micro Centaur) for 5 minutes to remove any unbound proteins and then spin washed in 10 ml buffer A. The beads were washed a further three times in 1 ml buffer A and then in 100 µl buffer A to remove any non-specifically bound proteins. The GST-tagged fusion proteins were eluted from the beads by incubation three sequential times with 350 µl 50 mM reduced glutathione in buffer A. 20 µl of each elution fraction and the remaining beads were analysed by SDS-PAGE (using a 10% polyacrylamide gel) and stained with Coomassie brilliant blue (National Diagnostics) to visualise the proteins.

The following day, the eluted fractions were combined and dialysed using Millipore mini-dialysis tubes in buffer B for 2-3 hours at room temperature. The dialysed samples were run on a 10% SDS-PAGE gel alongside BSA standards, and the gel stained with Coomassie brilliant blue to quantify the relative protein concentrations.

2.5 Cell culture methods

2.5.1 Cells

The cell lines used throughout this study and their growth media are detailed in **Table 2.5**. The purpose of use of the cell lines are described throughout this section. All reagents and media used in cell culture were sourced from Invitrogen unless otherwise stated.

Table 2.5 Cell lines and their growth media

Cells	Characteristics	Growth medium	Reference
HEK-293T	Human embryonic kidney cells	Dulbecco's modified Eagle's medium (DMEM) with 10% fetal calf (bovine) serum (FBS) and 0.1% penicillin/streptomycin	Provided by Anne Orr, CVR
U2OS	Human osteosarcoma cells		Provided by Anne Orr, CVR
HF	Human fibroblasts		A gift from Thomas Stamminger (Erlangen)
HepaRG	Human hepatocellular carcinoma cells	William's medium E with 10% FBS Gold (PAA laboratories), 2 mM glutamine, 0.5 µM hydrocortisone (Sigma-Aldrich) and 5 µg/ml insulin, 0.1% penicillin/streptomycin	Gripon *et al.*, 2002
HA-TetR	HepaRG cells transduced with lentivirus derived from pLKOneo.CMV.EGFPnlsTetR		Everett *et al.*, 2009
HA-IE1/pp71	Express HCMV IE1 and pp71 proteins after doxycycline induction		Everett *et al.*, 2013
BHK-21	Baby hamster kidney fibroblasts (clone 21)	Glasgow modified Eagle's medium with 100 units/ml penicillin, 100 µg/ml streptomycin, 10% new-born calf serum (NBCS) and 10% tryptose phosphate broth (E&O Laboratories Ltd)	Stoker & Macpherson, 1964

2.5.2 Growth and passaging of cells

Cells were grown in their respective growth media (**Table 2.5**) in 75 cm^2 flasks (Nunc Fisher Scientific UK Ltd) at 37 °C in the presence of 5% CO_2. The cells were passaged once the cell monolayers were 80-90% confluent. To passage the cells, the monolayers were washed in 5 ml versene in PBS (E&O Laboratories Ltd) and then incubated with 1 ml 1% trypsin (Sigma-Aldrich) in versene solution for 2-5 minutes. Disassociated cells were resuspended in the appropriate media and a dilution of this was used to seed a new flask, with the dilution ranging from 1/3 to 1/10, depending on the cell type.

2.5.3 Cell seeding

Resuspended cells were counted using a Neubauer haemocytometer to calculate the number of cells per ml. The cells were seeded at the appropriate density in plates or multi-

well dishes as appropriate (**Table 2.6**), with the tissue culture plastics all sourced from Nunc Fisher Scientific UK Ltd.

Table 2.6 Cell seeding densities

	Seeding density
24 well plate	1×10^5
12 well plate	2×10^5
35 mm dish	4×10^5
60 mm dish	1×10^6

2.5.4 Freezing and thawing of cell stocks for long term storage

Confluent cells were washed with versene and then 1% trypsin/versene solution, leaving a small volume of the latter on the cells. After the cells had dissociated, the cells were resuspended in 10 ml of culture media. The cell suspension was transferred to a 15 ml Falcon tube and centrifuged at 2000 rpm for 5 minutes in a bench top centrifuge (Thermo Scientific Heraeus Megafuge 16R). The cell pellets were resuspended in 4 ml freezing mix, which consisted of the appropriate growth media, with an additional 20% FBS and 10% DMSO (cryoprotective agent, Sigma-Aldrich). The resuspended cell pellets were aliquoted into 1 ml amounts, distributed into 1.5 ml cryo-vials, then frozen slowly to -70 °C, and kept there for short term storage or transferred to liquid nitrogen for long term storage.

To revive cells from frozen, the cryovials were placed on dry ice and thawed quickly at 37 °C and pipetted into a flask with the appropriate pre-warmed medium. Once the cells had attached to the tissue culture flask, the medium was replaced to remove residual DMSO.

2.5.5 Lentiviral transduction of cell lines

The plasmids used and their purposes in the generation of lentiviruses and in the transduction of cell lines for the production of the ICP0 inducible cell lines are described in **Table 2.7**.

Table 2.7 Plasmids used for generation of cell lines

Plasmid	Purpose	Source
pVSV-G	Expression of VSV envelope protein for lentivirus production.	BD Biosciences
pCMV.DR.8.91	Lentivirus helper vector, providing capsid (gag) reverse transcriptase polymerase (pol), Rev, and Tat helper functions	A gift from D. Trono (http://tronolab.epfl.ch)
pLKO.DCMV.TetO.cICP0 based plasmids	Lentiviral vector plasmids that express ICP0 and relevant mutants under doxycycline inducible control	Everett *et al.*, 2009, this study

HEK-293T cells were plated at 1.5 x 10^6 per 60 mm plate in complete DMEM medium. A mixture of 8 µl PLUS reagent (Invitrogen) and 250 µl of serum-free DMEM was added to Falcon tubes containing 3 µg pLKO.DCMV.TetO.cICP0 lentivirus plasmid, 3 µg pVSV-G (expressing the vesicular stomatitis virus envelope protein G) and 3 µg pCMV-DR.8.91 (expressing all necessary lentivirus helper functions), and incubated for 15 minutes at room temperature. A second mixture of 12 µl lipofectamine (Invitrogen) and 250 µl serum free DMEM was dispensed into the DNA-PLUS mixtures and incubated for 15 minutes at room temperature. Finally, 900 µl of serum free DMEM was added to the DNA mixture, which was added to the serum-free DMEM washed cells. After 3 hours, 4 ml of conditioned medium (in which the cells had previously been growing) was added to the cells, which were then incubated overnight at 37 °C. The following day, the transfection mix was removed and 4 ml DMEM added. The next day, the supernatant was collected and 4 ml DMEM and 30% FBS were added to the cells. The supernatant collection was repeated the following day and added to the 48 hour supernatant, which was then centrifuged at 1500 rpm for 5 minutes and filtered through a 0.45 micron filter. HA-TetR cells plated at 6 x 10^5 in 60 mm dishes the previous day were infected with 1 ml of the filtered lentiviral supernatant and 5 µg/ml polybrene (to aid virus adsorption), and adsorbed for 1 hour. The supernatant was removed, and the cells were infected with another 1 ml aliquot of the lentiviral supernatant. For the third repeat, 4 ml lentivirus supernatant and 1 µl polybrene were added, and the cells were incubated overnight. Puromycin (Sigma-Aldrich) selection (1 µg/ml initially, reduced to 0.5 µg/ml for the following days and general cell maintenance) was applied to the cells until the cells on the mock infected plate, which contained no antibiotic resistant lentivirus, had died. After this, the cells were expanded into larger scale cultures for use in the experiments.

2.6 Virus construction

2.6.1 Virus construction buffers and solutions

Eagles A

0.1495 g $CaCl_2.2H_2O$ (Sigma-Aldrich), 0.1495 g $MgSO_4.7H_2O$ (Sigma-Aldrich), dH_20 to 500 ml. Aliquot 100 ml into 200 ml bottles. Autoclave at 15 psi for 15 minutes. Store at 4 °C.

Amino acid solution (produced in house, CVR)

0.84 g L-Arginine mono-HCl, 0.48 g L-cysteine, 0.384 g L-histidine mono-HCl, 1.048 g L-isoleucine, 1.048 g leucine, 1.462 g L-lysine mono-HCl, 0.66 g L-phenylalanine, 0.952 g L-threonine, 0.16 g L-tryptophan, 0.724 g L-tyrosine, 0.936 g L-valine, 0.3 g L-methionine, 0.07 g inositol, 55 g $NaHCO_3$, 30 ml phenol red 1%, dH_20 to 1000 ml.

Salt solution (produced in house, CVR)

102.4 g NaCl, 6.4 g KCl, 2.4 g $NaH_2PO_4.2H_2O$, 72 g glucose, 16 ml ferric nitrate 0.01%, 4.68 g L-glutamine, 16 ml (1.6×10^6 units) penicillin, 1.6 g steptomycin sulphate, 16 ml 0.02% antimycotic, dH_20 to 1000 ml.

Vitamins solution (produced in house, CVR)

0.05 g choline chloride, 0.05 g folic acid, 0.05 g nicotinamide, 0.05 g DL-pantothenic acid, CA salt, 0.05 g pyridoxal-HCl, 0.05 g thiamine-HCl, 0.005 g riboflavine, dH_20 to 100 ml.

Eagle's B (produced in house, CVR)

250 ml salt solution, 200 ml amino acid solution, 16 ml vitamin solution, dH_20 to 500 ml. Aliquot 20 ml into universal bottles.

Noble agar	6.4 g Difco Noble agar, dH_2O to 200 ml. Aliquot 30 ml into 100 ml bottles. Autoclave at 15 psi for 15 minutes. Store at 4 °C.

2.6.2 Fragments for homologous recombination

The desired ICP0 mutations or deletions were sub-cloned into the p111 plasmid backbone, and 20 µg DNA was digested with *Sac*I and *Pvu*II at 37 °C for 2 hours. This digestion produces a 4.8 kb fragment that included the complete ICP0 genomic region with the 3' flanking sequence and the IE1 promoter, thus enabling insertion into viral DNA by homologous recombination. The restriction mix was then heat inactivated at 80 °C for 20 minutes and ethanol precipitated by increasing the volume of the restriction mix with 1x TE to 100 µl, and adding 5 µl NaCl and 250 µl EtOH. The sample was incubated at -20 °C for 10 minutes, and the pellet was spin-washed with 80% EtOH before being resuspended in 40 µl 1x TE. A 1-2 µl aliquot of the fragment sample was run on an agarose gel to check that the fragment was the correct size and concentration.

2.6.3 Transfection

BHK cells (or HA-IE1/pp71 cells in the case of the deletion mutants downstream of the RING finger domain ICP0Δ197-222) were seeded at 4 x 10^5 cells per 35 mm dish. The next day, 2 µl *dl*1403 purified viral DNA (2 kb deletion within both copies of ICP0 gene) (provided by Anne Orr, CVR) and 2 µg precipitated restriction digest mix containing *Sac*I-*Pvu*II fragment from p111 plasmid backbone (see above) were added to a 15 ml Falcon tube. The DNA was mixed with 4 µl PLUS reagent (used in conjugation with lipofectamine to improve transfection efficiencies) and 100 µl serum-free media per transfection and incubated at room temperature for 15 minutes. Then, 4 µl lipofectamine and 100 µl serum-free media were added to the DNA/PLUS mix and incubated for a further 15 minutes at room temperature. The cells were washed in serum-free media, and the conditioned media in which the cells had been grown in was retained. An additional 500 µl serum-free media was added to each reaction mix, and this mixture was added to the freshly washed cells. The cells and transfection mixture were incubated at 37 °C for 3 hours with gentle agitation every 10 minutes, and at 3 hours post transfection they were overlaid with 1.5 ml conditioned medium, and the incubation was continued at 37 °C until cytopathic effect (c.p.e) was apparent (after 3-4 days).

2.6.4 Plaque purification

When extensive c.p.e was apparent after transfection, the cells and supernatant were harvested and sonicated. After clarification by centrifugation, the virus stocks were passaged twice on HFs plated at 1 x 10^6 cells per 60 mm dishes, using a range of virus inputs. Because most ICP0 mutations do not cause a defect as pronounced as the large deletion of the gene in *dl*1403, this step enriches for the desired recombinants. The passaged stocks were then plaque purified on 4 x 10^5 BHK cells in 35 mm dishes at dilutions ranging from neat to 10^{-5} and adsorbed for an hour at 37 °C with occasional agitation. The overlay solution was composed of Eagle's A, Eagle's B, NBCS and Noble agar. The Eagle's B solution was warmed at 37 °C until the precipitate had dissolved, and 20 ml was added to 90 ml Eagle's A and 5 ml NBCS. 12 ml of the Eagle's A/B/NBCS mixture was aliquoted into a 25 ml glass bottle and warmed to 50 °C. The Noble agar was melted in the microwave and kept in a water bath at 50 °C to prevent it solidifying. All the virus dilutions were removed from the cells so that no liquid remained, 3 ml Noble agar was added to the Eagle's A/B/NBCS mixture, and the cells were overlaid with 2 ml of this mixture. The plates were left to cool at room temperature until the agar had solidified and then incubated at 37 °C for 2-3 days until plaques had developed.

Plaques were identified using dark field illumination on a light microscope, and their positions were marked on the plastic. Pipette tips were used to pierce the agar and take up a single plaque and the cells associated with it, and these were transferred to an Eppendorf tube containing 100 µl BHK medium. BHK cells were plated the previous day in 24 well plates at 1 x 10^5 cells per well, and 50 µl of the plaque-purified sample was adsorbed onto the cells for an hour with occasional agitation at 37 °C. After adsorption, the cells were overlaid with 500 µl BHK medium. After 2-3 days, when c.p.e was apparent, the supernatant was harvested and stored at -70 °C, while the cells were washed in PBS and harvested in 70 µl of 1x boiling mix and analysed for the presence of ICP0 by Western blotting (**Section 2.3.3**). A positive sample identified from the Western blot was used to undergo at least another two rounds of plaque purification, and the presence of ICP0 was confirmed by Western blotting and immunofluorescence (**section 2.8**). When all required plaque samples positive for ICP0 expression by Western blot had been identified, one positive sample was used to produce small scale virus stocks, which were grown on BHK cells in 60 mm plates (**section 2.7.2**) from the plaque purified supernatant.

2.6.5 Sequencing of viral DNA

To confirm that the isolated viruses contained the desired mutations, the viral DNA was sequenced directly. BHK cells were seeded at 1 x 10^5 cells per well in 24 well plates and infected the following day at an MOI of 1 with the mutant viruses. The infected cells were harvested into the medium after c.p.e was apparent, and the DNA was extracted using the DNeasy tissue kit (Qiagen). PCR was performed on the samples with 50 ng of DNA per reaction, and the products were separated on a 1.5% agarose gel and the band extracted. When necessary, if the yield of the PCR product was insufficient, the PCR was repeated with the same primers, using the initial PCR product as the template. The gel extraction was repeated and the PCR product was submitted for DNA sequencing (University of Dundee) to confirm that the desired mutations were present.

2.7 Virology methods

2.7.1 Viruses

Viruses that had been isolated previously and that were used throughout this study are listed in **Table 2.8**. Virus mutants that were constructed during the course of this study are described in **section 2.2**. All HSV-1 strains were propagated in BHK cells (**section 2.7.2**) and titrated on U2OS cells (**section 2.7.3**).

Table 2.8 Viruses provided for use in this study.

Viruses	Characteristics
wt HSV-1 strain 17 syn+ (17+)	wt HSV-1 syn 17+ strain (Brown *et al.*, 1973)
HSV-1 ICP0 deletion mutant FXE	Expresses ICP0 with a deletion of amino acid residues 106-149 within the RING finger domain (Everett, 1989)
HSV-1 ICP0 substitution mutant K144E	Derivatives of wt 17+ HSV-1 containing point mutations within ICP0 at the position indicated, replacing the residue identified by the initial letter (single letter amino acid code) with that at the end (Everett *et al.*, 1995).
HSV-1 ICP0 substitution mutant W146A	
HSV-1 ICP0 substitution mutant Q148E	
HSV-1 ICP0 substitution mutant N151D	
*in*1374	Defective HSV-1 that cannot enter lytic replication under restrictive conditions as it contains a deletion of the ICP0 gene, a mutation within VP16 so is unable to stimulate IE gene expression and a temperature sensitive mutation within ICP4 which disrupts its function. It also contains a β-galactosidase reporter gene under the control of the HCMV IE promoter/enhancer (Preston & Nicholl, 2005)
*dl*1403	Contains a 2 kb deletion within both copies of the ICP0 gene of HSV-1 strain 17 syn+ (Stow & Stow, 1986)
*in*1863	Contains a HCMV promoter and *lacZ* expression cassette inserted into the thymidine kinase gene of wt HSV-1 (provided by C. Preston)
*dl*1403/CMV*lac*Z	Contains a HCMV promoter and *lacZ* expression cassette inserted into the thymidine kinase gene of *dl*1403 (provided by C. Preston)

2.7.2 Propagation of viral stocks

Viral stocks were propagated in BHK cells seeded at 1 x 10^6 in 60 mm dishes. Cells were infected in 1 ml volume at a range of MOIs (0.01 to 0.001), depending on the expected viral replication defect, and the virus was adsorbed for 1 hour at 37 °C with agitation every 10 minutes. The cells were overlaid with 2 ml of fresh medium and incubated at 37 °C for 2-3 days until extensive c.p.e was apparent. The supernatant containing cell-released virus was harvested and centrifuged at 3000 rpm (Thermo Scientific Heraeus Megafuge 16R) for 5 minutes to remove any cellular debris. Aliquots of the virus were stored short-term at 4 °C until the viral titre was determined. The aliquots were stored at -70 °C in the long term.

2.7.3 Titration of viral stocks

Titration of viral stocks was carried out in U2OS cells, as ICP0 is not required for efficient HSV-1 replication in this cell type (Yao & Schaffer, 1995). Cells were seeded at 2 x 10^5 cells per well in 12 well plates and infected with 10^{-2} to 10^{-5} virus dilutions in a total volume of 100 µl for 1 hour at 37 °C, with agitation every 10 minutes. The cells were overlaid with complete DMEM media containing 1% human serum (MP Biomedicals) to neutralise any cell-released virus and allow the virus to spread from cell to cell to create plaques. The plates were incubated at 37 °C for 48 hours or until plaques had developed. The medium was removed and the cell monolayer was stained with Giemsa stain (VWR International Ltd) for 5 minutes and then washed with dH_2O. The plaques were counted under a light microscope.

The viral titres were calculated using the formula below:
Viral titre or plaque forming units (PFU) per ml
= number of plaques x dilution factor x 10 (used 100µl inoculum and titre given per ml)

2.7.4 Viral infections

Cells were seeded at the appropriate density (**section 2.5.3, Table 2.6**) and the medium was removed to leave enough to cover the cells. The amount of virus added to the cells was calculated on the basis of the MOI. The virus was added to the cells and absorbed for 1 hour, with gentle agitation every 5-10 minutes. After 1 hour, the cells were overlaid with the appropriate media.

2.7.5 Plaque assays – 'blue plaque assays' and standard viral plaque assays

So-called 'blue plaque assays' were used when the virus in question contained the β-galactosidase reporter gene. Cells were seeded at 1 x 10^5 cells per well of a 24-well plate and then, when appropriate, treated with 0.1 µg/ml doxycycline to induce ICP0 expression the following day. The day following doxycycline induction, the cells were infected with sequential ten-fold dilutions of *in*1863 (wt) or ICP0-null mutant *dl*1403/CMVlacZ, which both contain an inserted *LacZ* gene coding for β-galactosidase (controlled by the HCMV promoter/enhancer and inserted into the *tk* locus). After virus adsorption, the cells were overlaid with complete WME containing 1% human serum (and 0.1 µg/ml doxycycline if

the cells had been induced). The plates were stained for β-galactosidase 24 hours later by washing with PBS and incubating the cells in PBS/1% glutaraldehyde for 40 minutes. The cells were washed with PBS and incubated at 37 °C with pre-warmed reagent solution (see below) for 30-120 minutes.

Reagent solution	In PBS: 5 mM potassium ferricyanide (Sigma-Aldrich), 5 mM potassium ferrocyanide (Sigma-Aldrich), 2 mM $MgCl_2$ (VWR International Ltd), 0.01% NP 40, X-gal (Melford Laboratories Ltd) in DMSO (40 mg/ml) added to a final concentration of 2.4 mM

When the virus in question did not contain the β-galactosidase reporter gene, cells were seeded into 12-well plates at 2 x 10^5 cells per well and infected with sequential ten-fold dilutions of wt/mutant viruses the following day. After virus adsorption for 1 hour at 37 °C with agitation every 5-10 minutes, the cells were overlaid with medium containing 1% human serum. After 48 hours, the plates were stained using Giemsa stain and the plaques counted.

2.7.6 Viral yield assays

Human fibroblasts (HFs) and HepaRG cells seeded at 2 x 10^5 cells per well in 12 well plates were infected at a range of MOIs (0.1, 0.01 and 0.001). Cells and supernatant were harvested at 24 hours post infection, sonicated (to release cell-associated virus) and titrated as sequential ten-fold dilutions on U2OS cells (seeded at 2 x 10^5 cells per well in 12 well plates the previous day). The plates were stained 48 hours later using Giemsa stain, and the plaques produced were counted.

2.7.7 Viral quiescence assays

HepaRG cells were seeded at 1 x 10^5 cells per well in 24 well plates. The following day, the cells were infected with *in*1374 virus at MOI of 5 and incubated at 38.5 °C overnight. The next day, the cells were super-infected with wt/mutant virus at an MOI of 5 at 37 °C. After virus adsorption for 1 hour at 37 °C with agitation every 5-10 minutes, the cells were overlaid with medium containing 10 μM ACV (a guanosine analogue that prevents viral DNA synthesis) and 1% human serum, and incubated at 38.5 °C for 8 hours. The cells were then fixed and stained for β-galactosidase activity by washing with PBS and

incubating in PBS/1% glutaraldehyde for 40 minutes. The cells were washed with PBS and incubated at 37 °C with pre-warmed reagent solution for staining (see **section 2.7.5**) for 30-120 minutes.

2.8 Immunofluorescence and confocal microscopy

2.8.1 Solutions used during immunofluorescence

Formaldehyde fix solution	1 ml formaldehyde solution (37% w/v, Sigma-Aldrich), 0.4 g sucrose, 19 ml PBS
Permeablisation solution	2 g sucrose, 1 ml 10% NP40, 19 ml PBS

2.8.2 Immunofluorescence protocol

Cells were seeded onto circular 13 mm glass coverslips in a 24 well plate at a seeding density of 1 x 10^5 cells per well. After the experimental procedure was carried out, the coverslips were transferred to a fresh 24 well plate and washed once in PBS. The cells were fixed by incubation with 0.5 ml formaldehyde fix solution for 5 minutes at room temperature. The coverslips were washed three times in 1 ml PBS, and the cells were permeabilised by incubating for 5 minutes at room temperature with 0.5 ml permeabilising solution. The cells were washed three times in PBS containing 2% FBS, and were stored at 4 °C in this buffer until required.

Primary antibodies were diluted as appropriate (**Table 2.3**) in PBS containing 5% FBS, and 35 µl of the antibody dilution was placed onto the coverslip with the cell side facing up and incubated for 1 hour at room temperature. The coverslips were washed six times in PBS containing 2% FBS and incubated with secondary antibodies (**Table 2.4**), as described above. After six washes with PBS/2% FBS, the coverslips were rinsed in dH_2O to remove any salt residue, and air dried before mounting cell side down on Citifluor AF1 mounting agent, and fixed in place using clear nail varnish.

Confocal microscopy was carried out using a Zeiss LSM 710 confocal microscope with 488, 561 and 633 nm laser lines, scanning each channel separately under conditions that

eliminated channel overlap. Images were exported as Tif files using Zen browser software, edited minimally using Abode Photoshop, and figures compiled in Abode Illustrator.

2.9 *In vitro* assays

2.9.1 Polyubiquitination assay

Polyubiquitination assays were carried out in reactions containing 2.5 µg ubiquitin (Sigma-Aldrich), 10 ng 6xHis-E1 ubiquitin activating enzyme (provided by the laboratory of Chris Boutell), titrated amounts of 6xHis-E2 ubiquitin conjugating enzyme (10, 20, 40 ng) (provided by the laboratory of Chris Boutell) and 30 ng wt or ICP0 mutant forms of a GST-ICP0 fusion protein encompassing the first 241 residues of ICP0 (GST-241). The mixture was incubated at 37 °C for 45 minutes, and then the reaction was stopped by the addition of 6 µl 3x boiling 'super mix' containing urea (30% SGB, 30% glycerol, 6.5% SDS powder, 9 M urea, 100 mM DL-dithiothreitol (DTT), bromophenol blue) and incubating at 95 °C for 10 minutes. The samples were run on a Biochem/Novex NuPAGE® pre-poured 4-12% bis-tris gradient protein gel (Invitrogen) run in NuPAGE® MOPS SDS running buffer (Invitrogen) at 160 volts. The proteins in the gel were transferred to a nitrocellulose membrane by electroblotting in NuPAGE® transfer buffer (Invitrogen) at 30 volts (~200 mA) for 1 hour. The membrane was blocked for 1 hour in blocking buffer, and then ubiquitin chain formation and autoubiquitination were detected using a P4D1 mouse monoclonal antibody and a 27-4577-01 anti-GST antibody, respectively.

2.10 Yeast-two-hybrid reagents and methods

Yeast-two-hybrid assays were used to test for protein interactions, and were conducted using the Matchmaker^{TM} GAL4 Two-Hybrid System 3 (Clonetech). An overview of the yeast-two-hybrid system is described in **Figure 2.4**, with the materials and methods for each step being detailed throughout this section.

2.10.1 Yeast strains

The *Saccharomyces cerevisiae* Y187 and AH109 yeast strains used throughout the yeast two hybrid study were obtained from Clonetech. Their genotypes are described in **Table 2.9**.

Table 2.9 Yeast strains used in this study.

Strain	Genotype	Reporter genes
Y187	*MATα, ura3-52, his3-200, ade2-101, trp1-901, leu2-3, 112, gal4Δ, gal80Δ, met⁻,* *URA3* : : $GAL1_{UAS}$-$GAL1_{TATA}$-*lacZ*	*MEL1, lacZ*
AH109	*MATa, trp1-901, leu2-3, 112, ura3-52, his3-200, gal4Δ, gal80Δ, LYS2* : $GAL1_{UAS}$-$GAL1_{TATA}$-*HIS3,* $GAL2_{UAS}$-$GAL2_{TATA}$-*ADE2,* *URA3* : $MEL1_{UAS}$-$MEL1_{TATA}$-*lacZ*	*HIS3, ADE2, MEL1, lacZ*

2.10.2 Plasmids used in yeast-two-hybrid assays

The plasmids used in the yeast-two-hybrid assay are detailed in **Table 2.10**, with their sources, main characteristics and purpose of use described.

Table 2.10 Plasmids used in yeast-two-hybrid assays

Plasmid	Purpose
pGADT7 (Clonetech)	Expression of DNA-activating domain fusion proteins *GAL4* $_{(768\text{-}881)}$ AD, *LEU2*, amp resistance, HA epitope tag Selection on –Leu SD (lacking essential aa) medium. Negative control.
pGAD-ICP0	wt ICP0 (1-775 aa) as a fusion protein to the *GAL*4 activation domain (AD). Selection on –Leu. (Boutell *et al.*, 2011; Vanni *et al.*, 2012)
pGAD-N151D **pGAD-K144E**	Mutant version of pGAD-ICP0 with single point mutations in the ICP0 RING finger have been previously described (Vanni *et al.*, 2012) or, in the case of K144E, were provided by the group of Chris Boutell. Selection on –Leu.
pGAD-KE/ND	Mutant version of pGAD-ICP0 with double point mutation K144E/N151D was constructed from the GST-tagged ICP0 RING finger construct (**section 2.10.6**) during the course of this study. Selection on –Leu.
pGAD-ICP0-2C	Mutant version of pGAD-ICP0 containing mutations in double cysteine zinc-binding residues (C116G/C156A) Selection on –Leu. (Vanni *et al.*, 2012).
pGBKT7 (Clonetech)	*GAL4*$_{(1\text{-}147)}$ DNA-BD, *TRP1*, kan resistance, c-myc epitope tag. Expression of DNA binding domain fusion proteins. Selection on –Trp (-W). Negative control.
BK-USP7	USP7 fused to the GAL4 DNA-binding domain. Selection on –Trp (-W). Positive control for ICP0 interaction. (Vanni *et al.*, 2012)
BK-UBE2D1 **BK-UBE2E1** **BK-UBE2N** **BK-UBE2V1** **BK-UBE2W**	E2 ubiquitin-conjugating enzymes fused to the GAL4-binding domain. Selection on –Trp (-W). UBE2D1, UBE2E1 (Vanni *et al.*, 2012), others provided by the group of Chris Boutell.

2.10.3 Yeast reagents and solutions

10x TE	0.1 M Tris-HCl, 10 mM EDTA pH7.5, autoclaved
10x lithium acetate (LiAC)	1 M LiAc (Sigma-Aldrich) pH 7.5, autoclaved
50% polyethylene glycol (PEG)	50 g PEG (Sigma-Aldrich) per 100 ml dH_2O, autoclaved
1x TE/LiAc solution	1 ml 10x TE, 1 ml 10x LiAc, 8 ml dH_2O
TE/LiAc/PEG solution	1 ml 10x TE, 1 ml 10x LiAc, 8 ml 50 % PEG
80% glycerol	8 ml glycerol, 2 ml dH_2O, autoclaved
0.2% adenine hemisulphate (Sigma-Aldrich) solution	0.2 g in 100 ml dH_2O, autoclaved
3-amino-1,2,4-triazole (3-AT)	1 M 3-AT (Sigma-Aldrich). Autoclaved
40% X-gal in N,N-dimethylformamide (DMF)	0.16 g X-gal powder in 400 µl N,N-dimethylformamide (DMF) (Sigma-Aldrich)
K_2HPO_4 (BDH Chemical Ltd)	1 M solution, filter sterilised
KH_2PO_4 (BDH Chemical Ltd)	1 M solution, filter sterilised
KPO_4 solution	61.5 ml K_2HPO_4, 38.5 ml KH_2PO_4
1% agarose in dH_2O	1 g agarose per 100 ml dH_2O

Agarose/X-gal staining solution

5 ml KPO_4 solution, 600 µl DMF (which permeabilises yeast cells), 50 µl 20% SDS, 100 µl 40% X-gal solution in DMF and 5 ml 1% agarose in dH_2O.

2.10.4 Yeast media and agar plates

Yeast strains were cultured in YPD broth, a media base including essential amino acids, or minimal SD base (Clonetech), which is a basic (drop out) medium lacking certain essential amino acids, e.g. -L to select for LEU2 (leucine biosynthesis) expression, -W to select for TRP1 (tryptophan biosynthesis) expression and –L-W to select for both LEU2 and TRP1 expression. After autoclaving adenine hemisulfate was added to YPD broth or agar (YPDA) to a final concentration of 0.003% to minimise yeast strains harbouring ADE1 and ADE2 which produce white colonies, so pink/red colour of colonies without the mutations were selected.

2.10.5 Reviving yeast glycerol stocks

Frozen yeast strains from -70 °C glycerol stocks were streaked onto pre-warmed YPDA agar plates or the appropriate drop out agar plates and incubated at 30 °C. Colonies of the yeast strains were then picked and re-streaked onto fresh agar plates after three days or once the colony exceeded 2 mm in diameter.

2.10.6 Transforming competent yeast cells using the polyethylene glycerol (PEG)/LiAc based method

Yeast strain AH109 was used for the transformation of the pGADT7-derived plasmids, and yeast strain Y187 was used for the transformation of the pGBKT7-derived plasmids. Empty vectors pGADT7 and pGBKT7 were transformed as the appropriate negative controls.

A culture containing four colonies of the appropriate yeast stain (AH109 or Y187) that had been passaged for less than three weeks was added to 3 ml YPDA media and incubated overnight at 30 °C with constant horizontal agitation. The following day, 750 µl of the overnight culture was diluted in 15 ml YPDA medium in a 15 ml Falcon tube and

incubated for 3.5 hours with horizontal agitation at 30 °C. The culture was centrifuged at 3500 rpm (Thermo Scientific Heraeus Megafuge 16R) for 5 minutes, and the pellet was resuspended in 2 ml dH_2O. The pellets were spin washed a further two times in dH_2O. The pellets were then centrifuged as before, resuspended in 2 ml 1xLiAc 0.1M/TE pH 8.0, spin-washed a further two times, and resuspended in 1xLiAc 0.1M/TE pH 8.0 buffer. After treatment with LiAc, the cells are fragile and cannot be vortexed. After the final spin-wash, the cells were resuspended in 1/200 of the culture volume (75 µl of 1xLiAc / TE pH8.0). After this, the yeast cells were competent for transformation.

The transformation mix contained 50 µl resuspended yeast cells, 25 µg denatured herring testes carrier DNA (Invitrogen, boiled for 30 minutes at 100 °C and cooled on ice prior to use) and 1-2 µg plasmid DNA (pGAD-KE/ND). The mixture was incubated at room temperature for 15 minutes, 150 µl of PEG 50% LiAc 0.1 M final/ TE pH 8.0 was added, and the tubes were inverted gently to mix. PEG enhances the binding of plasmid DNA to yeast cell surfaces during transformation. The mixture was incubated at 30 °C for 1 hour with horizontal agitation and then heat shocked for 20 minutes at 42 °C. After the heat shock, 700 µl dH_2O was added to the transformation mix, and the cells were centrifuged for 1 minute at 6000 rpm (MSE Micro Centaur). The pellet was resuspended in 400 µl selective medium (–L or –W, determined by the plasmid). AH109 was used to transform pGAD plasmids that allow growth in the absence of leucine (–L), and Y187 was used to transform pGBK plasmids that allow growth in the absence of tryptophan (–W). Aliquots (200 µl) of the mixture were plated onto pre-warmed selective agar plates (if the transformation efficiency was high, 1/10 or 1/100 dilutions were also plated). The colonies were incubated at 30 °C for 3-4 days until they were about 2-3 mm in diameter. The colonies were then ready for restreaking, and when restreaked a further two times, they were then ready to mate.

2.10.7 Mating

Mating cultures of the AH109 and Y187 yeast strains were set up in 500 µl YPDA. Five colonies approximately 2 mm in diameter from each of the –L and –W plates were placed into the YPDA and incubated at 30 °C overnight with horizontal agitation. The following day, the overnight cultures were diluted 1/10 and 100 µl plated onto –L-W plates to select for diploids that contained both pGADT7 (selection on –L) and pGBKT7 (selection on –W) derived plasmids. The plates were incubated at 30 °C for about four days until the colonies reached 2-3 mm in diameter.

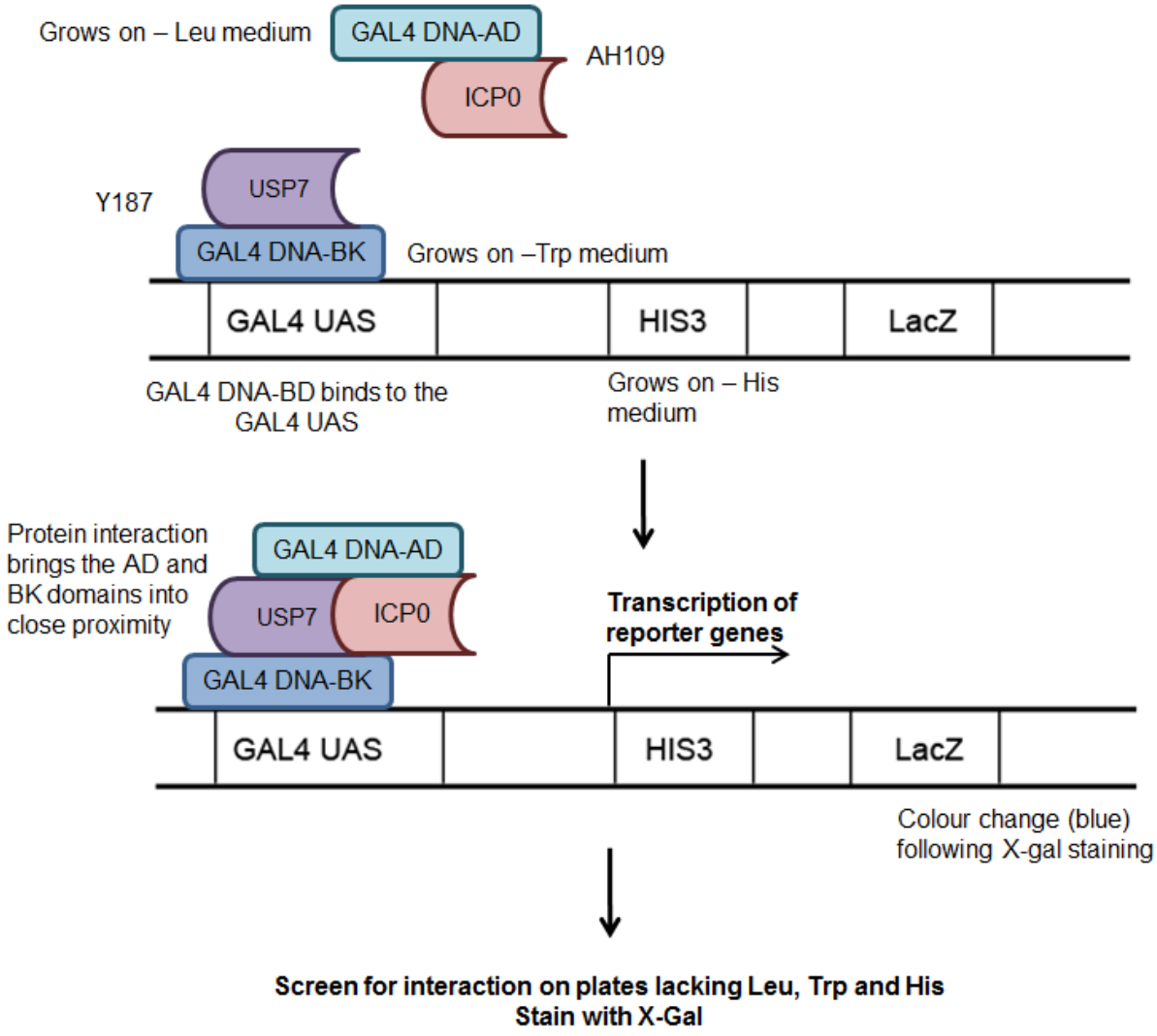

Figure 2.4 Studying protein-protein interactions using the yeast-two-hybrid system. The *GAL4* transcription factor is divided into two fragments, the binding domain (BK) in pGBK-T7 plasmids and activating domain (AD) in pGAD-T7 plasmids. Proteins of interest are expressed as fusion proteins with the BK and AD domains. The pGBK plasmids are transformed into Y187 yeast strain grown on agar lacking Trp (-W), and the pGAD plasmids are transformed into AH109 yeast strain grown on agar lacking Leu (-L). After mating, the yeast strains are grown on agar lacking –Leu/-Trp (-L/-W) to select for the presence of both proteins. The BK domain binds to the GAL UAS located upstream of the reporter genes, and, if the two tested proteins interact, the BK and AD are brought into close proximity and activate transcription of downstream reporter genes *HIS3* and *LacZ*. Detection of protein interactions are confirmed by growth on agar plates lacking –Leu/-Trp/-His (-L/-W/-H), and can be visualised by X-gal staining.

2.10.8 Yeast-two-hybrid plating

Five colonies each 2-3 mm in diameter were picked from the mating plates lacking Leu and Trp, put into an Eppendorf tube containing 500 µl of –L-W broth, and incubated overnight at 30 °C with constant horizontal agitation. The following day, the samples were vortexed, 7 µl was pipetted onto agar plates (listed below), and the plates were incubated at 30 °C for 2-3 days.

a) Lacking Leu and Trp: selects for diploids containing pGADT7 and pGBKT7 based plasmids
b) Lacking Leu, Trp and His: selecting for expression of the downstream reporter gene *HIS3*, indicating an interaction between the two proteins tested.
c) Lacking Leu, Trp and His plus 1 mM 3-amino-1,2,4-triazole (3-AT): 3-AT is a competitive inhibitor of the *HIS3* gene product, imidaxoleglycerol phosphate dehydratase, and it enables greater selection for positive interactions in yeast-two-hybrid system and eliminates background growth on –H selection plates.
d) Lacking Leu, Trp and His plus 5 mM 3-AT: the most stringent selection used for positive interactions

2.10.9 X-gal staining

Colonies growing on the agar plates lacking Leu, Trp and His with 1 or 5 mM 3-AT were further analysed for positive protein interactions by X-gal staining to detect β-galactosidase expression from the *LacZ* reporter gene downstream of the *HIS3* reporter gene. The agar plates were imaged prior to X-gal staining, and the buffers were pre-warmed to 50 °C prior to use to prevent X-gal crystal formation. The agarose/X-gal staining solution (containing DMF which permeabilises yeast cells) was added to the plates, and, once dried, the plates were incubated at 37 °C overnight. The following day, the plates were imaged in colour, with a blue colour indicating β-galactosidase activity and an interaction between the two proteins, whereas colonies that remained white indicated no interaction.

3 Results - Analysis of the alpha-helix RING finger ICP0 mutants using an inducible cell line system

3.1 Introduction

The tertiary structure of the RING finger domain of the equine herpesvirus 1 (EHV-1) protein, which is highly related to ICP0, shows that it consists of an amphipathic alpha-helix that lies between the second and third strands of the triple stranded anti-parallel beta sheets (**Figure 1.4**) (Barlow *et al.*, 1994). Several polar and charged side chains extend off the alpha-helix, and it has been shown by site-directed mutagenesis that some of these side chains are required for fully efficient ICP0 activity in gene expression reporter assays and also a limited number of virus infection assays (Barlow *et al.*, 1994; Everett *et al.*, 1995). These alpha-helix mutations do not appear to reduce *in vitro* E3 ligase activity of ICP0 in combination with E2 ubiquitin-conjugating enzyme UBE2D1 (Boutell *et al.*, 2002).

This chapter investigates mutations in the alpha-helix of the RING finger domain of ICP0, namely N151D and K144E. These mutations are located in the charged side chains that are exposed on the surface of the alpha-helix and which may therefore form an interface with ICP0 interaction partners. Recently, Vanni et al. (2012), using an inducible ICP0 expression system, found that mutation N151D was defective in inducing reactivation of quiescent HSV-1, but was only slightly defective in complementing lytic infection of an ICP0-null mutant HSV-1 (Vanni *et al.*, 2012). This observation raises the possibility that complementation and reactivation involve differential activities of ICP0. This was an exciting and potentially extremely important finding that merited confirmation and further investigation. Therefore, based on this observation, one of the aims of the work presented in this chapter was to repeat the investigation of the N151D mutation and extend the studies to include the nearby K144E mutation which has previously been analysed in transfection and virus based assays and had phenotypes similar to the N151D mutation (Barlow *et al.*, 1994; Everett *et al.*, 1995). Therefore, these two mutations were analysed in parallel to investigate in more detail their effects on ND10, complementation of an ICP0-null mutant virus, and reactivation of quiescent HSV-1. These studies aimed to elucidate in greater detail the role of the RING finger alpha-helix in the functions of ICP0.

These mutants were initially studied using an ICP0 inducible expression system, (**Figure 2.2**) (Everett *et al.*, 2009), which expresses ICP0 in an inducible manner to levels

comparable to the early stages of HSV-1 infection. This system is advantageous in many assays, as it allows direct analysis of ICP0-specific functions in the absence of other viral proteins, whereas attempts at long term ICP0 expression would be detrimental for cell survival (Everett *et al.*, 2009). Using the inducible ICP0 cell line avoids problems associated with comparing defects of ICP0 mutant HSV-1 that depend on factors such as cell type and input MOI, and the limitations of transfection experiments that can expresses the protein of interest at very high non-physiological levels. These complications with virus infection and transfection-based systems in certain assays can be minimised by using the inducible cell line system. However, studies of the effects of the mutations in the context of the viral genome remain important, and these studies will be presented in a later chapter.

3.2 Results

3.2.1 The RING finger alpha-helix mutant proteins colocalise with PML but have reduced abilities to induce its dispersal

At the early stages of infection, ICP0 shows colocalisation with PML, but as the infection progresses ND10 are disrupted, with the RING finger domain of ICP0 inducing the degradation of PML, particularly its SUMO-modified isoforms (Boutell *et al.*, 2011; Everett *et al.*, 1998a; Everett & Maul, 1994; Maul & Everett, 1994; Maul *et al.*, 1993). PML is involved in host cell restriction of HSV-1 infection, and this can be counteracted by ICP0 inducing the degradation of PML, thereby lifting its repressive effects (Everett *et al.*, 2006; Parkinson & Everett, 2000). The effects of the RING finger mutations K144E and N151D on ICP0 localisation and degradation of PML were investigated using the inducible ICP0 expression system. Initially, the RING finger mutants K144E and N151D were transferred into the pLKO.DCMV.TetO.cICP0 plasmid (Everett *et al.*, 2009) (**section 2.2.3**). Inducible cell lines were established by transducing HA-TetR cells with lentivirus produced from pLKO.DCMV.TetO.cICP0 plasmids expressing wt or K144E and N151D mutants.

Cells were treated with 0.1 µg/ml doxycycline for 24 hours to induce ICP0 expression, and the localisation of ICP0 and dispersal of PML were analysed by immunofluorescence (**Figure 3.1**). The control HA-TetR cells showed no ICP0 expression after treatment with doxycycline, showing that ICP0 expression was specific to cells transduced with the ICP0 lentivirus. In these control cells, the PML remained in distinct foci that were distributed

throughout the nucleus. In cells expressing wt or mutant forms of ICP0, the ICP0 was widely expressed in a high proportion of transduced cells and was both dispersed throughout the nucleoplasm and present in discrete foci. In wt ICP0 expressing cells, the PML was almost completely dispersed, whereas in K144E and N151D expressing cells, although ICP0 was widely expressed at apparently higher levels than seen with wt ICP0, in most cells the PML remained in distinct foci that showed a high degree of colocalisation with ICP0.

These results show that although the K144E and N151D mutant proteins are expressed at high levels and colocalise with PML, they induce its dispersal inefficiently. These results confirm previous results using transfection assays that showed that the N151D and K144E mutant forms of ICP0 colocalise with PML at ND10 but fail to disperse PML (Everett *et al.*, 1995), and also the more recent analysis of mutant N151D in the inducible cell line system (Vanni *et al.*, 2012).

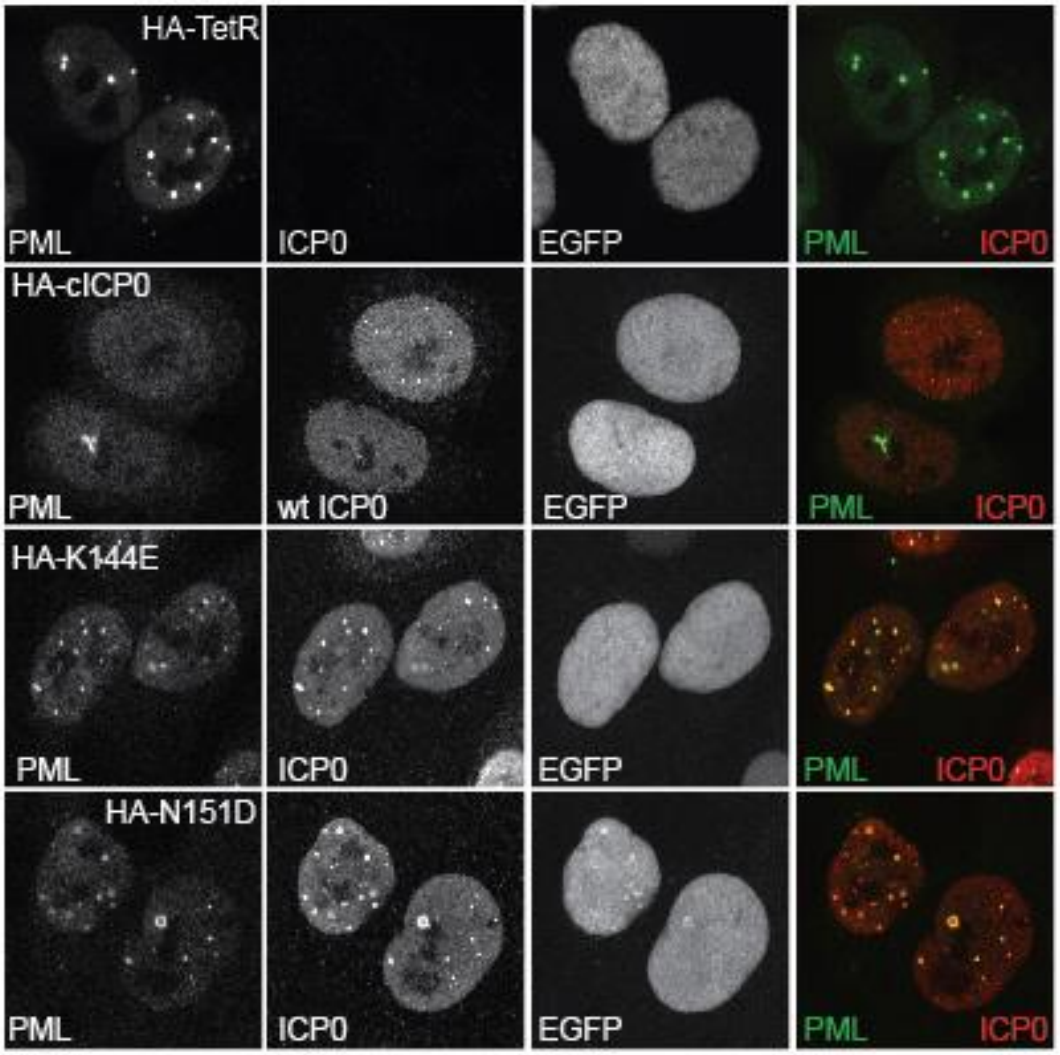

Figure 3.1 Analysis of ICP0 expression in wt and mutant HA-ICP0 cells and the dispersal of PML.
HA-TetR, HA-cICP0 or cells expressing the RING finger mutants were treated for 24 hours with doxycycline to induce ICP0 expression, and the ability of these proteins to colocalise with and disperse PML was analysed. The cells were stained using rabbit anti-PML polyclonal antibody and the mouse anti-ICP0 monoclonal antibody 11060. EGFP autofluorescence from expression of the EGFP-linked tetracycline repressor protein is shown for all cells. The images are representative of a large number of cells that were examined.

3.2.2 The N151D and K144E RING finger mutant proteins are only slightly defective in complementation of the plaque formation defect of an ICP0-null mutant virus

The plaque formation defect of an ICP0-null mutant virus can be complemented by the expression of ICP0 (Everett *et al.*, 2004a). The ICP0 inducible cell line can completely complement the plaque formation defect of an ICP0-null mutant virus (*dl*1403/CMVlacZ)

following wt ICP0 induction, whereas the RING finger deletion mutant does not complement this defect in PFE (Everett *et al.*, 2009). The ability of the N151D and K144E RING finger mutant protein to complement an ICP0-null mutant virus in comparison to wt ICP0 were investigated.

Cells with or without doxycycline treatment to induce expression of wt or mutant ICP0 were analysed by plaque assay following infection with wt (*in*1863) or ICP0-null mutant (*dl*1403/CMVlacZ) HSV-1 virus (**Table 3.1, Figure 3.2)**. Parental HA-TetR cells, which do not contain ICP0, were included as a control. Relative PFEs were calculated in comparison to wt ICP0. The wt virus had similar PFEs in all cell types without ICP0 induction. After ICP0 induction, wt ICP0 caused a slight (about 2-fold) increase in wt HSV-1 plaque formation, and all the mutants showed slight decreases in plaque numbers compared to wt ICP0, but this was always less than a two-fold difference. Wt and mutant ICP0 cells without ICP0 induction showed comparable but very low plaque numbers following infection with the ICP0-null mutant virus (**Table 3.1)**. ICP0-null mutant virus plaque numbers increased by about 200-fold after induction of wt ICP0 expression compared to HA-TetR control cells. The RING finger mutants N151D and K144E also increased *dl*1403/CMVlacZ plaque formation to levels about two-fold less efficient than wt ICP0 in this system. In the absence of doxycycline induction, there was little difference in ICP0-null mutant virus plaque numbers between HA-TetR and wt ICP0 cells, and this was also the case for both ICP0 mutants. The plaque assay data show that the ICP0 mutants analysed here are able to complement ICP0-null mutant HSV-1 plaque formation to levels within two-fold of the wt protein. This confirms the previous observation using mutant N151D (Vanni *et al.*, 2012) and demonstrates that in this respect the nearby K144E mutant has a similar phenotype.

Table 3.1 Plaque count data in cells expressing N151D and K144E following infection with wt or ICP0-null mutant HSV-1 viruses.
Cells were treated with doxycycline for 24 hours to induce ICP0 expression or left untreated. The following day the cells were infected with sequential three-fold dilutions (dil) of wt (*in*1863) or ICP0-null mutant (*dl*1403CMV/lacZ) HSV-1 viruses. The plaque counts at each dilution (tmtc – too many to count), the average plaque counts and the relative value of each cell type compared to wt ICP0 (HA-cICP0) are shown from two repeat experiments.

A) Wt HSV-1 minus doxycycline

Cells HA-	**Dil**	**1**	**1/3**	**1/9**	**1/27**	**Average**	**Relative % compared to wt**	**Ave relative values**
TetR	**10^{-4}**	tmtc	124	59	32	58900000	71.8	**90.1**
		tmtc	tmtc	100	31	86850000	108.4	
cICP0	**10^{-4}**	tmtc	265	101	28	82000000	100.0	**100.0**
		tmtc	tmtc	115	21	80100000	100.0	
cICP0. K144E	**10^{-4}**	tmtc	144	78	0	56700000	69.1	**71.9**
		tmtc	tmtc	61	24	59850000	74.7	
cICP0. N151D	**10^{-4}**	tmtc	241	103	26	78400000	95.6	**102.0**
		tmtc	tmtc	109	28	86850000	108.4	

B) Wt HSV-1 plus doxycycline (0.1 µg/ml)

Cells HA-	**Dil**	**1**	**1/3**	**1/9**	**1/27**	**Average**	**Relative % compared to wt**	**Ave relative values**
TetR	**10^{-4}**	tmtc	163	81	19	57700000	37.0	**44.3**
		tmtc	tmtc	84	16	59400000	51.6	
cICP0	**10^{-4}**	tmtc	tmtc	179	56	156150000	100.0	**100.0**
		tmtc	tmtc	118	46	115200000	100.0	
cICP0. K144E	**10^{-4}**	tmtc	161	63	0	52500000	33.6	**64.1**
		tmtc	tmtc	116	42	108900000	94.5	
cICP0. N151D	**10^{-4}**	tmtc	tmtc	149	31	108900000	69.7	**81.0**
		tmtc	tmtc	119	39	106200000	92.2	

C) ICP0-null mutant HSV-1 minus doxycycline

Cells HA-	Dil	1	1/3	1/9	1/27	Average	Relative % compared to wt	Ave relative values
TetR	**10^{-2}**	tmtc	tmtc	357	22	1903500	89.8	**122.5**
		tmtc	tmtc	176	22	1089000	155.1	
cICP0	**10^{-2}**	tmtc	tmtc	312	53	2119500	100.0	**100.0**
		tmtc	tmtc	105	17	702000	100.0	
cICP0. K144E	**10^{-2}**	tmtc	tmtc	64	15	490500	23.1	**65.7**
		tmtc	tmtc	133	12	760500	108.3	
cICP0. N151D	**10^{-2}**	tmtc	tmtc	236	23	1372500	64.8	**96.2**
		tmtc	tmtc	136	21	895500	127.6	

D) ICP0-null mutant HSV-1 virus plus doxycycline (0.1 µg/ml)

Cells HA-	Dil	1	1/3	1/9	1/27	Average	Relative % compared to wt	Ave relative values
TetR	**10^{-2}**	tmtc	tmtc	93	14	607500	0.5	**0.5**
		tmtc	tmtc	184	25	1165500	0.6	
cICP0	**10^{-4}**	tmtc	tmtc	121	50	121950000	100.0	**100.0**
		tmtc	tmtc	204	77	195750000	100.0	
cICP0. K144E	**10^{-4}**	tmtc	131	53	33	58700000	48.1	**42.7**
		tmtc	191	66	38	73100000	37.3	
cICP0. N151D	**10^{-4}**	tmtc	172	89	18	60100000	49.3	**47.8**
		tmtc	263	106	36	90500000	46.2	

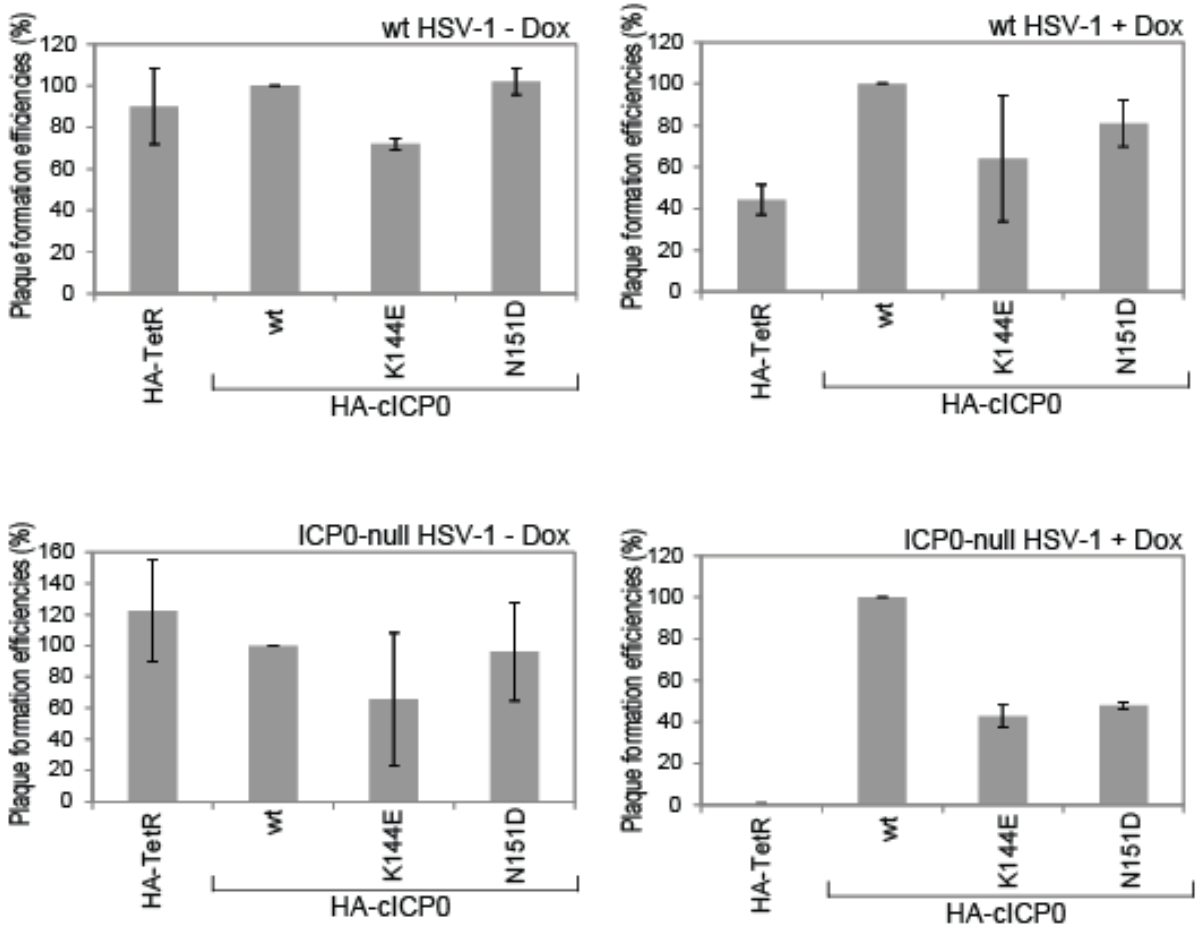

Figure 3.2 Plaque formation efficiency of cells expressing N151D and K144E following wt HSV-1 and ICP0-null mutant HSV-1 infection.
The experiments for both the wt HSV-1 (*in*1863) and ICP0-null mutant (*dl*1403 CMV/lacZ) HSV-1 were carried out with or without induction of ICP0 expression using doxycycline (0.1 μg/ml) for 24 hours before infection. Cells were infected with sequential three-fold dilutions of virus, then stained for β-galactosidase activity 24 hours later. The graph from the data in Table 3.1 shows the average plaque forming abilities from two repeat experiments, expressed as a percentage of PFE in HA-cICP0 cells (expressing wt ICP0). The error bars represent the higher and lower percentage values obtained from two repeat experiments.

3.2.3 RING finger mutants are defective in inducing the reactivation of quiescent HSV-1 genomes

One common characteristic of all herpesviruses is their ability to establish latency from which they can periodically reactivate. ICP0-null mutant viruses that are unable to initiate

a lytic infection are maintained in a quiescent or latent state (reviewed in Efstathiou & Preston, 2005). In *in vitro* quiescence models using non-neuronal cells, ICP0 can reverse the silencing of quiescent HSV genomes (Coleman *et al.*, 2008; Ferenczy *et al.*, 2011; Harris *et al.*, 1989; Samaniego *et al.*, 1998), and this has been shown to be dependent on the RING finger domain of ICP0 (Everett *et al.*, 2009; Ferenczy *et al.*, 2011). In animal models, latent ICP0-null mutant viruses show inefficient reactivation (Cai *et al.*, 1993; Halford & Schaffer, 2001). However, there is some debate whether the defect in reactivation efficiency of ICP0-null mutant viruses is due to defects in ability to reactivate from latency or due to failure to enter productive lytic infections after reactivation (reviewed in Nicoll *et al.*, 2012).

One method to investigate the initiation of viral gene expression from quiescent genomes is a cell culture model system using *in*1374 virus (Preston & Nicholl, 2005). The *in*1374 virus cannot enter lytic replication under restrictive conditions as it contains a deletion of the ICP0 gene, a temperature-sensitive mutation within ICP4 and a mutation within VP16 so that it is unable to stimulate IE gene transcription. Therefore, the *in*1374 virus establishes quiescence very efficiently (Preston & Nicholl, 2005). The virus also contains a marker *Lac*Z gene so that β-galactosidase expression can be analysed to investigate the derepression of the *Lac*Z gene within the viral genome.

Cells expressing wt or mutant ICP0 were infected with *in*1374 at the non-permissive temperature so that quiescence could be established, and ICP0 expression was induced by the addition of doxycycline the following day (**Figure 3.3A)**. Following induction with doxycycline, a large proportion of wt ICP0 cells expressed β-galactosidase from the *Lac*Z gene (indicated by the blue colour), demonstrating reactivated viral gene transcription. In contrast, the control HA-TetR and the HA-cICP0 cells before induction showed little or no *LacZ* gene transcription. The N151D and K144E RING finger mutant proteins showed a substantially reduced proportion of cells expressing β-galactosidase compared to wt ICP0, indicating that reactivation of the quiescent genomes was relatively inefficient, particularly with K144E.

The plate image data were quantified by taking two random fields of view of each well and counting the cells positive and negative for β-galactosidase expression. The percentage of positive cells were calculated and the results presented as a proportion of cells expressing β-galactosidase as a percentage of that obtained through wt ICP0 expression (**Figure**

3.3B). The results showed that there were very few β-galactosidase positive cells in HA-cICP0 cells that had not been induced and also in the induced HA-TetR control cells, indicating that reactivation of gene expression from quiescent HSV-1 is ICP0-dependent. The RING finger N151D mutation and particularly the K144E mutation had a considerable defect in inducing viral gene expression in quiescently infected cells. These results are in agreement with previous results showing that N151D had a substantial defect in inducing gene expression from quiescent viral genomes (Vanni *et al.*, 2012).

The results for the ICP0 mutants T67A and R8507 shown in **Figure 3.3** are not relevant to the results presented in this chapter, but will be discussed later in **chapter 6**. It was necessary to present them here to avoid cropping the image of the plate.

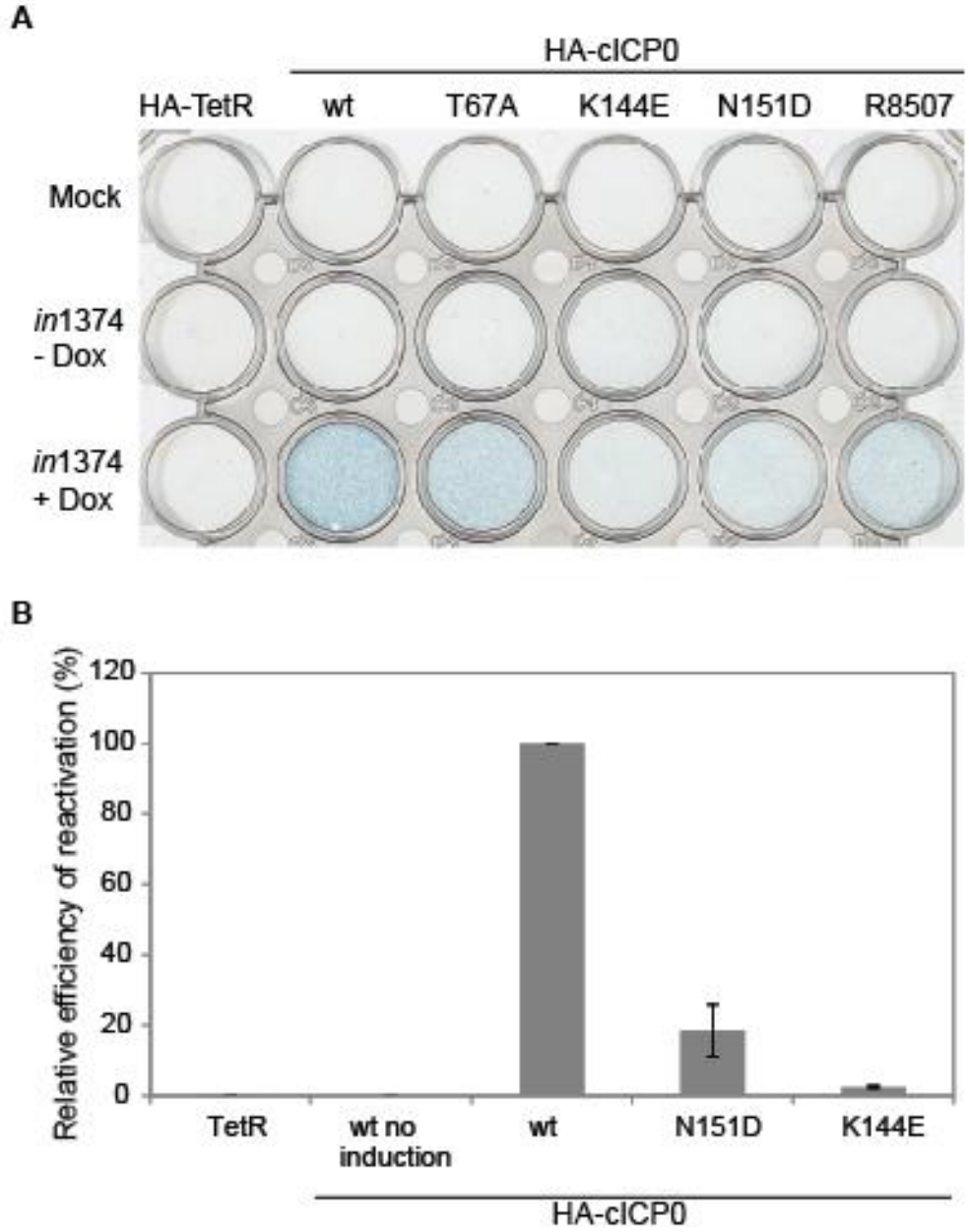

Figure 3.3 Reactivation of viral gene expression by wt and mutant ICP0.
A) HA-TetR, HA-cICP0 and RING finger mutant ICP0 cells (except the mock infected control wells) were infected with *in*1374 (MOI 5), and 24 hours later ICP0 expression was induced with doxycycline (0.1 µg/ml) as indicated. The cells were stained for β-galactosidase activity 24 hours later, where a blue colour indicated cells positive for reactivated viral gene transcription while negative cells gave a clear background.
B) Quantification of the reactivation of gene expression by wt and mutant ICP0. Two random fields of view of the cells infected with *in*1374 and induced with doxycycline were imaged from a single plate. The cells positive and negative for reactivated gene expression were counted, and the percentage of positive cells for each cell type calculated which was then presented as a percentage of that in the HA-cICP0 cells expressing wt ICP0. The bars show the mean result from the two fields of view, and the error bars represent the higher and lower percentages.

3.3 Analysis of the double mutant K144E/N151D (KE/ND) in the ICP0-inducible cell line

3.3.1 Introducing both the K144E and N151D mutations into the same protein in the inducible cell line system

The apparent differential effects between complementation of plaque formation of an ICP0-null mutant virus and reactivation of gene expression from quiescent viral genomes of the N151D and K144E mutants could be because these mutations affect a function that is preferentially required for reactivation. For example, stimulation of lytic infection involves activities on viral genomes immediately after their entry into the nucleoplasm while in an unchromatinised state. In contrast, reactivation is thought to involve events on compacted, repressed chromatin. Thus, different mechanisms could be involved. Alternatively, it is possible that the mechanisms involved are similar, but that greater ICP0 activity is required for reactivation than for complementation, perhaps because of the differences in viral chromatin structure. It is likely that the N151D and K144E mutations affect the same ICP0 interface, and therefore the same inherent function. These two mutations may disrupt a binding site of a cofactor that is involved in reactivation of latent HSV-1 through altering the surface charge of the alpha-helix. To further investigate why these mutations caused a greater defect in reactivation of quiescent viral genomes compared to complementation, the double mutation K144E/N151D (KE/ND) was cloned into the pLKO.DCMV.TetO.cICP0 plasmid, and an inducible cell line expressing the double mutation KE/ND within ICP0 was created. If the K144E and N151D mutations affect a function that is specific for reactivation, it would be expected that the double mutant KE/ND would be defective for this activity, while retaining significant complementation activity. However, if these residues affect a function or binding interface that is required for both lytic infection and reactivation, but greater ICP0 activity is required for reactivation than complementation, then KE/ND might be expected to have a larger defect in the lytic replication assays than the individual mutants. Therefore, the double mutant KE/ND was analysed alongside the single mutants K144E and N151D to analyse if the effect of these two mutations were additive.

3.3.2 Double mutant KE/ND fails to complement the plaque formation defect of an ICP0-null mutant HSV-1

The ability of the double mutant KE/ND to complement an ICP0-null mutant HSV-1 (*dl*1403/CMVlacZ) was analysed by plaque assay (**Table 3.2**, **Figure 3.4**). In parallel, the ICP0 single mutant cell lines, as well as the HA-TetR control cells, with or without doxycycline induction, were examined as described previously (**see section 3.2.2**). ICP0-null mutant virus plaque numbers were increased by about 600-fold in this series of experiments after induction of wt ICP0 expression compared to HA-TetR control cells (**Table 3.2**). Mutant N151D had a less than two fold decrease compared to wt complementation, whereas mutant K144E had more than a three-fold decrease compared to wt. These results are similar to those of the earlier series of experiments (**Figure 3.2**). The double mutant KE/ND, however was highly defective in complementation, with over a 30-fold decrease in plaque numbers compared to wt. Compared to the HA-TetR cells, the double mutant was not entirely negative and was able to increase the ICP0-null mutant virus plaque formation by 20-fold. This is unlike the complete RING finger deletion mutant, however, which had no activity at all in this assay (Everett *et al.*, 2009). Therefore, introducing both of these mutations within the ICP0 protein produces a major defect in complementation of an ICP0-null mutant virus, and a greater defect than the single mutations alone.

Table 3.2 Plaque count data in cells expressing KE/ND following infection with an ICP0-null mutant HSV-1 after induction with doxycycline.
Cells were treated with doxycycline (0.1 µg/ml) for 24 hours to induce ICP0 expression and the following day infected with sequential three-fold dilutions of ICP0-null mutant (*dl*1403CMV/lacZ) HSV-1. The starting dilution for the HA-TetR cells was 10^{-2}, and 10^{-4} in the other cell types. The plaque counts at each dilution, the average plaque counts and the relative value of each cell type compared to wt ICP0 (HA-cICP0) are shown from three repeat experiments.

Cells HA-	**Dil**	**1**	**1/3**	**1/9**	**1/27**	**Average**	**Relative % compared to wt**	**Ave relative values**
TetR	**10^{-2}**	81	15	0	1	51000	0.1	**0.1**
		108	8	4	0	56000	0.2	
		61	18	1	0	41333	0.1	
cICP0	**10^{-4}**	324	137	65	18	45150000	100.0	**100.0**
		229	94	40	5	25150000	100.0	
		239	120	52	17	38150000	100.0	
cICP0. K144E	**10^{-4}**	151	70	33	5	19825000	43.9	**55.1**
		149	53	19	7	16700000	66.4	
		223	71	21	8	21025000	55.1	
cICP0. N151D	**10^{-4}**	90	18	6	7	9675000	21.4	**29.7**
		63	26	7	1	5775000	23.0	
		150	61	21	6	17100000	44.8	
cICP0. KE/ND	**10^{-4}**	6	5	1	1	1425000	3.2	**2.8**
		11	2	1	0	866667	3.4	
		7	2	0	0	650000	1.7	

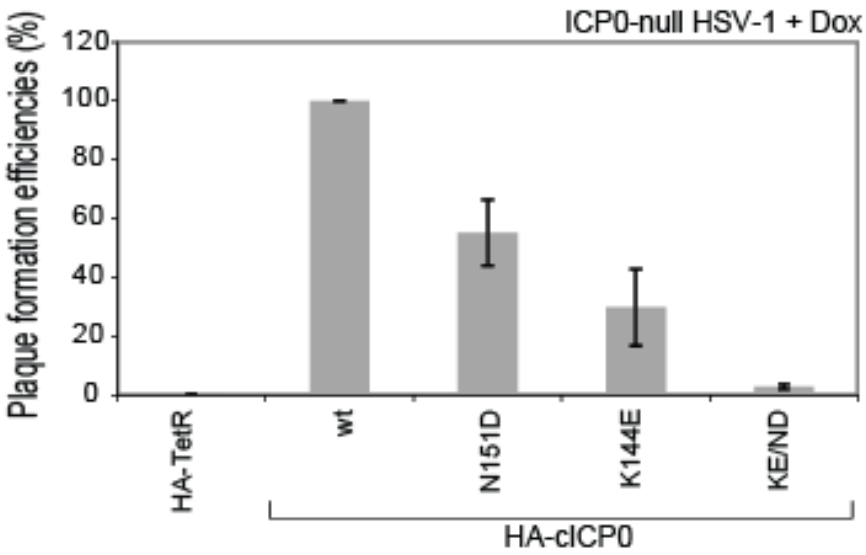

Figure 3.4 Effect of the RING finger mutations on ICP0-null mutant HSV-1 plaque formation.
The ICP0 inducible cells were treated with 0.1 µg/ml doxycycline to induce ICP0 expression and 24 hours later infected with sequential three-fold dilutions of ICP0-null mutant virus (*dl*1403/CMVlacZ). The graph represents the data in **Table 3.2**, with the average plaque forming ability from three repeat experiments, and the PFE in each cell type is expressed as a percentage of that in HA-cICP0 cells that express wt ICP0. The error bars represent the standard deviation from the three repeat experiments.

3.3.3 Double mutant KE/ND is highly defective in inducing gene expression from quiescent viral genomes

The ability of the double mutant KE/ND to reactivate gene expression from quiescent viral genomes was studied using *in*1374 virus (**Figure 3.5**), as described previously and using the same protocol (**section 3.2.3**). As before, the reactivation efficiency was quantified by taking three random fields of view of each well of a cell culture plate and calculating the percentage of cells positive for reactivation as a proportion of wt ICP0. The results with the single substitution mutants K144E and N151D confirm the results seen in **section 3.2.3,** demonstrating that these mutations cause substantial defects in the induction of gene expression from quiescent viral genomes. The double mutant KE/ND was even more defective, producing only minimal numbers of positive cells that were less than 0.5% of wt ICP0 levels.

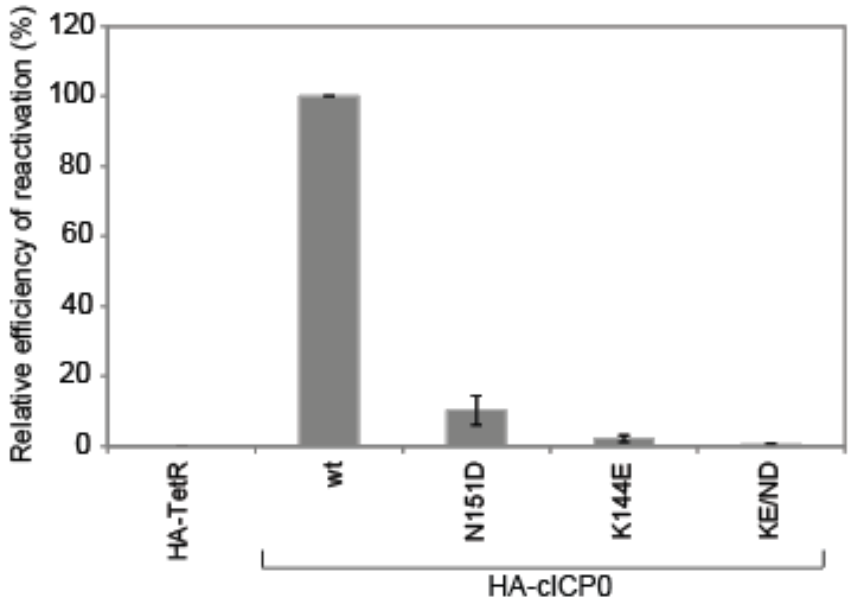

Figure 3.5 Reactivation of gene expression by wt ICP0 and the RING finger mutants. HA-TetR, HA-cICP0 and RING finger mutant ICP0 cells were infected with *in*1374 HSV-1 mutant virus, and 24 hours later ICP0 expression was induced with doxycycline (0.1 µg/ml). The cells were stained for β-galactosidase activity 24 hours later. Three random fields of view of each cell type induced with doxycycline were imaged from a single plate. The cells positive and negative for reactivated transcription were counted, and the percentage of positive cells for each cell type was calculated and plotted as a percentage of that in positive control HA-cICP0 cells. The bars show the mean results from the three fields of view from a single plate, and the error bars represent the standard deviation.

3.3.4 The RING finger mutants have a defect in PML degradation and express ICP0 to higher levels compared to wt in the inducible cell system

Expression of wt and RING finger mutant ICP0 proteins and their effects on PML were analysed by Western blotting (**Figure 3.6)**. Expression of ICP0 occurred in all induced cells except the HA-TetR control cells. The level of ICP0 expression was greatly increased in the RING finger mutants K144E, N151D and KE/ND compared to wt ICP0, and this cannot be attributed to loading differences (see actin). The higher expression levels observed in the RING finger mutants were reproducible in a number of Western blot experiments. In the HA-TetR control cells, and uninduced cells including HA-cICP0, there was no degradation of any of the PML isoforms. After induction, all of the PML isoforms were degraded in wt ICP0 cells. All the RING finger mutants showed some degradation of the SUMO modified and unmodified forms of PML, but all were less efficient than the wt in the degradation of PML, with the double mutant being the least efficient. These results show that, despite the high expression levels of ICP0 and the extended time of expression, the RING finger mutants were defective in PML degradation,

despite colocalising with PML in ND10 (**Figure 3.1**). The reduced efficiency of PML degradation as detected by Western blot correlates with less effective disruption of ND10 detected by immunofluorescence analysis of the single mutants (**section 3.2.1**).

The ICP0 RING finger possesses E3 ligase activity and can induce its own auto-ubiquitination (Boutell *et al.*, 2002; Canning *et al.*, 2004). Auto-ubiquitination of ICP0 makes it less stable, and ICP0 is stabilised by interacting with USP7, a deubiquitinating enzyme (Everett *et al.*, 1999b). It is unlikely that the RING finger mutants affect the interaction with USP7, as the USP7 binding motif is located in the C-terminal third of ICP0 (Meredith *et al.*, 1995; Meredith *et al.*, 1994) (within residues 618-634 (Everett *et al.*, 1999b)), whereas the RING finger domain is located in the N-terminal third. The auto-ubiquitination activity may be disrupted in these RING finger mutants, which could explain why they express higher levels of ICP0.

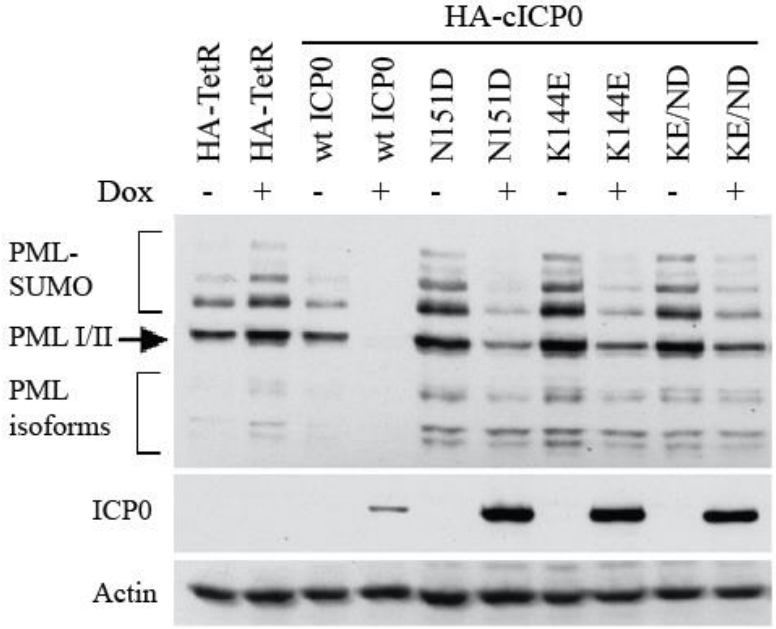

Figure 3.6 Western blot analysis of the degradation of different PML and SUMO isoforms by wt and mutant forms of ICP0.
HA-TetR, HA-cICP0 and RING finger mutant ICP0 cells were induced with doxycycline (0.1µg/ml) for 24 hours or left untreated. PML and ICP0 were detected using the mouse monoclonal antibodies 5E10 and 11060, respectively. Actin was used as a loading control and was detected using the mouse monoclonal antibody AC-40.

3.4 Conclusion and Discussion

Previous work using the ICP0 inducible expression system showed that mutant N151D had a much greater defect in reactivation of quiescent HSV-1 compared to complementation of an ICP0-null mutant virus (Vanni *et al.*, 2012). In addition to N151D, this chapter includes analysis of another single mutation within ICP0, K144E, with both these residues located in the polar side chains exposed by the alpha-helix. These single ICP0 mutations were analysed in the inducible ICP0 expression system for their ability to complement the plaque formation defect of an ICP0-null mutant virus and to induce the reactivation of quiescent HSV-1 as well as their effect on the major ND10 protein PML. The results obtained here for the N151D mutant confirmed those seen in Vanni et al. (2012), that N151D had less than a two-fold defect when complementing the plaque formation efficiency of an ICP0-null mutant virus but had less than 20% of wt levels for reactivation of quiescent HSV-1. The effect with K144E was even more marked, with this mutant having only a three-fold decrease in complementation efficiency compared to wt, but less than 5% reactivation of quiescent HSV-1 compared to wt ICP0 expressing cells.

The N151D and K144E mutant proteins colocalised with PML, but did not induce ND10 disruption efficiently (**Figure 3.1** and **Figure 3.6**). PML is involved in the intrinsic resistance to HSV-1 infection, and its expression is enhanced by interferon (Chelbi-Alix *et al.*, 1995). Depletion of PML increases the replication of ICP0-null mutant HSV-1 (Cuchet *et al.*, 2011; Everett *et al.*, 2006). Therefore, the inability of the RING finger mutants to degrade PML could lead to increased repression of the viral genome and a reduced ability to reactivate from latency. It is known that ICP0 is important for the reactivation of quiescent genomes (Leib *et al.*, 1989), but other viral or cellular factors may also play a role. Therefore, these two mutations may disrupt a binding site of a cofactor that is involved in the reactivation of latent HSV-1 through altering the surface charge of the alpha-helix.

To investigate the differences between the ICP0 mutants with regard to complementation and reactivation, ICP0 containing both the K144E and N151D mutations was expressed in the inducible cell line system. The results showed the double mutant had severe defects in both complementation and reactivation with levels less than 5% of wt levels for both (**Figure 3.4** and **Figure 3.5**). The double mutant was also more defective for PML degradation. Therefore, since the double mutant is defective for both complementation and reactivation, the results suggest that these mutations do not affect a function that is specific

for reactivation alone. These mutations could affect the surface charge, binding site or function that is required for ICP0 activity in general, but greater activity from ICP0 is required for reactivation rather than complementation during lytic infection. In this hypothesis, the single mutants retain sufficient activity for complementation but this level of activity is not enough for efficient reactivation, whereas in the double mutant the function of the alpha-helix is reduced to an extent that then produces a more severe phenotype in the complementation assays.

The inducible ICP0 expression system used for the experiments in this chapter is a valuable tool for studying ICP0 mutants. However, the system does have some limitations, such as the level of expression of ICP0 cannot be tightly controlled, the time course of ICP0 expression is different from that during viral infection, and ICP0 does not accumulate to the levels seen during a normal infection. Lowering the concentration of doxycycline could reduce ICP0 expression, but this may result in a reduction in the percentage of cells expressing ICP0, and increasing the concentration of doxycycline does not lead to higher ICP0 expression. The experiments using the inducible cell line are limited by the cell type, as they are all based on HA-TetR cells which are derivatives of HepaRG cells. HepaRG cells are highly restrictive, with ICP0-null mutant viruses having a 500-fold defect (Everett, 2010; Everett *et al.*, 2009), but these are not the normal epithelial cells that HSV-1 would infect. For the experiments in this study, cells were induced for 24 hours with doxycycline to induce ICP0 expression to ensure that over 90% of cells were positive for ICP0 expression. Therefore, the inducible cell line has different kinetics from natural virus infection. For these reasons, it was also valuable to study the effects of these mutations in the context of the viral genome, as described in the following chapter.

4 Results - Study of ICP0 RING finger alpha-helix mutants in the context of the viral genome

4.1 Introduction

The results using the inducible ICP0 expression system in **Chapter 3** found that mutations in the alpha-helix of ICP0's RING finger domain (N151D and K144E) had two- to three-fold defects in the complementation efficiency of ICP0-null mutant HSV-1 compared to wt ICP0, and had more pronounced defects in reactivation of quiescent HSV-1. Due to certain limitations of the inducible cell line system, described in **section 3.4**, including extended expression times during the experiments, limited cell types and lack of control over expression kinetics, it was also important to study the effects of these mutations in the context of mutant virus infection. The inducible cell system allows the properties of ICP0 to be studied without the complications of virus infection, while virus studies are valuable as they are more realistic than the inducible cell line as all viral proteins are present, and primary cells such as human fibroblasts (HFs) can be used.

This chapter investigates the phenotype of the RING finger mutants K144E and N151D during the context of viral infection. For these experiments, mutant viruses W146A and Q148E were analysed as controls in parallel to the K144E and N151D mutant viruses. Like K144E and N151D, mutations W146A and Q148E are also located in the RING finger alpha-helix, but these have been previously characterised and found to cause no serious defects (Boutell *et al.*, 2002; Everett *et al.*, 1995; Everett, 2000; Vanni *et al.*, 2012). Since the time of the original virus infection studies, the assays and available approaches for studying ICP0-null mutant viruses have improved and expanded considerably, thus justifying a reinvestigation of the RING finger alpha-helix mutant viruses in more detail. The deletion mutant FXE was used as the negative control throughout. FXE contains a deletion of amino acid residues 106-149 (Everett, 1989), which includes a large proportion of the RING finger domain of ICP0 (amino acid residues 116-156) (Barlow *et al.*, 1994). The experiments in this chapter were carried out in HFs and human hepatocellular HepaRG cells. Both cell types require ICP0 for efficient HSV-1 replication, but HFs are the more restrictive cell type (Everett, 2010; Everett *et al.*, 2004a; Everett *et al.*, 2009).

4.2 Results

4.2.1 Plaque formation efficiencies of ICP0 mutant viruses

The defect in plaque formation efficiency of an ICP0 mutant virus is cell type dependent. HFs are one of the most restrictive cell types with an ICP0-null mutant virus having a 1000-fold defect compared to wt HSV-1 (Everett *et al.*, 2004a), whereas in HepaRG cells the defect is 500-fold (Everett, 2010; Everett *et al.*, 2009). However, in the osteosarcoma cell line U2OS, an ICP0 null mutant virus replicates as efficiently as wt virus, meaning that ICP0 is not required for HSV-1 replication in this cell type (Yao & Schaffer, 1995). Therefore, titres in U2OS cells provide a true measure of potentially infectious virus without the complication of the ICP0 defect. Therefore in all experiments in this thesis, the titres of all virus stocks were determined in U2OS cells, and these values were used to calculate input multiplicities for all infected cell types.

Plaque assays were conducted in HepaRG cells and HFs, to take into account the differences in restriction of the different cell types. Cells were infected with sequential ten-fold dilutions of wt or ICP0 mutant viruses over a range such that plaques formed and could be easily counted. The dilution range was adjusted for each virus according to its phenotype. The cells were overlaid with medium containing human serum that contained antibodies to HSV-1, to prevent cell-free virus infecting neighbouring cells and allowing plaques to form by cell to cell spread. Plaques that formed in HepaRG cells and HFs were calculated as a ratio of those produced in U2OS cells, and normalised to the percentage of plaque forming ratio of the wt virus (**Figure 4.1**).

The results show that the positive control mutants W146A and Q148E produced more plaques than wt virus in HFs but had comparable PFEs to the wt virus in HepaRG cells. The N151D virus was about 20% as effective as wt virus, with HFs being the more restrictive cell type. Mutant K144E had a 30-fold defect in plaque forming ability compared to wt in HepaRG cells, and was almost as defective as the FXE deletion mutant in HFs. These results broadly follow the trend of the ICP0 inducible cell lines presented in the previous chapter (**chapter 3**), except that the defects caused by mutations N151D and especially K144E were more marked in this lytic replication virus infectivity assay.

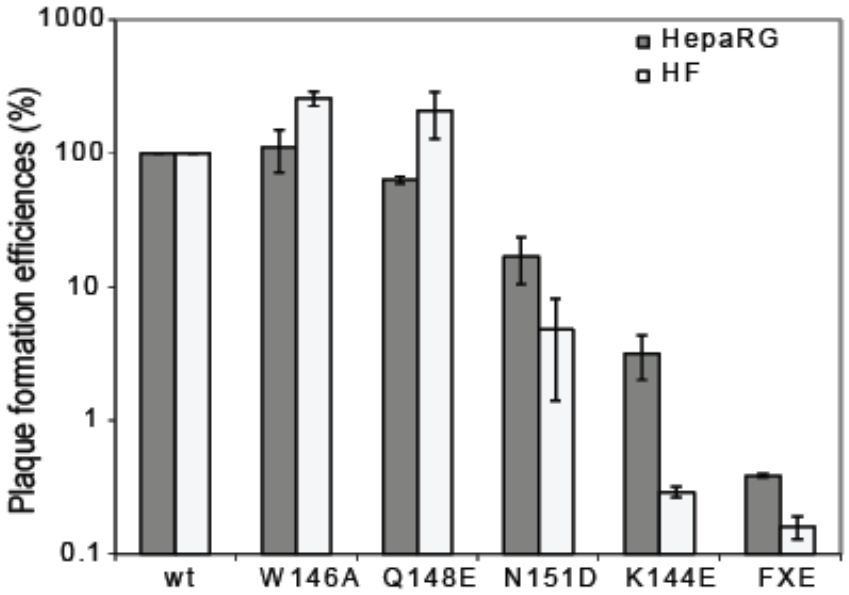

Figure 4.1 PFEs of ICP0 mutant viruses in HF and HepaRG cells.
Plaque assays were conducted in cells infected with wt HSV-1 or ICP0 mutant viruses. The average PFE of each virus in HF and HepaRG cells were calculated as a ratio of plaques formed in U2OS cells and presented as a percentage of the wt value. The error bars represent the higher and lower percentages obtained from two repeats.

4.2.2 Investigation of the yields of RING finger mutant viruses in single step growth experiments in HFs and HepaRG cells

In addition to cell type, input multiplicity can also influence the apparent phenotype of ICP0 mutant viruses. At low MOI in restrictive cell types, mutant viruses have a high probability of entering a latent or quiescent infection, whereas above a certain input multiplicity ICP0 null mutant viruses replicate as efficiently as wt HSV-1 (Everett *et al.*, 2004a). Therefore, the yields of ICP0 mutant viruses were investigated at a range of input multiplicities from 0.1 to 0.001. HFs and HepaRG cells were infected at input multiplicities of 0.1, 0.01 or 0.001, and assayed for the presence of new progeny virus 24 hours later by titration on U2OS cells **(Figure 4.2).** Viral yield assays take into account any difference in plaque sizes that are not immediately apparent by plaque assays.

At the higher MOI of 0.1, mutants Q148E, W146A and K144E produced similar yields of infectious virus in both cell types and were comparable to that of the wt. Mutants N151D and FXE showed a decrease in viral yields compared to wt and the other mutants, but this decrease was less than 10-fold. At MOI 0.01, Q148E and W146A mutant viruses still replicated as efficiently as the wt virus, with similar yields of infectious virus produced and

this remained the case even at the lower MOI of 0.001. In N151D infected cells the viral yield dropped around 30-fold in the two cell types as the MOI was reduced from 0.1 to MOI 0.001. FXE and K144E infected cells showed a two orders of magnitude decrease in viral yield in HepaRG cells and three to four order of magnitude decrease in HFs when comparing infections at MOI 0.1 and MOI 0.01, and the viral yields at MOI 0.001 were very substantially reduced from the wt yields at MOI 0.001.

The results showed that at high viral inputs the mutant viruses replicated as efficiently as wt with similar yields of virus produced in both cell types. However at low MOIs the effects of the RING finger mutations can be observed, with K144E and FXE giving lowest yields of infectious virus.

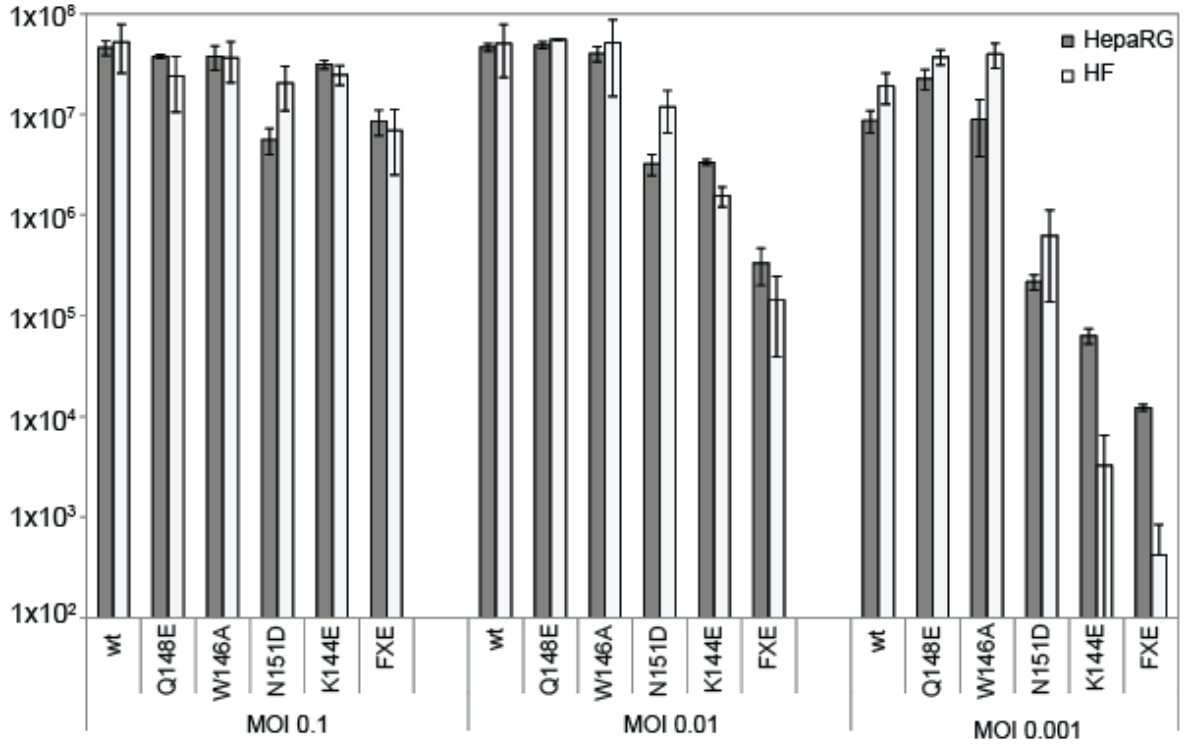

Figure 4.2 Viral yield assays of ICP0 mutant viruses in HepaRG cells and HFs using a range of MOIs.
Cells were infected using a range of MOIs (0.1, 0.01 and 0.001) and overlaid with medium (inoculum not washed off), then 24 hours later the cells and supernatants were harvested, sonicated and titrated on U2OS cells as sequential ten-fold dilutions to calculate PFEs. The error bars represent the higher and lower values obtained from two repeat experiments.

4.2.3 Effects of ICP0 mutant viruses on PML

Use of the inducible ICP0 expression system demonstrated that N151D and K144E colocalised with PML and showed some degradation of the SUMO-modified and unmodified forms of PML, but were less active at degrading PML than wt, despite expressing ICP0 to greater levels than wt (**sections 3.2.1** and **3.3.4)**. The ability of the RING finger mutants to colocalise with and degrade PML was investigated in the context of viral infections. These experiments were done at high MOI to ensure that all cells were infected.

HFs and HepaRG cells were infected with wt or mutant ICP0 viruses at an MOI of 10, and the cells were harvested at two, four and six hours post infection (**Figure 4.3**). ICP0 was expressed at increasing amounts in each virus as the infection progresses, with the levels comparable between all viruses. There was no increased expression of the RING finger mutant ICP0 proteins relative to wt, in contrast to what was observed in the inducible cell line experiments (**Figure 3.6**). In the wt infected cells, all PML isoforms were degraded by two hours after infection of HepaRG cells, and this was slightly delayed to four hours in HFs. Virus Q148E degraded PML at similar rates to wt, with the majority of PML being degraded by two hours post infection. Mutant N151D had a slight delay in degrading PML in HepaRG cells compared to wt, with the majority of PML isoforms being degraded by four hours post infection. In HFs, however, there was only minimal degradation of PML by the six hour time-point in N151D infected cells. Mutant K144E caused slight degradation of PML by six hours post infection in HepaRG cells, but there was minimal degradation of PML in HFs at this time point. FXE did not degrade any of the PML isoforms by six hours post infection in either of the cell types.

For the immunofluorescence analysis, cells were infected at MOI 5 and stained two or four hours post infection (**Figure 4.4**). The results show that at both two and four hours post infection, in cells infected with wt virus the majority of ND10 were disrupted and the signal dispersed, and this also occurred in W146A and Q148E infected cells. In contrast, mutant viruses K144E, N151D and FXE were unable to disrupt PML, but instead ICP0 and PML colocalised in distinct foci under these experimental conditions.

The Western blot and immunofluorescence data confirm the previous results obtained using the inducible cell lines (**Figure 3.1, Figure 3.6**). In HFs infected with mutant viruses K144E and N151D, ICP0 colocalised with PML, but did not induce the dispersal or

efficient degradation of PML. In HepaRG cells, which are less restrictive, mutant N151D induced the degradation of all PML isoforms, but this was slightly delayed compared to wt infection.

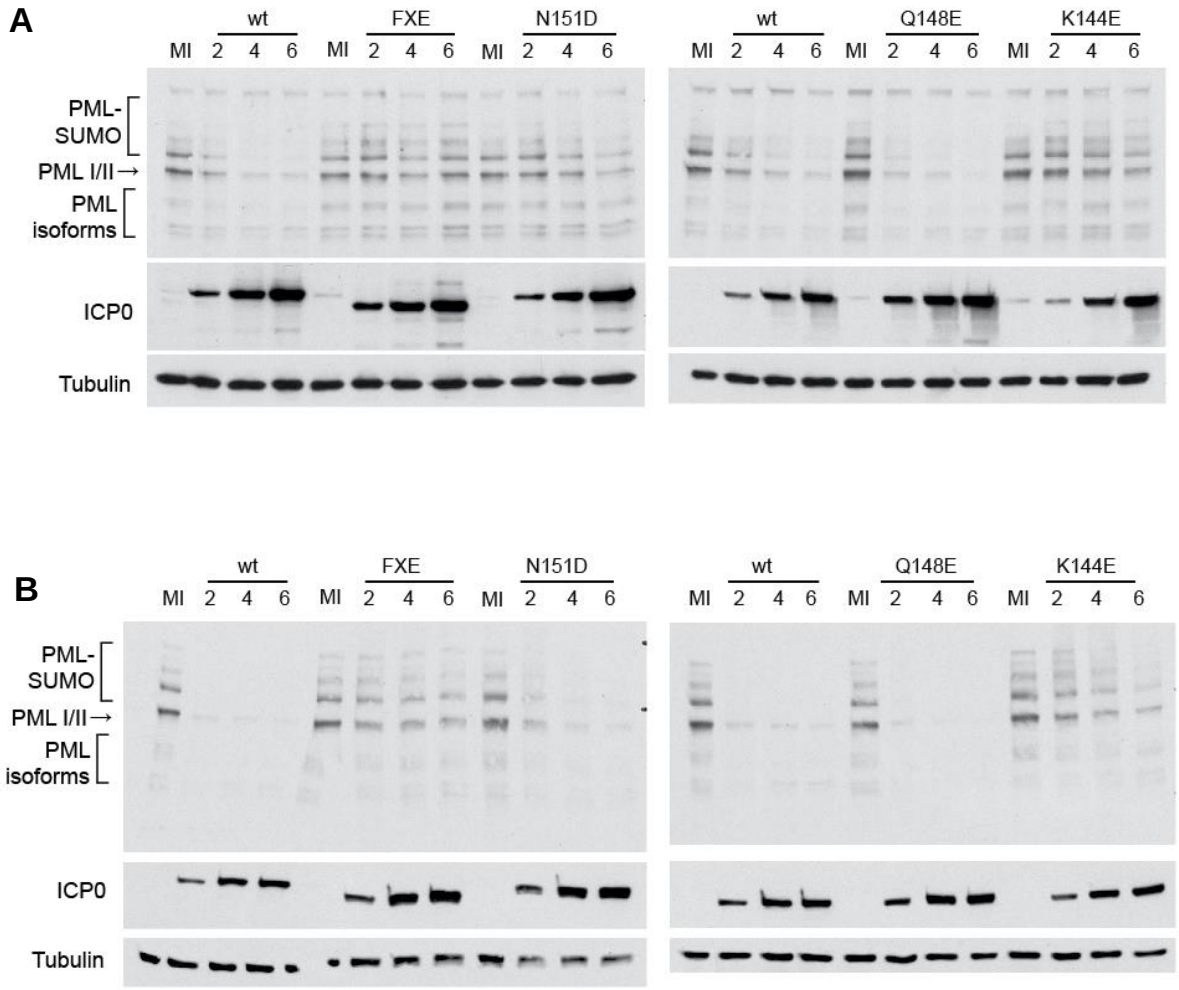

Figure 4.3 Western blot analysis of the degradation of different PML isoforms during infection with wt and mutant viruses.
HFs (A) or HepaRG (B) cells were infected with wt or ICP0 mutant viruses at MOI of 10 or left uninfected (MI mock infection) and harvested at 2, 4 and 6 hours post infection in SDS gel loading buffer. The proteins were resolved on a 7.5% gel and then transferred to a nitrocellulose membrane and detected by probing for PML, ICP0 and tubulin.

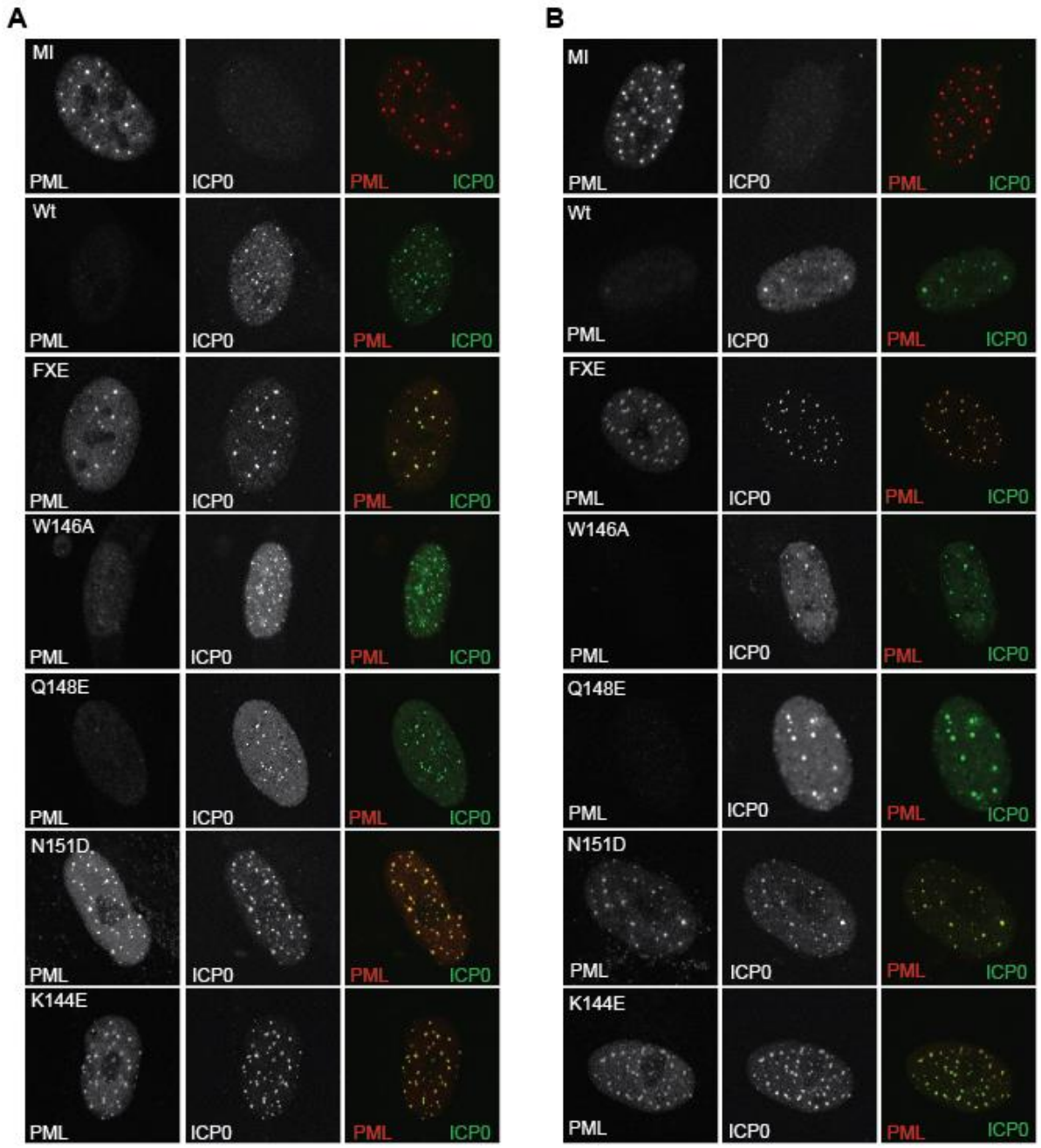

Figure 4.4 Analysis of ICP0 expression in wt and ICP0 mutant virus infected HFs and the dispersal of PML.
HFs were infected at MOI 5 with wt and ICP0 mutant virus and at (A) 2 hours and (B) 4 hours post infection cells were fixed. The cells were stained using rabbit anti-PML polyclonal antibody (red) and the mouse anti-ICP0 monoclonal antibody 11060 (green).

4.2.4 Reactivation/derepression of quiescent HSV-1 genomes

The reactivation (or more properly the derepression) of viral gene expression was investigated using the *in*1374 virus that establishes quiescence very effectively (described in detail in **section 3.2.3**). HepaRG cells were infected with *in*1374 (MOI 5) at non-permissive temperature, followed by infection with wt or ICP0 mutant viruses (MOI 5) the next day (**Figure 4.5**). In the absence of the second infection, all gene expression from *in*1374 was efficiently repressed. The reactivation of viral gene expression was measured by expression of β-galactosidase from the *LacZ* marker gene. The plate image in **Figure 4.5A** shows that a large proportion of *in*1374 and wt co-infected cells expressed β-galactosidase from the *lacZ* gene, indicating reactivated transcription of the *in*1374 virus, whereas this appeared inefficient in the RING finger mutant co-infections. This experiment was quantified by counting the cells positive for β-galactosidase expression out of the total cell population and expressing this as a percentage of the proportion of positive wt co-infected cells (**Figure 4.5B**). This quantification showed that viruses containing mutations N151D and K144E caused significant defects in the efficiency of reactivation, with less than 10% of wt levels, however they have higher levels of reactivation than FXE.

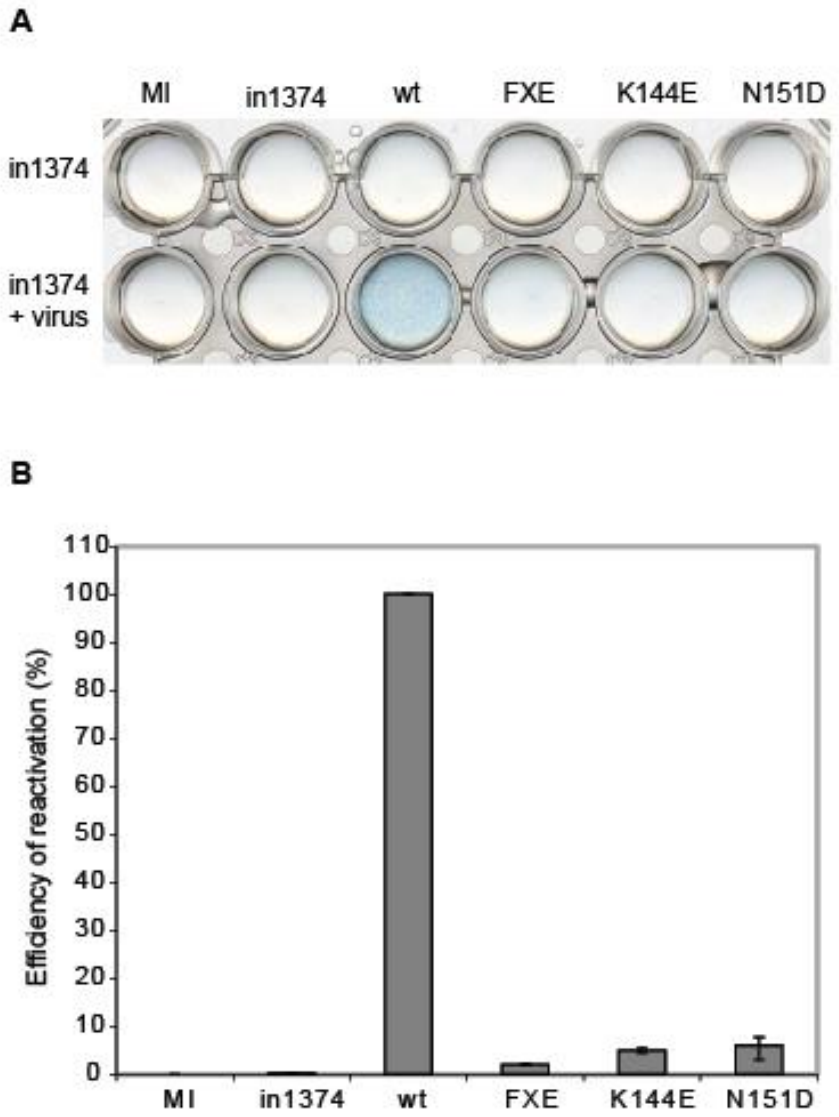

Figure 4.5 Reactivation of *in*1374 viral gene expression by ICP0 RING finger mutants.

(**A**) HepaRG cells (except the mock) were infected with *in*1374 at MOI 5, and 24 hours later super-infected with wt or mutant viruses (MOI 5). After virus adsorption, the cells were overlaid with medium containing 10 μM ACV and 1% human serum. The cells were stained for β-galactosidase activity 24 hours later, where a blue colour indicated cells positive for reactivated transcription while negative cells gave a clear background.

(**B)** Quantification of the reactivation of gene expression by wt and mutant ICP0 viruses shown in A, a single plate was analysed. Three random fields of view of the cells were imaged. The cells positive and negative for reactivated transcription were counted, and the percentage of positive cells for each virus calculated which was then plotted as a percentage of wt virus. The bars show the mean result from the three fields of view and the error bars represent the standard deviations.

Reactivation of gene expression in quiescent *in*1374 genomes was also investigated by immunofluorescence in parallel to the method described above. Cells treated as described above were stained for β-galactosidase and ICP0 proteins (**Figure 4.6**). This approach allowed calculation of the proportion of ICP0 positive cells in which β-galactosidase was expressed (**Figure 4.6B**), thus overcoming uncertainties about the proportions of doubly infected cells inherent in the assays of **Figure 4.5**. The results were expressed as a percentage of the wt reactivation levels as described above. The reactivation efficiency of FXE compared to wt was 9%, whereas K144E and N151D infected cells had 10% and 17% of the reactivation levels seen in wt. These results gave higher reactivation efficiency for the RING finger mutants compared to the results in **Figure 4.5b.** The immunofluorescence method for detecting reactivation appears to be a more sensitive method of detecting cells with reactivated gene expression compared to counting cells for β-galactosidase expression out of the total cell population, as the reactivated cells are calculated as a percentage of cells that are also expressing ICP0. The differences between the two assays for detecting reactivated gene expression highlight the importance of threshold of detection in the two different assays.

The fact that some reactivation is detectable in cells super-infected with the FXE mutant is initially surprising on the basis of most of the previously published analysis (Harris *et al.*, 1989; Harris & Preston, 1991; Minaker *et al.*, 2005; Russell *et al.*, 1987). However, when examined in great detail, some reactivating cells are detectable even in cells infected with an ICP0 deletion mutant (Preston, 2007). The great sensitivity of the immunofluorescence staining method may be revealing this ICP0-independent derepression. Nonetheless, the results are basically similar to those in **Figure 4.5**; with the mutant K144E a little more active than FXE in this assay, and N151D retaining higher levels of activity.

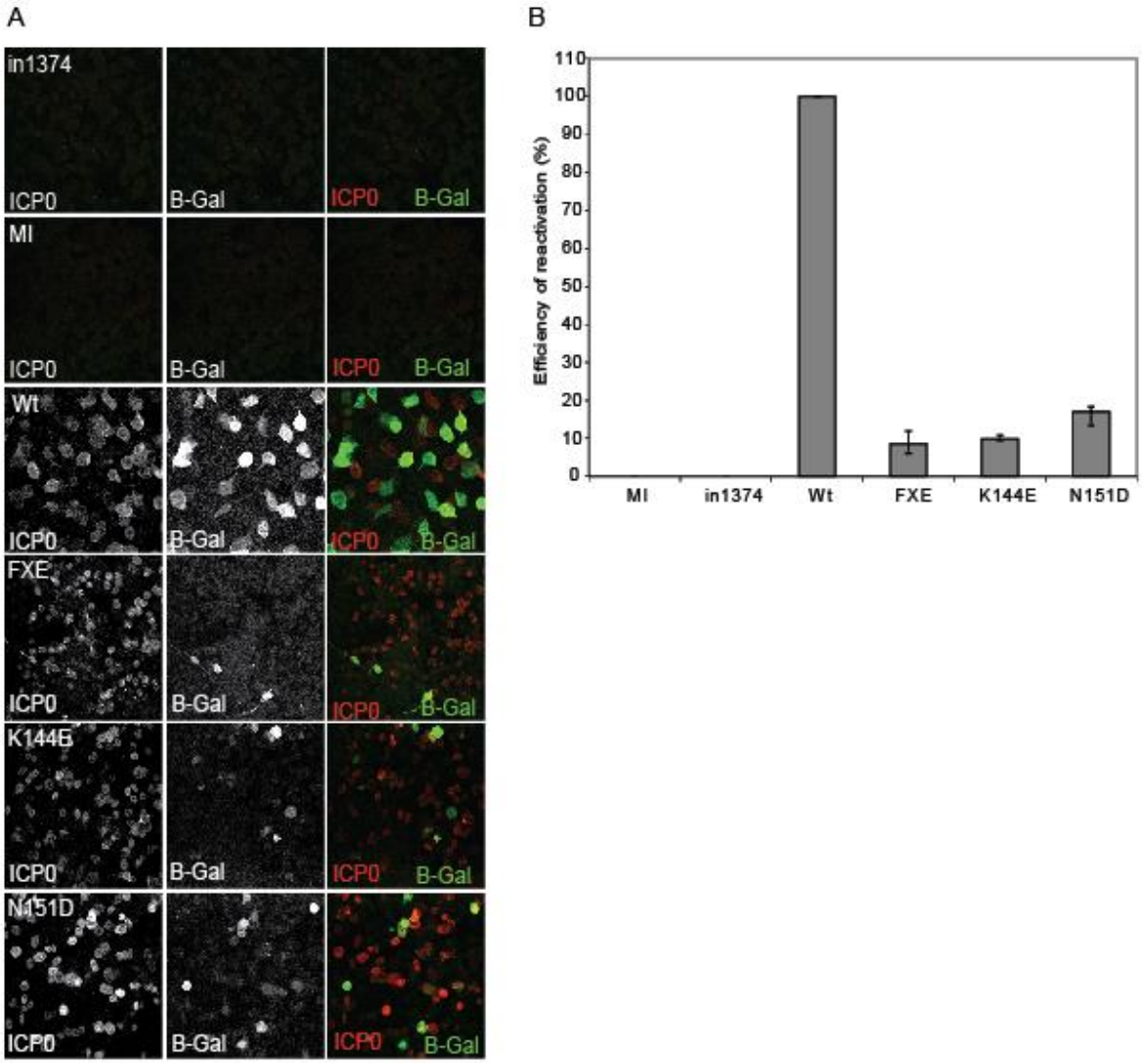

Figure 4.6 Immunofluorescence analysis of the reactivation of *in*1374 gene expression by wt and mutant ICP0 virus.

(A) Coverslips were treated the same way as the cells in the reactivation experiment (Figure 4.5) and fixed and permeabilised 24 hours after infection with wt and mutant ICP0 virus. The coverslips were stained for ICP0 (red) and β-galactosidase (green), with cells positive for β-galactosidase indicating reactivated viral gene expression.

(B) Quantification of cells on a single coverslip in (A) displaying reactivated gene expression compared to those expressing ICP0. Three random fields of view of cells infected with *in*1374 and wt or mutant ICP0 viruses were imaged. The cells expressing β-galactosidase were counted and calculated as a percentage of those positive for ICP0 expression, and the results shown as a percentage of the wt super-infected sample. The error bars represent the standard deviation obtained from three images.

4.3 Analysis of K144E/N151D double mutant virus infection

4.3.1 Construction of a recombinant virus which expresses ICP0 with both K144E and N151D mutations

Section 4.2.2 showed that at high input MOIs mutant viruses K144E and N151D replicated as efficiently as wt, but that at low MOIs these mutant viruses gave lower yields of infectious virus, particularly the K144E mutant, which had only slightly higher yields than FXE. Both mutant ICP0 proteins localised to ND10 but did not induce its dispersal efficiently, and K144E in particular showed delays in the rate of degradation of PML compared to wt infection. In addition, mutants K144E and N151D both had substantial defects on the efficiency of reactivation of quiescent HSV-1 genomes.

While the results of the previous chapter confirmed and extended those of Vanni *et al*. (Vanni *et al.*, 2012), which suggested that it was possible to separate the activities of ICP0 during lytic infection and reactivation/derepression, the results using the virus mutants showed a greater correlation between relative defects in plaque formation and reactivation. As explained in **Chapter 3**, a cell line expressing ICP0 with both these mutations was constructed to test whether the RING finger alpha-helix had a specific function in reactivation. The results showed that ICP0 containing both the K144E and N151D mutations had severe defects in both complementation of an ICP0-null mutant virus and reactivation of quiescent viral genomes, with less than 5% of wt ICP0 activity. The KE/ND results suggest that lytic infection and reactivation from quiescence do not affect an ICP0 function specific for reactivation, and the differences observed with the single substitution mutants may reflect a requirement for stronger ICP0 activity during reactivation. Therefore, to further analyse how these mutations affect ICP0's functions, and to determine if this was also the case in virus infection when other viral proteins are present, a virus containing both mutations was constructed.

The K144E and N151D double mutant (KE/ND) virus was constructed by transfecting cells with infectious *dl*1403 DNA, which contains a large deletion of the ICP0 gene (Stow & Stow, 1986), and a fragment of an ICP0 plasmid containing the complete ICP0 gene (including promoter, introns and 3' untranslated region) with both the K144E and N151D mutations (**section 2.6**). The ICP0 region containing the mutations recombined with the *dl*1403 DNA by homologous recombination. The virus stock produced from the

transfected cells was passaged on HFs to enrich for the presence of ICP0, the resulting virus populations were plaque purified, and single plaques were screened for the presence of ICP0 by Western blotting. After three rounds of plaque purification, the viral DNA of the final isolate was directly sequenced and was confirmed to have the desired KE/ND mutation. The initial passaging of the virus mixtures on HFs enriches for viruses having some ICP0 function, an approach which works very efficiently for those with wt activity, but which is less effective for mutants with only residual function, as in this case. Therefore it was necessary to screen a large number of plaques before the required isolate was identified.

The following sections describe the use of this double point mutant virus in the same assays used to investigate the single point mutants described previously. For comparison purposes, it was necessary to include the single point mutant viruses as controls in these experiments. Therefore some of the data below replicate data presented previously, in some cases illustrating differences in detail that often occur in the analysis of ICP0 mutant viruses due to technical aspects of their phenotype.

4.3.2 Mutant K144E and double mutant KE/ND have significant defects on plaque forming ability compared to wt HSV-1, especially in HFs.

To analyse the PFE of the double mutant KE/ND virus, plaque assays were conducted in HepaRG cells and HFs as described previously in **section 4.2.1.** Results were calculated as a ratio of plaques formed on U2OS cells and displayed as PFEs as a percentage of the ratio observed with wt virus (**Figure 4.7**). In this series of experiments, the PFEs of the positive control viruses Q148E and W146A viruses were lower than wt, but this was not considered significant as it was less than a two-fold reduction. These results differ slightly from those of the earlier series of experiments (**Figure 4.1**), but not in a way that affects the interpretation; differences of this magnitude in plaque assays are within normal experimental variation. In this series of experiments, mutant N151D plaque formation was reduced by three-fold compared to wt virus, whereas mutant K144E and the double mutant KE/ND had reduced plaque forming ability compared to wt by at least three orders of magnitude, a defect comparable to that of the RING finger deletion mutant FXE, with HFs producing fewer plaques than HepaRG cells.

Of note, mutant N151D had a higher PFE in this series of experiments (HepaRG cells 32%, HFs 25%) compared to the plaque assays in **section 4.2.1,** in which its plaque formation activity was reduced to a greater extent (HepaRG cells 17%, HFs 5%). These differences illustrate some of the difficulties of handling ICP0 mutant virus data, and in this case the final percentages depend on four different titration values for each mutant (titres of wt and mutant virus in the cells in question and U2OS cells). Even with replicate experiments, the usual variations in plaque assay data could explain the two-fold difference in HepaRG cell data between the two series of experiments with mutant N151D. Plaque assay data are even more variable in HFs due to the lack of linearity of plaque numbers with respect to dilution of ICP0-defective viruses (Everett *et al.*, 2004a). Therefore comparison between the absolute data for a given virus between different series of experiments is liable to variation, especially with the more defective viruses. Comparisons between different viruses within the same series of experiments are generally more reliable, at least in terms of indicating relative defects.

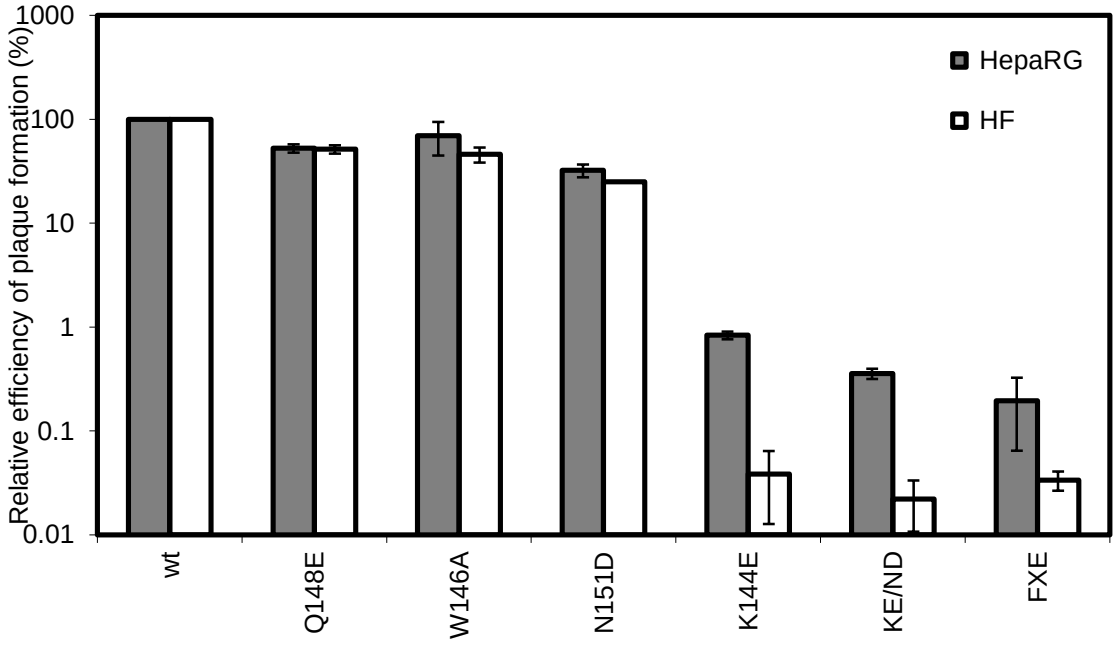

Figure 4.7 Plaque formation efficiencies of ICP0 mutant viruses in HepaRG cells and HFs.
Cells were infected with sequential ten-fold dilutions of wt or ICP0 mutant HSV-1. After adsorption, the cells were overlaid with medium containing human serum. The average PFE of each virus in both cell types was calculated as a ratio of plaques formed in U2OS cells and presented as a percentage of wt PFE ratio. The error bars represent the standard deviation obtained from three repeat experiments.

4.3.3 Mutants K144E and KE/ND give lower yields of infectious virus

Section 4.2.2, Figure 4.2 showed that the phenotype of the ICP0 alpha-helix mutants was most prominent in low multiplicity infections. Therefore, the yields of RING finger mutant viruses were investigated at MOI 0.01 and 0.001, in both HepaRG cells and HFs. At the lower MOI of 0.001, KE/ND and FXE failed to produce any infectious virus that could be counted on the titration plates, so this MOI was at the limit of detection for some of the mutants. Therefore, viral yield assays were carried out at MOI 0.01 only, infecting cells and titrating the virus produced after 24 hours on U2OS cells to calculate PFEs (**Figure 4.8**). As with the experiments presented at the beginning of this chapter, the W146A and Q148E mutant viruses were used as positive controls and were analysed alongside the double mutant KE/ND and single point mutants K144E and N151D.

As before, mutant viruses Q148E and W146A replicated as efficiently as wt with similar yields of infectious virus in both cell types. Mutant N151D showed lower viral yields in HepaRG cells and HFs compared to wt, but the defect was less than 5-fold (which is again a lesser defect than the corresponding results in the previous experiment of **Figure 4.2**). The yields of mutant viruses K144E and KE/ND were reduced by two orders of magnitude compared to wt in HepaRG cells. Within HFs, the reduction with K144E and N151D was three to four orders of magnitude, with KE/ND having viral titres only slightly above the input virus used for the experiment.

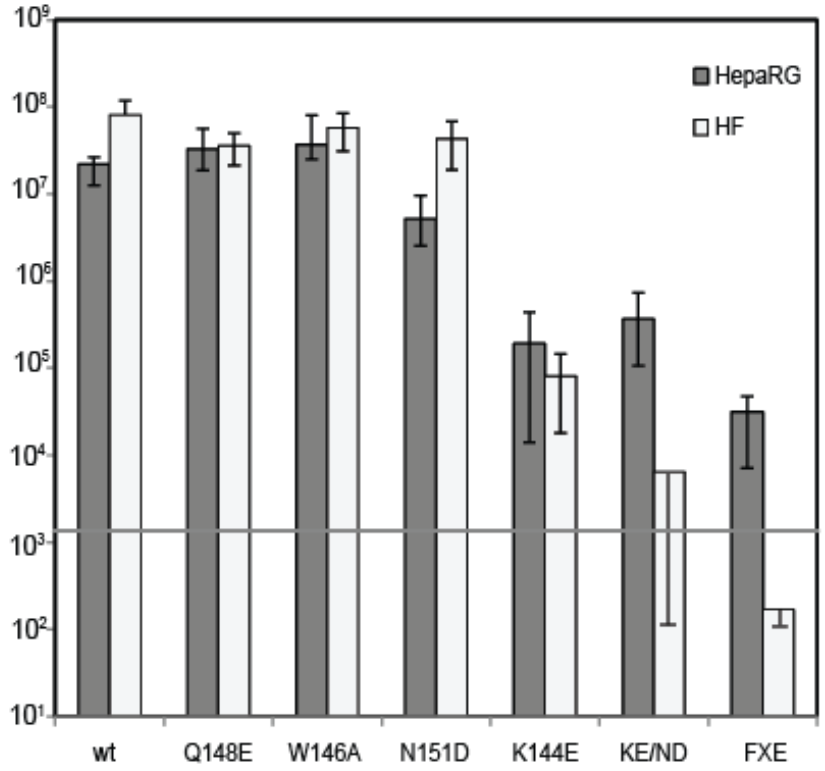

Figure 4.8 Viral yield assays of ICP0 mutant viruses in HepaRG cells and HFs at MOI 0.01.
HepaRG cells and HFs were infected at MOI 0.01, then 24 hours later the cells and supernatant were harvested, sonicated and titrated on U2OS cells as ten-fold dilutions to calculate PFEs. The error bars represent the standard deviation obtained from three repeat experiments (two repeats in the case of KE/ND and FXE, and the lower error bar representing the lowest detectable plaque number). The line on the graph at 10^3 represents the amount of input virus.

4.3.4 Virus mutants K144E and KE/ND colocalise with PML but have reduced abilities to degrade it

To investigate the effect of the RING finger mutants on ND10 proteins, the colocalisation of these proteins with ND10 protein component PML was investigated, as well as the rate of PML degradation. These experiments were carried out at a high MOI of 5 or 10 to ensure that all the cells were infected and therefore that comparisons of rates of protein degradation could be properly compared. The rate of degradation of PML was investigated over a time course of infection with samples harvested at 2, 4, 6 and 8 hours (**Figure 4.9**). In HepaRG cells (**Figure 4.9A**) infected with wt HSV-1, the majority of PML was degraded by two hours post infection, with only minimal amounts of unmodified PML remaining. This was also the case for the N151D mutant infected cells. In mutant K144E infected HepaRG cells, the majority of sumoylated PML was degraded by six hours post

infection, whereas in KE/ND infected cells there was no detectable PML degradation by the eight hour time-point, as was the case with FXE. The results with the single mutants here are consistent with those of **Figure 4.3**.

The rate of degradation of PML in HFs (**Figure 4.9B**) was delayed compared to HepaRG infected cells. Mutants K144E and KE/ND showed greatly reduced abilities to degrade PML in HFs, giving results that were comparable to the FXE deletion mutant. PML degradation was delayed in N151D infected cells compared to wt infection, with the majority of PML isoforms degraded at six hours post infection as opposed to four hours in wt infected cells. The differences observed in the rate of degradation of PML in both cell types is not related to the amount of ICP0 expressed, as all of the mutants had similar levels of expression of ICP0 as wt at each time-point. There is a clear correlation between the efficiencies of plaque formation, replication and the rate of PML degradation in HFs of the single and double mutant viruses.

During lytic infection, gene expression proceeds in a temporally regulated cascade that can be divided into three phases; IE, early and late. Gene expression of each class of genes was analysed at the same time as PML degradation at MOI 5 (**Figure 4.9**). However, at such a high MOI the potential deleterious effects of the ICP0 mutations on viral gene expression would be at least partially marked. In HepaRG infected cells (**Figure 4.9A**), the expression of the early protein UL42, a DNA replication accessory protein, showed only a slight decrease in expression in the RING finger mutants compared to wt at this MOI, but expression in FXE infected cells was delayed. The late capsid protein VP5 expression was slightly delayed in N151D and K144E infected cells, with more of a delay occurring in KE/ND and FXE infected cells. In HFs (**Figure 4.9B**), UL42 expression was delayed in the RING finger mutant virus infections, and this was more pronounced in K144E and KE/ND infected cells. Late gene expression was slightly lower in N151D infected cells compared to wt, but expression levels showed a considerable delay in K144E and KE/ND infected cells and were comparable to FXE.

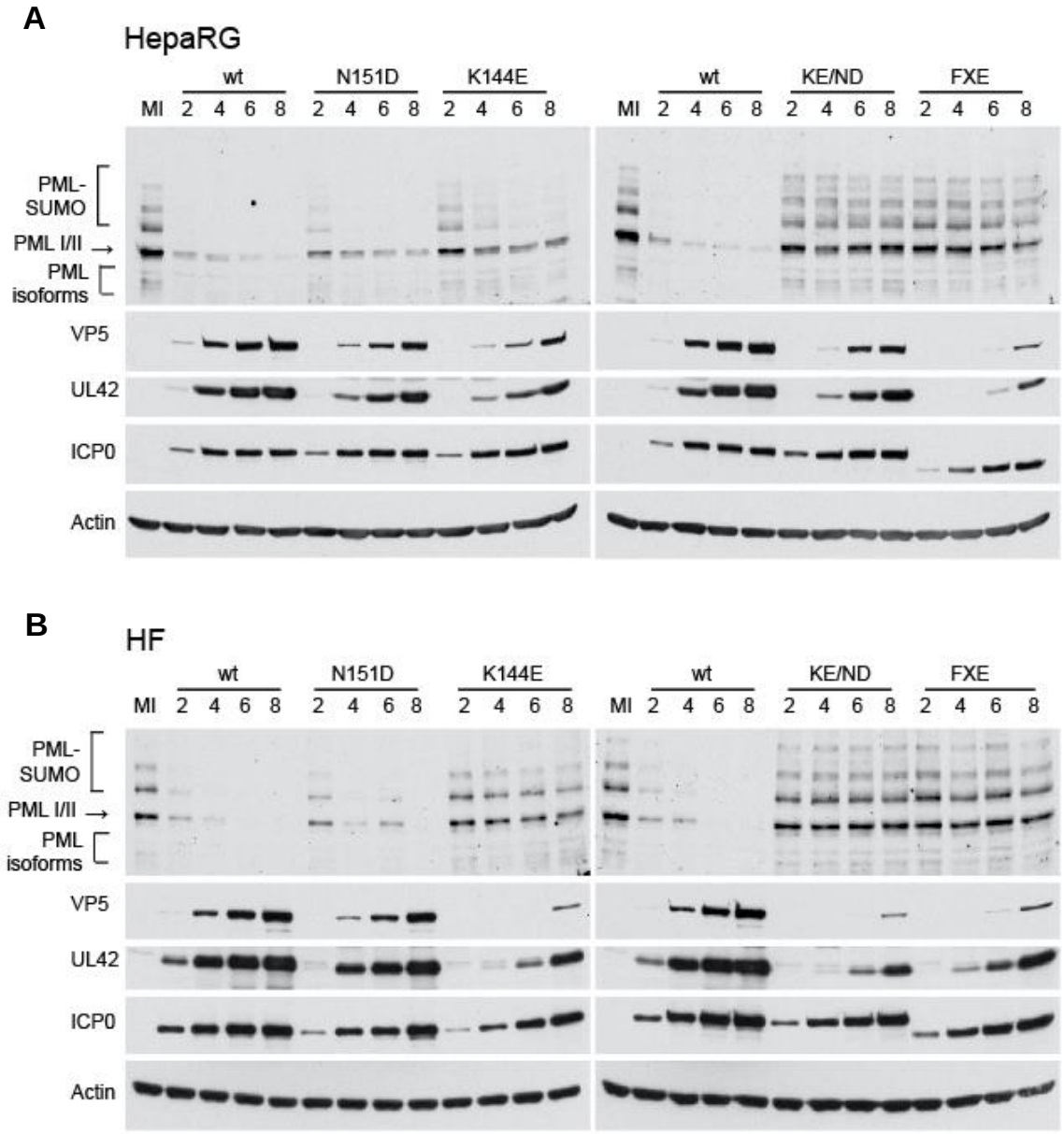

Figure 4.9 The degradation of PML isoforms and viral gene expression during infection by wt ICP0 and mutant viruses in HepaRG cells and HFs.
HepaRG cells (A) and HFs (B) were infected with wt or mutant viruses at MOI of 5 and harvested at 2, 4, 6 and 8 hours post infection. The proteins were resolved on a 7.5% SDS gel, transferred to a nitrocellulose membrane and detected by probing for PML, ICP0, UL42, and VP5 representing IE, early and late classes of viral proteins.

The effects of the alpha-helix mutations on the localisation and dispersal of PML were investigated by immunofluorescence (**Figure 4.10**). HFs were infected at MOI 10, and the localisation of PML was analysed at two and four hours post infection by staining for PML and ICP0. As expected, the results showed that in uninfected cells the PML was in distinct nuclear foci, whereas in wt infected cells by two hours post infection the PML had been dispersed. In mutant N151D infected cells at two hours post infection the majority of PML

had been dispersed but in a minority of cells (about 10%) the PML remained in distinct foci that showed colocalisation with ICP0. By the four hour time-point however, in all N151D infected cells the PML had been dispersed. In K144E and KE/ND infected cells, the PML remained in distinct foci that colocalised with ICP0, and these mutants behaved like FXE at two and four hours post infection. These results correlate with the relative rates of PML degradation as assayed by western blotting.

The immunofluorescence of cells infected with mutant N151D at MOI 10 showed that in the majority of cells the PML is dispersed by two hours post infection and is dispersed in all cells by four hours post infection. This result is different to that of the experiment done at MOI 5 (**Figure 4.4**), which showed by four hours post infection N151D mutant ICP0 showed colocalisation with PML and did not induce its dispersal. At the higher MOI, N151D is more likely to initiate lytic infection more efficiently, thereby producing more ICP0 and inducing the degradation of PML more quickly than at the lower MOI. This is consistent with the increased rate of PML degradation induced by the N151D mutant virus in these later experiments (compare **Figures 4.3** and **Figure 4.9**). However, it is also true that plaque formation and replication of the N151D mutant stock used in these experiments were more efficient in these later experiments. These apparent inconsistencies probably reflect the inherent difficulties of working with ICP0 mutant viruses, as the results are very sensitive to input MOI, which is dependent on accuracy of the stock titres, which in turn may vary enough to affect the detail of experimental outcomes due to factors such as the relative status of the cells when the titres were determined.

The infection experiments carried out at high MOIs showed that the N151D induced the dispersal of PML, whereas, in the inducible cell line experiments (**section 3.2.1**), ICP0 showed colocalisation and did not induce PML dispersal after 24 hours of ICP0 expression. One possible explanation for the differing results between the two experimental systems is the antibodies used. The inducible cell line immunofluorescence experiments were carried out using anti-PML antibody (Bethyl) that was later shown to cross-react with ICP0 when expressed at high levels, which is what occurs in these RING finger mutants. Therefore, a different antibody was used for these virus infection studies.

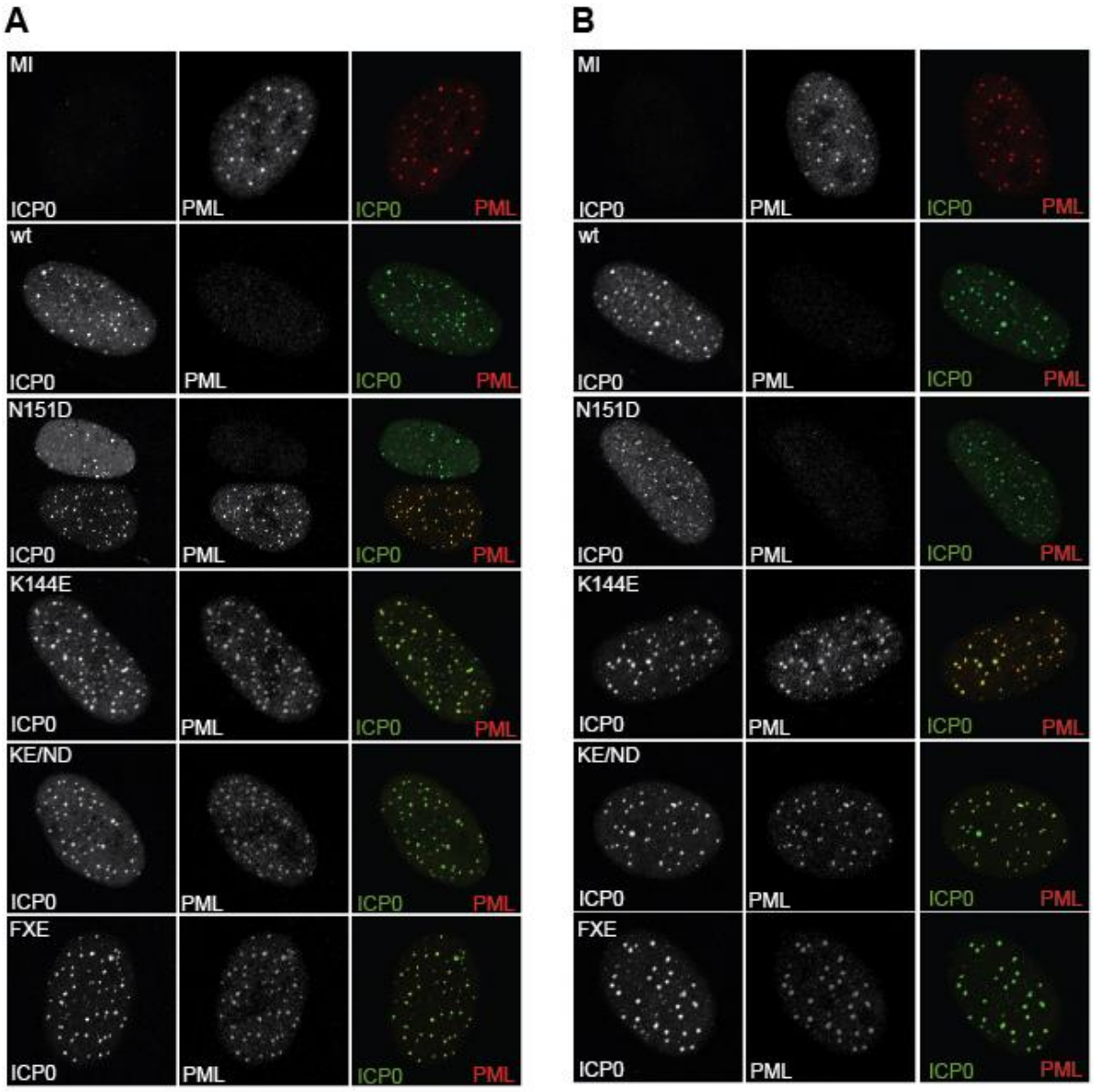

Figure 4.10 ICP0 expression and PML dispersal in wt and ICP0 mutant virus infected HFs at two and four hours post infection.
HFs were infected at MOI 10 with the indicated viruses, and at two (**A**) and four (**B**) hours post infection the cells were fixed and stained for ICP0 (green) and PML (red).

4.3.5 Degradation of SUMO-modified Sp100 during infection with the RING finger mutants

Sp100 is a permanent ND10-associated protein that exists in several isoforms due to alternative splicing and can be modified by SUMO. SUMO-modification of Sp100 is not required for its localisation to ND10, but this is PML-dependent (Muller & Dejean, 1999; Sternsdorf *et al.*, 1997). During HSV-1 infection, the RING finger domain of ICP0 induces the degradation of SUMO-modified Sp100 (Chelbi-Alix & de The, 1999; Muller

& Dejean, 1999). However, depletion of PML in uninfected cells also leads to the desumoylation of Sp100 (Everett *et al.*, 2006), and therefore it is possible that ICP0 does not target Sp100 directly, and that its desumolyation is an indirect consequence of PML degradation.

The rates of Sp100 degradation in HepaRG cells and HFs were investigated (**Figure 4.11**) at MOI 5, over the course of an eight hour infection with the ICP0 alpha-helix mutants. The results in HepaRG cells (**Figure 4.11A**) showed that wt virus caused degradation of SUMO-modified Sp100 by two hours post infection, with only unmodified Sp100 being detected. The degradation of SUMO-modified Sp100 was slightly delayed in N151D mutant infected cells, to four hours post infection. In cells infected with mutants K144E and KE/ND, the majority of SUMO-modified Sp100 had been degraded by the eight hour time-point, and there was also some degradation in FXE infected cells. The relative loss of the sumoylated form of Sp100 in KE/ND and FXE mutant infected cells contrasts with the failure of these mutants to degrade PML, which suggests that different mechanisms may be operating between the different cellular proteins, PML and Sp100. Within infected HFs (**Figure 4.11B**), there was a two hour delay in the degradation of SUMO-modified Sp100 by wt HSV-1 and the N151D mutant compared to the rates seen in HepaRG cells. By eight hours post infection, KE/ND and FXE infected cells had levels of SUMO-modified Sp100 similar to those in the wt infection at two hours, with K144E exhibiting an intermediate phenotype. That at least some loss of sumoylated Sp100 occurred, again contrasts with the apparent failure of these mutants to affect PML under similar experimental conditions, suggesting that loss of SUMO-modified Sp100 is PML-independent under these experimental conditions.

Despite differences in detail in their effects on PML and sumoylated Sp100, the overall relative activities of the mutants follow a similar pattern in these assays. Therefore, mutants K144E and KE/ND have the most greatly reduced abilities to degrade PML and reduce the sumolylated forms of Sp100. Also, the efficiency of the degradation of the ND10 proteins correlates with the efficiency of plaque formation and replication.

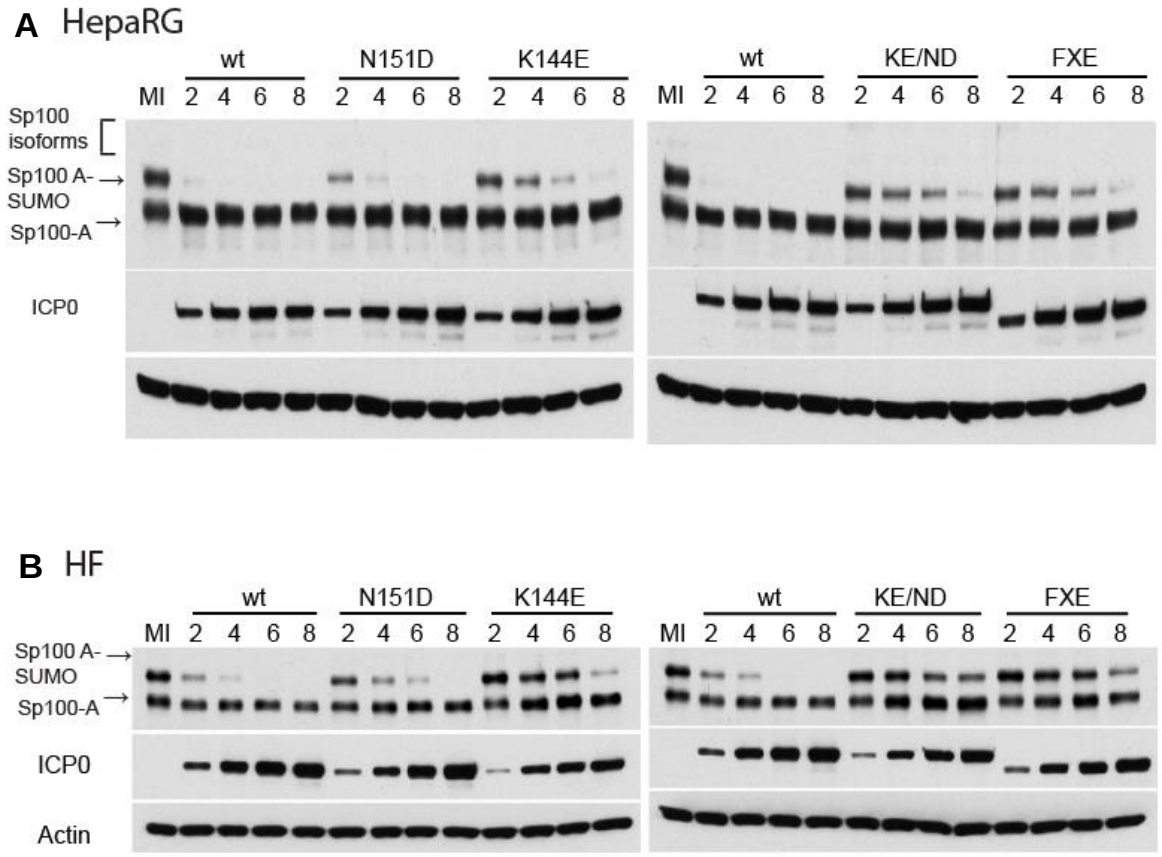

Figure 4.11 The rate of degradation of sumoylated Sp100 during infection with wt and RING finger mutant viruses in HepaRG cells and HFs.
HepaRG cells (A) and HFs (B) were infected with wt ICP0 or mutant viruses at MOI 5 and harvested at two, four, six and eight hours post infection. The proteins were resolved on a 7.5% SDS gel, transferred to a nitrocellulose membrane and detected by probing for Sp100, ICP0 and actin.

4.3.6 Viral gene expression is delayed in the alpha-helix mutant virus infections

At the high MOI of 5, the rate of viral gene expression was not greatly affected in the RING finger mutant infections of HepaRG cells, and was only substantially delayed for late protein VP5 in K144E and KE/ND mutant infected HFs (**Figure 4.9)**. However, the effects of the ICP0 mutations on viral gene expression might be concealed due to the high MOI. Therefore, viral gene expression was investigated using a lower MOI (MOI 1) over the course of an eight hour infection (**Figure 4.12**).

In the wt ICP0 and alpha-helix mutant infected HepaRG cells (**Figure 4.12A**), there was a similar level of ICP0 expression, which was slightly delayed in FXE infected cells.

Expression of the early protein UL42 was detected in wt infected cells from four hours onwards, and this was also the case in N151D infected cells, although the level of expression was lower at each time-point. K144E and KE/ND infected cells exhibited substantially delayed UL42 expression compared to wt, with strong expression only occurring at the eight hour time-point. VP5 expression was extensively delayed in the RING finger mutants, with K144E and KE/ND having the greatest effect on VP5 expression. FXE infected cells showed very low expression levels of UL42 at eight hours post infection and no detectable expression of the VP5 capsid protein. In infected HFs (**Figure 4.12B**), ICP0 expression was similar in the RING finger point mutants compared to wt, with levels of ICP0 expression delayed in FXE infected cells. UL42 expression was delayed in N151D infected cells, with strong expression occurring at eight hours post infection as opposed to six hours in wt infected cells, and this was the same for VP5 expression. There was no detectable expression of UL42 or VP5 proteins in K144E and KE/ND infected cells throughout the eight hours, and this was the same with FXE infected cells.

The differences between the gene expression profiles at MOI 5 (**Figure 4.9**) and MOI 1 (**Figure 4.12**) highlight the substantial effect that choice of MOI has on experimental output when analysing ICP0 mutant viruses. Given inherent variations in determination of virus titre stocks, these data suggest that even two-fold differences between true and determined virus titres could have substantial experimental consequences. The viral gene expression during virus infection results confirm previous results using transfection assays that used different concentrations of plasmid DNA and found that both the N151D and K144E mutations had a significant effect on ICP0's ability to activate gene expression, but that K144E had the most substantial defect and was comparable to FXE (Everett *et al.*, 1995).

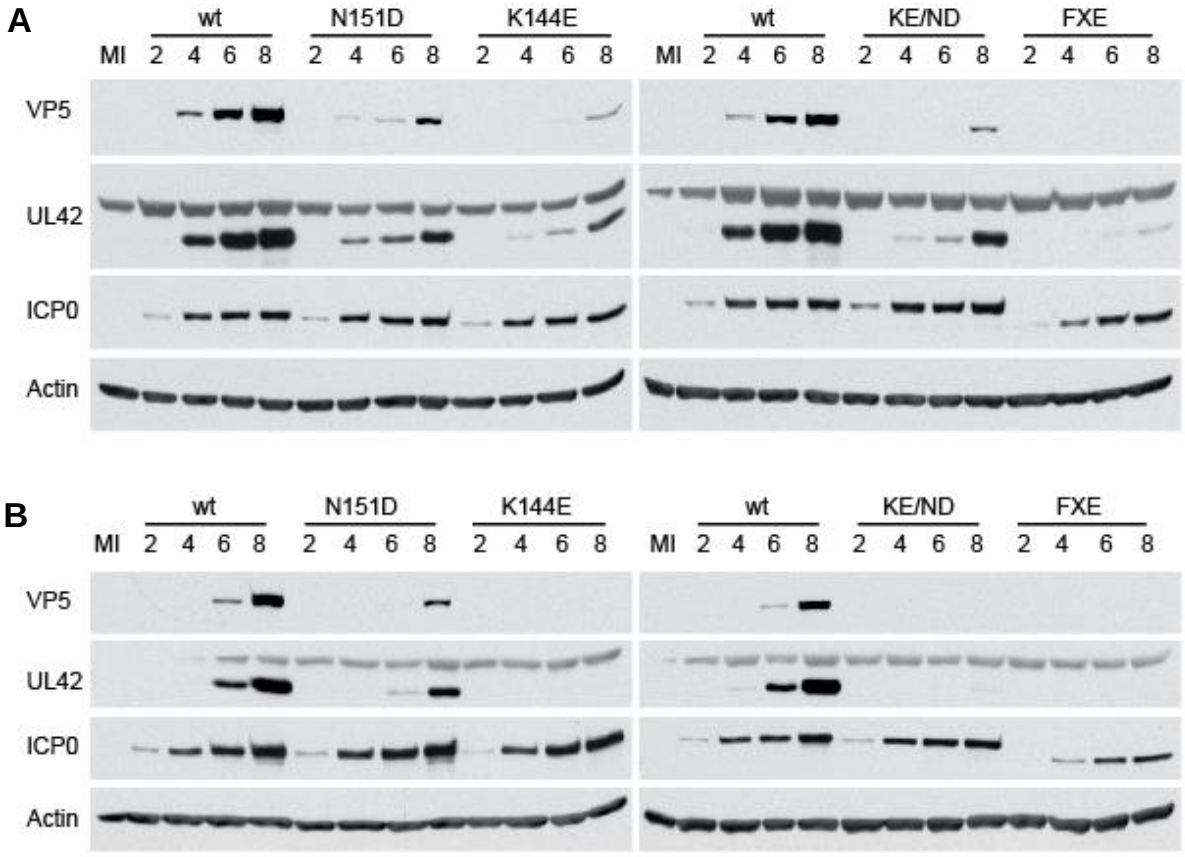

Figure 4.12 Viral gene expression during infection with RING finger mutants compared to wt HSV-1 in HepaRG cells and HFs.
HepaRG cells (A) and HFs (B) were infected at MOI 1 and harvested at two, four, six and eight hours post infection. Samples were analysed by Western blotting using antibodies against ICP0, UL42 and VP5, to represent the IE, early and late classes of genes, respectively. Actin was used as a loading control.

4.3.7 Analysis of the abilities of the ICP0 alpha-helix mutant viruses to inhibit the recruitment of ND10 proteins to viral genomes.

ICP4 is an IE protein and functions as a transcriptional activator of early and late gene transcription by interacting with the transcriptional preinitiation complex (Smith *et al.*, 1993). ICP4 binds strongly to viral DNA and is recruited to replicating viral genomes at the early stages of infection to form discrete foci, most of which are associated with ND10 (Everett *et al.*, 2003). At early stages of viral infection, ICP4 shows an asymmetric arch-like distribution inside the nucleus of newly infected cells or cells at the edges of a developing plaque (Everett & Murray, 2005). In the absence of ICP0, ND10 components including PML and Sp100 are recruited to sites associated with the ICP4 complexes and with the viral genomes (Everett & Murray, 2005; Everett *et al.*, 2004b). This recruitment also occurs in wt infected cells, but due to ICP0 disrupting ND10 and inducing the

degradation and/or dispersal of PML and other ND10 proteins, this process is transient and difficult to detect (Everett & Murray, 2005). Unlike the formation of ND10 which is PML-dependent (Ishov *et al.*, 1999; Zhong *et al.*, 2000), the recruitment of Sp100 and hDaxx proteins to viral genomes occurs independently of PML (Everett *et al.*, 2006).

The recruitment of ND10 proteins (PML, Sp100 and hDaxx) was investigated by immunofluorescence staining for ICP4 and the ND10 proteins (**Figure 4.13**). In wt infected HFs, the majority of PML signal was dispersed, and any remaining foci were not recruited to sites associated with viral genomes. PML was also dispersed in the majority of N151D infected cells. However, in less than 5% of N151D infected cells, there was some faint recruitment of PML to viral genomes, which occurred in cells that had very low amounts of ICP4. In contrast, there was marked recruitment of PML in cells infected with K144E, KE/ND or FXE viruses (**Figure 4.13A**). There was also recruitment of Sp100 in N151D infected cells when ICP4 levels were low, but no recruitment was detected when the ICP4 foci were better developed. Sp100 (**Figure 4.13B**) and hDaxx (**Figure 4.13C**) recruitment supported the PML results with K144E and the double mutant KE/ND. These results therefore suggest K144E and KE/ND mutations in ICP0 are defective in their ability to inhibit the recruitment of these cellular repressors to viral genome sites through their inefficient degradation.

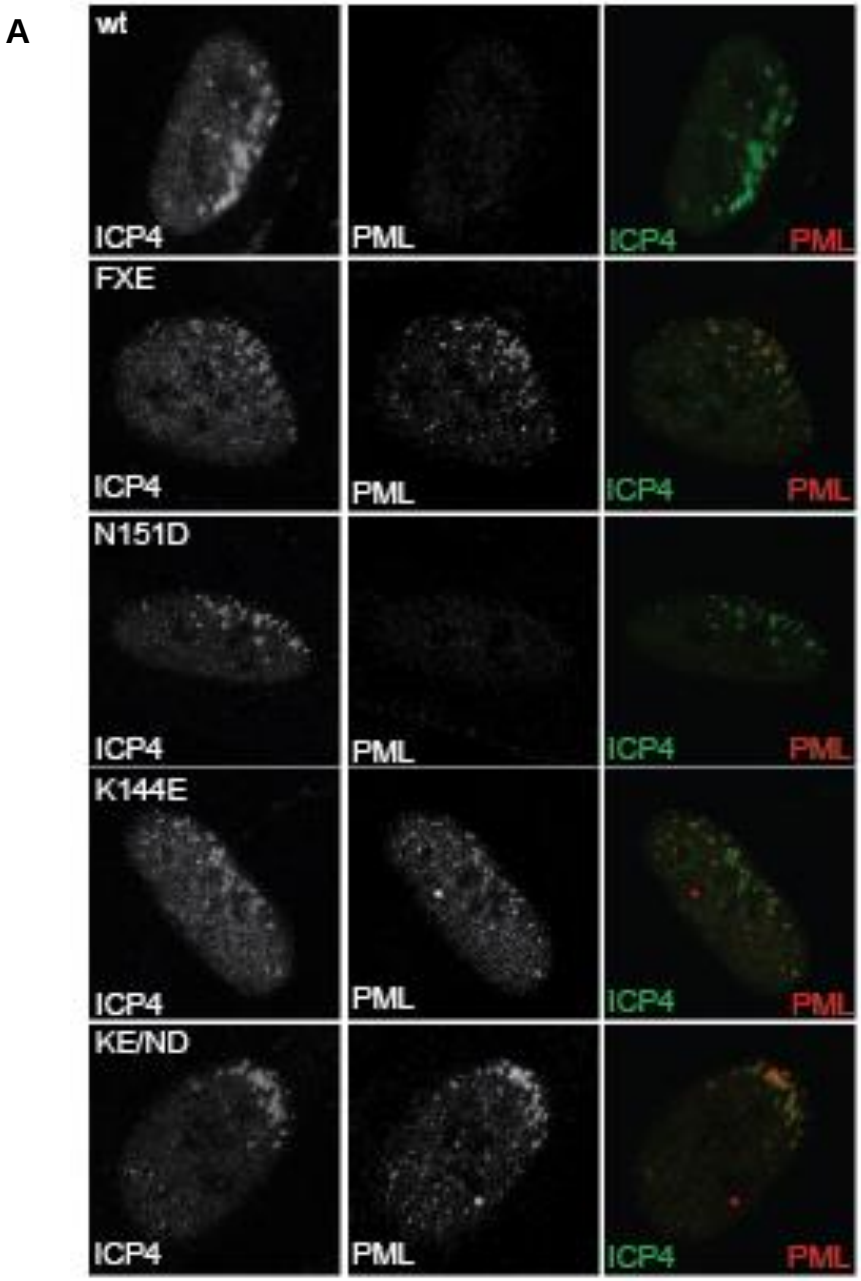

Figure 4.13 Immunofluorescence analysis of the recruitment of ND10 proteins to viral genomes at the early stages of HSV-1 infection by wt and RING finger mutant viruses.

Cells were infected with wt/mutant viruses at low MOI and stained for ICP4 (green) and ND10 proteins (red), PML (**A**), Sp100 (**B**) and hDaxx (**C**) the following day. Cells at the edges of plaques showing an asymmetric distribution of ICP4 were selected, as these cells represent the early stages of infection, with ICP4 indicating the location of the viral genomes.

B

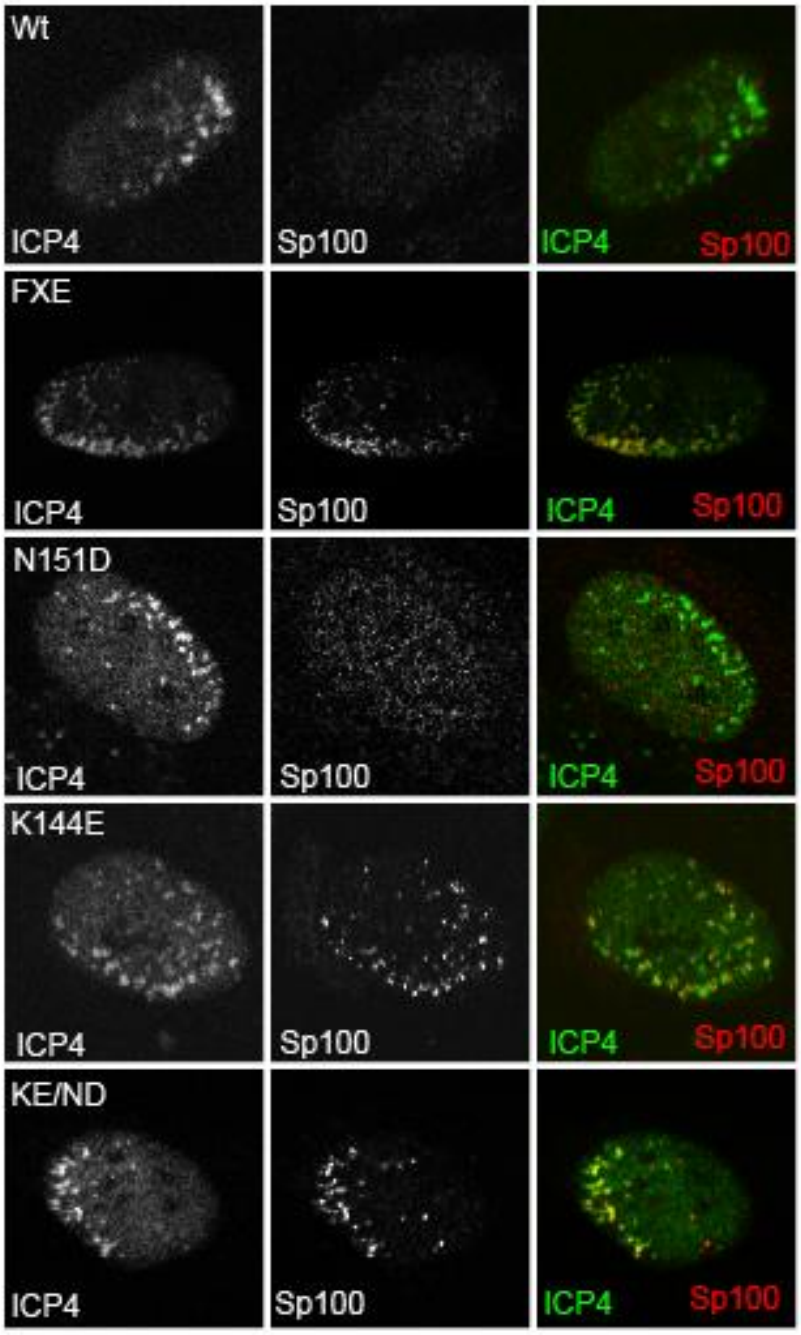
Wt
ICP4
Sp100
ICP4
Sp100
FXE
ICP4
Sp100
ICP4
Sp100
N151D
ICP4
Sp100
ICP4
Sp100
K144E
ICP4
Sp100
ICP4
Sp100
KE/ND
ICP4
Sp100
ICP4
Sp100

C

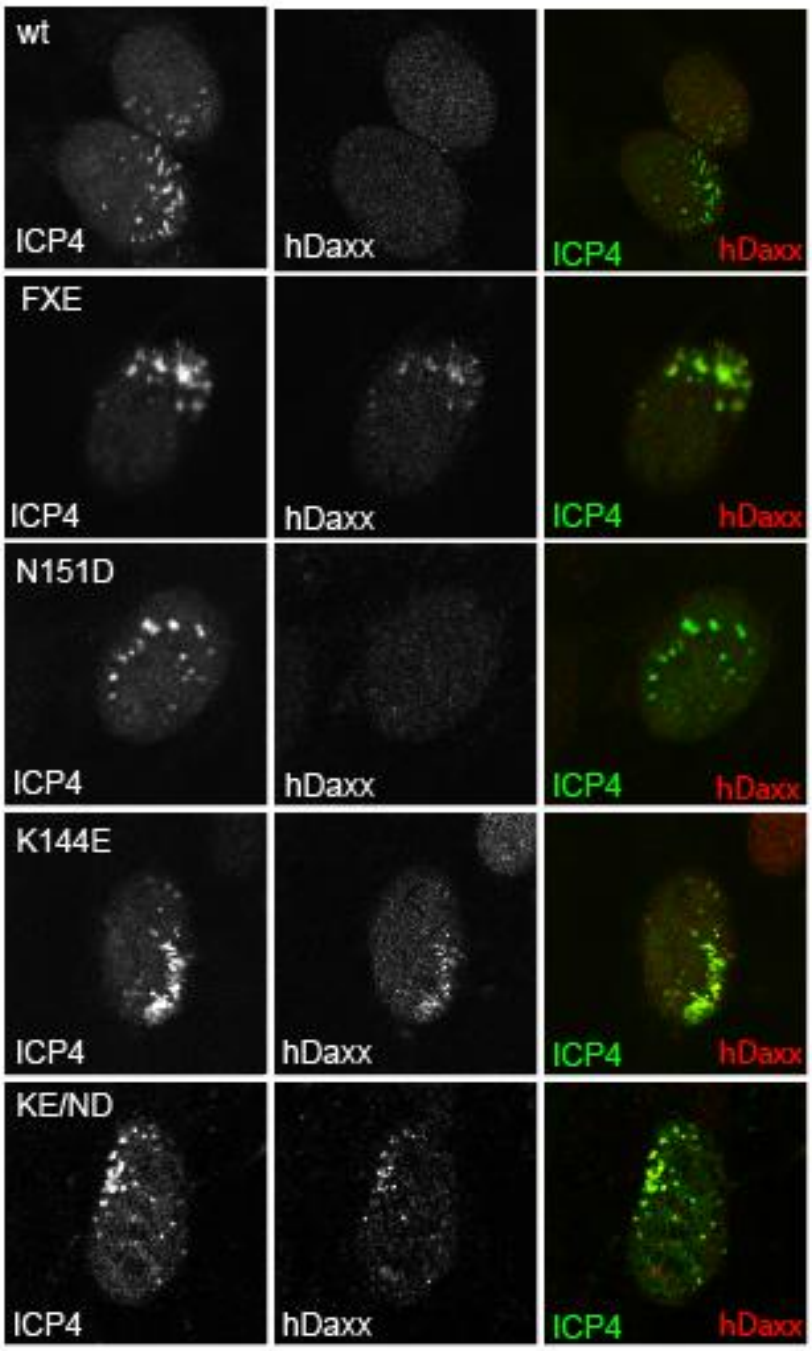
wt
ICP4
hDaxx
ICP4
hDaxx
FXE
ICP4
hDaxx
ICP4
hDaxx
N151D
ICP4
hDaxx
ICP4
hDaxx
K144E
ICP4
hDaxx
ICP4
hDaxx
KE/ND
ICP4
hDaxx
ICP4
hDaxx

4.3.8 Investigation of the degradation of a further ICP0 substrate

It is possible that the mutations in the alpha-helix of the RING finger domain affect ICP0's interactions with substrates, components of the ubiquitin conjugation machinery, or both. They could therefore cause differential defects in the rate of degradation amongst different ICP0 substrates. The effects of the alpha-helix mutations on the degradation of two main ICP0 substrates (PML and Sp100) have been presented in **section 4.3.4** and **section 4.3.5,** with each substrate having a similar degradation profile. Therefore, the degradation of another recently identified ICP0 substrate was investigated.

Protein ZBTB10 (zinc finger and BTB domain protein 10) belongs to a family of proteins that has been implicated in transcriptional regulation, particularly repression of transcription (reviewed in Lee & Maeda, 2012. The C-terminal end of ZBTB proteins contains a zinc finger domain that binds specific DNA sequences, and the N-terminal BTB domain mediates interactions with other proteins (reviewed in Lee & Maeda, 2012). ZBTB10 was identified as a potential ICP0 substrate in a screen for proteins that were destabilized during HSV-1 infection (E. Sloan, unpublished data), and the rate of degradation of the ZBTB10 protein was investigated during infection with the RING finger mutant viruses.

HepaRG cells were infected at a MOI 5 and the results (**Figure 4.14**) showed that in wt infected cells ZBTB10 was degraded at early time points of infection, with the majority being degraded by the four hour time-point. Mutants N151D and K144E showed a delay in degrading ZBTB10, and this delay was more pronounced in K144E infected cells. The double mutant KE/ND achieved only slight degradation of ZBTB10 at eight hours post infection and was comparable to FXE, showing that the double mutant was defective in degrading ZBTB10. The defects in RING finger mutants in degrading ZBTB10 were not due to differences in the levels of ICP0 expression, as the levels of ICP0 during infection with the mutant viruses were similar to the expression level of the wt virus. ZBTB10 degradation followed the same pattern as PML and Sp100 degradation, with the rate of degradation by mutants N151D and K144E delayed, with K144E showing the greater effect, and only minimal degradation occurring in the double mutant KE/ND infected cells.

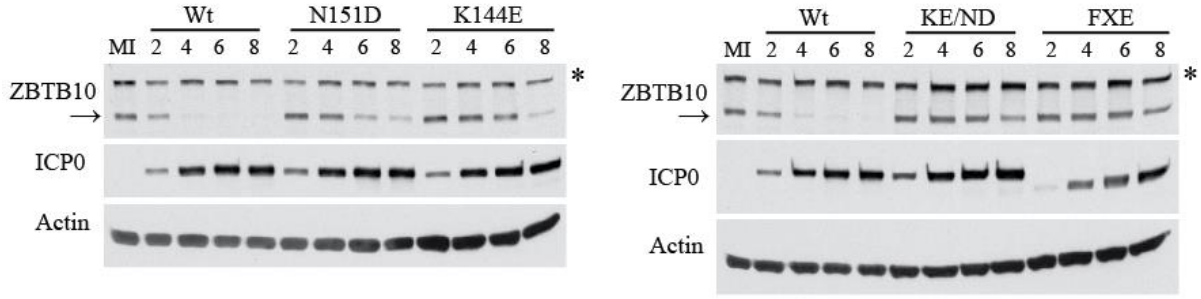

Figure 4.14 Rate of degradation of ZBTB10 during infection by the RING finger mutant viruses.
HepaRG cells were infected at MOI 5 and harvested at two, four, six and eight hours post infection. The arrow indicates the ZBTB10 specific band and the asterisk denotes a non-specific band.

4.3.9 Mutants K144E and KE/ND greatly reduce the efficiency of reactivation in quiescently infected cells while the N151D mutation caused a lesser defect

In a final experiment to analyse the phenotype of the KE/ND double mutant virus, reactivation of β-galactosidase expression in HepaRG cells quiescently infected with *in*1374 was analysed by immunofluorescence (**Figure 4.15**), using the same methodology as described for **Figure 4.6**. Quantification of the immunofluorescence images showed that mutant N151D was 40% as effective as wt in reactivating viral gene expression in quiescently infected cells, whereas mutants K144E and KE/ND had significant defects on reactivation. Of note was that infections with wt and mutant viruses were done at MOI 5, under conditions in which lytic infection with the RING finger mutants was progressing at a similar rate to wt with regard to viral gene expression (see **Figure 4.9**).

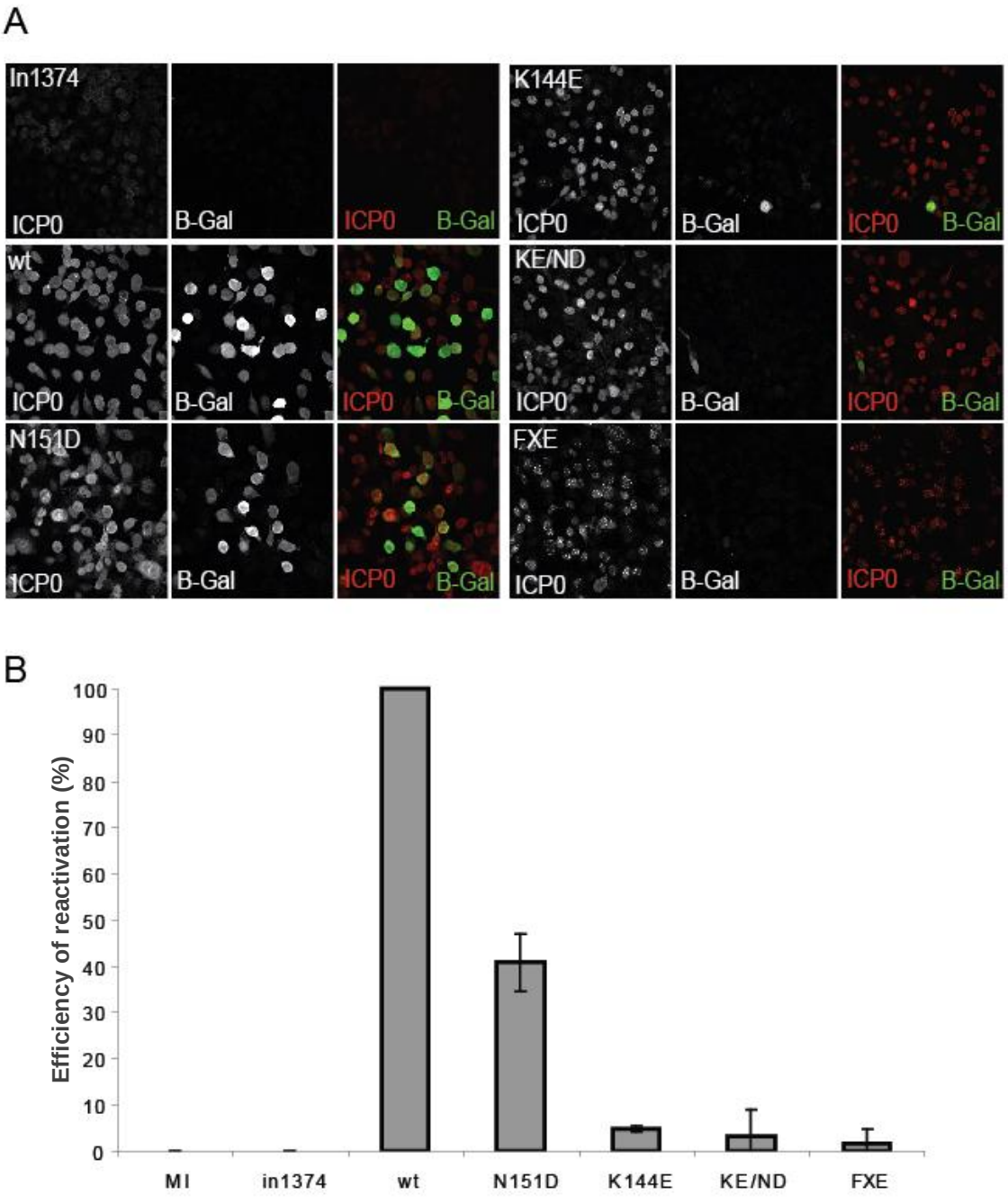

Figure 4.15 Immunofluorescence analysis of the reactivation of viral gene expression by wt and mutant ICP0 virus.

(A) Cells on coverslips were infected with *in*1374 at MOI 5, and 24 hours later superinfected with wt or ICP0 mutant viruses at MOI 5. After virus adsorption, the cells were overlaid with medium containing 50 μM ACV and 1% human serum. The cells were fixed and permeabilised 24 hours later, then stained for ICP0 (red) and β-galactosidase protein (green). Cells positive for β-galactosidase indicate reactivated viral gene expression of the *in*1374 virus.

(B) Quantification of cells displaying reactivated viral gene expression compared to those expressing ICP0 as seen in (A). Three random fields of view of cells were imaged and the cells expressing β-galactosidase protein were counted and calculated as a percentage of those positive for ICP0 expression. The results are shown as a percentage of the wt ratio. The error bars represent the standard deviation obtained from three images.

The results from each of the reactivation experiments correlate with those obtained for the plaque assays with each of the mutants (**Figure 4.1** and **Figure 4.7**). However, during the reactivation experiment, the infections with the alpha-helix mutant viruses and wt were carried out at an MOI 5, at which all the cells should have been productively infected over a 24 hour period if ACV was not present. In HepaRG cells infected at MOI 5 (**Figure 4.9**), the IE and early gene expression in the alpha-helix mutants is comparable to wt expression levels, and late gene expression is only slightly delayed in these mutants. Therefore, the defect in reactivation efficiency seen with mutants K144E, KE/ND and FXE occurs under conditions in which lytic gene expression should be progressing normally (see **Figure 4.9**). It has previously been thought that failure of ICP0 mutant viruses to reactivate quiescent HSV-1 genomes, despite lytic replication of the superinfecting virus, could be due to genome competition resulting from the high MOI required to get the mutants replicating. However, in the experiments presented here this should have been overcome by the use of ACV and MOIs based on titres in U2OS cells, and thus the number of superinfecting viral genomes should have been equivalent in all infections. Therefore, there appears to be a differential in the results for reactivation over lytic infection under these experimental conditions, which was especially the case for K144E. However, before this can be confirmed the viral gene expression of early and late genes in the reactivated cells should be confirmed to show that gene expression has proceeded beyond the IE stage and ICP0 expression. Nonetheless, based on the gene expression profiles of the mutants at the same MOIs (**Figure 4.9**), this is expected over a 24 hour period.

Reactivation efficiency for N151D in this assay was considerably higher than the previous reactivation assay (**Figure 4.5** and **Figure 4.6**), and this was also the case for N151D PFE. As discussed previously, the higher activity of N151D observed here could be due to slight differences in the viral titres of the stocks used for each set of assays.

4.4 Conclusion and Discussion

The viral infection experiments described in this chapter show that at high input MOIs the alpha-helix mutants replicated as efficiently as wt and had no major defects in early and late gene expression. However, mutants K144E and KE/ND had a substantial delay in degrading PML compared to wt. At lower MOIs, the phenotypes of the RING finger mutants were more noticeable, with K144E and KE/ND giving lower yields of infectious virus and the expression of early and late genes by all the RING finger mutants was

delayed compared to wt, with the delay more pronounced with VP5 (a typical late protein). In all the above assays, the N151D mutant was less defective than the other mutants. The ability of the mutants to reactivate gene expression in quiescently infected cells correlates with their relative abilities to degrade PML and their activities in viral yield and plaque formation assays. Again, mutant N151D was the least defective, with mutants K144E and KE/ND having substantial defects that were comparable to the RING finger deletion mutant FXE.

In the later series of assays carried out alongside the double mutant KE/ND, mutant N151D had increased activity in assays of PFE, viral yield and reactivation efficiency (**sections 4.3.2-4.3.9**) compared to the assays carried out at the beginning of this chapter (**sections 4.2.1-4.2.4**). This could be due to slight differences in viral titres as a fresh plate stock of virus was produced for each set of assays. However, both sets of assays show that N151D activity was greater than that of the FXE, K144E and KE/ND mutants, and is closer to that of wt virus, especially in HepaRG cells. Mutants K144E and KE/ND were highly defective in both sets of assays, with the double mutant tending to be even more defective than K144E and quite similar in phenotype to that of the deletion mutant FXE.

It was possible that the mutations in the alpha helix of the RING finger domain affect ICP0 interactions with substrates and it is likely that the mutations also affected the degradation of other ICP0 substrates (other proteins that have repressive effects), in a similar manner to that of PML. This was shown to be the case with the rates of degradation of Sp100 and ZBTB10 mirroring those of PML. Therefore, PML may be a good indicator of ICP0 activity but not necessarily the only important target (indeed, it is highly likely that there are several biologically relevant substrates of ICP0).

The data from the virus infected cell experiments do not fit easily with the original hypothesis arising from the work of Vanni et al. (2012) that, as demonstrated by mutant N151D, which has a greater defect in reactivation compared to complementation of an ICP0 null mutant virus, the activities of ICP0 involved in stimulating lytic infection may be separable from those required for reactivation. This hypothesis suggests that the RING finger helix provides an interface that is required mainly for the former function. The results using mutant N151D in the inducible cell line chapter were by and large consistent with the work of Vanni et al., and were extended to mutant K144E which showed a similar phenotype. However, as discussed in chapter 3, the results from the double mutant KE/ND

(which has substantial defects on both lytic infection and reactivation from quiescence) were more consistent with the hypothesis that greater ICP0 activity is required for reactivation than for the initial stimulation of lytic infection, and that the RING finger helix is required for both functions. At first sight, the virus infected cell experiments also show a good correlation between lytic infection and reactivation from quiescence in terms of the relative defects of the mutants examined. There is one important qualification to this conclusion, however. The viral infection reactivation experiments were performed at an MOI at which ICP0 is not essential for lytic viral gene expression (as illustrated by expression of UL42 and VP5 in parallel experiments), yet induction of reactivation was very inefficient. This suggests that ICP0 is almost essential for reactivation or derepression of quiescent HSV-1 genomes in cultured cells, even under conditions in which it is dispensable for lytic infection.

The efficiency of reactivation by each of the alpha-helix mutants correlates with PML degradation, viral yield and PFE. The differences in ICP0's activity in the RING finger helix mutants may be due to effects on the efficiency of substrate recognition by ICP0, or they may affect its E3 ligase activity by hindering its interactions with the E2 ubiquitin-conjugating enzymes. Indeed, it has been previously shown that the alpha-helix and loop regions of the RING finger domain of ICP0 are involved in the interactions with E2 ubiquitin-conjugating enzymes (Vanni *et al.*, 2012). On the basis of the original results of Vanni et al., it seemed possible that ICP0 may utilise different E2 ubiquitin-conjugating enzymes for different functions, and hence it is possible that these mutations in the RING finger alpha-helix may differentially affect the interactions with E2 ubiquitin conjugating enzymes and the stimulation of lytic infection and reactivation from quiescence. Although the results presented so far in this thesis now make this hypothesis less likely to be true, it was still of value to assess the biochemical activity of these mutants and their interactions with different E2 ubiquitin-conjugating enzymes. These studies are presented in the next chapter.

5 Results - Interactions of ICP0 alpha-helix mutants with components of the ubiquitin conjugation pathway

5.1 ICP0 interactions with the ubiquitin conjugation pathway proteins

ICP0, an E3 ubiquitin ligase, binds to E2 ubiquitin-conjugating enzymes and targets proteins to promote their (poly)ubiquitination and degradation via the 26S proteasome. The RING finger domains of E3 ubiquitin ligases bind to E2 ubiquitin-conjugating enzymes, allowing the E2 enzyme and substrate to come into close proximity, enabling the direct transfer of ubiquitin from the E2 ubiquitin-conjugating enzyme to the substrate protein (reviewed in Deshaies & Joazeiro, 2009). RING finger E3 ubiquitin ligases have been shown to be able to interact with multiple E2 ubiquitin-conjugating enzymes (van Wijk *et al.*, 2009), and therefore it may be possible that ICP0 interacts with multiple E2 enzymes during infection. It has previously been established that the RING finger domain of ICP0 interacts with the highly homologous E2 ubiquitin-conjugating enzymes UBE2D1 and UBE2E1 (also known as UbcH5a and UbcH6) and catalyses the formation of unanchored polyubiquitin chains *in vitro* (Boutell *et al.*, 2002). It has been shown that the alpha-helix and loop regions of the RING finger domain of ICP0 are involved in the interactions with UBE2D1 (Vanni *et al.*, 2012).

This chapter follows on from and extends the work of Vanni *et al*. (2012), and was done in collaboration with Dr Chris Boutell, investigating the E3 ubiquitin ligase activity of the RING finger alpha-helix mutants and the interactions of these mutants with components of the ubiquitin conjugation pathway. Given the results of Vanni *et al*. (2012) and from the virus infected cell studies in **chapter 4**, the underlying hypothesis was that ICP0 may utilise different E2s for its various functions, and hence it was possible that mutations in the RING finger alpha-helix may differentially affect the interactions with E2 ubiquitin conjugating enzymes and the stimulation of lytic infection and reactivation from quiescence.

5.2 Results

5.2.1 Characterisation of the effects of RING finger mutations on ICP0 interactions with E2 ubiquitin conjugating enzymes using yeast-two-hybrid assay

The alpha-helix and loop regions of the RING finger domain of ICP0 have been shown to be important for the interaction of ICP0 with UBE2D1 (Vanni *et al.*, 2012), and therefore mutations in the RING finger alpha-helix could affect ICP0's interactions with E2 ubiquitin-conjugating enzymes or components of the ubiquitin conjugation reaction. The Vanni *et al*. (2012) study included ICP0 mutant N151D, but not K144E or the double mutant constructed during the course of this thesis. Therefore, to extend the previous results, a yeast-two-hybrid experiment was carried out to test the interactions of wt ICP0 and the RING finger mutants with a panel of E2 ubiquitin-conjugating enzymes (**Figure 5.1**).

The wt ICP0 and the RING finger ICP0 mutants were expressed as fusion proteins to the *GAL4*-activating domain (AD), and the E2 ubiquitin-conjugating enzymes were expressed as fusion proteins to the *GAL4*-binding domain (BK). If the proteins fused to the binding domain and activation domain moieties interact, then an active transcription factor is assembled which binds to the GAL4-binding sites in the reporter promoter and transcription of downstream reporter genes (*HIS3* and *lacZ*) occurs (**section 2.10, Figure 2.4**). USP7 was used as a positive control for ICP0 interaction, as USP7 interacts strongly with ICP0 via the interaction motif located in the C-terminal third of ICP0 (614-630 aa) (Everett *et al.*, 1997; Meredith *et al.*, 1995; Meredith *et al.*, 1994). Diploids expressing only the AD or BK domains were used as negative controls for protein interaction.

The results from the yeast-two-hybrid assay (**Figure 5.1**) show that wt ICP0 interacted with the E2 ubiquitin conjugating enzymes UBE2D1, UBE2E1, UBE2V1 (albeit relatively weakly) and UBE2W, but failed to interact with UBE2N. The RING finger mutant ICP0-2C, which lacks two of the RING finger cysteine residues (C116G, C156A) that are required for zinc binding (Lium & Silverstein, 1997) and therefore the stability of the RING finger, interacted with USP7 but did not interact with any of the E2 enzymes tested, showing that the integrity of the RING finger domain is important for the interaction of ICP0 with these E2 ubiquitin-conjugating enzymes. The alpha-helix RING finger mutants K144E and the double KE/ND mutant interacted with UBE2D1, UBE2E1, and UBE2W to the same extent as wt, but their interactions with UBE2V1 were reduced below detectable

levels. This latter point was also true of N151D, but in these experiments the interactions of this mutant with UBE2D1 and UBE2E1 also appeared reduced under the most stringent conditions. The double mutant also lost the ability to interact with UBE2W on the most stringent selection plate (–Leu-Trp-His + 5 mM 3-AT) but still interacted with UBE2W in the presence of 1 mM 3-AT (**Figure 5.1**).

Using high level expression of a dominant negative mutant, evidence has been presented that UBE2D1 is important for the degradation of PML and Sp100 (Gu & Roizman, 2003). The functions of the other E2 conjugating enzymes analysed in **Figure 5.1** during HSV-1 infection have not been investigated. UBE2V1 has no ubiquitin ligase activity on its own, as it is enzymatically inactive due to the lack of an active site cysteine residue (Sancho *et al.*, 1998), and instead it forms a functional heterodimer with the enzymatically active E2 UBE2N (Hofmann & Pickart, 1999; VanDemark *et al.*, 2001). In previous studies, the UBE2N-UBE2V1 complex was found to catalyse the synthesis of Lys63-linked polyubiquitin chains that are not thought to be involved in protein degradation by the proteasome, but may play a role in the DNA repair pathway (Hofmann & Pickart, 1999) or IKK activation (Deng *et al.*, 2000). Unlike other E2 ubiquitin-conjugating enzymes, where ubiquitin is covalently attached via the C-terminal carboxy group of ubiquitin and the ε-amino group of a lysine residue on target proteins, UBE2W catalyses the linkages between the C-terminus of ubiquitin and the N-terminal α-amino groups of target substrates, and this only results in mono-ubiquitination events (Tatham *et al.*, 2013).

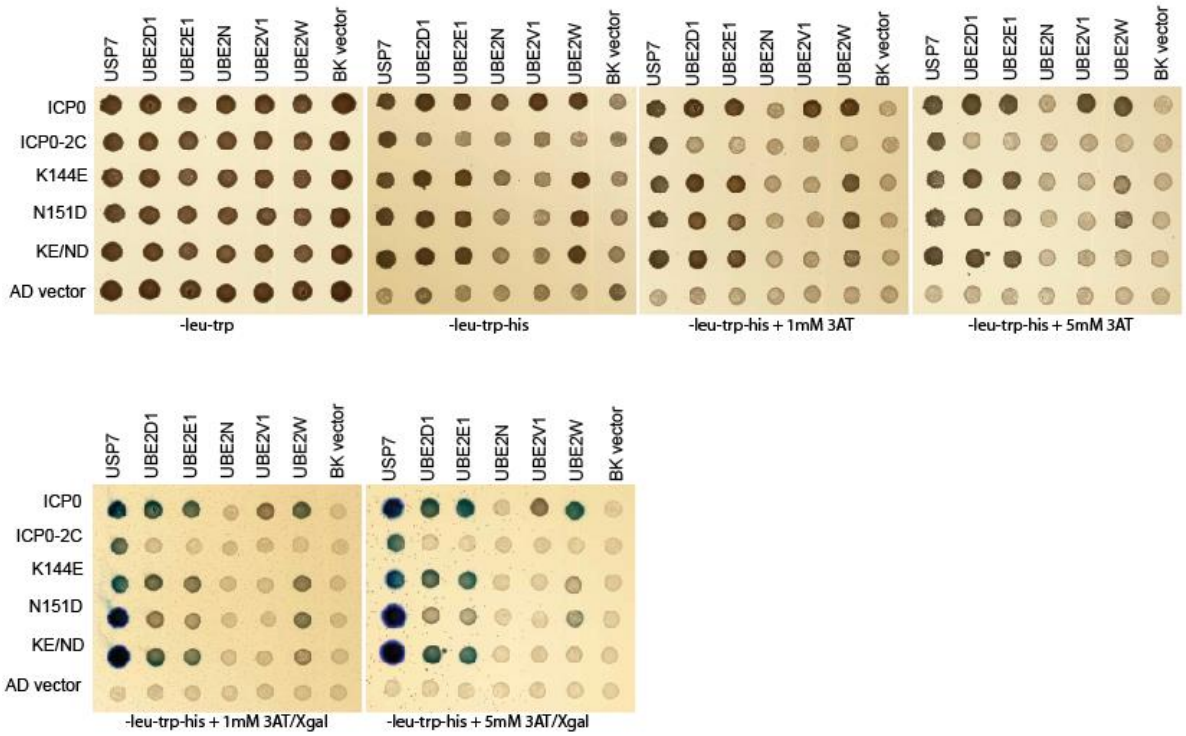

Figure 5.1 Yeast-two-hybrid testing the interactions of wt ICP0 and RING finger mutants with a panel of E2 ubiquitin-conjugating enzymes.
wt ICP0 and RING finger mutants were linked to the *GAL4* DNA-activating domain (AD) and tested for interaction with USP7 and a panel of E2 ubiquitin-conjugating enzymes (UBE2) linked to the *GAL4*-binding domain (BK). Protein interaction was analysed by plating diploids containing both AD and BD plasmids onto medium lacking leucine, tryptophan and histidine, supplemented with 1 mM or 5 mM 3-AT, and stained with X-gal (lower panel plates only). The blue colour indicates β-galactosidase activity and thus an interaction between the two proteins.

5.2.2 ICP0 RING finger mutations affect polyubiquitin chain formation by the UBE2N-UBE2V1 complex

The loss of interaction of the ICP0 RING finger mutants with UBE2V1 may contribute to the phenotypes seen with these mutants shown in previous chapters and the reduced ability of these mutants to reactivate quiescent HSV-1. To further investigate the interactions of the alpha-helix mutants with the E2 ubiquitin-conjugating enzymes UBE2D1 and UBE2N-UBE2V1, the first 241 residues of ICP0 and the RING finger mutants were fused to GST. These GST constructs were then analysed for their abilities to catalyse the formation of polyubiquitin chains *in vitro* or to undergo auto-ubiquitination in the presence of titrated amounts of UBE2D1 and UBE2N-UBE2V1 (**Figure 5.2**). The reactions also included the E1 activation enzyme, ATP and wt ubiquitin.

The yeast-two-hybrid results showed that the mutations in the alpha-helix did not affect the interaction of ICP0 with UBE2D1, and in the presence of UBE2D1 the RING finger mutants could catalyse the formation of polyubiquitin chains to similar levels as seen with the wt ICP0 protein. This confirms previous results that K144E and N151D had no significant effect on the *in vitro* polyubiquitin chain formation with UBE2D1 (Boutell *et al.*, 2002; Vanni *et al.*, 2012). The interaction of UBE2V1 was lost with these RING finger mutants in the yeast-two-hybrid experiment. To test whether the ICP0 mutants could catalyse the formation of polyubiquitin chains with UBE2V1, reactions were carried out with equal amounts of UBE2N and UBE2V1, as these two ubiquitin conjugating enzymes work together as a UBE2N-UBE2V1 heterodimer (**Figure 5.2**). The results showed that wt ICP0 forms polyubiquitin chains with UBE2N-UBE2V1 and that this activity was lost with the negative control mutant ICP0-2C. The N151D mutant had a reduced ability to catalyse the formation of polyubiquitin chains in the presence of UBE2N-UBE2V1 compared to wt, and this activity was even less with the K144E mutant. The level of polyubiqutin chain formation with the double mutant KE/ND was higher than the level seen with the ICP0-2C mutant but was also greatly reduced compared to wt levels.

ICP0 can undergo auto-ubiquitination that makes it less stable, and this can be counteracted by the interaction of ICP0 with USP7, a deubiquitinating enzyme (Canning *et al.*, 2004). The wt ICP0 and the RING finger mutants (except ICP0-2C) undergo auto-ubiquitination in the presence of UBE2D1, but no auto-ubiquitination was detected in the presence of UBE2N-UBE2V1 with wt ICP0 or the RING finger mutants (**Figure 5.2**).

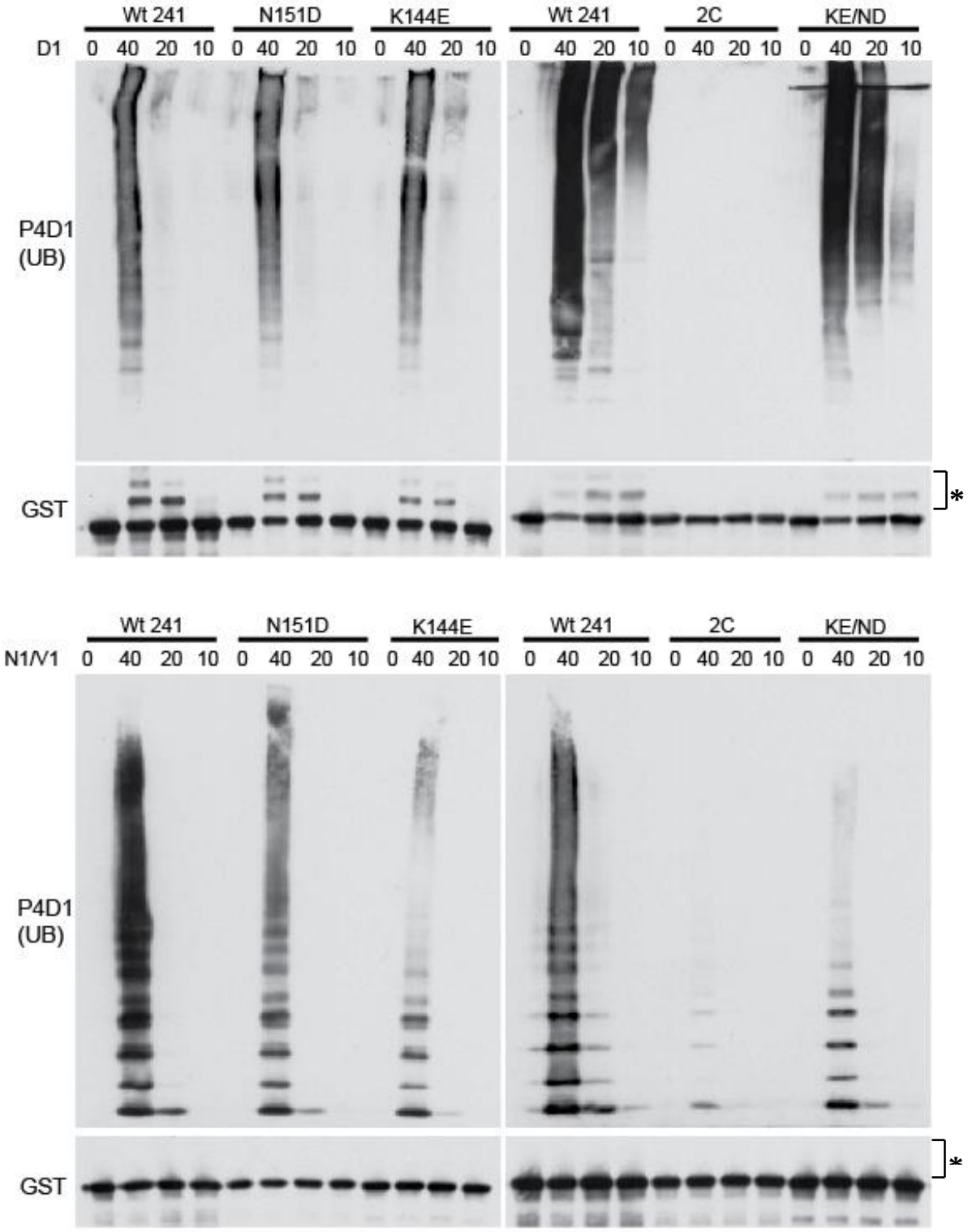

Figure 5.2 wt ICP0 and RING finger mutants E3 ubiquitin ligase activity *in vitro* in the presence of UBE2D1 and UBE2N-UBE2V1.

GST-tagged wt ICP0 and RING finger mutants were analysed for their abilities to catalyse the formation of polyubiquitin chains in the presence of wt ubiquitin, and to undergo auto-ubiquitination in the presence of titrated amounts of UBE2D1 (D1) and UBE2N-UBE2V1 (N/V1) (40, 20, 10 ng). Polyubiquitin chain formation was detected using P4D1 antibody and auto-ubiquitination was detected using anti-GST antibody (labelled by asterisks).

5.2.3 Double mutant KE/ND fails to form colocalising conjugated ubiquitin foci in infected cells

The results of the *in vitro* E3 ubiquitin ligase assays of the ICP0 mutants with E2 ubiquitin-conjugating enzymes gave some interesting results, which imply at the least that ICP0 may utilise a number of different E2 enzymes. However, it is also important to investigate the functional activity of ICP0 and the interactions of ICP0 and the mutants with components of the ubiquitin pathway in the context of infection. The RING finger activity of the ICP0 mutants in infected cells can be studied by analysing the formation and localisation of conjugated ubiquitin by immunofluorescence (**Figure 5.3)** using monoclonal antibody FK2, which recognises ubiquitin-protein conjugates but not free ubiquitin (Fujimuro *et al.*, 1994). HFs were infected at MOI 10 with the wt and mutant ICP0 viruses, and stained two hours post infection. The results showed that in non-infected cells the ubiquitin was mainly dispersed throughout the nucleus, with a few punctate foci, but in wt infected cells the ubiquitin formed discrete foci that showed strong colocalisation with ICP0. In N151D and K144E infected cells, the conjugated ubiquitin also showed a high degree of colocalisation with ICP0. In the RING finger deletion mutant FXE infected cells, there were some ubiquitin foci that colocalised with ICP0, but the majority of the ubiquitin signal was dispersed throughout the nucleus, as in uninfected cells. This was also the case with the double mutant KE/ND infected cells.

These results obtained with the K144E and N151D mutant viruses, showing the formation of conjugated ubiquitin colocalising with ICP0, are different from those published previously. Everett (2000) and Vanni *et al*. (2012) found that HEp-2 cells (human epithelial cells originated from a human laryngeal carcinoma) transfected with a plasmid containing mutated forms of ICP0 had between 10-20% of wt ability to induce the colocalisation of conjugated ubiquitin (Everett, 2000; Vanni *et al.*, 2012). The discrepancies between the sets of results could be due to the different systems used; high MOI virus infected HFs stained 2 hours post infection compared to transfected HEp-2 cells stained six to 24 hours post transfection. From these infected cell data, it appears that the formation of colocalising conjugated ubiquitin by the K144E mutant may reflect polyubiquitin chain formation and the auto-ubiquitination seen *in vitro* in the presence of UBE2D1, rather than UBE2N-UBE2V1 catalysed reactions.

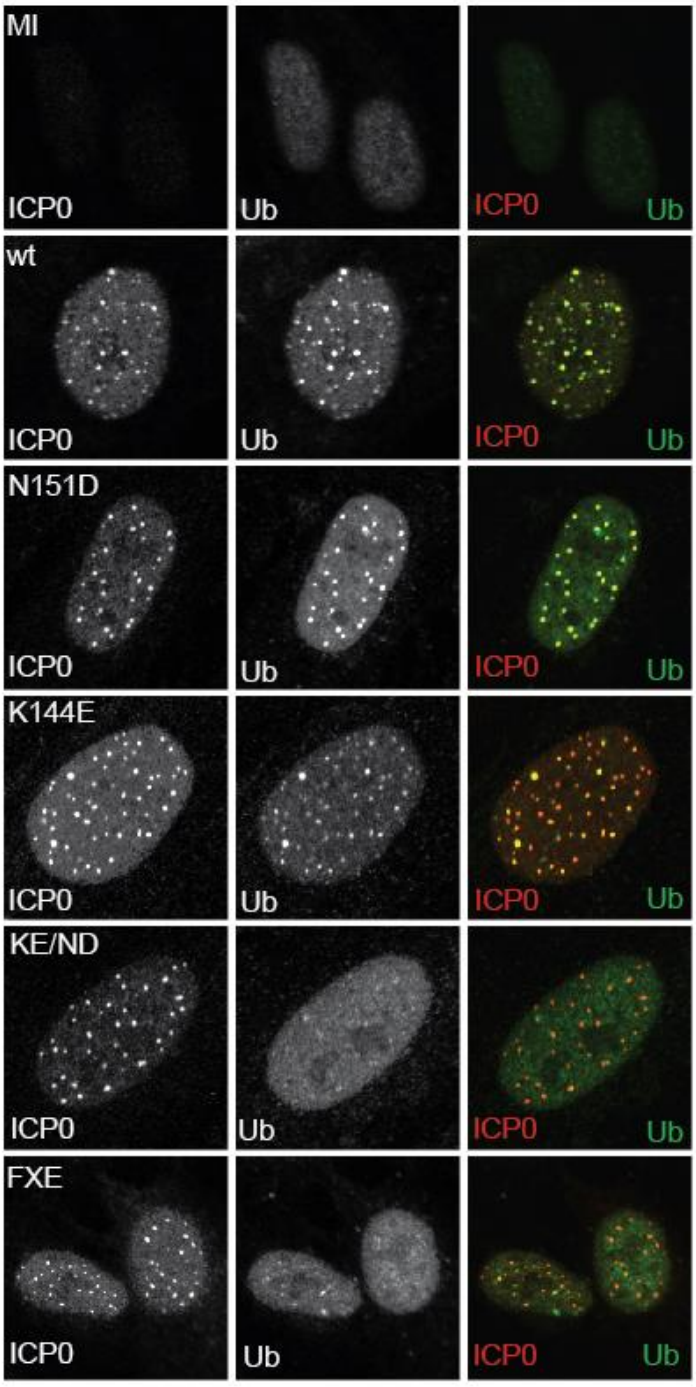

Figure 5.3 The ability of the RING finger mutants to induce the formation of colocalising conjugated ubiquitin.
HFs were infected at MOI 10 and the virus adsorbed for 1 hour before overlaying cells with medium containing 1% human serum. Cells were fixed, permeablised and stained two hours post infection. ICP0 (red) was detected using rabbit polyclonal R190 antibody and ubiquitin (ub, green) was detected using the mouse monoclonal antibody FK2, which detects ubiquitin-protein conjugates but not free ubiquitin. The images are representative of a large number cells that were examined.

5.2.4 E2 ubiquitin-conjugating enzyme localisation in cells expressing wt and RING finger mutant ICP0

The defect in degradation (and by implication ubiquitination) of target proteins such as PML by the RING finger mutants, particularly K144E and KE/ND, may be due to effects on the RING finger helix interaction interface between ICP0 with the E2 ubiquitin-conjugating enzyme and target proteins. The cellular distribution of UBE2D1 and UBE2E1 has been previously investigated in cells transfected with plasmids expressing tagged E2 ubiquitin conjugating enzymes and ICP0 (Boutell *et al.*, 2002). In these studies, ICP0 and the E2 ubiquitin conjugating enzymes showed nuclear colocalisation but the intensity of colocalisation was stronger in some cells than others. There was no recruitment of either of the E2 ubiquitin conjugating enzymes with the RING finger deletion mutant FXE (Boutell *et al.*, 2002).

The localisation of UBE2D1 and UBE2V1 was investigated with regards to ICP0 and the RING finger mutants by immunofluorescence. This was achieved by either transfecting plasmids expressing ICP0 and the flag-tagged E2 ubiquitin conjugating enzymes into cells simultaneously, or by transfecting the flag-tagged E2 plasmids and then infecting the cells with wt or mutant viruses 24 hours later. Different cell types (U2OS and HepaRG cells), transfection reagents (GeneJuice®, Lipofectamine® and Lipofectamine® LTX) and varying amounts of transfected E2 plasmids (50-1000 ng) were investigated. Problems were experienced in getting enough cells that expressed both the E2 enzyme and ICP0 simultaneously, especially by the infection method, as the majority of cells expressed only the tagged form of the E2 ubiquitin conjugating enzyme or ICP0, and less than 5% of cells expressed both. In cells expressing wt ICP0, there was colocalisation with UBE2D1 or UBE2V1, but in cells expressing FXE there were variable results, with some cells showing no colocalisation of the E2 enzyme and ICP0 but other cells showing a strong colocalisation, as seen with the wt. These cells were invariably expressing the ICP0 protein at exceptionally high levels. In general, transfection gave a very wide range of expression levels among positive cells in a sample, and the degree of any colocalisation with ICP0 was influenced by expression level. While cells could be selected for examination in which expression levels appeared closer to physiological levels, this would always be subject to observer bias. Therefore, no conclusion could be reached using this method as to the relative colocalisation of the various mutant forms of ICP0 with the E2 ubiquitin conjugating enzymes tested.

5.3 Conclusions and Discussion

The results of the yeast-two-hybrid experiments and the *in vitro* E3 ubiquitin ligase assays show that ICP0 has the potential for functionally relevant interactions with E2 ubiquitin conjugating enzymes other than the previously described roles of UBE2D1 and UBE2E1. ICP0 formed polyubiquitin chains *in vitro* in the presence of UBE2N-UBE2V1 and also interacted with UBE2V1 and UBE2W in the yeast two hybrid experiments. The results show the RING finger region of ICP0 may influence E2 interactions, as the RING finger mutants lost their ability to interact with UBE2V1 in the yeast-two-hybrid and N151D exhibited less polyubiquitin chain formation compared to wt, with lower levels still with K144E and KE/ND. The results for the *in vitro* E3 ubiquitin ligase activity of the ICP0 mutants in the presence of UBE2N-UBE2V1 are broadly consistent with the results of the yeast-two-hybrid experiments, given that the reduced activity in the *in vitro* ligase assay may derive from a residual interaction with the E2 enzyme that is below the level of detection in the yeast-two-hybrid assay. The two assays are consistent in regard to interaction and activity of the mutants with UBE2D1.

On the basis of the yeast-two-hybrid experiments and E3 ubiquitin ligase assays, there is an implication that UBE2V1 interaction with the RING finger domain may be important for ICP0 activity. From these data, it appears that ICP0's activity in conjunction with UBE2N-UBE2V1 correlates more closely with ICP0 activity in some assays than the interaction with UBE2D1. For example, the levels of polyubiquitin chain formation *in vitro* with UBE2N-UBE2V1 (**Figure 5.2**) with each of the mutants mirror their activities in terms of PML degradation (**Figures 4.9, 4.10**), viral infectivity (**Figures 4.7, 4.8**) and reactivation induction (**Figure 4.15**). This is surprising given the current understanding of the differential roles of UBE2D1 and UBE2N-UBE2V1 in protein degradation and ubiquitin-mediated signalling. The lack of formation of colocalising conjugated ubiquitin in KE/ND infected cells also correlates with the lack of PML degradation in cells infected by this virus, and this again points to the potential role of UBE2N/UBE2V1 in ICP0 activity, rather than UBE2D1. On the other hand, the results with K144E fit better with the hypothesis that the formation of intracellular co-localising conjugated ubiquitin depends on UBE2D1 rather than UBE2N/UBE2V1. Thus, no simple picture emerges from the combination of the complete data of all of these assays.

These results should be interpreted with caution, as there is a potential difficulty in correlating E3 ligase activity and E2 ubiquitin conjugating enzyme interaction data *in vitro*

with what occurs *in vivo*. For example, UBE2D1 has been shown to be important for the degradation of PML and Sp100 (Gu & Roizman, 2003), but K144E and KE/ND interacted with UBE2D1 in the yeast-two-hybrid and formed polyubiquitin chains *in vitro* in the presence of UBE2D1 to levels comparable to wt, but they do not degrade PML efficiently *in vivo*, at least in infected HFs. These results therefore raise the question whether the *in vitro* and yeast-two-hybrid results truly reflect ICP0 mediated ubiquitin ligase activity in the intracellular environment. Therefore, more work will be needed to investigate whether these residues in the alpha-helix are important for interactions with components of the ubiquitin conjugation pathway in infected cells, and the potential roles of different E2 ubiquitin conjugating enzymes in the HSV-1 life cycle. Future work could therefore investigate E2 ubiquitin conjugating enzyme requirements for ICP0 activity by knock-down or knock-out methodologies. As yet, there is no clear indication that different E2 ubiquitin conjugating enzymes are required for lytic infection and reactivation.

6 Results - Investigation of motifs within ICP0 that show sequence similarity to other viruses or that are involved in interactions with cellular proteins

6.1 Introduction

Among the ICP0-homologue proteins of alphaherpesviruses, the RING finger domain shows the highest sequence similarity due to its conserved function as an E3 ubiquitin ligase (Boutell & Everett, 2013), and this region has been extensively studied. There are other regions of ICP0 that contain motifs with functions attributed to them, such as the nuclear localisation signal, the USP7 binding motif, and a less well defined region required for ND10 localisation. However, there are other regions throughout ICP0 that contain motifs or sequences with similarity to those present within other viral proteins, including other herpesviruses, which have not previously been studied in detail. Therefore, the aim of this chapter was to investigate motifs and residues that are conserved between herpesviruses or that show similarity to motifs in other viral proteins that interact with cellular proteins, including E3 ubiquitin ligases.

6.2 Motifs that are reported to interact with cellular E3 ubiquitin ligases

There is a growing list of E3 ubiquitin ligases that interact with other E3 ligases, including an HECT E3 ligase NEDD4 that interacts with and targets the RING finger E3 ligase casitas B-lineage lymphoma (CBL) protein for degradation (reviewed in Weissman *et al.*, 2011). Part of this chapter will investigate motifs within ICP0 that show similarity to motifs within other viral proteins and/or that interact with cellular E3 ubiquitin ligases, including those involved in the DNA damage response (**section 6.2.1**) and viral budding (**section 6.2.2**).

6.2.1 ICP0 interacts with the cellular E3 ubiquitin ligase RNF8 that is involved in the DNA damage response

The DNA damage response can be activated in response to viral infection, and viruses have evolved ways to manipulate this pathway for their own benefit by activating some aspects while inhibiting others (reviewed in Weitzman *et al.*, 2010). HSV-1 has been shown to activate the DNA damage response, and interact with or induce the degradation

of cellular proteins involved in these pathways to promote viral replication (Lilley *et al.*, 2005; Mohni *et al.*, 2011; Weller, 2010). One example of this during HSV-1 infection is the ICP0 induced degradation of the DNA-PK catalytic subunit (Lees-Miller *et al.*, 1996; Parkinson *et al.*, 1999) that is involved in DNA double-strand break repair and V(D)J recombination (reviewed in Lees-Miller, 1996). Other than a requirement for the ICP0 RING finger, the mechanism of this degradation has not been established.

The DNA damage response pathway consists of a variety of cellular proteins and signalling pathways for sensing and repairing DNA damage within cells. Double-stranded DNA breaks are detected by the sensor proteins Mre11, Rad50 and Nbs1 (the MRN complex), which then activates protein kinases, including ATM kinase. Activation of the ATM kinase leads to phosphorylation of the histone H2AX, which acts as a marker for the site of DNA damage. The mediator of DNA damage checkpoint protein 1 (Mdc1) binds the phosphorylated H2AX, and this leads to further recruitment of proteins involved in the DNA damage response (reviewed in Chaurushiya *et al.*, 2012; Weitzman *et al.*, 2010). The cellular repair proteins and those involved in chromatin modification are recruited to the sites of DNA damage via a process that requires the action of cellular RING finger E3 ubiquitin ligases RNF8 (Huen *et al.*, 2007; Kolas *et al.*, 2007; Mailand *et al.*, 2007) and RNF168 (Doil *et al.*, 2009; Stewart *et al.*, 2009).

ICP0 inhibits the formation of DNA damage repair foci after the stage of H2AX phosphorylation by inducing the degradation of the cellular ubiquitin ligase RNF8, which is involved in histone ubiquitination and anchoring repair factors at DNA damage sites (Lilley *et al.*, 2010). Later, after the experiments of this thesis were completed, it was shown that RNF8 and RNF168 are recruited to incoming HSV-1 genomes and are involved in intrinsic restriction of HSV-1 infection (Lilley *et al.*, 2011). RNF8 binds to the phosphorylated TQXF clusters on Mdc1 (Mailand *et al.*, 2007). ICP0 contains a STDTELF motif at residues 64-70, and during HSV-1 infection, the T67 residue is phosphorylated by cellular casein kinase 1, thus imitating the phosphorylation sites on Mdc1, enabling ICP0 to bind to RNF8. This leads to the proteasome-mediated degradation of RNF8, and there is evidence that this enhances viral replication (Chaurushiya *et al.*, 2012).

ICP0 interacts with the DNA damage response pathway via the phosphorylated T67 residue binding to RNF8 and targeting it for degradation. As treatments such as UV light

can cause DNA damage and induce reactivation of quiescent genomes, it is possible that these two pathways are linked and this may occur via the T67 residue. As part of a collaborative interaction between the Everett and Weitzman laboratories, ICP0 containing a threonine to alanine mutation at residue 67 (T67A) was made available. The aim here was to study the effects of this mutation on ICP0-null mutant complementation and reactivation using the ICP0 inducible cell line system, prior to the later isolation of a mutant virus in the Weitzman laboratory.

6.2.1.1 Analysis of the effects of the T67A mutation on the ability of ICP0 to complement an ICP0-null mutant HSV-1

The ability of ICP0 mutant T67A that is unable to interact with RNF8 was analysed for its ability to complement an ICP0-null mutant virus using the doxycycline inducible ICP0 expression system (described in **chapter 2.2.3, Figure 2.2**). The wt virus infected HA-TetR control cells and HA-T67A cells gave similar plaque numbers compared to HA-cICP0 expression cells without ICP0 induction (**Table 6.1, Figure 6.1**). After ICP0 induction, the HA-TetR and HA-T67A cells showed slight decreases in wt virus plaque numbers compared to HA-cICP0 cells, but this was by less than two-fold for HA-T67A cells. Cells expressing wt and mutant ICP0 protein without ICP0 induction all showed comparable plaque numbers when infected with an ICP0-null mutant *dl*1403 virus. When complementing the ICP0-null mutant virus, the HA-T67A cells showed a slight decrease in plaque formation ability compared to HA-cICP0 after induction, with 75% of wt activity. This difference, however, cannot be considered biologically significant in this experimental approach.

Table 6.1 Plaque count data in cells expressing T67A following infection with wt or ICP0-null mutant HSV-1 after 24 hours induction with doxycycline or left untreated. Cells were treated with doxycycline (0.1 µg/ml) for 24 hours to induce ICP0 expression or left untreated, and the following day infected with sequential three-fold dilutions of wt (in1863) or ICP0-null mutant (*dl*1403CMV/lacZ) HSV-1. The starting dilutions varied between the cell types and viruses. The plaque counts at each dilution, the average plaque counts and the relative value of each cell type compared to wt ICP0 (HA-cICP0) are shown from two repeat experiments.

A) Wt HSV-1 minus doxycycline

Cells HA-	**Dil**	**1**	**1/3**	**1/9**	**1/27**	**Average**	**Relative % compared to wt**	**Ave relative values**
TetR	**10^{-4}**	tmtc	124	59	32	58900000	**71.8**	90.1
		tmtc	tmtc	100	31	86850000	**108.4**	
cICP0	**10^{-4}**	tmtc	265	101	28	82000000	**100.0**	100.0
		tmtc	tmtc	115	21	80100000	**100.0**	
cICP0. T67A	**10^{-4}**	tmtc	235	97	22	72400000	**88.3**	88.5
		tmtc	tmtc	92	22	71100000	**88.8**	

B) Wt virus plus doxycycline

Cells HA-	**Dil**	**1**	**1/3**	**1/9**	**1/27**	**Average**	**Relative % compared to wt**	**Ave relative values**
TetR	**10^{-4}**	tmtc	163	81	19	57700000	**37.0**	44.3
		tmtc	tmtc	84	16	59400000	**51.6**	
cICP0	**10^{-4}**	tmtc	tmtc	179	56	156150000	**100.0**	100.0
		tmtc	tmtc	118	46	115200000	**100.0**	
cICP0. T67A	**10^{-4}**	tmtc	228	104	26	77400000	**49.6**	68.3
		tmtc	tmtc	109	38	100350000	**87.1**	

C) ICP0 null mutant HSV-1 minus doxycycline

Cells HA-	**Dil**	**1**	**1/3**	**1/9**	**1/27**	**Average**	**Relative % compared to wt**	**Ave relative values**
TetR	**10^{-2}**	tmtc	tmtc	357	22	1903500	**89.8**	122.5
		tmtc	tmtc	176	22	1089000	**155.1**	
cICP0	**10^{-2}**	tmtc	tmtc	312	53	2119500	**100.0**	100.0
		tmtc	tmtc	105	17	702000	**100.0**	
cICP0. T67A	**10^{-2}**	tmtc	tmtc	172	40	1314000	**62.0**	107.3
		tmtc	tmtc	175	21	1071000	**152.6**	

D) ICP0 null mutant HSV-1 plus doxycycline

Cells HA-	Dil	1	1/3	1/9	1/27	Average	Relative % compared to wt	Ave relative values
TetR	**10^{-2}**	tmtc	tmtc	93	14	607500	0.5	**0.5**
		tmtc	tmtc	184	25	1165500	0.6	
cICP0	**10^{-4}**	tmtc	tmtc	121	50	121950000	100.0	**100.0**
		tmtc	tmtc	204	77	195750000	100.0	
cICP0. T67A	**10^{-4}**	tmtc	tmtc	104	45	107550000	88.2	**75.4**
		tmtc	tmtc	128	48	122400000	62.5	

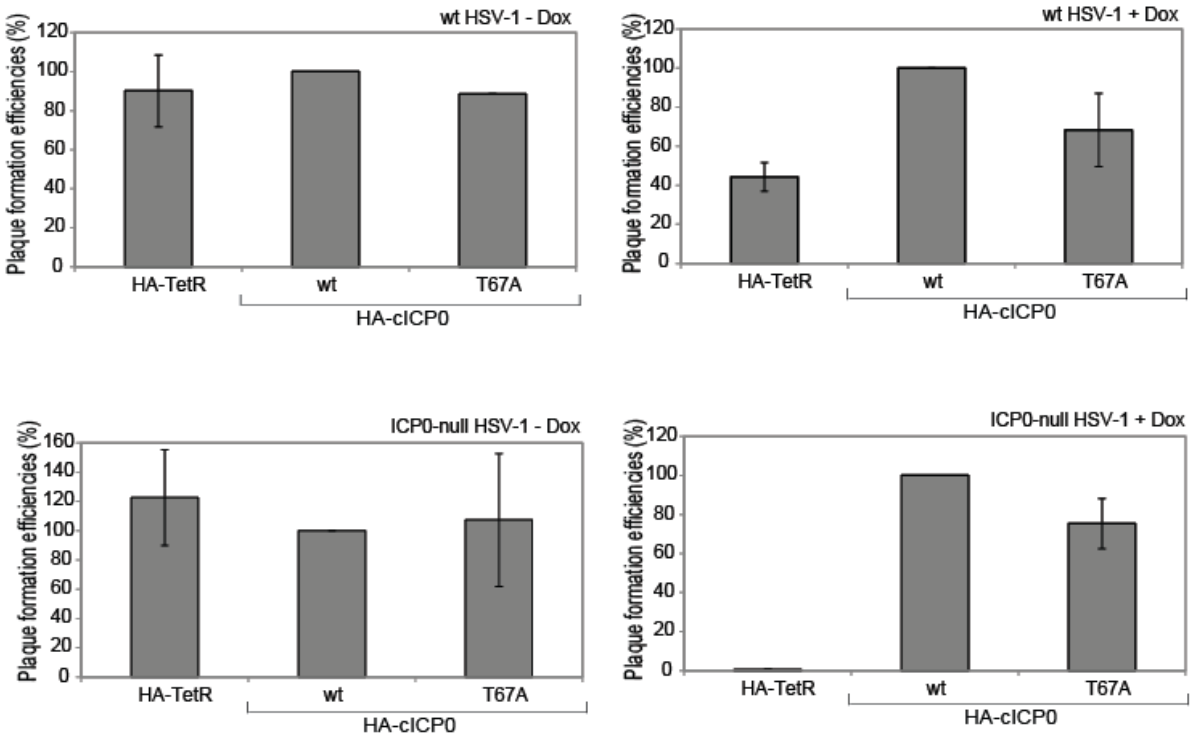

Figure 6.1 Effect of T67A mutation within ICP0 on wt HSV-1 and ICP0-null mutant HSV-1 plaque formation efficiency.
HA-cICP0 and HA-T67A cells were infected with wt HSV-1 (*in*1863) or ICP0-null mutant (*dl*1403/CMVlacZ) HSV-1, and the following day ICP0 expression was induced with doxycycline (0.1 μg/ml) if required. The plates were stained for β-galactosidase activity 24 hours later. The results from the data in **Table 6.1** show the average plaque forming ability from two repeat experiments and are presented as a percentage of that in HA-cICP0 cells. The error bars represent the range between the two repeat experiments.

The experiments reported here were intended to provide a relatively rapid test of the role of residue T67. That this mutation causes a decrease in the stimulation of plaque formation efficiency of the ICP0-null mutant virus of less than two-fold compared to wt ICP0, while retaining over a 100-fold improvement of plaque formation compared to the control HA-TetR cells, implies that any effect on viral replication efficiency of the interaction between T67 and RNF8 is not substantial in HepaRG cells. Later studies, however, showed that depletion of RNF8 increases the efficiency of ICP0 null mutant HSV-1 infection in murine embryonic fibroblasts (Lilley *et al.*, 2011; Lilley *et al.*, 2010). A virus carrying the T67A mutation had a replication defect on ICP27 gene expression in low MOI infections in HepaRG cells compared to wt by around six-fold. This defect was improved in cells expressing a shRNA targeting RNF8 but did not restore replication to wt levels. Later experiments also showed that the T67A virus had around a 10-fold defect in viral yield in HFs compared to wt (Chaurushiya *et al.*, 2012). One factor in the inducible cell line approach that could explain the differing results is that ICP0 expression is induced 24 hours before infection, perhaps allowing time for slight defects in overall ICP0 activity to be masked by the extended time of expression.

6.2.1.2 The T67A mutation does not affect ICP0's ability to degrade ND10 proteins in the inducible cell line system

Expression of the T67A mutant ICP0 protein and its effects on PML and Sp100 degradation was analysed by Western blotting (using the Bethyl Laboratories rabbit anti-PML antibody) (**Figure 6.2**). The results with mutant R8507 shown in this figure is not relevant to the results presented in this section, but are discussed in **section 6.3**. The figure also shows results with mutants K144E and N151D, which were studied in previous chapters. These particular results are not presented elsewhere as the PML Bethyl Laboratories antibody used for this Western blot was found to cross-react with ICP0 when ICP0 is expressed in high amounts, as seen with these mutants, giving the impression that unmodified species of PML were not degraded in these cell types. It was necessary to present the results with these mutants here to avoid cropping the Western blot image.

Expression of ICP0 occurred in the cells that were induced with doxycycline except in the HA-TetR control cells. The level of ICP0 expression was similar in wt ICP0 and the T67A mutant cells. The T67A mutant after induction showed extensive degradation of all PML proteins, with only low levels of PML I/II remaining, and there was also loss of SUMO-modified Sp100, with only unmodified Sp100 being expressed. In retrospect, and with

reference to the studies which were published after these experiments were conducted, this result is not surprising, as while the T67A mutant prevented the degradation of RNF8, other substrates of ICP0 including DNA-PK, USP7 and RNF168 were shown to be degraded by infection with HSV-1 containing the T67A mutation (Chaurushiya *et al.*, 2012). Although PML, Sp100, DNA-PK and USP7 (and also RNF8) are targeted for degradation by the RING finger domain of ICP0, these results imply that residue T67 is required only for binding to and targeting RNF8, and therefore the other substrates must be recognised for degradation using sequences that are different from that used for RNF8.

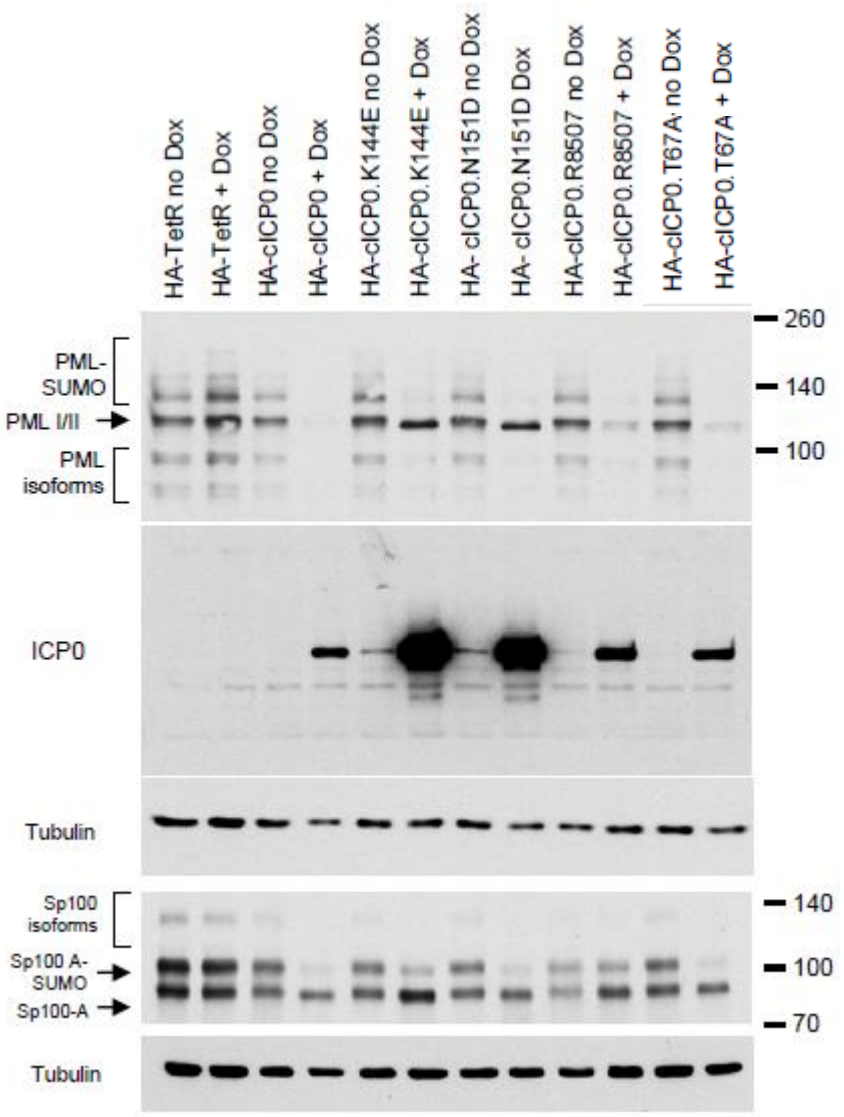

Figure 6.2 Western blot analysis of the degradation of different PML and Sp100 isoforms by wt and mutant forms of ICP0.
HA-TetR, HA-ICP0 and mutant ICP0 cells were induced with doxycycline (0.1 µg/ml) for 24 hours or left untreated. The proteins were resolved on a 7.5% SDS gel and then transferred to a nitrocellulose membrane and detected by probing for PML, ICP0, Sp100 and tubulin. The numbers on the right are molecular masses (kilodaltons). One thing to note was that the PML Bethyl antibody showed cross reactivity with ICP0 when ICP0 was expressed at very high levels as seen with K144E and N151D. These mutants are included to prevent the need to crop the image.

6.2.1.3 The T67A mutation does not have any substantial effects on the efficiency of reactivation of quiescent HSV-1 in the inducible cell line system

The DNA damage response pathway and reactivation from quiescence could be linked, as stimuli such as UV light causes DNA damage and also induces reactivation. Therefore, the T67A mutation within ICP0, which prevents the degradation of a cellular ligase component of the DNA damage response and prevents its downstream effects, may have an effect on the reactivation of quiescent HSV-1. The effect of this mutation on reactivation of quiescent HSV-1 was investigated using the *in*1374 virus, which establishes quiescence very effectively (described in **Table 2.8**). This reactivation assay was performed using HA-cICP0 and HA-T67A cells, which express ICP0 following induction with doxycycline. The expression of β-galactosidase indicated reactivation of viral gene expression that could be quantified as a percentage of positive cells in the total cell population, which was expressed as a proportion of the reactivation observed in HA-cICP0 cells (**Figure 6.3**). The T67A mutation caused a slight defect in reactivation of gene expression from quiescent HSV-1, with 67% of the levels seen following induction of wt ICP0, but this was less than a two-fold difference and was similar to its ability to complement the plaque formation deficiency of an ICP0-null mutant virus. Therefore, the T67A mutation does not appear to have a substantial effect on inducing the reactivation of quiescent HSV-1 in cultured cells.

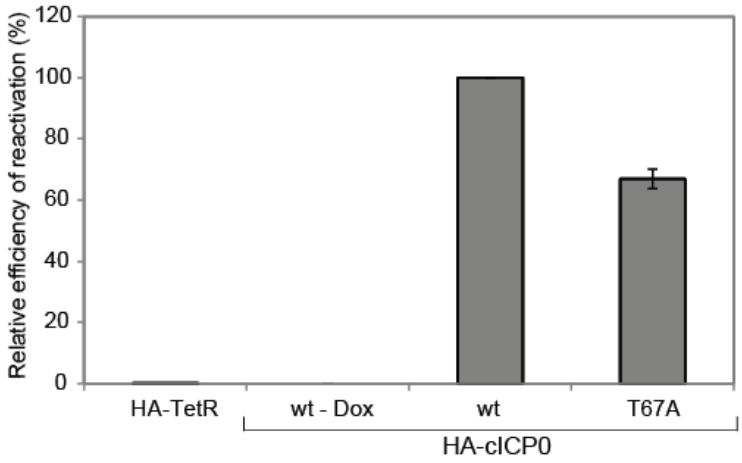

Figure 6.3 Quantification of the reactivation of viral gene expression by mutant T67A.
Two random fields of view of the cells infected with *in*1374 and 24 hours later induced with doxycycline (**Figure 3.3**) were imaged. The cells positive and negative for reactivated gene expression were counted, and the percentage of positive cells for each cell type calculated. These were then represented as a percentage of the positive cells in HA-cICP0 cells expressing wt ICP0. The bars show the mean result from the two fields of view from a single plate, and the error bars represent the higher and lower percentages from the two repeat experiments. HA-TetR (plus doxycycline) and HA-cICP0 (no doxycycline) were included as negative controls.

6.2.1.4 Conclusions and Discussion

The T67A mutant behaved similarly to wt ICP0 in regards to PML and Sp100 degradation, and only had slight defects in complementation of an ICP0-null mutant virus and reactivation of gene expression from quiescent HSV-1, showing a less than two fold reduction when compared to wt ICP0. As stimuli such as UV can activate the DNA damage response and induce reactivation, it seems unlikely that these two pathways are linked, at least via the T67-RNF8 interaction. Later published studies using a T67A mutant virus and RNF8 depletion implied that degradation of RNF8 was required to counteract its repressive effects on viral transcription. It is possible that these issues are affected by cell type or species of origin, as some of the experiments were carried out in murine embryonic fibroblasts lacking RNF8, or that the inducible cell line expression system is insufficiently sensitive to detect relatively small changes in intrinsic ICP0 activity.

6.2.2 The PPEYPTAP motif and SIAH-1 interaction motifs within ICP0 that are involved in interactions with cellular E3 ubiquitin ligases

HSV-1 ICP0 contains the sequence PPEYPTAP at residues 717-724, which is highly related to PTAP and PPXY motifs in other viral proteins that have been shown to be involved in interactions with cellular E3 ubiquitin ligases, including HECT and Nedd4 (reviewed in Bieniasz, 2006). Retroviral Gag proteins contain conserved motifs termed late domains that contain PTAP, PPXY or YXXL motifs that play a role in regulating viral budding (reviewed in Freed, 2002). The PTAP motif within the HIV-1 Gag protein binds to Tsg101, an E2 ubiquitin-conjugating enzyme variant protein and a component of the endosomal complexes (ESCRT-1) required for transport that regulates viral budding and receptor endocytosis (Garrus *et al.*, 2001; Göttlinger *et al.*, 1991; Martin-Serrano *et al.*, 2001; VerPlank *et al.*, 2001). The PPXY motif within the gag proteins of retroviruses including Rous sarcoma virus (Kikonyogo *et al.*, 2001), human T-cell leukaemia virus (Blot *et al.*, 2004; Bouamr *et al.*, 2003; Sakurai *et al.*, 2004) and Pfizer monkey virus (Yasuda *et al.*, 2002) play a role in viral budding by interacting with E3 ubiquitin ligases including the Nedd4 family. The matrix (M) proteins of vesicular stomatitis virus and rabies virus (Harty *et al.*, 1999), and the Ebola Vp40 protein (Harty *et al.*, 2000; Yasuda *et al.*, 2003) also contain the PPXY motifs that play roles in viral budding. Schreiner et al. (2012) reported that the PPXY motif located in protein VI of adenovirus was important for capsid transport to the nucleus and efficient viral replication, and that it also mediates interaction with Nedd4 ubiquitin ligases. Protein VI has been shown to localise to ND10, and its PPXY motif counteracts the Daxx mediated repression of viral transcription (Schreiner *et al.*, 2012).

ICP0 also contains the cellular ubiquitin ligase SIAH-1 binding motif PXAXVXPXXR at residues 401-410. SIAH-1 functions as an E3 ubiquitin ligase of the RING finger class, and most substrates of SIAH-1 contain a PXAXVXP motif for interaction (House *et al.*, 2003). A yeast-two-hybrid experiment showed that SIAH-1 and ICP0 interact and that SIAH-1 and ICP0 colocalised in discrete nuclear foci (Nagel *et al.*, 2011). Overexpression of ICP0 resulted in the stabilisation of SIAH-1, whereas silencing SIAH-1 led to increased ICP0 stability during infection (Nagel *et al.*, 2011). Prior to this report, work in this laboratory had also detected a possible interaction between ICP0 and SIAH-1 in a yeast-two-hybrid screen (N. Rauch and R.D. Everett, unpublished results). Therefore, it is possible that SIAH-1 and ICP0 act together to regulate their functions.

SIAH-1 has also been shown to interact with KSHV ORF45 in yeast-two-hybrid and co-immunoprecipitation experiments (Abada *et al.*, 2008). ORF45 is an IE protein that plays a role in the inhibiting the host antiviral response (Zhu *et al.*, 2010) by interacting with interferon regulatory factor 7 (IRF-7), thereby preventing the activation of type I IFN signalling (Zhu *et al.*, 2002). ORF45 contains a partially conserved SIAH-1 interaction motif (KPVAVVAGRVR) at amino acid residues 140-151. SIAH-1 promotes the ubiquitination of ORF45 and its subsequent degradation via the proteasome through a RING finger domain-dependent mechanism (Abada *et al.*, 2008).

One of the objectives of this chapter was to analyse the function of the PPEYPTAP motif and SIAH-1 interaction (PXAXVXPXXR) motif within ICP0 in the context of HSV-1. To achieve this objective, mutations were introduced into these motifs, the PPEYPTAP motif was mutated to AAEYATAA (termed the PPEYPTAP mutant), and the SIAH-1 interaction motif mutated from RPRAAVAPCVR to RPRAAGAGCVR (termed SIAH-IM, which changes the central two core conserved amino acids of the consensus motif) (**chapter 2.2.3**). These motifs were initially studied using the ICP0 inducible expression system (Everett *et al.*, 2009) (**chapter 2..2.3, Figure 2.2**), in which doxycycline induces ICP0 expression, but later these mutations were studied in the context of HSV-1 infection.

6.2.2.1 The PPEYPTAP mutant and SIAH-IM have less than a two-fold defect in complementing ICP0-null mutant HSV-1

The ability of ICP0 proteins with mutations in the PPEYPTAP and SIAH-1 interaction motifs to complement HSV-1 wt and ICP0-null mutant virus were analysed using the doxycycline inducible ICP0 expression system (**Table 6.2, Figure 6.4**). During wt HSV-1 infection, in the absence of doxycycline induction the HA-PPEYPTAP and HA-SIAH-IM cells gave similar PFEs to HA-cICP0 and the control HA-TetR cells. After induction with doxycycline, wt HSV-1 plaque formation decreased slightly in HA-PPEYPTAP and HA-SIAH-IM infected cells compared to that in HA-cICP0 expressing cells, but this decrease was less than two-fold. Similar results were seen when infecting these cells with the ICP0-null mutant virus without doxycycline induction. After induction, the HA-PPEYPTAP cells complemented the plaque formation defect of an ICP0-null mutant virus to 66% of wt levels and this figure was 53% in the HA-SIAH-IM cells. Therefore, the mutations in the PPEYPTAP sequence and SIAH-1 interaction motif do not appear to cause substantial defects in complementation of an ICP0-null mutant virus.

The two-fold defect in complementation of an ICP0-null mutant virus in HA-SIAH-IM cells compared to HA-cICP0 cells is in agreement with previous literature, which showed that deletion of the SIAH-1 interaction motif reduced the ability to stimulate plaque formation compared to wt ICP0 in cells transfected with ICP0 null mutant DNA and ICP0 plasmid with a deletion in the SIAH-1 interaction motif (Nagel *et al.*, 2011).

Table 6.2 Plaque count data in cells expressing mutations in the PPEYPTAP and SIAH-1 interaction motif following infection with wt or ICP0-null mutant HSV-1.
Cells were treated with doxycycline (0.1 µg/ml) for 24 hours to induce ICP0 expression or left untreated, and the following day infected with sequential three-fold dilutions of wt (in1863) or ICP0-null mutant (*dl*1403CMV/lacZ) HSV-1. The starting dilutions varied between the cell types and viruses. The plaque counts at each dilution, the average plaque counts and the relative value of each cell type compared to wt ICP0 (HA-cICP0) are shown from three repeat experiments.

A) Wt HSV-1 minus doxycycline

Cells HA-	**Dil**	**1**	**1/3**	**1/9**	**1/27**	**Average**	**Relative % compared to wt**	**Ave relative values**
TetR	**10^{-4}**	tmtc	tmtc	104	49	112950000	74.3	**85.3**
		tmtc	321	158	45	120000000	113.9	
		tmtc	331	149	40	113800000	67.8	
cICP0	**10^{-4}**	tmtc	tmtc	158	60	152100000	100.0	**100.0**
		tmtc	334	132	36	105400000	100.0	
		tmtc	379	199	78	167800000	100.0	
cICP0. PTAP	**10^{-4}**	tmtc	272	103	47	100400000	66.0	**89.9**
		tmtc	359	178	48	132500000	125.7	
		tmtc	409	173	42	130600000	77.8	
cICP0. SIAH	**10^{-4}**	tmtc	255	107	36	90000000	59.2	**91.2**
		tmtc	474	172	49	143100000	135.8	
		tmtc	435	127	56	132000000	78.7	

B) wt HSV-1 plus doxycycline

Cells HA-	**Dil**	**1**	**1/3**	**1/9**	**1/27**	**Average**	**Relative % compared to wt**	**Ave relative values**
TetR	**10^{-4}**	tmtc	tmtc	136	39	113850000	72.3	**67.5**
		tmtc	247	103	37	88900000	51.4	
		tmtc	226	110	30	82600000	78.8	
cICP0	**10^{-4}**	tmtc	tmtc	134	72	157500000	100.0	**100.0**
		tmtc	tmtc	213	57	172800000	100.0	
		tmtc	tmtc	137	32	104850000	100.0	
cICP0. PTAP	**10^{-4}**	tmtc	285	116	34	93900000	59.6	**88.7**
		tmtc	385	182	64	150700000	87.2	
		tmtc	314	174	46	125000000	119.2	
cICP0. SIAH	**10^{-4}**	tmtc	236	119	22	79100000	50.2	**78.7**
		tmtc	472	223	74	180700000	104.6	
		tmtc	281	109	27	85100000	81.2	

C) ICP0 null mutant HSV-1 minus doxycycline

Cells HA-	**Dil**	**1**	**1/3**	**1/9**	**1/27**	**Average**	**Relative % compared to wt**	**Ave relative values**
TetR	**10^{-2}**	54	12	12	0	60000	15.8	**51.3**
		157	44	11	3	117250	79.8	
		221	41	9	5	140000	58.5	
cICP0	**10^{-2}**	438	127	24	18	380250	100.0	**100.0**
		225	52	17	2	147000	100.0	
		307	88	22	7	239500	100.0	
cICP0. PTAP	**10^{-2}**	67	17	9	4	76750	20.2	**67.1**
		150	40	12	6	135000	91.8	
		269	63	26	6	213500	89.1	
cICP0. SIAH	**10^{-2}**	104	14	9	2	70250	18.5	**55.8**
		125	32	15	2	102500	69.7	
		201	63	23	6	189750	79.2	

D) ICP0 null mutant HSV-1 plus doxycycline

Cells HA-	**Dil**	**1**	**1/3**	**1/9**	**1/27**	**Average**	**Relative % compared to wt**	**Ave relative values**
TetR	**10^{-2}**	49	11	4	2	43000	0.1	**0.3**
		151	42	5	3	100750	0.2	
		tmtc	72	18	5	171000	0.4	
cICP0	**10^{-4}**	274	84	22	16	28900000	100.0	**100.0**
		tmtc	148	64	20	52000000	100.0	
		276	90	55	18	38175000	100.0	
cICP0. PTAP	**10^{-4}**	159	70	24	10	21375000	74.0	**65.6**
		281	152	49	8	34850000	67.0	
		186	75	19	10	21300000	55.8	
cICP0. SIAH	**10^{-4}**	173	45	17	3	13550000	46.9	**52.8**
		267	112	53	10	33750000	64.9	
		185	70	14	7	17750000	46.5	

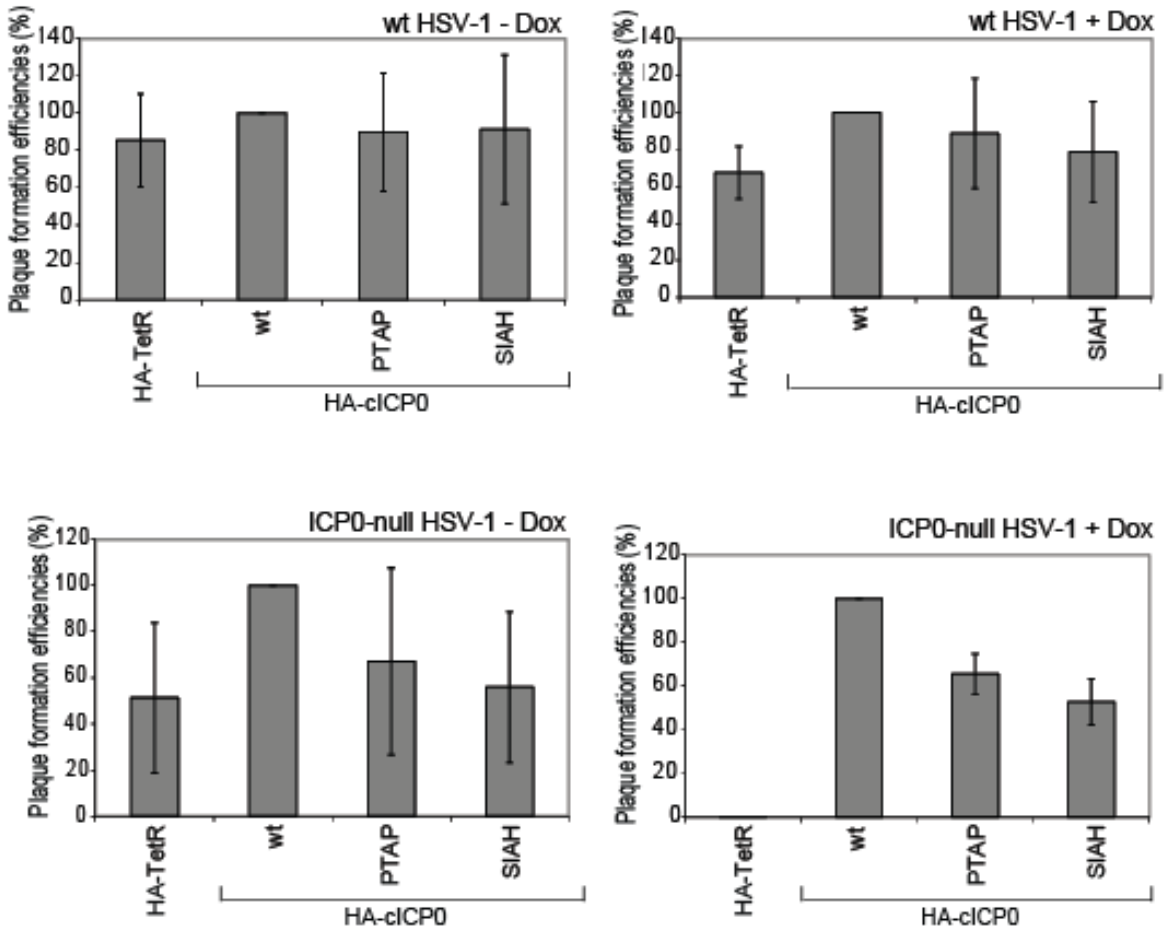

Figure 6.4 Effect of PPEYPTAP motif and SIAH-1 interaction motif mutations within ICP0 on wt HSV-1 and ICP0-null mutant HSV-1 plaque formation efficiency.
The experiments for each virus were carried out using HA-cICP0, HA-PPEYPTAP and HA-SIAH-IM cells, with or without doxycycline induction (0.1 µg/ml), 24 hours before staining for β-galactosidase activity. The graphs from data in **Table 6.2** show the average PFE from three replicate experiments as a percentage of HA-cICP0 cells. The error bars represent the standard deviation from three repeat experiments.

6.2.2.2 Construction of PPEYPTAP and SIAH-IM mutant viruses

The PPEYPTAP motif and SIAH-1 interaction motif are involved in interactions with cellular E3 ubiquitin ligases, so it is conceivable that they are involved with phenotypes that are more easily studied in the context of a mutant virus infection. Viruses containing the same mutations in these motifs as those in the inducible cell line (**section 6.2.2.1**) and described in **chapter 2.2.3** were constructed by homologous recombination with *dl*1403 infectious DNA and plaque purified, as described in **chapter 2.6**.

6.2.2.3 Plaque formation efficiency of PPEYPTAP and SIAH-IM mutant viruses during infection of HFs and HepaRG cells

Plaque assays were conducted in HepaRG cells and the more restrictive HFs. Since ICP0 is not required for efficient HSV-1 replication in U2OS cells, the results were presented as a ratio of plaques formed on these cells, and presented as a percentage of those formed in wt infected cells (**Figure 6.5**). The SIAH-IM virus had comparable plaque formation efficiency to wt virus in HepaRG cells, and this was almost 50% higher in HFs, which was surprising as this is a more restrictive cell type. The reasons for this are unknown, but it may simply reflect inherent variation in plaque formation assays. The PPEYPTAP mutant virus had greatly increased PFE compared to wt in HepaRG cells with around 1.7-fold increase, but showed around a two-fold defect in HFs in relation to wt.

Mutations in the SIAH-1 interaction motif did not seem to reduce the ability of the virus to form plaques. This was somewhat surprising, based on results from the inducible cell line (**section 6.2.2.1**) that showed SIAH-IM had a two-fold defect compared to wt ICP0, and previous results showing transfected ICP0 lacking the SIAH-1 interaction motif had reduced plaque forming ability in cells co-transfected with ICP0-null mutant virus DNA (Nagel *et al.,* 2011). The previous results were based on a deletion of the whole SIAH-1 interaction motif from residues 410-420 in HSV-2 ICP0, whereas in this study mutations were created in two residues of the SIAH-1 interaction motif mutating from RPRAAVAPCVR to RPRAAGAGCVR. Therefore, the mutations in SIAH-IM may not have been sufficient to completely abolish the interaction with SIAH-1. However, it could not be confirmed if the mutant still interacted with SIAH-1 (see **section 6.2.2.5**).

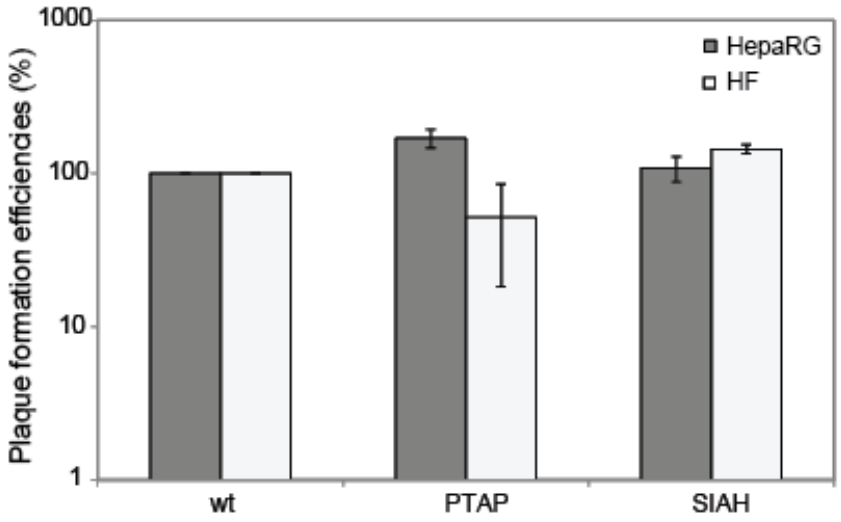

Figure 6.5 Plaque formation efficiencies of PPEYPTAP mutant and SIAH-IM viruses in HFs and HepaRG cells.
Plaque assays were conducted in cells infected with sequential ten-fold dilutions of wt or mutant viruses. The average plaque formation efficiency from each virus in HFs and HepaRG cells were calculated as a ratio of plaques formed in U2OS cells and presented as a percentage of the wt value. The error bars represent the higher and lower percentages obtained from two repeat experiments.

6.2.2.4 PPEYPTAP mutant and SIAH-IM viruses efficiently induce the dispersal of PML in infected cells, but the PPEYPTAP mutation affects ICP0's translocation to the cytoplasm at late times of infection.

The PPXY motif of protein VI of adenovirus has been reported to displace hDaxx from ND10 (Schreiner *et al.*, 2012). SIAH-1 is able to bind to and induce the proteasome-mediated degradation of PML (Fanelli *et al.*, 2004), and it has been reported that ICP0 lacking the SIAH-1 interaction motif was more efficient at inducing the degradation of PML (Nagel *et al.*, 2011). The effects of the PPEYPTAP and SIAH-1 interaction motif mutations on PML, one of the main ND10 proteins, and the localisation of ICP0 were investigated by immunofluorescence in HFs during infection at MOI 10 (**Figure 6.6**) at two and eight hours post infection.

At two hours post infection, the majority of PML had been dispersed in cells infected with mutant PPEYPTAP and SIAH-IM virus, which was comparable to the wt virus. The PML had been dispersed in SIAH-IM infected cells, even in cells expressing a low amount of ICP0. This agrees with previous literature that found PML was degraded efficiently in cells transfected with ICP0 lacking the SIAH-1 interaction motif (Nagel *et al.*, 2011). At

two hours post infection, ICP0 showed a nuclear distribution, whereas at eight hours post infection, in wt and SIAH-IM infected cells, the ICP0 was cytoplasmic. This is expected, as at later times of infection ICP0 relocalises to the cytoplasm (Kawaguchi *et al.*, 1997). However, in PPEYPTAP infected cells at later times of infection, there was a small percentage of cytoplasmic ICP0, though the majority remained in distinct foci in the nucleus. Previous work with virus D14, which contains a deletion of ICP0 residues 680-720 that overlaps with the PPEYPTAP mutation, ICP0 was retained in the nucleus at later times of infection and did not relocate to the cytoplasm (Everett & Maul, 1994). Mutations in multiple SLS located in the C-terminal region of ICP0 also affect the intracellular localisation of ICP0 by causing retention of ICP0 in the nucleus at later times of infection (Everett *et al.*, 2014), although none of these SLS motifs overlap with the PPEYPTAP motif. Therefore, the mutations in the PPEYPTAP motif most likely affect a more extensive region of ICP0 that includes the SLS motifs and that is likely to play a role in the redistribution of ICP0 from the nucleus to the cytoplasm at later times of infection.

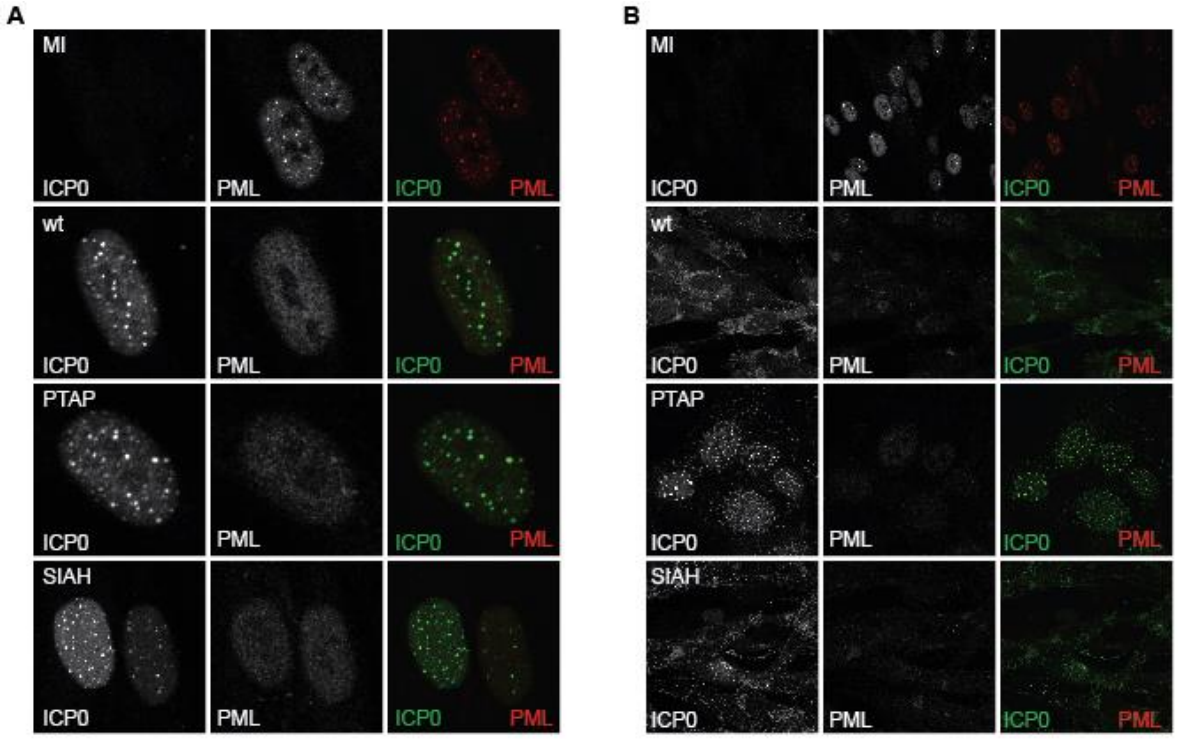

Figure 6.6 Analysis of ICP0 and PML expression in PPEYPTAP mutant and SIAH-IM virus infected HFs.
HFs on coverslips were infected at an MOI of 10 with wt or mutant virus, and at 2 hours (A) and 8 hours (B) post infection cells were fixed and permeablised. The cells were analysed by immunofluorescence staining for ICP0 (green) and PML (red). (A) is an image of the cell's nucleus whereas (B) is a wide-field image of a number of cells, as in some cells ICP0 was cytoplasmic at this time-point.

6.2.2.5 Colocalisation between ICP0 and SIAH-1 in infected cells could not be detected

SIAH-1 and ICP0 have been reported to colocalise in discrete nuclear foci in HSV-1 infected cells (Nagel *et al.*, 2011). Immunofluorescence was carried out to investigate whether ICP0 containing mutations in the SIAH-1 interaction motif would still show localisation with ICP0. HFs were infected with wt or SIAH-IM virus at MOI 2 and fixed and stained for ICP0 and SIAH-1 at two and four hours post-infection. In wt infected cells, no colocalisation between SIAH-1 and ICP0 could be detected, and SIAH-1 showed a diffuse nuclear staining and no colocalisation with the ICP0 foci. The fact that no colocalisation between SIAH-1 and ICP0 was observed may be due to antibody specificity, and due to time constraints and reagent availability, no other antibodies against SIAH-1 could be tested. Therefore, it could not be confirmed if the mutations in the SIAH-1 interaction motif abolished the interaction with SIAH-1 completely, or indeed if the published interaction between SIAH-1 and ICP0 could be verified independently by this method.

6.2.2.6 Conclusion and Discussion

While mutations in the SIAH-1 interaction motif caused a two-fold defect in plaque forming ability when complementing an ICP0-null mutant virus in the inducible cell line system, mutations in this motif in the context of the HSV-1 genome did not affect plaque forming ability in either HepaRG cells or HFs, and did not affect the dispersal of PML within infected cells at early times of infection, which was comparable to wt virus. This is surprising based on previous transfection results that showed deletion in the SIAH-1 interaction motif reduced plaque forming ability (Nagel *et al.*, 2011). Therefore, the results may show that abolishing the interaction with SIAH-1 does not affect ICP0 functions within the context of viral infection to any substantial degree, or that the function of SIAH-1 is redundant and other cellular proteins can play the role of SIAH-1. However, it could not be confirmed if the interaction with SIAH-1 was abolished in SIAH-IM virus, as no interaction could be detected between wt ICP0 and the SIAH-1 protein (at least in terms of co-localisation). Therefore, the mutations introduced into the SIAH-1 interaction motif may not have abolished the interaction with SIAH-1 completely (although they do affect known important residues), and it is conceivable that the protein could still bind and therefore behave as wt ICP0 and give similar results to wt infection. To investigate this in more detail, different antibodies to the SIAH-1 protein should be analysed to investigate the interaction between SIAH-1 and ICP0, and to test if this is lost in the SIAH-IM virus.

It may be necessary to mutate the whole SIAH-1 interaction motif before it can be concluded that this motif does not have an effect during HSV-1 infection.

The PPEYPTAP motif in retroviral gag proteins is involved in interactions with E3 ubiquitin ligases and is important for regulating viral budding. HSV-1 ICP0 containing mutations in this motif had a slightly reduced PFE in HFs, but this was not the case in the less restrictive HepaRG cells (indeed the mutant virus appeared to have an enhanced plaque forming ability in these cells) (**Figure 6.5**). The mutant virus dispersed PML as rapidly as wt virus, but at late times of infection ICP0 remained nuclear and did not relocate into the cytoplasm. Different parts of the C-terminal region of ICP0 have been shown to be important for the redistribution of ICP0 from the nucleus to the cytoplasm at later times of infection. Therefore, mutations in this motif are likely to contribute to this mechanism rather than being fully responsible for this effect. They may affect the protein folding or binding of ICP0 to the cell's transport machinery.

As PPEYPTAP motifs in retroviral gag proteins have been shown to interact with cellular E3 ubiquitin ligases, a yeast-two-hybrid screen could be carried out to analyse whether this motif within ICP0 interacts with different E3 ligases of the NEDD4 family. Co-immunoprecipitation experiments could be used to confirm any interactions found. As PPEYPTAP motifs are involved in viral budding in retroviruses, the effects of this motif on HSV-1 egress could be investigated by immunofluorescence, staining for proteins of the nuclear egress complex and investigating if virus containing mutations in the PPEYPTAP motif behave in a similar manner to wt virus.

6.3 The role of the sequence within ICP0 implicated in the binding to CoREST

ICP0 contains a region of amino acids (resides 537 to 613) that shows some homology to a sequence in the N-terminal part of the cellular protein CoREST (Gu *et al.*, 2005). CoREST is a corepressor for the cellular protein REST, that along with HDAC1 and HDAC2, forms a transcriptional repressor complex and has a role in chromatin modification (You *et al.*, 2001). In non-neuronal cells, ICP0 has been shown to bind to CoREST during infection with HSV-1, leading to the displacement of HDAC1 from the REST/CoREST/HDAC complex (Gu *et al.*, 2005). Subsequent studies showed that the ICP0 residues 671 (aspartic acid) and 673 (glutamic acid) are required for ICP0 binding to CoREST (Gu & Roizman, 2009). It was shown that PML was largely but not fully degraded in cells infected with the

double point mutant R8507 (D671A/E673A) in the CoREST binding region and viral replication was delayed (Gu & Roizman, 2009). This region is within the D14 deletion mutation which showed decreased ICP0 activity in the presence of ICP4 (Everett, 1988).

Roizman and Gu (2009) suggested that the REST/CoREST/HDAC complex may repress viral gene expression in the absence of ICP0, and therefore may have a role in the reactivation/derepression of viral gene expression. However, Ferenczy et al. (2011) found that R8507 and wt virus activated quiescent genomes to an equivalent extent in a cell-based system that quantified GFP expression from a reporter gene in a mutant virus that readily establishes quiescent infections in cell culture. This conclusion was based on the proportion of cells that became GFP positive after superinfection with R8507 or wt HSV-1, although GFP mRNA was reduced compared to wt (Ferenczy *et al.*, 2011). Therefore, the aim of this section (which was initiated before publication of the Ferenczy et al. study) was to investigate the double point mutant R8507 (D671A/E673A) to determine if it plays any role in the reactivation/derepression of viral gene expression from quiescent genomes using the inducible ICP0 expression system.

6.3.1 Ability of R8507 mutant ICP0 to complement an ICP0 null mutant HSV-1 virus using the inducible ICP0 expression system

The mutations defined as R8507 in the original publications from the Roizman laboratory were independently introduced into the HSV-1 strain 17 ICP0 sequence. For simplicity, the mutant ICP0 protein produced here was also termed R8507. The ability of the R8507 mutant to complement ICP0-null mutant (*dl*1403/CMVLacZ) and wt HSV-1 (*in*1863) infection was analysed by plaque assay with or without doxycycline to induce ICP0 expression (**Table 6.3, Figure 6.7**). HA-TetR control cells, HA-cICP0 and HA-R8507 cells infected with the wt virus all had similar plaque numbers without ICP0 induction. After ICP0 induction of wt infected HA-R8507 cells, there was a slight decrease in plaque numbers compared to HA-cICP0 wt infected cells, though this was less than two-fold. In cells infected with an ICP0-null mutant (*dl*1403) virus and in the absence of induction, there was no difference in plaque numbers between HA-TetR cells and HA-cICP0 cells, with HA-R8507 cells showing a slight decrease. ICP0-null mutant virus plaque numbers were increased by about 200-fold after induction of wt ICP0 expression compared to HA-TetR control cells. The ICP0-null mutant virus infected HA-R8507 cells induced with

doxycycline were 50% as effective as HA-cICP0, and therefore had only a slight defect in the complementation of ICP0-null mutant virus.

Table 6.3 Plaque count data in cells expressing R8507 following infection with wt or ICP0-null mutant HSV-1.
Cells were treated with doxycycline (0.1 µg/ml) for 24 hours to induce ICP0 expression or left untreated, and the following day infected with sequential three-fold dilutions of wt (in1863) or ICP0-null mutant (*dl*1403CMV/lacZ) HSV-1. The starting dilutions varied between the cell types and viruses. The plaque counts at each dilution, the average plaque counts and the relative value of each cell type compared to wt ICP0 (HA-cICP0) are shown from three repeat experiments.

A) Wt HSV-1 minus doxycycline

Cells HA-	**Dil**	**1**	**1/3**	**1/9**	**1/27**	Average	Relative % compared to wt	**Ave relative values**
TetR	**10^{-4}**	tmtc	124	59	32	58900000	71.8	**90.1**
		tmtc	tmtc	100	31	86850000	108.4	
cICP0	**10^{-4}**	tmtc	265	101	28	82000000	100.0	**100.0**
		tmtc	tmtc	115	21	80100000	100.0	
cICP0. R8507	**10^{-4}**	tmtc	308	133	38	104900000	127.9	**113.1**
		tmtc	tmtc	97	26	78750000	98.3	

B) Wt HSV-1 plus doxycycline

Cells HA-	**Dil**	**1**	**1/3**	**1/9**	**1/27**	Average	Relative % compared to wt	**Ave relative values**
TetR	**10^{-4}**	tmtc	163	81	19	57700000	37.0	**44.3**
		tmtc	tmtc	84	16	59400000	51.6	
cICP0	**10^{-4}**	tmtc	tmtc	179	56	156150000	100.0	**100.0**
		tmtc	tmtc	118	46	115200000	100.0	
cICP0. R8507	**10^{-4}**	tmtc	tmtc	106	40	101700000	65.1	**60.1**
		tmtc	tmtc	72	23	63450000	55.0	

C) ICP0 null mutant HSV-1 minus doxycycline

Cells HA-	**Dil**	**1**	**1/3**	**1/9**	**1/27**	**Average**	**Relative % compared to wt**	**Ave relative values**
TetR	**10^{-2}**	tmtc	tmtc	357	22	1903500	89.8	**122.5**
		tmtc	tmtc	176	22	1089000	155.1	
cICP0	**10^{-2}**	tmtc	tmtc	312	53	2119500	100.0	**100.0**
		tmtc	tmtc	105	17	702000	100.0	
cICP0. R8507	**10^{-2}**	tmtc	tmtc	132	23	904500	42.7	**59.8**
		tmtc	tmtc	78	14	540000	76.9	

D) ICP0 null mutant HSV-1 plus doxycycline

Cells HA-	**Dil**	**1**	**1/3**	**1/9**	**1/27**	**Average**	**Relative % compared to wt**	**Ave relative values**
TetR	**10^{-2}**	tmtc	tmtc	93	14	607500	0.5	**0.5**
		tmtc	tmtc	184	25	1165500	0.6	
cICP0	**10^{-4}**	tmtc	tmtc	121	50	121950000	100.0	**100.0**
		tmtc	tmtc	204	77	195750000	100.0	
cICP0. R8507	**10^{-4}**	tmtc	139	68	21	53200000	43.6	**50.2**
		tmtc	278	143	45	111200000	56.8	

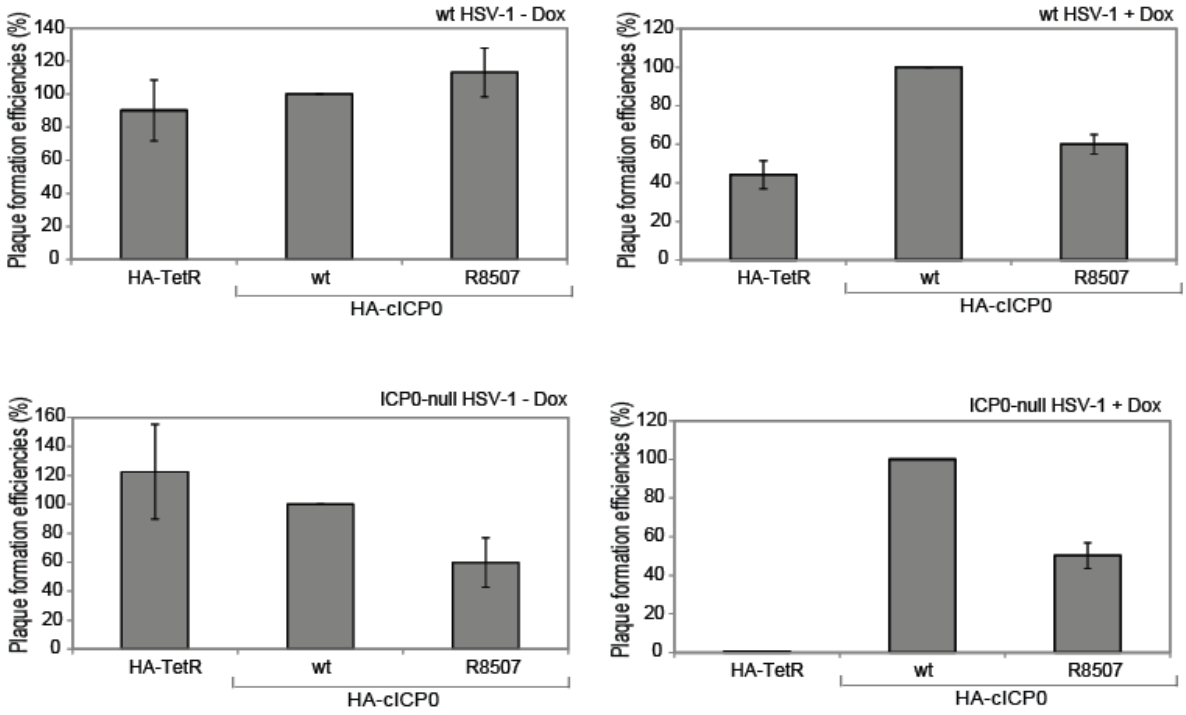

Figure 6.7 PFE of cells expressing R8507 following wt HSV-1 and ICP0-null mutant HSV-1 infection.
HA-TetR, HA-cICP0 and HA-R8507 cells were infected with wt HSV-1 (*in*1864) or ICP0-null mutant virus (*dl*1403) and either induced with doxycycline (0.1 µg/ml) or left untreated. The following day the cells were stained for β-galactosidase activity to visualise plaque formation. The graphs from the data in **Table 6.3** show the average plaque forming ability of HA-TetR and HA-R8507 as a percentage of plaques formed in HA-cICP0 cells. The error bars represent the range between two repeat experiments.

6.3.2 The R8507 mutation affects the rate of degradation of ND10 proteins

R8507 is located within the C-terminal quarter of ICP0, which is required for efficient localisation to ND10 (Maul & Everett, 1994), and Gu and Roizman found that PML degradation was delayed in R8507 infected cells (Gu & Roizman, 2009). Therefore, the effects of the R8507 mutation on PML and Sp100 degradation in the ICP0 inducible expression system were investigated by Western blotting (**Figure 6.2**). After doxycycline induction, wt ICP0 (HA-cICP0) caused extensive degradation of all PML proteins and SUMO-modified Sp100, with only unmodified Sp100 remaining. HA-R8507 cells after induction showed degradation of the different PML isoforms, with only low levels of PML I/II remaining. The R8507 mutant did not degrade SUMO modified Sp100 as efficiently as wt ICP0, with some SUMO modified Sp100 remaining, but this was at lower levels than in the HA-TetR control cells.

6.3.3 R8507 had a two-fold reduction in reactivating viral gene expression compared to wt ICP0.

It has been suggested that the REST/CoREST/HDAC complex may play a role in reactivation/derepression of viral gene expression in the absence of ICP0 (Gu & Roizman, 2009). The ICP0 residues required for binding to CoREST (D671A/E673A), leading to displacement of HDAC1 from the complex, were investigated for their role in the reactivation/derepression of viral gene expression from quiescent genomes in the inducible ICP0 expression system.

HA-cICP0 and HA-R8507 cells were infected with *in*1374 virus, and the following day ICP0 expression was induced by the addition of doxycycline. The percentage of cells positive for β-galactosidase expression were calculated and presented as a percentage expression of HA-cICP0 cells (**Figure 6.8**). The results showed that R8507 mutant has slight defects in reactivating gene expression, with 50% of wt levels. The reactivation efficiency of mutant R8507 correlates with the complementation ability of an ICP0-null mutant virus, with both showing a two-fold reduction compared to wt.

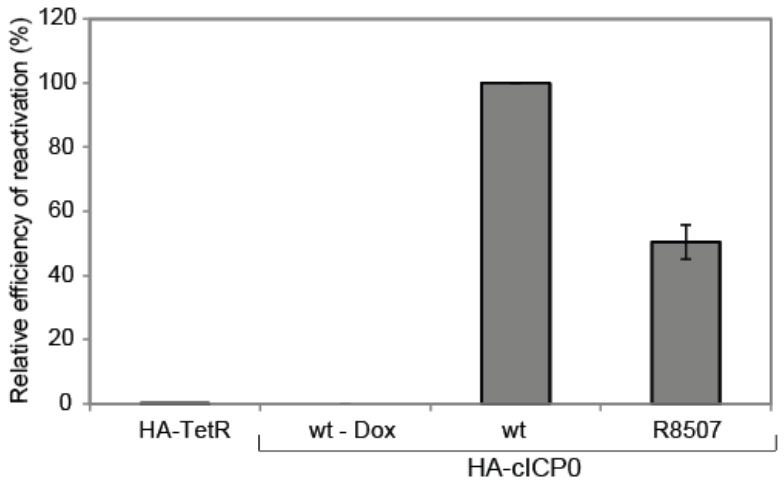

Figure 6.8 Quantification of reactivated viral gene expression by ICP0 mutant R8507. HA-cICP0 and HA-R8507 cells infected with *in*1374 virus and ICP0 expression induced by doxycycline (except where indicated) the next day were stained 24 hours later to detect β-galactosidase activity (**Figure 3.3**). The cells from a single plate were imaged, and the proportion of cells expressing β galactosidase for each cell type was represented as a percentage of HA-cICP0 reactivation efficiency. The error bars represent the higher and lower percentages obtained from two images.

6.3.4 Conclusion and Discussion

Using the inducible ICP0 expression system, it was found that cells expressing R8507 mutant ICP0 had a two-fold reduction compared to wt ICP0 protein when complementing an ICP0-null mutant virus and in reactivation of quiescent viral gene expression. As mutations in the residues involved in CoREST binding did not have a major effect on complementing the PFE of an ICP0-null mutant virus or reactivation, it is unlikely that this mechanism plays a major role in the reactivation of viral gene expression.

Cells expressing R8507 did not degrade PML completely to wt levels, with some SUMO unmodified PMLI/II remaining. This is in agreement with previous work that showed that PML degradation is delayed in cells infected with R8507 (Gu & Roizman, 2009). Recent work has shown that R8507 virus had a three-fold defect in plaque forming ability in HepaRG cells, while in HFs it was found not to be defective, and it was confirmed that PML degradation was slightly delayed in R8507 infected cells (Everett *et al.*, 2014). Given that the R8507 mutations lie in a region that has some effects on ICP0 localisation and the rate of PML degradation (Ciufo *et al.*, 1994; Everett *et al.*, 2014; Everett & Maul, 1994; Maul & Everett, 1994), it is not possible to conclude whether the slight defects in the activity of the R8507 ICP0 protein can be attributed to its lack of interaction with CoREST or to ND10-related phenomena.

6.4 Deletion of residues downstream from ICP0 RING finger domain that show sequence similarity between different alphaherpesviruses

The region downstream from the RING finger domain of ICP0 shows sequence similarity between HSV-1, HSV-2 and herpesvirus B of macaque monkey (**Figure 6.9**). This region has been shown to be important for the E3 ligase activity of ICP0, as deletion between residues 162-188, which does not include the RING finger domain, was E3 ligase negative *in vitro* (Boutell *et al.*, 2002). Further downstream from this region, a deletion mutant lacking residues 197-222 was negative for the ability to induce accumulations of conjugated ubiquitin (Everett, 2000).

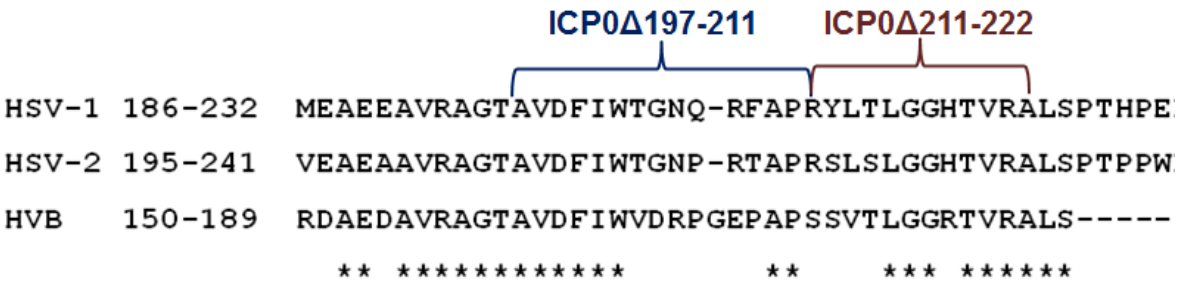

Figure 6.9 The region downstream of the RING finger domain is conserved in HSV-1, HSV-2 and HVB.
The asterisks denote completely conserved residues from the three herpesviruses. Labelled are the deletion mutants ICP0Δ197-211 and ICP0Δ211-222, that were analysed in this study.

In this section, the region downstream from the ICP0 RING finger domain between residues 197 and 222 was investigated (**Figure 6.9**). This region contains two distinct sections of high sequence similarity between the related proteins referred to above. These could be substantially altered separately using existing ICP0 mutants that contain insertions of sequences including an *EcoR*I site, namely E13, R3 and E32. As described in the Methods chapter (**section 2.2.4**), plasmids were constructed that included deletions between the E13 and R3, or the R3 and E32 insertion sites. These plasmids were used to isolate mutant viruses containing deletions within ICP0 of residues 197-211 (ICP0Δ197-211) and residues 211-222 (ICP0Δ211-222) by homologous recombination. Isolation of a virus containing a deletion of this whole region from residues 197-222, which has been studied previously in the context of plasmid transfection experiments, was attempted but was not successful as any virus made repeatedly reverted back to an ICP0-null mutant virus.

The aim of this section was to investigate the region downstream of the RING finger domain, to characterise the phenotypes of viruses containing deletions within this region, and to analyse their importance in the context of viral infection.

6.4.1 The ICP0Δ211-222 virus has substantial defects in the plaque formation efficiency in HFs and HepaRG cells.

Cell type can influence the apparent phenotypes of ICP0 mutant viruses and their PFE. Therefore, plaque assays were carried out in HepaRG cells and the more restrictive HFs,

and the plaques formed in these cell types were calculated as a ratio of those produced on the permissive U2OS cells. The results are presented on a log scale as a proportion of plaques produced compared to wt virus (**Figure 6.10**).

The deletion mutant ICP0Δ197-211 did not have a substantial defect in the formation of plaques in HFs, with 79% of wt activity. In HepaRG cells this was lower at 56% of wt activity, but this is less than a two-fold reduction. The deletion ICP0Δ211-222 caused a substantial decrease in PFE compared to wt, with over a 70-fold reduction in plaque numbers compared to wt in HepaRG cells, and a 500-fold reduction in the more restrictive HFs.

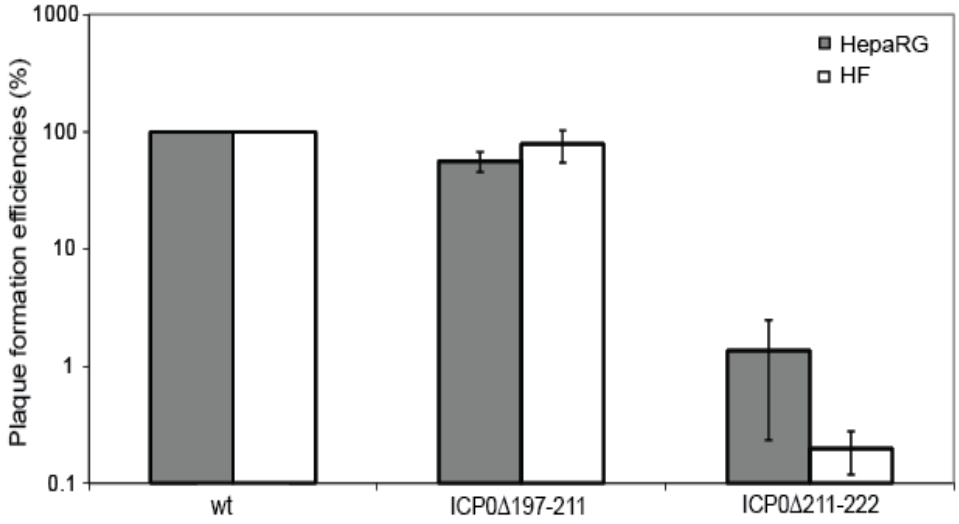

Figure 6.10 PFE of ICP0Δ197-211 and ICP0Δ211-222 viruses in HepaRG cells and HFs.
Plaque assays were conducted in cells infected with wt HSV-1 or ICP0 mutant viruses. The average PFE of the viruses in each cell type was calculated as a ratio of plaques formed in U2OS cells, and shown as a percentage of the wt value. The error bars represent the higher and lower percentages obtained from two repeat experiments.

6.4.2 ICP0Δ211-222 virus fails to degrade PML despite showing colocalisation

In transfection experiments, a deletion within ICP0 from residues 197 to 222 was shown to be negative in the accumulation of conjugated ubiquitin (Everett, 2000). The formation and localisation of conjugated ubiquitin is a good indicator of E3 ligase activity and the ability to induce the degradation of substrates via the proteasome. Therefore, due to this deletion effect on the accumulation of ubiquitin, the mutants ICP0Δ197-211 and ICP0Δ211-222 that span this deletion were investigated for their abilities to colocalise with and degrade PML.

The ability of the deletion mutants to colocalise with PML was investigated by immunofluorescence in HFs infected at MOI 10, and stained at two and four hour post infection (**Figure 6.11**). In wt infected cells, the PML had been dispersed by two hours post infection. This contrasts with non-infected cells, where the PML remained in distinct foci that were scattered throughout the nucleus. In cells infected with ICP0Δ197-211, the PML signal was also dispersed at two hours post infection and was comparable to wt infected cells. The ICP0Δ211-222 mutant did not induce the dispersal of PML even at four hours post infection, and ICP0 showed colocalisation with the PML foci.

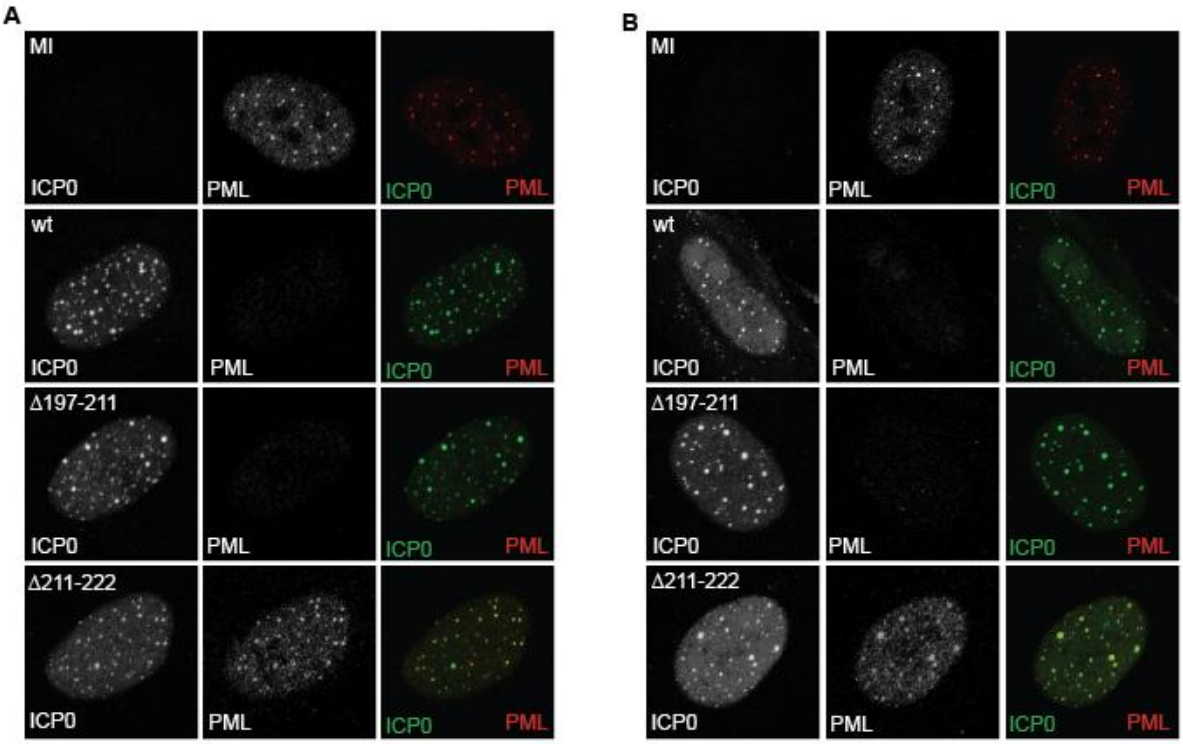

Figure 6.11 Expression of ICP0 in HFs infected with ICP0Δ197-211 and ICP0Δ211-222 and the ability of the mutants to colocalise with and disperse PML in infected cells.
HF cells were infected at MOI of 10 with wt and mutant virus stained for ICP0 (green) and PML (red) at 2 hours (A) and 4 hours (B) post infection.

The rate of PML degradation and viral gene expression in the mutant viruses was investigated by Western blot in HFs infected at an MOI 5 (**Figure 6.12**). In wt infected cells, the majority of PML was degraded by two hours post infection, with only minimal amounts of unmodified PML remaining. PML degradation was slightly delayed to four hours post infection in ICP0Δ197-211 infected cells. ICP0Δ211-222 showed reduced degradation of PML at the two and four hours post infections, which is consistent with the immunofluorescence results (**Figure 6.11**). Some degradation of PML had occurred in ICP0Δ211-222 infected cells by the six hour and eight hour time-points.

Viral gene expression was analysed at the same time as PML degradation at MOI 5 (**Figure 6.12**). Even at this high MOI which can potentially mask the true effects of ICP0 mutations on viral gene expression, ICP0Δ211-222 shows a substantial delay in gene expression of the early UL42 and late capsid protein VP5, whereas the effect on ICP0 expression was not as apparent.

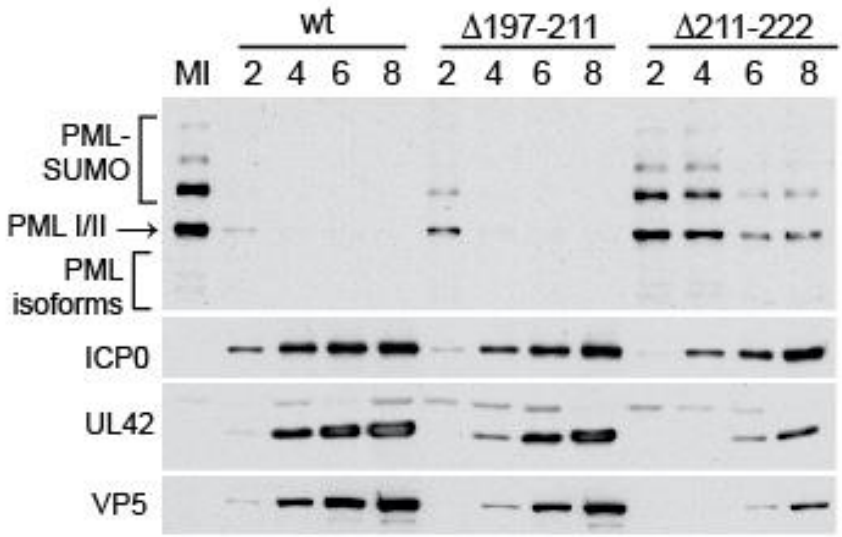

Figure 6.12 Ability of ICP0Δ197-211 and ICP0Δ211-222 mutant viruses to degrade PML and their effects on the rate of viral gene expression during an eight hour infection.
HFs were infected with wt or mutant viruses at an MOI of 5 and samples harvested at 2, 4, 6 and 8 hours post infection. The proteins were resolved on a 7.5% SDS gel, transferred to a nitrocellulose membrane, and detected by probing for ICP0, UL42 and VP5, representing IE, early and late classes of viral proteins, respectively.

6.4.3 Viral gene expression was substantially delayed in ICP0Δ211-222 virus infections

Viral gene expression was shown to be delayed in ICP0Δ211-222 infected cells, even at the high MOI of 5 (**Figure 6.12**). Therefore, the effects of the deletions downstream of the RING finger on viral gene expression were investigated at the lower MOI of 1 over the course of an eight hour infection in HFs. The results (**Figure 6.13**) show that the expression of ICP0 in both ICP0Δ197-211 and ICP0Δ211-222 was comparable to wt expression levels at each time point. The differences in gene expression become apparent for expression of the early UL42 protein and late VP5 capsid protein. In ICP0Δ197-211 infected cells, gene expression of the early and late proteins was slightly lower than that seen with the wt virus but expression began at the same time points. However, ICP0Δ211-222 has a substantial effect on viral gene expression, with no expression of UL42 or VP5 by eight hours post infection. Therefore, although ICP0Δ211-222 does not have any considerable defect in ICP0 expression compared to wt, early and late gene expression is severely affected.

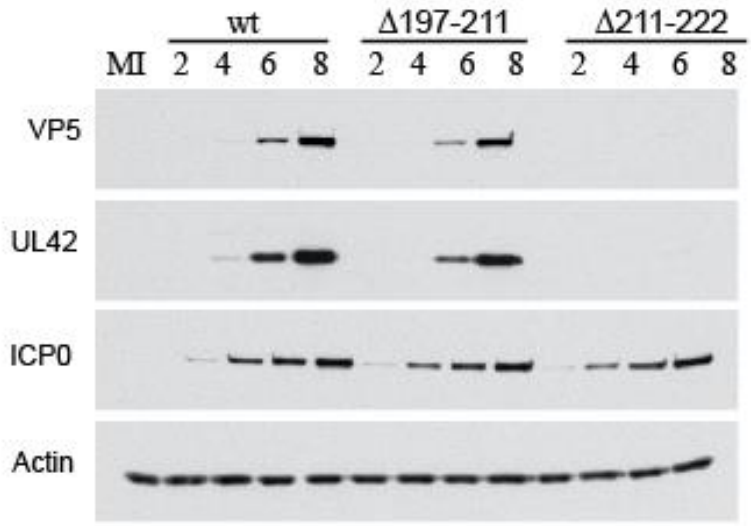

Figure 6.13 Comparison of the viral gene expression efficiencies of the ICP0Δ197-211 and ICP0Δ211-222 mutant viruses compared to wt.
HFs were infected at an MOI of 1 and then samples harvested at 2, 4, 6 and 8 hours post infection were analysed by Western blotting, probing for ICP0, UL42, and VP5 representing IE, early and late classes of viral proteins. Actin was the loading control.

6.4.4 Conclusions and Discussion

ICP0Δ197-211 showed a slight decrease in plaque forming ability compared to wt virus but was comparable to wt in gene expression and PML degradation. The ICP0Δ211-222 virus carrying deletion of residues directly downstream, however, showed major defects in PFE, PML degradation and gene expression of early and late proteins even in high MOI infections.

The ICP0Δ197-222 region has previously been shown to be negative for the accumulation of conjugated ubiquitin in transfection experiments (Everett, 2000), but, in the virus infected cell experiments ICP0Δ197-211 did not affect ICP0s ability to degrade PML, and in ICP0Δ211-222 infected cells, PML degradation was severely delayed, although there was some degradation at six hours post infection. Therefore, ICP0Δ211-222 must retain some ability to conjugate ubiquitin onto target proteins, albeit maybe less efficiently. The ability of these mutant proteins to conjugate ubiquitin could be further investigated by immunofluorescence staining for ICP0 and conjugated ubiquitin (FK2 antibody). Also, the E3 ligase activity of these mutants could be investigated *in vitro* for their ability to catalyse the formation of polyubiquitin chains in the presence of wt ubiquitin and E2 ubiquitin conjugating enzymes.

Residues 1-211 of ICP0 are active in *in vitro* ubiquitin conjugation assays (Boutell *et al.*, 2002), and therefore resides 211-222 cannot be absolutely required for core RING function. Yeast-two-hybrid experiments showed that the N-terminal region of ICP0 between residues 1-388 interacted with PML.I (Cuchet-Lourenço *et al.*, 2012), and virus deletion studies showed that residues 212-311 within ICP0 are involved in the dissociation and degradation of PML (Perusina Lanfranca *et al.*, 2013). Therefore, the defect of ICP0Δ211-222 in degrading PML could be due to this region being involved in substrate recognition. This hypothesis could be investigated by using cells expressing the different PML isoforms and analysing the effect that ICP0Δ197-211 (and ICP0Δ211-222) have on these compared to wt, in particular PML.I isoform cells. If residues 211-222 are involved in PML substrate recognition, this would not completely explain the observed phenotype of this virus, and therefore this deletion may affect binding to other cellular or viral proteins.

7 Summary, Discussion and Future Prospects

7.1 Summary

The RING finger domain of ICP0 acts as an E3 ubiquitin ligase (Boutell *et al.*, 2002), inducing the degradation and dispersal of ND10 proteins (Chelbi-Alix & de The, 1999; Everett & Maul, 1994; Parkinson & Everett, 2000), which are part of the cellular intrinsic antiviral defence mechanism. The RING finger domain contains an alpha-helix and loop regions (Barlow *et al.*, 1994), and these have been shown to be important for ICP0's interaction with E2 ubiquitin-conjugating enzymes (Barlow *et al.*, 1994; Vanni *et al.*, 2012). Some of the studies presented in this thesis aimed to contribute more detail to the understanding of the alpha-helix of the RING finger domain. Previous work using the inducible ICP0 expression system suggested that lytic infection and reactivation may involve differential activities of ICP0 that were revealed by a mutation in the alpha-helix, N151D (Vanni *et al.*, 2012). Therefore, to extend this work, mutations in the alpha-helix of ICP0 were investigated, including N151D and additionally K144E and the double mutant KE/ND using both the inducible ICP0 expression system and virus infection studies. The experiments with the ICP0 inducible expression system confirmed the previous results and showed that the single mutants had a greater defect during reactivation than complementation. The data using the virus infection studies showed a better correlation between the ability to degrade ICP0 substrates, and efficiencies of lytic infection and reactivation. However, the reactivation experiments were carried out at an MOI where lytic infection was not severely impeded. Therefore, residues K144 and N151 are important for ICP0's activity, especially for reactivation of quiescent HSV-1. These investigations indicated however that there is no strong evidence to suggest that ICP0 utilises differential activities of its RING finger to mediate reactivation and the stimulation of lytic infection, despite the likely dissimilar nature of the viral chromatin structure in the two situations.

Furthermore, as the RING finger shows a degree of sequence similarity among alphaherpesviruses, regions of homology that had not previously been investigated were studied along with motifs contained within ICP0 that had been reported to interact with E3 ubiquitin ligases or other cellular proteins. These studies indicated that a region downstream of the RING finger domain (residues 211-222) of ICP0 is important for

ICP0's activity, but no major role was detected for motifs that potentially interact with SIAH-1, Nedd4 family ubiquitin ligases, or CoREST.

7.2 Discussion

Conclusion and discussion points have been discussed at the end of each results chapter. Therefore to avoid overlap, only information not discussed in these chapters is reviewed here.

7.2.1 Residues in the alpha-helix are required for efficient ICP0 activity during the lytic phase and are important for reactivation

During lytic infection, mutant K144E was more defective than the N151D mutant, and this was especially apparent at low MOIs. It has previously been shown that mutations in the RING finger region of ICP0 could affect the levels of ICP0 contained within the tegument (Delboy *et al.*, 2010; Maringer & Elliott, 2010; Maringer *et al.*, 2012). It was reported that the virions of the K144E and FXE mutant viruses contained greatly reduced levels of tegument ICP0 and may have defects in transport of the capsid to the nucleus. However, mutant N151D virions contained wt levels of tegument ICP0, which was detected in the nuclear periphery (Delboy & Nicola, 2011; Delboy *et al.*, 2010). The results from this thesis, showing that the K144E mutation caused a greater defect than N151D during lytic infection, could in principle be explained by lack of tegument ICP0 in K144E virions and defects in transportation of the capsid to the nucleus. This would mean that fewer viral genomes entering the nucleus and therefore lower viral replication occurs. The role of tegument ICP0, however, remains incompletely understood, and independent verification of these studies is required. The replication of K144E virus was improved at higher MOIs, therefore genomes must be able to be transported and enter the nucleus if they are present in high enough copies, and the same must be true of ICP0 null mutant HSV-1. However, the hypothesis of tegument ICP0 being involved with capsid transport does not fully explain the phenotypes observed with the N151D mutant virus. Mutant N151D is reported to contain wt levels of tegument ICP0, but it shows an intermediate phenotype compared to wt during lytic infection. Therefore, the tegument levels of ICP0 in the RING finger

mutant viruses and their defects during lytic infection should be investigated to determine if the replication defects are correlated with lack of tegument ICP0 and transport to the nucleus.

The alpha-helix mutants reactivated quiescent HSV-1 poorly, even at multiplicities at which they replicated efficiently. The data suggest that there may be a greater requirement for ICP0 activity during reactivation of chromatinised quiescent genomes than for stimulating gene expression from unchromatinised genomes at the beginning of infection. These mutations and their effects on reactivation confirm that ICP0 is almost essential for reactivation of quiescent HSV-1 genomes in cultured cells, even under conditions such as high input MOI, where it is dispensable for lytic infection.

7.2.2 ICP0 has the ability to interact with multiple E2 ubiquitin conjugating enzymes and mutations in the alpha-helix may affect these interactions

The yeast-two-hybrid experiments showed that wt ICP0 has the potential to interact with the E2 ubiquitin conjugating enzymes UBE2V1 and UBE2W, as well as the previously described UBE2D1 and UBE2E1 enzymes (UbcH5a and UbcH6) (Boutell *et al.*, 2002; Vanni *et al.*, 2012). wt ICP0 could induce polyubiquitin chain formation in the presence of both UBE2D1 and the UBE2N-UBE2V1 heterodimer. However, auto-ubiquitination of ICP0 was detected in the presence of UBE2D1 but not with UBE2N-UBE2V1. These data are consistent with previous reports that UBE2N-UBE2V1 is involved in the formation of unanchored K63-linked polyubiquitin chains rather than the initial ubiquitin attachment event in the presence of E3 ubiquitin ligases CHIP and TRAF6 (Windheim *et al.*, 2008; Xu *et al.*, 2008).

The interaction of the alpha-helix mutants in ICP0 with UBE2V1 was below the limit of detection in the yeast-two-hybrid experiment. However, all the mutants retained some ability to catalyse polyubiquitin chains in the presence of UBE2N-UBE2V1, but these levels were below that of wt ICP0. N151D had reduced ability compared to wt, and this activity was reduced further with the K144E mutant, and KE/ND had levels only slightly above the ICP0-2C mutant.

In the yeast-two-hybrid experiment, the interaction between UBE2W and KE/ND was lost on the highest selection plate or was below the limit of detection. UBE2W attaches a single ubiquitin to the N-terminus of its substrates, as opposed to ubiquitination onto a ε-NH2 group of a lysine residue (Tatham *et al.*, 2013). N-terminal ubiquitin is not dependent on lysine residues and has been shown to be involved in the degradation of certain proteins including p21 (a regulator of the cell cycle and DNA replication (Bloom *et al.*, 2003)), MyoD (a transcription factor involved in muscle differentiation (Breitschopf *et al.*, 1998)), latent membrane protein 1 of EBV, which is essential for the transformation of B lymphocytes (Aviel *et al.*, 2000), and the E7 oncoprotein of human papillomavirus 16 (Reinstein *et al.*, 2000). These proteins do not show homology between their N-terminal domains, so recognition must involve different members of the ubiquitin pathway (Ciechanover & Ben-Saadon, 2004). The functional relevance of N-terminal ubiquitin remains unclear within the context of HSV-1 infection. However, as the interaction between KE/ND and UBE2W was lost in the yeast-two-hybrid experiment and this mutant was negative for its ability to conjugate ubiquitin and in the degradation of PML, the role of UBE2W should be investigated.

It is already known that different E2 enzymes produce different chain linkages or have different specificities. It is possible that ICP0 utilises different combinations of E2 ubiquitin conjugating enzymes for different functions, or that E2 ubiquitin conjugating enzymes work sequentially to produce polyubiquitin chains. KSHV encodes two RING finger like E3 ubiquitin ligases termed K3 and K5 (MIR1 and MIR2) (Coscoy *et al.*, 2001), and K3 has been shown to interact with UBE2D1-3 and UBE2N (Dodd *et al.*, 2004). To synthesise Lys63 linked chains, K3 uses the sequential action of two E2 ubiquitin conjugating enzymes. The ubiquitin is first attached to the substrate by UBE2D2-D3 and then subsequent ubiquitin is linked via Lys63 chains by UBE2N (Duncan *et al.*, 2006). The Lys63 polyubiquitin chains act in immune evasion by downregulating MHC class I to avoid CTL recognition (Duncan *et al.*, 2006). BRCA-1 RING finger E3 ubiquitin ligase has additionally been shown to interact with multiple E2 ubiquitin-conjugating enzymes, including UBE2E1, UBE2E2, UBE2N, UBE2K and UBE2W. UBE2E2 and UBE2W are involved in chain initiation, whereas UBE2N-UBE2V1 and UBE2K carry out chain elongation, forming Lys63 and Lys48 chains respectively (Christensen *et al.*, 2007). Therefore, like KSHV K3 and BRCA-1, ICP0 may interact with multiple E2 ubiquitin conjugating enzymes to achieve polyubiquitination with different chain specificities. For example, ICP0 may interact with one E2 ubiquitin-conjugating enzyme that carries out

chain initiation or mono-ubiquitination events, and another that is involved in chain elongation. As UBE2N-UBE2V1 is only involved in chain elongation, it is dependent on the initial mono-ubiquitination of a lysine residue within the substrate. Therefore, the interaction with UBE2N-UBE2V1 and ICP0 is only functionally relevant if ICP0 is still able to interact with the E2 enzyme that carries out the initial ubiquitination event.

7.2.3 Do the K144E and N151D mutations affect an interface that binds E2 ubiquitin conjugating enzymes?

A study by Vanni et al. (2012) using homology modelling and site directed mutagenesis aimed to map the interaction interface between the ICP0 RING finger and E2 ubiquitin conjugating enzyme UBE2D1. They found that ICP0 residues V118, T120, P154 and L155 located in the loop regions were likely to form contact residues with UBE2D1 (Vanni *et al.*, 2012). This thesis has found that residues N151 and K144 may also be involved in the interactions with E2 ubiquitin conjugating enzymes. N151 and K144 are both predicted to be exposed on the alpha-helix based on the structure from EHV and could form a binding interface (**Figure 7.1**). The double mutant KE/ND did not induce the degradation of PML and was defective in its ability to conjugate ubiquitin, although the single mutants retained the ability to conjugate ubiquitin and to degrade PML (albeit less efficiently, especially for K144E). Therefore, mutating both K144 and N151 within the same protein may greatly affect the E3 ligase ability of ICP0 or prevent the binding of E2 ubiquitin conjugating enzymes. The interaction of UBE2W was lost for KE/ND and *in vitro* polyubiquitin chain formation was greatly reduced for KE/ND.

Residue M147 is also predicted to be on the same interface as K144 and N151. The Vanni *et al.* study found that mutating the M147 residue affected ICP0's interaction with UBE2D1 and UBE2E1 and its ability to conjugate ubiquitin (Vanni *et al.*, 2012). Therefore, this alpha-helix interface may also contribute to the binding of E2 ubiquitin-conjugating enzymes. Therefore, if as predicted this edge of the alpha-helix forms a binding interface, this residue should be studied alone and in combination with K144 and N151 and the previously described resides to investigate if this hypothesis is correct. This study, along with previous studies, demonstrates that the alpha-helix residues are important for ICP0's activity and have the potential to interaction with E2 ubiquitin-conjugating enzymes. However, mapping the interaction interface is complicated by the lack of a

crystal structure for ICP0. At present, the structure of the ICP0 RING finger domain and alpha-helix can only be predicted based on the structure of EHV-1 ICP0.

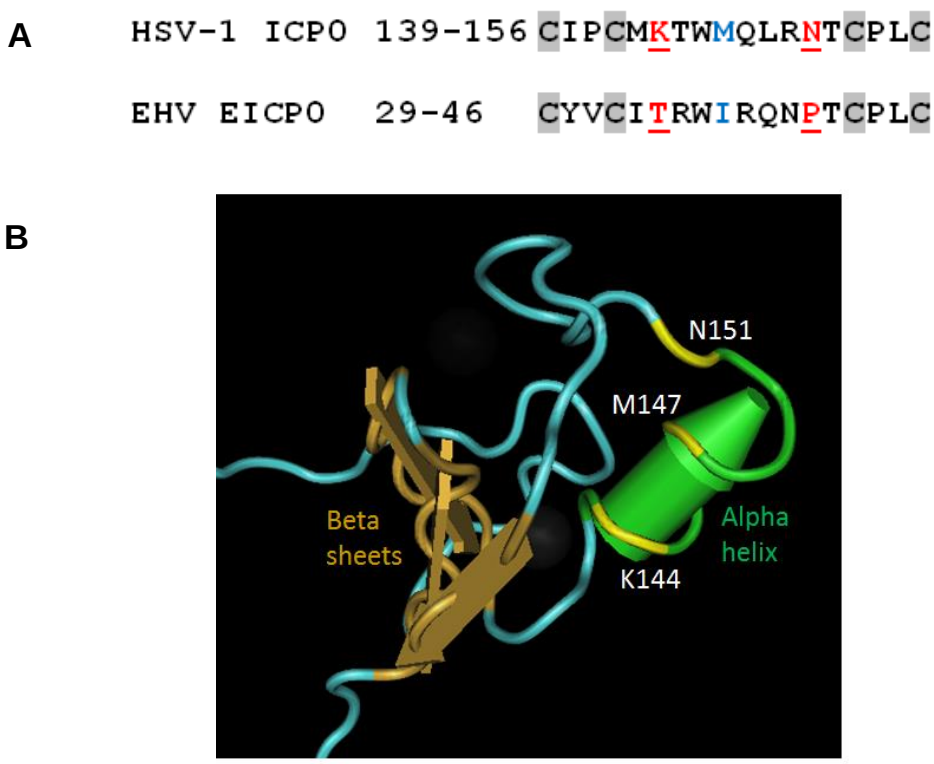

Figure 7.1 The RING finger domain of HSV-1 ICP0 modelled on EHV EICP0.
A) Comparison of ICP0 and its viral orthologue EICP0 from EHV. The zinc-binding resides are highlighted in grey and are conserved. The alpha-helix resides that were the focus of this thesis are highlighted in red. M147, which may form part of the same binding interface as K144 and N151, is highlighted in blue.
B) Locations of residues K144 and N151 in EHV ICP0. M147 may also form part of this binding interface and has been studied previously by Vanni *et al.* (2012).

7.2.4 Assay dependence of specific results

The results from this study appear to vary in detail between the different experimental systems used, such as the ICP0 inducible cell line and the virus infection studies in HFs and HepaRG cells. The results differ in terms of ND10 disruption and PML degradation, with no degradation/disruption occurring with N151D mutant in the inducible cell line compared to N151D behaving in a similar manner to wt in virus infection studies,

especially at high MOIs. The relative defects of the RING finger alpha-helix mutants also varied in detail between the two systems. For each of the systems used, the readout is assay-dependent and can be influenced by the amount of ICP0 expressed and the length of time that it is expressed (in the case of the inducible cell line), and the cell type and MOI during virus infection studies. All of these factors, which in many cases are the choice of the investigator, influence the results and their potential interpretation. However, despite the variations in relative defects of the mutants when comparing between different experiments and assays, the results follow a similar trend. Mutant N151D had an intermediate defect that was less visible during higher MOI infections, a larger defect was observed with K144E, and the double mutant KE/ND was highly defective in all the assays and in both virus infection studies and the inducible cell line.

The results about the E3 ligase activity of the alpha-helix mutants and their interactions with E2 ubiquitin conjugating enzymes should also be interpreted with care. These assays may not truly represent the mutants' ICP0 mediated ubiquitin ligase activity *in vivo*. Therefore, more work will be needed to investigate whether these residues in the alpha-helix are important for interactions with components of the ubiquitin pathway in infected cells, and the potential roles of different E2 enzymes in the HSV-1 life cycle.

7.2.5 Region downstream of the RING finger domain may be involved in substrate targeting

The ICP0Δ211-222 virus had a severe plaque forming defect, exhibited poor expression of early and late proteins, and was defective in the ability to induce the degradation of PML. This region is however, outside of the core domain required for E3 ubiquitin ligase activity *in vitro* (Boutell *et al.*, 2002), although it overlaps a larger deletion that was defective for production of conjugated ubiquitin chains in transfected cells (Everett, 2000). Previous studies have suggested that the region downstream from the RING finger domain may be involved in interacting with and degradation of PML.I (Cuchet-Lourenço *et al.*, 2012; Perusina Lanfranca *et al.*, 2013). Therefore, the region of ICP0 within the deletion 211-222 may play a role in the targeting of PML to the proteasome. ICP0 targets a number of proteins for substrate mediated degradation, however, except for USP7 and RNF8, for most of these proteins the binding region between ICP0 and the target protein is unknown. ICP0 interacts with USP7 through a motif located in its C-terminal third between residues

618-634 (Meredith *et al.*, 1995), and the cellular E3 ligase RNF8 via residue T67 (Chaurushiya *et al.*, 2012). The hypothesis that the 211-222 region is involved in PML targeting can be investigated using a yeast-two-hybrid experiment looking for interaction between full length ICP0 and PML.I and truncated ICP0 mutants, including ICP0Δ211-222. Cells expressing different PML isoforms could be used to analyse the ability of ICP0Δ211-222 virus to induce PML degradation, in particular PML.I. If this region does play a role in substrate targeting, this would not fully explain the observed phenotype of the virus, and therefore this region may affect interactions with other viral or cellular proteins. Therefore, the E3 ligase activity of ICP0Δ211-222 should be investigated as well as interactions with key E2 ubiquitin conjugating enzymes.

7.3 Future Prospects

7.3.1 Do analogous alpha-helix mutations in other alphaherpesviruses have the same phenotype as those in ICP0

The RING finger domain shows high sequence conservation of the zinc-binding residues due to structural constraints imposed by their binding (Barlow *et al.*, 1994), and mutating these conserved cysteine and histidine residues impairs ICP0 activity (Lium & Silverstein, 1997). However, apart from the zinc-binding residues, there is only limited conserved homology within the RING finger domain with substantial diversity among sequences of different alphaherpesvirus proteins (**Figure 7.2**). The alpha-helix lies in between the third and fourth pairs of zinc-binding residues, and therefore the orientations of the alpha-helix among related alphaherpesvirus ICP0 proteins is likely to be similar.

An area of research that would be interesting for further study is to investigate the alpha-helix region of related ICP0 proteins, such as those expressed by EHV-1 (EICP0), bovine herpesvirus 1 (BICP0), VZV protein Orf61 and pseudorabies virus protein EP0. The advantage of including EICP0 is that there is a known structure available (Barlow *et al.*, 1994), so any apparent phenotype could be modelled and interaction partners investigated. EICP0, BICP0 and EP0 all have been shown to act as E3 ubiquitin ligases *in vitro* and are able to complement an ICP0-null mutant HSV-1 in the inducible cell line system (Everett *et al.*, 2010). Therefore, it could be investigated whether analogous mutations to K144E

and N151D in those alpha-helices cause the same phenotype, and further investigate mutations within these proteins that may affect the same interface. Residue W146 is conserved among the alphaherpesviruses, however a number of studies have shown that this residue does not affect ICP0's function when mutated (Boutell *et al.*, 2002; Everett *et al.*, 1995; Everett, 2000; Vanni *et al.*, 2012). This study has confirmed previous studies that mutating the conserved tryptophan residue does not have an effect in the context of ICP0's activity during HSV-1 infections.

Mutations in these ICP0 homologues could be investigated using the inducible cell line to investigate complementation of HSV-1 ICP0-null mutant virus, reactivation of quiescent virus, and effects on ND10. All of these homologues of ICP0 have been shown to disrupt ND10, although their ability to degrade PML and Sp100 varies greatly between proteins (Everett *et al.*, 2010). It would be advantageous to analyse VZV, as it is the only other virus in the group to infect humans (HSV-1 and HSV-2 are similar). For the others, it is not known if they utilise species specific E2 ubiquitin-conjugating enzymes or if there is a high conservation amongst E2 enzymes between species. These experiments would give further insight into the role of the alpha-helix, as if the analogous mutations have similar phenotypes, it may point to an interaction interface and the phenotype caused by loss of interaction with a co-factor or protein.

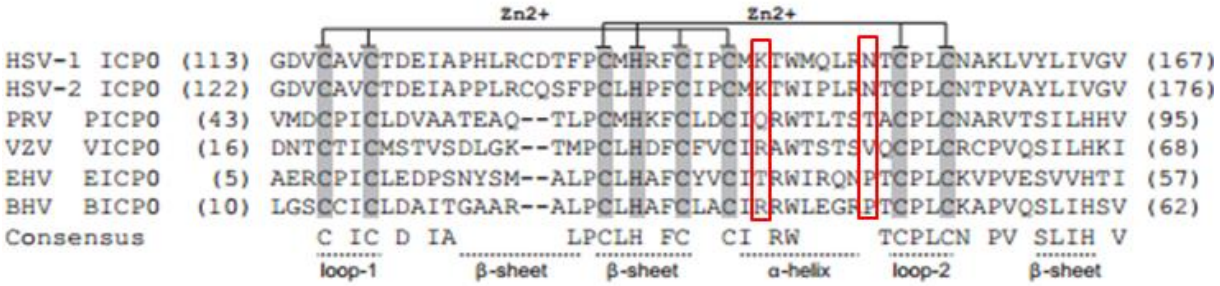

Figure 7.2 Amino acid alignment of the RING finger domains of ICP0 and related alphaherpesvirus proteins.
The zinc coordinating residues are highlighted in grey and show homology within the alphaherpesviruses. Residues K144 and N151 within ICP0 and the corresponding residues within the other viral proteins are highlighted in red and show no conservation (except between HSV-1 and HSV-2). Adapted from Boutell & Everett (2013).

7.3.2 Do mutations K144E and N151D affect ICP0s interactions with proteins or cofactors important for ICP0 activity

This study suggests that mutations in the RING finger alpha helix may affect ICP0's interactions with components of the ubiquitin pathway. To investigate if K144E and N151D mutations either alone or in combination affect ICP0's interactions with other proteins pull down experiments and mass spectrometry could be carried out. The protocol, described in (Brymora *et al.*, 2004), uses GST fusion proteins to pull down interacting proteins. This could be investigated during virus infection or overexpressing the protein of interest however this has limitations due to non-physiological levels of protein being expressed. Binding proteins could then be identified by SDS-PAGE, trypsin digests and mass spectrometry against known protein databases. This process relies on direct protein-protein interactions. Each of the mutants could be analysed against wt ICP0 and mutant FXE to identify interaction partners for each virus and to determine which are common or if any interactions are lost in the alpha-helix mutants. The results may also contain non-specific contaminants that bind to the protein of interest non-specifically. This method may not be sensitive enough to detect all the binding partners of ICP0, and it is not known if E2 ubiquitin conjugating enzyme interactions would be detected as they may be transient. Any protein that was detected using this method would need to be confirmed by another method such as co-immunoprecipitation or knock-out methods to detect a positive interaction and if it is functionally relevant.

7.3.3 Investigate the requirements of different E2 ubiquitin-conjugating enzymes for ICP0 activity

This study has shown that ICP0 has the ability to interact with different E2 ubiquitin-conjugating enzymes, but at present it is unknown if these interactions are functionally relevant during the course of HSV-1 infection. Therefore, it would be of value to investigate the requirements of different E2 ubiquitin-conjugating enzymes for ICP0 activity and whether they act in combination with other E2 enzymes. This could be investigated *in vivo* in the context of virus infection by immunofluorescence. However, the lack of antibodies against endogenous E2 enzymes is problematic. Therefore, the E2 enzymes could be myc-tagged at their N-terminal end and expressed using the inducible cell line. Using the inducible expression system may avoid toxicity issues of long term

over-expression of E2 ubiquitin conjugating proteins. These tools could be used to investigate the localisation of E2 enzymes within cells and if they show colocalisation with ICP0.

Knock-out or silencing methodologies, such as the use of siRNA to deplete endogenous E2 ubiquitin-conjugating enzymes, could also be used to investigate if their absence impacts ICP0's ability during lytic infection or reactivation. This should be used to further investigate the role of UBE2W and UBE2N-UBE2V1 during HSV-1 infection, as in the RING finger mutants, the interactions with these enzymes could be impaired, which may explain their phenotypes. *In vitro* E3 ubiquitin assays could be utilised to investigate whether E2 enzymes work as heterodimers such as in the case of UBE2N-UBE2V1, as ICP0 is likely to interact with multiple E2 ubiquitin-conjugating enzymes, some of which are only involved in chain initiation and elongation. This should be explored, as if ICP0 uses UBE2N-UBE2V1 *in vivo*, it must also interact with another E2 enzyme to initiate chain formation, as these enzymes are only involved in chain elongation. Different E2 ubiquitin-conjugating enzymes also govern chain linkage specificity and therefore function. Chain linkage could be examined using linkage-specific antibodies or mass spectrometry to determine which chains ICP0 utilise and what role they play in the context of HSV-1 infection.

References

Abada, R., Dreyfuss-Grossman, T., Herman-Bachinsky, Y., Geva, H., Masa, S.-R. & Sarid, R. (2008). SIAH-1 interacts with the Kaposi's sarcoma-associated herpesvirus-encoded ORF45 protein and promotes its ubiquitylation and proteasomal degradation. *J Virol* **82**, 2230-2240.

Adamson, A. L. & Kenney, S. (2001). Epstein-Barr virus immediate-early protein BZLF1 is SUMO-1 modified and disrupts promyelocytic leukemia bodies. *J Virol* **75**, 2388-2399.

Ahn, J. H. & Hayward, G. S. (1997). The major immediate-early proteins IE1 and IE2 of human cytomegalovirus colocalize with and disrupt PML-associated nuclear bodies at very early times in infected permissive cells. *J Virol* **71**, 4599-4613.

Arthur, J. L., Scarpini, C. G., Connor, V., Lachmann, R. H., Tolkovsky, A. M. & Efstathiou, S. (2001). Herpes simplex virus type 1 promoter activity during latency establishment, maintenance, and reactivation in primary dorsal root neurons in vitro. *J Virol* **75**, 3885-3895.

Ascoli, C. A. & Maul, G. G. (1991). Identification of a novel nuclear domain. *J Cell Biol* **112**, 785-795.

Aviel, S., Winberg, G., Massucci, M. & Ciechanover, A. (2000). Degradation of the Epstein-Barr virus latent membrane protein 1 (LMP1) by the ubiquitin-proteasome pathway: targeting via ubiquitination of the N-terminal residue. *J Biol Chem* **275**, 23491-23499.

Barcy, S. & Corey, L. (2001). Herpes simplex inhibits the capacity of lymphoblastoid B cell lines to stimulate CD4+ T cells. *J Immunol* **166**, 6242-6249.

Barlow, P. N., Luisi, B., Milner, A., Elliott, M. & Everett, R. (1994). Structure of the C3HC4 domain by 1H-nuclear magnetic resonance spectroscopy. A new structural class of zinc-finger. *J Mol Biol* **237**, 201-211.

Bieniasz, P. D. (2004). Intrinsic immunity: a front-line defense against viral attack. *Nature Immunol* **5**, 1109-1115.

Bieniasz, P. D. (2006). Late budding domains and host proteins in enveloped virus release. *Virology* **344**, 55-63.

Bloom, J., Amador, V., Bartolini, F., DeMartino, G. & Pagano, M. (2003). Proteasome-mediated degradation of p21 via N-terminal ubiquitinylation. *Cell* **115**, 71-82.

Blot, V., Perugi, F., Gay, B., Prévost, M.-C., Briant, L., Tangy, F., Abriel, H., Staub, O., Dokhélar, M.-C. & Pique, C. (2004). Nedd4.1-mediated ubiquitination and subsequent recruitment of Tsg101 ensure HTLV-1 Gag trafficking towards the multivesicular body pathway prior to virus budding. *J Cell Sci* **117**, 2357-2367.

Boissière, S. L., Hughes, T. & O'Hare, P. (1999). HCF-dependent nuclear import of VP16. *EMBO J* **18**, 480-489.

Bottomley, M. J., Collard, M. W., Huggenvik, J. I., Liu, Z., Gibson, T. J. & Sattler, M. (2001). The SAND domain structure defines a novel DNA-binding fold in transcriptional regulation. *Nat Struct Mol Biol* **8**, 626-633.

Bouamr, F., Melillo, J. A., Wang, M. Q., Nagashima, K., de Los Santos, M., Rein, A. & Goff, S. P. (2003). PPPYEPTAP motif is the Late domain of human T-cell leukemia virus type 1 Gag and mediates its functional interaction with cellular proteins Nedd4 and Tsg101. *J Virol* **77**, 11882-11895.

Boutell, C., Canning, M., Orr, A. & Everett, R. D. (2005). Reciprocal activities between herpes simplex virus type 1 regulatory protein ICP0, a ubiquitin E3 ligase, and ubiquitin-specific protease USP7. *J Virol* **79**, 12342-12354.

Boutell, C., Cuchet-Lourenco, D., Vanni, E., Orr, A., Glass, M., McFarlane, S. & Everett, R. D. (2011). A viral ubiquitin ligase has substrate preferential SUMO

targeted ubiquitin ligase activity that counteracts intrinsic antiviral defence. *PLoS Pathog* **7**, e1002245.

Boutell, C. & Everett, R. D. (2013). Regulation of alphaherpesvirus infections by the ICP0 family of proteins. *J Gen Virol* **94**, 465-481.

Boutell, C., Sadis, S. & Everett, R. D. (2002). Herpes simplex virus type 1 immediate-early protein ICP0 and is isolated RING finger domain act as ubiquitin E3 ligases in vitro. *J Virol* **76**, 841-850.

Breitschopf, K., Bengal, E., Ziv, T., Admon, A. & Ciechanover, A. (1998). A novel site for ubiquitination: the N-terminal residue, and not internal lysines of MyoD, is essential for conjugation and degradation of the protein. *EMBO J* **17**, 5964-5973.

Brown, S. M., Ritchie, D. A. & Subak-Sharpe, J. H. (1973). Genetic studies with herpes simplex virus type 1. The isolation of temperature-sensitive mutants, their arrangement into complementation groups and recombination analysis leading to a linkage map. *J Gen Virol* **18**, 329-346.

Brymora, A., Valova, V. A. & Robinson, P. J. (2004). Protein-protein interactions identified by pull-down experiments and mass spectrometry. *Curr Protoc Cell Biol* **22**, 17.15.11–17.15.51.

Cai, W., Astor, T. L., Liptak, L. M., Cho, C., Coen, D. M. & Schaffer, P. A. (1993). The herpes simplex virus type 1 regulatory protein ICP0 enhances virus replication during acute infection and reactivation from latency. *J Virol* **67**, 7501-7512.

Campadelli-Fiume, G., Amasio, M., Avitabile, E., Cerretani, A., Forghieri, C., Gianni, T. & Menotti, L. (2007). The multipartite system that mediates entry of herpes simplex virus into the cell. *Rev Med Virol* **17**, 313-326.

Canning, M., Boutell, C., Parkinson, J. & Everett, R. D. (2004). A RING finger ubiquitin ligase is protected from autocatalyzed ubiquitination and degradation by binding to ubiquitin-specific protease USP7. *J Biol Chem* **279**, 38160-38168.

Cantrell, S. R. & Bresnahan, W. A. (2006). Human cytomegalovirus (HCMV) UL82 gene product (pp71) relieves hDaxx-mediated repression of HCMV replication. *J Virol* **80**, 6188-6191.

Cassady, K. A., Gross, M. & Roizman, B. (1998). The herpes simplex virus US11 protein effectively compensates for the γ134.5 gene if present before activation of protein kinase R by precluding its phosphorylation and that of the α subunit of eukaryotic translation initiation factor 2. *J Virol* **72**, 8620-8626.

Chang, J. T., Schmid, M. F., Rixon, F. J. & Chiu, W. (2007). Electron cryotomography reveals the portal in the herpesvirus capsid. *J Virol* **81**, 2065-2068.

Chang, Y., Cesarman, E., Pessin, M. S., Lee, F., Culpepper, J., Knowles, D. M. & Moore, P. S. (1994). Identification of herpesvirus-like DNA sequences in AIDS-associated Kaposi's sarcoma. *Science* **266**, 1865-1869.

Chau, V., Tobias, J., Bachmair, A., Marriott, D., Ecker, D., Gonda, D. & Varshavsky, A. (1989). A multiubiquitin chain is confined to specific lysine in a targeted short-lived protein. *Science* **243**, 1576-1583.

Chaurushiya, M. S., Lilley, C. E., Aslanian, A., Meisenhelder, J., Scott, D. C., Landry, S., Ticau, S., Boutell, C., Yates Iii, J. R., Schulman, B. A., Hunter, T. & Weitzman, M. D. (2012). Viral E3 ubiquitin ligase-mediated degradation of a cellular E3: viral mimicry of a cellular phosphorylation mark targets the RNF8 FHA domain. *Mol Cell* **46**, 79-90.

Chelbi-Alix, M. K. & de The, H. (1999). Herpes virus induced proteasome-dependent degradation of the nuclear bodies-associated PML and Sp100 proteins. *Oncogene* **18**, 935-941.

Chelbi-Alix, M. K., Pelicano, L., Quignon, F., Koken, M. H. M., Venturini, L., Stadler, M., Pavlovic, J., Degos, L. & de Thé, H. (1995). Induction of the PML protein by interferons in normal and APL cells. *Leukemia* **9**, 2027-2033.

Chen, J. & Silverstein, S. (1992). Herpes simplex viruses with mutations in the gene encoding ICP0 are defective in gene expression. *J Virol* **66**, 2916-2927.

Christensen, D. E., Brzovic, P. S. & Klevit, R. E. (2007). E2-BRCA1 RING interactions dictate synthesis of mono- or specific polyubiquitin chain linkages. *Nat Struct Mol Biol* **14**, 941-948.

Ciccia, A. & Elledge, S. J. (2010). The DNA damage response: making it safe to play with knives. *Mol Cell* **40**, 179-204.

Ciechanover, A. & Ben-Saadon, R. (2004). N-terminal ubiquitination: more protein substrates join in. *Trends Cell Biol* **14**, 103-106.

Ciufo, D. M., Mullen, M. A. & Hayward, G. S. (1994). Identification of a dimerization domain in the C-terminal segment of the IE110 transactivator protein from herpes simplex virus. *J Virol* **68**, 3267-3282.

Coleman, H. M., Connor, V., Cheng, Z. S., Grey, F., Preston, C. M. & Efstathiou, S. (2008). Histone modifications associated with herpes simplex virus type 1 genomes during quiescence and following ICP0-mediated de-repression. *J Gen Virol* **89**, 68-77.

Conway, J. F. & Homa, F. L. (2011). Nucleocapsid strucutre, assembly and DNA packaging of herpes simplex virus. In *Alphaherpesviruses: Molecular Virology*, pp. 175-194. Edited by S. K. Weller. Norfolk, UK: Caister Academic Press.

Coscoy, L., Sanchez, D. J. & Ganem, D. (2001). A novel class of herpesvirus-encoded membrane-bound E3 ubiquitin ligases regulates endocytosis of proteins involved in immune recognition. *J Cell Biol* **155**, 1265-1274.

Crawford, D. H. (2001). Biology and disease associations of Epstein-Barr virus. *Philos Trans R Soc Lond B Biol Sci* **356**, 461-473.

Cuchet-Lourenço, D., Vanni, E., Glass, M., Orr, A. & Everett, R. D. (2012). Herpes simplex virus 1 ubiquitin ligase ICP0 interacts with PML isoform I and induces its SUMO-independent degradation. *J Virol* **86**, 11209-11222.

Cuchet, D., Sykes, A., Nicolas, A., Orr, A., Murray, J., Sirma, H., Heeren, J., Bartelt, A. & Everett, R. D. (2011). PML isoforms I and II participate in PML-dependent restriction of HSV-1 replication. *J Cell Sci* **124**, 280-291.

Dai-Ju, J. Q., Li, L., Johnson, L. A. & Sandri-Goldin, R. M. (2006). ICP27 interacts with the C-terminal domain of RNA polymerase II and facilitates its recruitment to herpes simplex virus 1 transcription sites, where it undergoes proteasomal degradation during infection. *J Virol* **80**, 3567-3581.

Daubeuf, S., Singh, D., Tan, Y., Liu, H., Federoff, H. J., Bowers, W. J. & Tolba, K. (2009). HSV ICP0 recruits USP7 to modulate TLR-mediated innate response. *Blood* **113**, 3264-3275.

Davido, D. J., von Zagorski, W. F., Lane, W. S. & Schaffer, P. A. (2005). Phosphorylation site mutations affect herpes simplex virus type 1 ICP0 function. *J Virol* **79**, 1232-1243.

Davison, A., Eberle, R., Ehlers, B., Hayward, G., McGeoch, D., Minson, A., Pellett, P., Roizman, B., Studdert, M. & Thiry, E. (2009). The order *Herpesvirales*. *Arch Virol* **154**, 171-177.

Davison, A. J., Trus, B. L., Cheng, N., Steven, A. C., Watson, M. S., Cunningham, C., Deuff, R.-M. L. & Renault, T. (2005). A novel class of herpesvirus with bivalve hosts. *J Gen Virol* **86**, 41-53.

de Ruijter, A. J., van Gennip, A. H., Caron, H. N., Kemp, S. & van Kuilenburg, A. B. (2003). Histone deacetylases (HDACs): characterization of the classical HDAC family. *Biochem J* **370**, 737-749.

Delboy, M. G. & Nicola, A. V. (2011). A pre-immediate-early role for tegument ICP0 in the proteasome-dependent entry of herpes simplex virus. *J Virol* **85**, 5910-5918.

Delboy, M. G., Siekavizza-Robles, C. R. & Nicola, A. V. (2010). Herpes simplex virus tegument ICP0 is capsid associated, and its E3 ubiquitin ligase domain is important for incorporation into virions. *J Virol* **84**, 1637-1640.

Deng, L., Wang, C., Spencer, E., Yang, L., Braun, A., You, J., Slaughter, C., Pickart, C. & Chen, Z. J. (2000). Activation of the IκB kinase complex by TRAF6 requires a dimeric ubiquitin-conjugating enzyme complex and a unique polyubiquitin chain. *Cell* **103**, 351-361.

Deshaies, R. J. & Joazeiro, C. A. P. (2009). RING domain E3 ubiquitin ligases. *Annu Rev Biochem* **78**, 399-434.

Diao, L., Zhang, B., Fan, J., Gao, X., Sun, S., Yang, K., Xin, D., Jin, N., Geng, Y. & Wang, C. (2005). Herpes virus proteins ICP0 and BICP0 can activate NF-kappaB by catalyzing IkappaBalpha ubiquitination. *Cell Signal* **17**, 217-229.

Dodd, R. B., Allen, M. D., Brown, S. E., Sanderson, C. M., Duncan, L. M., Lehner, P. J., Bycroft, M. & Read, R. J. (2004). Solution structure of the Kaposi's sarcoma-associated herpesvirus K3 N-terminal domain reveals a novel E2-binding C4HC3-type RING domain. *J Biol Chem* **279**, 53840-53847.

Dohner, K., Wolfstein, A., Prank, U., Echeverri, C., Dujardin, D., Vallee, R. & Sodeik, B. (2002). Function of dynein and dynactin in herpes simplex virus capsid transport. *Mol Biol Cell* **13**, 2795-2809.

Doil, C., Mailand, N., Bekker-Jensen, S., Menard, P., Larsen, D. H., Pepperkok, R., Ellenberg, J., Panier, S., Durocher, D., Bartek, J., Lukas, J. & Lukas, C. (2009). RNF168 binds and amplifies ubiquitin conjugates on damaged chromosomes to allow accumulation of repair proteins. *Cell* **136**, 435-446.

Duncan, L. M., Piper, S., Dodd, R. B., Saville, M. K., Sanderson, C. M., Luzio, J. P. & Lehner, P. J. (2006). Lysine-63-linked ubiquitination is required for endolysosomal degradation of class I molecules. *EMBO J* **25**, 1635-1645.

Efstathiou, S. & Preston, C. M. (2005). Towards an understanding of the molecular basis of herpes simplex virus latency. *Virus Res* **111**, 108-119.

Ellison, K. S., Maranchuk, R. A., Mottet, K. L. & Smiley, J. R. (2005). Control of VP16 translation by the herpes simplex virus type 1 immediate-early protein ICP27. *J Virol* **79**, 4120-4131.

Everett, R., O'Hare, P., O'Rourke, D., Barlow, P. & Orr, A. (1995). Point mutations in the herpes simplex virus type 1 Vmw110 RING finger helix affect activation of gene expression, viral growth, and interaction with PML-containing nuclear structures. *J Virol* **69**, 7339-7344.

Everett, R. D. (1987). A detailed mutational analysis of Vmw110, a trans-acting transcriptional activator encoded by herpes simplex virus type 1. *Embo J* **6**, 2069-2076.

Everett, R. D. (1988). Analysis of the functional domains of herpes simplex virus type 1 immediate-early polypeptide Vmw110. *J Mol Biol* **202**, 87-96.

Everett, R. D. (1989). Construction and characterization of herpes simplex virus type 1 mutants with defined lesions in immediate early gene 1. *J Gen Virol* **70**, 1185-1202.

Everett, R. D. (2000). ICP0 induces the accumulation of colocalizing conjugated ubiquitin. *J Virol* **74**, 9994-10005.

Everett, R. D. (2010). Depletion of CoREST does not improve the replication of ICP0 null mutant herpes simplex virus type 1. *J Virol* **84**, 3695-3698.

Everett, R. D., Barlow, P., Milner, A., Luisi, B., Orr, A., Hope, G. & Lyon, D. (1993a). A novel arrangement of zinc-binding residues and secondary structure in the C3HC4 motif of an alpha herpes virus protein family. *J Mol Biol* **234**, 1038-1047.

Everett, R. D., Bell, A. J., Lu, Y. & Orr, A. (2013). The replication defect of ICP0-null mutant herpes simplex virus 1 can be largely complemented by the combined activities of human cytomegalovirus proteins IE1 and pp71. *J Virol* **87**, 978-990.

Everett, R. D., Boutell, C., McNair, C., Grant, L. & Orr, A. (2010). Comparison of the biological and biochemical activities of several members of the alphaherpesvirus ICP0 family of proteins. *J Virol* **84**, 3476-3487.

Everett, R. D., Boutell, C. & Orr, A. (2004a). Phenotype of a herpes simplex virus type 1 mutant that fails to express immediate-early regulatory protein ICP0. *J Virol* **78**, 1763-1774.

Everett, R. D., Boutell, C., Pheasant, K., Cuchet-Lourenço, D. & Orr, A. (2014). Sequences related to SUMO interaction motifs in herpes simplex virus 1 protein ICP0 act cooperatively to stimulate virus infection. *J Virol* **88**, 2763-2774.

Everett, R. D. & Chelbi-Alix, M. K. (2007). PML and PML nuclear bodies: implications in antiviral defence. *Biochimie* **89**, 819-830.

Everett, R. D., Cross, A. & Orr, A. (1993b). A truncated form of herpes simplex virus type 1 immediate-early protein Vmw110 is expressed in a cell type dependent manner. *Virology* **197**, 751-756.

Everett, R. D., Earnshaw, W. C., Findlay, J. & Lomonte, P. (1999a). Specific destruction of kinetochore protein CENP-C and disruption of cell division by herpes simplex virus immediate-early protein Vmw110. *Embo J* **18**, 1526-1538.

Everett, R. D., Freemont, P., Saitoh, H., Dasso, M., Orr, A., Kathoria, M. & Parkinson, J. (1998a). The disruption of ND10 during herpes simplex virus infection correlates with the Vmw110- and proteasome-dependent loss of several PML isoforms. *J Virol* **72**, 6581-6591.

Everett, R. D. & Maul, G. G. (1994). HSV-1 IE protein Vmw110 causes redistribution of PML. *Embo J* **13**, 5062-5069.

Everett, R. D., Meredith, M. & Orr, A. (1999b). The ability of herpes simplex virus type 1 immediate-early protein Vmw110 to bind to a ubiquitin-specific protease contributes to its roles in the activation of gene expression and stimulation of virus replication. *J Virol* **73**, 417-426.

Everett, R. D., Meredith, M., Orr, A., Cross, A., Kathoria, M. & Parkinson, J. (1997). A novel ubiquitin-specific protease is dynamically associated with the PML nuclear domain and binds to a herpesvirus regulatory protein. *Embo J* **16**, 1519-1530.

Everett, R. D. & Murray, J. (2005). ND10 components relocate to sites associated with herpes simplex virus type 1 nucleoprotein complexes during virus infection. *J Virol* **79**, 5078-5089.

Everett, R. D., Murray, J., Orr, A. & Preston, C. M. (2007). Herpes simplex virus type 1 genomes are associated with ND10 nuclear substructures in quiescently infected human fibroblasts. *J Virol* **81**, 10991-11004.

Everett, R. D., Orr, A. & Preston, C. M. (1998b). A viral activator of gene expression functions via the ubiquitin–proteasome pathway. *EMBO J* **17**, 7161-7169.

Everett, R. D., Parada, C., Gripon, P., Sirma, H. & Orr, A. (2008). Replication of ICP0-null mutant herpes simplex virus type 1 is restricted by both PML and Sp100. *J Virol* **82**, 2661-2672.

Everett, R. D., Parsy, M. L. & Orr, A. (2009). Analysis of the functions of herpes simplex virus type 1 regulatory protein ICP0 that are critical for lytic infection and derepression of quiescent viral genomes. *J Virol* **83**, 4963-4977.

Everett, R. D., Rechter, S., Papior, P., Tavalai, N., Stamminger, T. & Orr, A. (2006). PML contributes to a cellular mechanism of repression of herpes simplex virus type 1 infection that is inactivated by ICP0. *J Virol* **80**, 7995-8005.

Everett, R. D., Sourvinos, G., Leiper, C., Clements, J. B. & Orr, A. (2004b). Formation of nuclear foci of the herpes simplex virus type 1 regulatory protein ICP4 at early times of infection: localization, dynamics, recruitment of ICP27, and evidence for the de novo induction of ND10-like complexes. *J Virol* **78**, 1903-1917.

Everett, R. D., Sourvinos, G. & Orr, A. (2003). Recruitment of herpes simplex virus type 1 transcriptional regulatory protein ICP4 into foci juxtaposed to ND10 in live, infected cells. *J Virol* **77**, 3680-3689.

Fanelli, M., Fantozzi, A., De Luca, P., Caprodossi, S., Matsuzawa, S.-i., Lazar, M. A., Pelicci, P. G. & Minucci, S. (2004). The coiled-coil domain is the structural determinant for mammalian homologues of Drosophila Sina-mediated degradation of promyelocytic leukemia protein and other tripartite motif proteins by the proteasome. *J Biol Chem* **279**, 5374-5379.

Farrell, M. J., Dobson, A. T. & Feldman, L. T. (1991). Herpes simplex virus latency-associated transcript is a stable intron. *Proc Natl Acad Sci U S A* **88**, 790-794.

Ferenczy, M. W., Ranayhossaini, D. J. & DeLuca, N. A. (2011). Activities of ICP0 involved in the reversal of silencing of quiescent herpes simplex virus 1. *J Virol* **85**, 4993-5002.

Finley, D. (2009). Recognition and processing of ubiquitin-protein conjugates by the proteasome. *Annu Rev Biochem* **78**, 477-513.

Finley, D., Sadis, S., Monia, B. P., Boucher, P., Ecker, D. J., Crooke, S. T. & Chau, V. (1994). Inhibition of proteolysis and cell cycle progression in a multiubiquitination-deficient yeast mutant. *Mol Cell Biol* **14**, 5501-5509.

Freed, E. O. (2002). Viral Late domains. *J Virol* **76**, 4679-4687.

Friedman, H. M., Cohen, G. H., Eisenberg, R. J., Seidel, C. A. & Cines, D. B. (1984). Glycoprotein C of herpes simplex virus 1 acts as a receptor for the C3b complement component on infected cells. *Nature* **309**, 633-635.

Fruh, K., Ahn, K., Djaballah, H., Sempe, P., van Endert, P. M., Tampe, R., Peterson, P. A. & Yang, Y. (1995). A viral inhibitor of peptide transporters for antigen presentation. *Nature* **375**, 415-418.

Fujimuro, M., Sawada, H. & Yokosawa, H. (1994). Production and characterization of monoclonal antibodies specific to multi-ubiquitin chains of polyubiquitinated proteins. *FEBS Lett* **349**, 173-180.

Fukuyo, Y., Horikoshi, N., Ishov, A. M., Silverstein, S. J. & Nakajima, T. (2011). The herpes simplex virus immediate-early ubiquitin ligase ICP0 induces degradation of the ICP0 repressor protein E2FBP1. *J Virol* **85**, 3356-3366.

Full, F., Jungnickl, D., Reuter, N., Bogner, E., Brulois, K., Scholz, B., Stürzl, M., Myoung, J., Jung, J. U., Stamminger, T. & Ensser, A. (2014). Kaposi's sarcoma associated herpesvirus tegument protein ORF75 is essential for viral lytic replication and plays a critical role in the antagonization of ND10-instituted intrinsic immunity. *PLoS Pathog* **10**, e1003863.

Ganem, D. (2007). KSHV-induced oncogenesis. In *Human Herpesviruses: Biology, Therapy, and Immunoprophylaxis*. Edited by A. Arvin, G. Campadelli-Fiume, E. Mocarski, P. S. Moore, B. Roizman, R. Whitley & K. Yamanishi. Cambridge: Cambridge University Press.

Garrus, J. E., von Schwedler, U. K., Pornillos, O. W., Morham, S. G., Zavitz, K. H., Wang, H. E., Wettstein, D. A., Stray, K. M., Côté, M., Rich, R. L., Myszka, D. G. & Sundquist, W. I. (2001). Tsg101 and the vacuolar protein sorting pathway are essential for HIV-1 budding. *Cell* **107**, 55-65.

Gershon, A. A. & Gershon, M. D. (2013). Pathogenesis and current approaches to control of varicella-zoster virus infections. *Clin Microbiol Rev* **26**, 728-743.

Glass, M. & Everett, R. D. (2013). Components of promyelocytic leukemia nuclear bodies (ND10) act cooperatively to repress herpesvirus infection. *J Virol* **87**, 2174-2185.

Göttlinger, H. G., Dorfman, T., Sodroski, J. G. & Haseltine, W. A. (1991). Effect of mutations affecting the p6 gag protein on human immunodeficiency virus particle release. *Proc Natl Acad Sci U S A* **88**, 3195-3199.

Gripon, P., Rumin, S., Urban, S., Le Seyec, J., Glaise, D., Cannie, I., Guyomard, C., Lucas, J., Trepo, C. & Guguen-Guillouzo, C. (2002). Infection of a human hepatoma cell line by hepatitis B virus. *Proc Natl Acad Sci U S A* **99**, 15655-15660.

Gross, S., Catez, F., Masumoto, H. & Lomonte, P. (2012). Centromere architecture breakdown induced by the viral E3 ubiquitin ligase ICP0 protein of herpes simplex virus type 1. *PLoS ONE* **7**, e44227.

Grotzinger, T., Sternsdorf, T., Jensen, K. & Will, H. (1996). Interferon-modulated expression of genes encoding the nuclear-dot- associated proteins Sp100 and promyelocytic leukemia protein (PML). *Eur J Biochem* **238**, 554-560.

Grünewald, K., Desai, P., Winkler, D. C., Heymann, J. B., Belnap, D. M., Baumeister, W. & Steven, A. C. (2003). Three-dimensional structure of herpes simplex virus from cryo-electron tomography. *Science* **302**, 1396-1398.

Gu, H., Liang, Y., Mandel, G. & Roizman, B. (2005). Components of the REST/CoREST/histone deacetylase repressor complex are disrupted, modified, and translocated in HSV-1-infected cells. *Proc Natl Acad Sci U S A* **102**, 7571-7576.

Gu, H. & Roizman, B. (2003). The degradation of promyelocytic leukemia and Sp100 proteins by herpes simplex virus 1 is mediated by the ubiquitin-conjugating enzyme UbcH5a. *Proc Natl Acad Sci U S A* **100**, 8963-8968.

Gu, H. & Roizman, B. (2007). Herpes simplex virus-infected cell protein 0 blocks the silencing of viral DNA by dissociating histone deacetylases from the CoREST-REST complex. *Proc Natl Acad Sci U S A* **104**, 17134-17139.

Gu, H. & Roizman, B. (2009). The two functions of herpes simplex virus 1 ICP0, inhibition of silencing by the CoREST/REST/HDAC complex and degradation of PML, are executed in tandem. *J Virol* **83**, 181-187.

Guldner, H. H., Szostecki, C., Grotzinger, T. & Will, H. (1992). IFN enhance expression of Sp100, an autoantigen in primary biliary cirrhosis. *J Immunol* **149**, 4067-4073.

Guldner, H. H., Szostecki, C., Schroder, P., Matschl, U., Jensen, K., Luders, C., Will, H. & Sternsdorf, T. (1999). Splice variants of the nuclear dot-associated Sp100 protein contain homologies to HMG-1 and a human nuclear phosphoprotein-box motif. *J Cell Sci* **112 (Pt 5)**, 733-747.

Halford, W., Weisend, C., Grace, J., Soboleski, M., Carr, D., Balliet, J., Imai, Y., Margolis, T. & Gebhardt, B. (2006). ICP0 antagonizes Stat 1-dependent repression of herpes simplex virus: implications for the regulation of viral latency. *Virol J* **3**, 44.

Halford, W. P., Halford, K. J. & Pierce, A. T. (2005). Mathematical analysis demonstrates that interferons-beta and -gamma interact in a multiplicative manner to disrupt herpes simplex virus replication. *J Theor Biol* **234**, 439-454.

Halford, W. P. & Schaffer, P. A. (2001). ICP0 is required for efficient reactivation of herpes simplex virus type 1 from neuronal latency. *J Virol* **75**, 3240-3249.

Hancock, M. H., Cliffe, A. R., Knipe, D. M. & Smiley, J. R. (2010). Herpes simplex virus VP16, but not ICP0, is required to reduce histone occupancy and enhance histone acetylation on viral genomes in U2OS osteosarcoma cells. *J Virol* **84**, 1366-1375.

Hancock, M. H., Corcoran, J. A. & Smiley, J. R. (2006). Herpes simplex virus regulatory proteins VP16 and ICP0 counteract an innate intranuclear barrier to viral gene expression. *Virology* **352**, 237-252.

Hardy, W. R. & Sandri-Goldin, R. M. (1994). Herpes simplex virus inhibits host cell splicing, and regulatory protein ICP27 is required for this effect. *J Virol* **68**, 7790-7799.

Harris, R. A., Everett, R. D., Zhu, X. X., Silverstein, S. & Preston, C. M. (1989). Herpes simplex virus type 1 immediate-early protein Vmw110 reactivates latent herpes simplex virus type 2 in an in vitro latency system. *J Virol* **63**, 3513-3515.

Harris, R. A. & Preston, C. M. (1991). Establishment of latency in vitro by the herpes simplex virus type 1 mutant in1814. *J Gen Virol* **72**, 907-913.

Harris, S. L., Frank, I., Vee, A., Cohen, G. H., Eisenberg, R. J. & Friedman, H. M. (1990). Glycoprotein C of herpes simplex virus type 1 prevents complement-mediated cell lysis and virus neutralization. *J Infect Dis* **162**, 331-337.

Harty, R. N., Brown, M. E., Wang, G., Huibregtse, J. & Hayes, F. P. (2000). A PPxY motif within the VP40 protein of Ebola virus interacts physically and functionally with a ubiquitin ligase: implications for filovirus budding. *Proc Natl Acad Sci U S A* **97**, 13871-13876.

Harty, R. N., Paragas, J., Sudol, M. & Palese, P. (1999). A proline-rich motif within the matrix protein of vesicular stomatitis virus and rabies virus interacts with WW domains of cellular proteins: implications for viral budding. *J Virol* **73**, 2921-2929.

He, B., Gross, M. & Roizman, B. (1997). The γ134.5 protein of herpes simplex virus 1 complexes with protein phosphatase 1α to dephosphorylate the α subunit of the eukaryotic translation initiation factor 2 and preclude the shutoff of protein synthesis by double-stranded RNA-activated protein kinase. *Proc Natl Acad Sci U S A* **94**, 843-848.

Heckman, K. L. & Pease, L. R. (2007). Gene splicing and mutagenesis by PCR-driven overlap extension. *Nat Protocols* **2**, 924-932.

Heldwein, E. E. & Krummenacher, C. (2008). Entry of herpesviruses into mammalian cells. *Cell Mol Life Sci* **65**, 1653-1668.

Herold, B. C., WuDunn, D., Soltys, N. & Spear, P. G. (1991). Glycoprotein C of herpes simplex virus type 1 plays a principal role in the adsorption of virus to cells and in infectivity. *J Virol* **65**, 1090-1098.

Hill, A., Jugovic, P., York, l., Russ, G., Bennink, J., Yewdell, J., Ploegh, H. & Johnson, D. (1995). Herpes simplex virus turns off the TAP to evade host immunity. *Nature* **375**, 411-415.

Hoege, C., Pfander, B., Moldovan, G.-L., Pyrowolakis, G. & Jentsch, S. (2002). RAD6-dependent DNA repair is linked to modification of PCNA by ubiquitin and SUMO. *Nature* **419**, 135-141.

Hofmann, R. M. & Pickart, C. M. (1999). Noncanonical MMS2-encoded ubiquitin-conjugating enzyme functions in assembly of novel polyubiquitin chains for DNA repair. *Cell* **96**, 645-653.

Hollenbach, A. D., McPherson, C. J., Mientjes, E. J., Iyengar, R. & Grosveld, G. (2002). Daxx and histone deacetylase II associate with chromatin through an interaction with core histones and the chromatin-associated protein Dek. *J Cell Sci* **115**, 3319-3330.

House, C. M., Frew, I. J., Huang, H.-L., Wiche, G., Traficante, N., Nice, E., Catimel, B. & Bowtell, D. D. L. (2003). A binding motif for Siah ubiquitin ligase. *Proc Natl Acad Sci U S A* **100**, 3101-3106.

Huang, L., Kinnucan, E., Wang, G., Beaudenon, S., Howley, P. M., Huibregtse, J. M. & Pavletich, N. P. (1999). Structure of an E6AP-UbcH7 complex: insights into ubiquitination by the E2-E3 enzyme cascade. *Science* **286**, 1321-1326.

Huen, M. S. Y., Grant, R., Manke, I., Minn, K., Yu, X., Yaffe, M. B. & Chen, J. (2007). RNF8 transduces the DNA-damage signal via histone ubiquitylation and checkpoint protein assembly. *Cell* **131**, 901-914.

Ishov, A. M., Sotnikov, A. G., Negorev, D., Vladimirova, O. V., Neff, N., Kamitani, T., Yeh, E. T., Strauss, J. F. & Maul, G. G. (1999). PML is critical for ND10

formation and recruits the PML-interacting protein daxx to this nuclear structure when modified by SUMO-1. *J Cell Biol* **147**, 221-234.

Ishov, A. M., Vladimirova, O. V. & Maul, G. G. (2004). Heterochromatin and ND10 are cell-cycle regulated and phosphorylation-dependent alternate nuclear sites of the transcription repressor Daxx and SWI/SNF protein ATRX. *J Cell Sci* **117**, 3807-3820.

Janeway, C. A., Travers, P., Walport, M. & Shlomchik, M.J. (2001). The course of the adaptive response to infection. In *Immunobiology. The immune system in health and disease. 6th edition*. New York: Garland Science.

Jensen, K., Shiels, C. & Freemont, P. S. (2001). PML protein isoforms and the RBCC/TRIM motif. *Oncogene* **20**, 7223-7233.

Jin, J., Li, X., Gygi, S. P. & Harper, J. W. (2007). Dual E1 activation systems for ubiquitin differentially regulate E2 enzyme charging. *Nature* **447**, 1135-1138.

Jin, L., Williamson, A., Banerjee, S., Philipp, I. & Rape, M. (2008). Mechanism of ubiquitin-chain formation by the human anaphase-promoting complex. *Cell* **133**, 653-665.

Joazeiro, C. A. & Weissman, A. M. (2000). RING finger proteins: mediators of ubiquitin ligase activity. *Cell* **102**, 549-552.

Johnson, D. C., Frame, M. C., Ligas, M. W., Cross, A. M. & Stow, N. D. (1988). Herpes simplex virus immunoglobulin G Fc receptor activity depends on a complex of two viral glycoproteins, gE and gI. *J Virol* **62**, 1347-1354.

Johnson, K. E. & Knipe, D. M. (2010). HSV-1 infection causes the secretion of a type I interferon-antagonizing protein and inhibits signaling at or before Jak-1 activation. *Virology* **396**, 21-29.

Johnson, K. E., Song, B. & Knipe, D. M. (2008). Role for herpes simplex virus 1 ICP27 in the inhibition of type I interferon signaling. *Virology* **374**, 487-494.

Kamitani, T., Kito, K., Nguyen, H. P., Wada, H., Fukuda-Kamitani, T. & Yeh, E. T. (1998). Identification of three major sentrinization sites in PML. *J Biol Chem* **273**, 26675-26682.

Kaplan, L. D. (2013). Human herpesvirus-8: Kaposi sarcoma, multicentric Castleman disease, and primary effusion lymphoma. *Hematology AM Soc Hematol Educ Program* **2013**, 103-108.

Kawaguchi, Y., Bruni, R. & Roizman, B. (1997). Interaction of herpes simplex virus 1 alpha regulatory protein ICP0 with elongation factor 1 delta: ICP0 affects translational machinery. *J Virol* **71**, 1019-1024.

Kelly, B. J., Fraefel, C., Cunningham, A. L. & Diefenbach, R. J. (2009). Functional roles of the tegument proteins of herpes simplex virus type 1. *Virus Res* **145**, 173-186.

Kerscher, O., Felberbaum, R. & Hochstrasser, M. (2006). Modification of proteins by ubiquitin and ubiquitin-like proteins. *Annu Rev Cell Dev Biol* **22**, 159-180.

Kikonyogo, A., Bouamr, F., Vana, M. L., Xiang, Y., Aiyar, A., Carter, C. & Leis, J. (2001). Proteins related to the Nedd4 family of ubiquitin protein ligases interact with the L domain of Rous sarcoma virus and are required for gag budding from cells. *Proc Natl Acad Sci U S A* **98**, 11199-11204.

Kimberlin, D. W. (2004). Neonatal herpes simplex infection. *Clin Microbiol Rev* **17**, 1-13.

Knipe, D. M. & Cliffe, A. (2008). Chromatin control of herpes simplex virus lytic and latent infection. *Nat Rev Microbiol* **6**, 211-221.

Kolas, N. K., Chapman, J. R., Nakada, S., Ylanko, J., Chahwan, R., Sweeney, F. D., Panier, S., Mendez, M., Wildenhain, J., Thomson, T. M., Pelletier, L., Jackson, S. P. & Durocher, D. (2007). Orchestration of the DNA-damage response by the RNF8 ubiquitin ligase. *Science* **318**, 1637-1640.

Kristie, T. M., Vogel, J. L. & Sears, A. E. (1999). Nuclear localization of the C1 factor (host cell factor) in sensory neurons correlates with reactivation of herpes simplex virus from latency. *Proc Natl Acad Sci U S A* **96**, 1229-1233.

Kuddus, R. H. & DeLuca, N. A. (2007). DNA-dependent oligomerization of herpes simplex virus type 1 regulatory protein ICP4. *J Virol* **81**, 9230-9237.

Kurt-Jones, E. A., Chan, M., Zhou, S., Wang, J., Reed, G., Bronson, R., Arnold, M. M., Knipe, D. M. & Finberg, R. W. (2004). Herpes simplex virus 1 interaction with Toll-like receptor 2 contributes to lethal encephalitis. *Proc Natl Acad Sci U S A* **101**, 1315-1320.

Kyratsous, C. A. & Silverstein, S. J. (2009). Components of nuclear domain 10 bodies regulate varicella-zoster virus replication. *J Virol* **83**, 4262-4274.

Lakin, N. D., Palmer, R., Lillycrop, K. A., Howard, M. K., Burke, L. C., Thomas, N. S. B. & Latchman, D. S. (1995). Down regulation of the octamer binding protein Oct-1 during growth arrest and differentiation of a neuronal cell line. *Brain Res Mol Brain Res* **28**, 47-54.

Lavau, C., Marchio, A., Fagioli, M., Jansen, J., Falini, B., Lebon, P., Grosveld, F., Pandolfi, P. P., Pelicci, P. G. & Dejean, A. (1995). The acute promyelocytic leukaemia-associated PML gene is induced by interferon. *Oncogene* **11**, 871-876.

Lee, S.-U. & Maeda, T. (2012). POK/ZBTB proteins: an emerging family of proteins that regulate lymphoid development and function. *Immunol Rev* **247**, 107-119.

Lees-Miller, S. P. (1996). The DNA-dependent protein kinase, DNA-PK: 10 years and no ends in sight. *Biochem Cell Biol* **74**, 503-512.

Lees-Miller, S. P., Long, M. C., Kilvert, M. A., Lam, V., Rice, S. A. & Spencer, C. A. (1996). Attenuation of DNA-dependent protein kinase activity and its catalytic subunit by the herpes simplex virus type 1 transactivator ICP0. *J Virol* **70**, 7471-7477.

Leib, D. A., Coen, D. M., Bogard, C. L., Hicks, K. A., Yager, D. R., Knipe, D. M., Tyler, K. L. & Schaffer, P. A. (1989). Immediate-early regulatory gene mutants define different stages in the establishment and reactivation of herpes simplex virus latency. *J Virol* **63**, 759-768.

Leib, D. A., Harrison, T. E., Laslo, K. M., Machalek, M. A., Moorman, N. J. & Virgin, H. W. (1999). Interferons regulate the phenotype of wild-type and mutant herpes simplex viruses in vivo. *J Exp Med* **189**, 663-672.

Li, H., Leo, C., Zhu, J., Wu, X., O'Neil, J., Park, E. J. & Chen, J. D. (2000). Sequestration and inhibition of Daxx-mediated transcriptional repression by PML. *Mol Cell Biol* **20**, 1784-1796.

Lilley, C. E., Carson, C. T., Muotri, A. R., Gage, F. H. & Weitzman, M. D. (2005). DNA repair proteins affect the lifecycle of herpes simplex virus 1. *Proc Natl Acad Sci U S A* **102**, 5844-5849.

Lilley, C. E., Chaurushiya, M. S., Boutell, C., Everett, R. D. & Weitzman, M. D. (2011). The intrinsic antiviral defense to incoming HSV-1 genomes includes specific DNA repair proteins and is counteracted by the viral protein ICP0. *PLoS Pathog* **7**, e1002084.

Lilley, C. E., Chaurushiya, M. S., Boutell, C., Landry, S., Suh, J., Panier, S., Everett, R. D., Stewart, G. S., Durocher, D. & Weitzman, M. D. (2010). A viral E3 ligase targets RNF8 and RNF168 to control histone ubiquitination and DNA damage responses. *EMBO J* **29**, 943-955.

Lin, R., Noyce, R. S., Collins, S. E., Everett, R. D. & Mossman, K. L. (2004). The herpes simplex virus ICP0 RING finger domain inhibits IRF3- and IRF7-mediated activation of interferon-stimulated genes. *J Virol* **78**, 1675-1684.

Lium, E. K. & Silverstein, S. (1997). Mutational analysis of the herpes simplex virus type 1 ICP0 C3HC4 zinc ring finger reveals a requirement for ICP0 in the expression of the essential alpha27 gene. *J Virol* **71**, 8602-8614.

Lomonte, P. & Everett, R. D. (1999). Herpes simplex virus type 1 immediate-early protein Vmw110 inhibits progression of cells through mitosis and from G(1) into S phase of the cell cycle. *J Virol* **73**, 9456-9467.

Lomonte, P. & Morency, E. (2007). Centromeric protein CENP-B proteasomal degradation induced by the viral protein ICP0. *FEBS Lett* **581**, 658-662.

Lomonte, P., Sullivan, K. F. & Everett, R. D. (2001). Degradation of nucleosome-associated centromeric histone H3-like protein CENP-A induced by herpes simplex virus type 1 protein ICP0. *J Biol Chem* **276**, 5829-5835.

Lomonte, P., Thomas, J., Texier, P., Caron, C., Khochbin, S. & Epstein, A. L. (2004). Functional interaction between class II histone deacetylases and ICP0 of herpes simplex virus type 1. *J Virol* **78**, 6744-6757.

Long, M. C., Leong, V., Schaffer, P. A., Spencer, C. A. & Rice, S. A. (1999). ICP22 and the UL13 protein kinase are both required for herpes simplex virus-induced modification of the large subunit of RNA polymerase II. *J Virol* **73**, 5593-5604.

Loret, S., Guay, G. & Lippé, R. (2008). Comprehensive characterization of extracellular herpes simplex virus type 1 virions. *J Virol* **82**, 8605-8618.

Lukashchuk, V. & Everett, R. D. (2010). Regulation of ICP0-null mutant herpes simplex virus type 1 infection by ND10 components ATRX and hDaxx. *J Virol* **84**, 4026-4040.

Lukashchuk, V., McFarlane, S., Everett, R. D. & Preston, C. M. (2008). Human cytomegalovirus protein pp71 displaces the chromatin-associated factor ATRX from nuclear domain 10 at early stages of infection. *J Virol* **82**, 12543-12554.

Lund, J., Sato, A., Akira, S., Medzhitov, R. & Iwasaki, A. (2003). Toll-like receptor 9–mediated recognition of herpes simplex virus-2 by plasmacytoid dendritic cells. *J Exp Med* **198**, 513-520.

Mailand, N., Bekker-Jensen, S., Faustrup, H., Melander, F., Bartek, J., Lukas, C. & Lukas, J. (2007). RNF8 ubiquitylates histones at DNA double-strand breaks and promotes assembly of repair proteins. *Cell* **131**, 887-900.

Malm, G. & Engman, M.-L. (2007). Congenital cytomegalovirus infections. *Semin Fetal Neonatal Med* **12**, 154-159.

Mangeat, B., Turelli, P., Caron, G., Friedli, M., Perrin, L. & Trono, D. (2003). Broad antiretroviral defence by human APOBEC3G through lethal editing of nascent reverse transcripts. *Nature* **424**, 99-103.

Marcos-Villar, L., Lopitz-Otsoa, F., Gallego, P., Munoz-Fontela, C., Gonzalez-Santamaria, J., Campagna, M., Shou-Jiang, G., Rodriguez, M. S. & Rivas, C. (2009). Kaposi's sarcoma-associated herpesvirus protein LANA2 disrupts PML oncogenic domains and inhibits PML-mediated transcriptional repression of the survivin gene. *J Virol* **83**, 8849-8858.

Maringer, K. & Elliott, G. (2010). Recruitment of herpes simplex virus type 1 immediate-early protein ICP0 to the virus particle. *J Virol* **84**, 4682-4696.

Maringer, K., Stylianou, J. & Elliott, G. (2012). A network of protein interactions around the herpes simplex virus tegument protein VP22. *J Virol* **86**, 12971-12982.

Martin-Serrano, J., Zang, T. & Bieniasz, P. D. (2001). HIV-1 and Ebola virus encode small peptide motifs that recruit Tsg101 to sites of particle assembly to facilitate egress. *Nat Med* **7**, 1313-1319.

Matsumoto, M. L., Wickliffe, K. E., Dong, K. C., Yu, C., Bosanac, I., Bustos, D., Phu, L., Kirkpatrick, D. S., Hymowitz, S. G., Rape, M., Kelley, R. F. & Dixit, V. M. (2010). K11-linked polyubiquitination in cell cycle control revealed by a K11 linkage-specific antibody. *Mol Cell* **39**, 477-484.

Maul, G. G. & Everett, R. D. (1994). The nuclear location of PML, a cellular member of the C3HC4 zinc- binding domain protein family, is rearranged during herpes simplex virus infection by the C3HC4 viral protein ICP0. *J Gen Virol* **75**, 1223-1233.

Maul, G. G., Guldner, H. H. & Spivack, J. G. (1993). Modification of discrete nuclear domains induced by herpes simplex virus type 1 immediate early gene 1 product (ICP0). *J Gen Virol* **74**, 2679-2690.

McClelland, D. A., Aitken, J. D., Bhella, D., McNab, D., Mitchell, J., Kelly, S. M., Price, N. C. & Rixon, F. J. (2002). pH reduction as a trigger for dissociation of herpes simplex virus type 1 scaffolds. *J Virol* **76**, 7407-7417.

McGeoch, D. J., Dalrymple, M. A., Davison, A. J., Dolan, A., Frame, M. C., McNab, D., Perry, L. J., Scott, J. E. & Taylor, P. (1988). The complete DNA sequence of the long unique region in the genome of herpes simplex virus type 1. *J Gen Virol* **69**, 1531-1574.

Melchjorsen, J., Sirén, J., Julkunen, I., Paludan, S. R. & Matikainen, S. (2006). Induction of cytokine expression by herpes simplex virus in human monocyte-derived macrophages and dendritic cells is dependent on virus replication and is counteracted by ICP27 targeting NF-κB and IRF-3. *J Gen Virol* **87**, 1099-1108.

Melroe, G. T., DeLuca, N. A. & Knipe, D. M. (2004). Herpes simplex virus 1 has multiple mechanisms for blocking virus-induced interferon production. *J Virol* **78**, 8411-8420.

Meredith, M., Orr, A., Elliott, M. & Everett, R. (1995). Separation of sequence requirements for HSV-1 Vmw110 multimerisation and interaction with a 135-kDa cellular protein. *Virology* **209**, 174-187.

Meredith, M., Orr, A. & Everett, R. (1994). Herpes simplex virus type 1 immediate-early protein Vmw110 binds strongly and specifically to a 135-kDa cellular protein. *Virology* **200**, 457-469.

Mettenleiter, T. C., Klupp, B. G. & Granzow, H. (2006). Herpesvirus assembly: a tale of two membranes. *Curr Opin Microbiol* **9**, 423-429.

Mettenleiter, T. C., Klupp, B. G. & Granzow, H. (2009). Herpesvirus assembly: an update. *Virus Res* **143**, 222-234.

Minaker, R. L., Mossman, K. L. & Smiley, J. R. (2005). Functional inaccessibility of quiescent herpes simplex virus genomes. *Virol J* **2**, 85.

Mittnacht, S., Straub, P., Kirchner, H. & Jacobsen, H. (1988). Interferon treatment inhibits onset of herpes simplex virus immediate-early transcription. *Virology* **164**, 201-210.

Mohni, K. N., Livingston, C. M., Cortez, D. & Weller, S. K. (2010). ATR and ATRIP are recruited to herpes simplex virus type 1 replication compartments even though ATR signaling is disabled. *J Virol* **84**, 12152-12164.

Mohni, K. N., Mastrocola, A. S., Bai, P., Weller, S. K. & Heinen, C. D. (2011). DNA mismatch repair proteins are required for efficient herpes simplex virus 1 replication. *J Virol* **85**, 12241-12253.

Mori, Y. & Yamanishi, K. (2007). HHV-6A, 6B, and 7: pathogenesis, host response, and clinical disease. In *Human Herpesviruses: Biology, Therapy, and Immunoprophylaxis*. Edited by A. Arvin, G. Campadelli-Fiume, E. Mocarski, P. S. Moore, B. Roizman, R. Whitley & K. Yamanishi. Cambridge: Cambridge University Press.

Mullen, M. A., Ciufo, D. M. & Hayward, G. S. (1994). Mapping of intracellular localization domains and evidence for colocalization interactions between the IE110 and IE175 nuclear transactivator proteins of herpes simplex virus. *J Virol* **68**, 3250-3266.

Muller, S. & Dejean, A. (1999). Viral immediate-early proteins abrogate the modification by SUMO-1 of PML and Sp100 proteins, correlating with nuclear body disruption. *J Virol* **73**, 5137-5143.

Nagel, C.-H., Albrecht, N., Milovic-Holm, K., Mariyanna, L., Keyser, B., Abel, B., Weseloh, B., Hofmann, T. G., Eibl, M. M. & Hauber, J. (2011). Herpes

simplex virus immediate-early protein ICP0 is targeted by SIAH-1 for proteasomal degradation. *J Virol* **85**, 7644-7657.

Ndjamen, B., Farley, A. H., Lee, T., Fraser, S. E. & Bjorkman, P. J. (2014). The herpes virus Fc receptor gE-gI mediates antibody bipolar bridging to clear viral antigens from the cell surface. *PLoS Pathog* **10**, e1003961.

Neil, S. J. D., Zang, T. & Bieniasz, P. D. (2008). Tetherin inhibits retrovirus release and is antagonized by HIV-1 Vpu. *Nature* **451**, 425-430.

Neumann, J., Eis-Hübinger, A. M. & Koch, N. (2003). Herpes simplex virus type 1 targets the MHC class II processing pathway for immune evasion. *J Immunol* **171**, 3075-3083.

Newcomb, W. W., Juhas, R. M., Thomsen, D. R., Homa, F. L., Burch, A. D., Weller, S. K. & Brown, J. C. (2001). The UL6 gene product forms the portal for entry of DNA into the herpes simplex virus capsid. *J Virol* **75**, 10923-10932.

Nicoll, M. P., Proença, J. T. & Efstathiou, S. (2012). The molecular basis of herpes simplex virus latency. *FEMS Microbiol Rev* **36**, 684-705.

Oxman, M. N. (2010). Zoster vaccine: current status and future prospects. *Clin Infect Dis* **51**, 197-213.

Paladino, P. & Mossman, K. L. (2009). Mechanisms employed by herpes simplex virus 1 to inhibit the interferon response. *J Interferon Cytokine Res* **29**, 599-608.

Parkinson, J. & Everett, R. D. (2000). Alphaherpesvirus proteins related to herpes simplex virus type 1 ICP0 affect cellular structures and proteins. *J Virol* **74**, 10006-10017.

Parkinson, J., Lees-Miller, S. P. & Everett, R. D. (1999). Herpes simplex virus type 1 immediate-early protein vmw110 induces the proteasome-dependent degradation of the catalytic subunit of DNA- dependent protein kinase. *J Virol* **73**, 650-657.

Pelzer, C., Kassner, I., Matentzoglu, K., Singh, R. K., Wollscheid, H.-P., Scheffner, M., Schmidtke, G. & Groettrup, M. (2007). UBE1L2, a novel E1 enzyme specific for ubiquitin. *J Biol Chem* **282**, 23010-23014.

Perry, L. J., Rixon, F. J., Everett, R. D., Frame, M. C. & McGeoch, D. J. (1986). Characterization of the IE110 gene of herpes simplex virus type 1. *J Gen Virol* **67**, 2365-2380.

Perusina Lanfranca, M., Mostafa, H. H. & Davido, D. J. (2013). Two overlapping regions within the N-terminal half of the herpes simplex virus 1 E3 ubiquitin ligase ICP0 facilitate the degradation and dissociation of PML and dissociation of Sp100 from ND10. *J Virol* **87**, 13287-13296.

Piret, J. & Boivin, G. (2011). Resistance of herpes simplex viruses to nucleoside analogues: mechanisms, prevalence, and management. *Antimicrob Agents Chemother* **55**, 459-472.

Piret, J. & Boivin, G. (2014). Antiviral drug resistance in herpesviruses other than cytomegalovirus. *Rev Med Virol* **24**, 186-218.

Preston, C. M. (1979). Control of herpes simplex virus type 1 mRNA synthesis in cells infected with wild-type virus or the temperature-sensitive mutant tsK. *J Virol* **29**, 275-284.

Preston, C. M. (2007). Reactivation of expression from quiescent herpes simplex virus type 1 genomes in the absence of immediate-early protein ICP0. *J Virol* **81**, 11781-11789.

Preston, C. M. & Nicholl, M. J. (2005). Human cytomegalovirus tegument protein pp71 directs long-term gene expression from quiescent herpes simplex virus genomes. *J Virol* **79**, 525-535.

Preston, C. M. & Nicholl, M. J. (2006). Role of the cellular protein hDaxx in human cytomegalovirus immediate-early gene expression. *J Gen Virol* **87**, 1113-1121.

Preston, C. M. & Nicholl, M. J. (2008). Induction of cellular stress overcomes the requirement of herpes simplex virus type 1 for immediate-early protein ICP0 and reactivates expression from quiescent viral genomes. *J Virol* **82**, 11775-11783.

Proença, J. T., Coleman, H. M., Connor, V., Winton, D. J. & Efstathiou, S. (2008). A historical analysis of herpes simplex virus promoter activation in vivo reveals distinct populations of latently infected neurones. *J Gen Virol* **89**, 2965-2974.

Proença, J. T., Coleman, H. M., Nicoll, M. P., Connor, V., Preston, C. M., Arthur, J. & Efstathiou, S. (2011). An investigation of herpes simplex virus promoter activity compatible with latency establishment reveals VP16-independent activation of immediate-early promoters in sensory neurones. *J Gen Virol* **92**, 2575-2585.

Qi, J., Kim, H., Scortegagna, M. & Ronai, Z. e. (2013). Regulators and effectors of Siah ubiquitin ligases. *Cell Biochem Biophys* **67**, 15-24.

Rajčáni, J., Andrea, V. & Ingeborg, R. (2004). Peculiarities of herpes simplex virus (HSV) transcription: an overview. *Virus Genes* **28**, 293-310.

Randall, R. E. & Goodbourn, S. (2008). Interferons and viruses: an interplay between induction, signalling, antiviral responses and virus countermeasures. *J Gen Virol* **89**, 1-47.

Reddenhase, M. J. (2013). *Cytomegaloviruses: From Molecular Pathogenesis to Intervention*. London, UK: Caister Academic Press.

Reichelt, M., Wang, L., Sommer, M., Perrino, J., Nour, A. M., Sen, N., Baiker, A., Zerboni, L. & Arvin, A. M. (2011). Entrapment of viral capsids in nuclear PML cages is an intrinsic antiviral host defense against varicella-zoster virus. *PLoS Pathog* **7**, e1001266.

Reinstein, E., Scheffner, M., Oren, M., Ciechanover, A. & Schwartz, A. (2000). Degradation of the E7 human papillomavirus oncoprotein by the ubiquitin-proteasome system: targeting via ubiquitination of the N-terminal residue. *Oncogene* **19**, 5944-5950.

Rice, S. A., Long, M. C., Lam, V., Schaffer, P. A. & Spencer, C. A. (1995). Herpes simplex virus immediate-early protein ICP22 is required for viral modification of host RNA polymerase II and establishment of the normal viral transcription program. *J Virol* **69**, 5550-5559.

Roizman, B. & Pellett, P. E. (2001). The Family *Herpesviridae*: A Brief Introduction. In *Fields Virology*, Fourth edn, pp. 2381 - 2397. Edited by D. M. Knipe & P. M. Howley. Philadelphia: Lippincott Williams and Wilkins.

Russell, J., Stow, N. D., Stow, E. C. & Preston, C. M. (1987). Herpes simplex virus genes involved in latency in vitro. *J Gen Virol* **68**, 3009-3018.

Sainz, B. & Halford, W. P. (2002). Alpha/beta interferon and gamma interferon synergize to inhibit the replication of herpes simplex virus type 1. *J Virol* **76**, 11541-11550.

Sakurai, A., Yasuda, J., Takano, H., Tanaka, Y., Hatakeyama, M. & Shida, H. (2004). Regulation of human T-cell leukemia virus type 1 (HTLV-1) budding by ubiquitin ligase Nedd4. *Microbes Infect* **6**, 150-156.

Samaniego, L. A., Neiderhiser, L. & DeLuca, N. A. (1998). Persistence and expression of the herpes simplex virus genome in the absence of immediate-early proteins. *J Virol* **72**, 3307-3320.

Sampath, P. & DeLuca, N. A. (2008). Binding of ICP4, TATA-binding protein, and RNA polymerase II to herpes simplex virus type 1 immediate-early, early, and late promoters in virus-infected cells. *J Virol* **82**, 2339-2349.

Sànchez, R. & Mohr, I. (2007). Inhibition of cellular 2′-5′ oligoadenylate synthetase by the herpes simplex virus type 1 Us11 protein. *J Virol* **81**, 3455-3464.

Sancho, E., Vilá, M. R., Sánchez-Pulido, L., Lozano, J. J., Paciucci, R., Nadal, M., Fox, M., Harvey, C., Bercovich, B., Loukili, N., Ciechanover, A., Lin, S. L., Sanz, F., Estivill, X., Valencia, A. & Thomson, T. M. (1998). Role of UEV-1,

an inactive variant of the E2 ubiquitin conjugating enzymes, in in vitro differentiation and cell cycle behavior of HT-29-M6 intestinal mucosecretory cells. *Mol Cell Biol* **18**, 576-589.

Sandri-Goldin, R. M. (2011). The many roles of the highly interactive HSV protein ICP27, a key regulator of infection. *Future Microbiol* **6**, 1261-1277.

Sawtell, N. M. (1997). Comprehensive quantification of herpes simplex virus latency at the single-cell level. *J Virol* **71**, 5423-5431.

Sawtell, N. M. (1998). The probability of in vivo reactivation of herpes simplex virus type 1 increases with the number of latently infected neurons in the ganglia. *J Virol* **72**, 6888-6892.

Schenck, P., Pietschmann, S., Gelderblom, H., Pauli, G. & Ludwig, H. (1988). Monoclonal antibodies against herpes simplex virus type 1-infected nuclei defining and localizing the ICP8 protein, 65K DNA-binding protein and polypeptides of the ICP35 family. *J Gen Virol* **69**, 99-111.

Schreiner, S., Martinez, R., Groitl, P., Rayne, F., Vaillant, R., Wimmer, P., Bossis, G., Sternsdorf, T., Marcinowski, L., Ruzsics, Z., Dobner, T. & Wodrich, H. (2012). Transcriptional activation of the adenoviral genome is mediated by capsid protein VI. *PLoS Pathog* **8**, e1002549.

Scoular, A., Norrie, J., Gillespie, G., Mir, N. & Carman, W. F. (2002). Longitudinal study of genital infection by herpes simplex virus type 1 in western Scotland over 15 years. *BMJ* **324**, 1366-1367.

Sheehy, A. M., Gaddis, N. C. & Malim, M. H. (2003). The antiretroviral enzyme APOBEC3G is degraded by the proteasome in response to HIV-1 Vif. *Nat Med* **9**, 1404-1407.

Showalter, S. D., Zweig, M. & Hampar, B. (1981). Monoclonal antibodies to herpes simplex virus type 1 proteins, including the immediate-early protein ICP 4. *Infect Immun* **34**, 684-692.

Smith, C. A., Bates, P., Rivera-Gonzalez, R., Gu, B. & DeLuca, N. A. (1993). ICP4, the major transcriptional regulatory protein of herpes simplex virus type 1, forms a tripartite complex with TATA-binding protein and TFIIB. *J Virol* **67**, 4676-4687.

Spence, J., Sadis, S., Haas, A. L. & Finley, D. (1995). A ubiquitin mutant with specific defects in DNA repair and multiubiquitination. *Mol Cell Biol* **15**, 1265-1273.

Sternsdorf, T., Guldner, H. H., Szostecki, C., Grotzinger, T. & Will, H. (1995). Two nuclear dot-associated proteins, PML and Sp100, are often co-autoimmunogenic in patients with primary biliary cirrhosis. *Scand J Immunol* **42**, 257-268.

Sternsdorf, T., Jensen, K. & Will, H. (1997). Evidence for covalent modification of the nuclear dot-associated proteins PML and Sp100 by PIC1/SUMO-1. *J Cell Biol* **139**, 1621-1634.

Stevens, J. G., Wagner, E. K., Devi-Rao, G. B., Cook, M. L. & Feldman, L. T. (1987). RNA complementary to a herpesvirus alpha gene mRNA is prominent in latently infected neurons. *Science* **235**, 1056-1059.

Stewart, G. S., Panier, S., Townsend, K., Al-Hakim, A. K., Kolas, N. K., Miller, E. S., Nakada, S., Ylanko, J., Olivarius, S., Mendez, M., Oldreive, C., Wildenhain, J., Tagliaferro, A., Pelletier, L., Taubenheim, N., Durandy, A., Byrd, P. J., Stankovic, T., Taylor, A. M. R. & Durocher, D. (2009). The RIDDLE syndrome protein mediates a ubiquitin-dependent signaling cascade at sites of DNA damage. *Cell* **136**, 420-434.

Stoker, M. & Macpherson, I. (1964). Syrian hamster fibroblast cell line BHK21 and its derivatives. *Nature* **203**, 1355-1357.

Stow, E. C. & Stow, N. D. (1989). Complementation of a herpes simplex virus type 1 Vmw110 deletion mutant by human cytomegalovirus. *J Gen Virol* **70**, 695-704.

Stow, N. D. & Stow, E. C. (1986). Isolation and characterization of a herpes simplex virus type 1 mutant containing a deletion within the gene encoding the immediate early polypeptide Vmw110. *J Gen Virol* **67**, 2571-2585.

Stremlau, M., Owens, C. M., Perron, M. J., Kiessling, M., Autissier, P. & Sodroski, J. (2004). The cytoplasmic body component TRIM5[alpha] restricts HIV-1 infection in Old World monkeys. *Nature* **427**, 848-853.

Stuurman, N., de Graaf, A., Floore, A., Josso, A., Humbel, B., de Jong, L. & van Driel, R. (1992). A monoclonal antibody recognizing nuclear matrix-associated nuclear bodies. *J Cell Sci* **101**, 773-784.

Sullivan, V., Talarico, C.L., Stanat, S.C., Davis, M., Coen, D.M. & Biron, K.K. (1992). A protein kinase homologue controls phosphorylation of ganciclovir in human cytomegalovirus-infected cells. *Nature* **358**, 162-164.

Tatham, M. H., Plechanovova, A., Jaffray, E. G., Salmen, H. & Hay, R. T. (2013). Ube2W conjugates ubiquitin to alpha-amino groups of protein N-termini. *Biochem J* **453**, 137-145.

Tavalai, N., Papior, P., Rechter, S., Leis, M. & Stamminger, T. (2006). Evidence for a role of the cellular ND10 protein PML in mediating intrinsic immunity against human cytomegalovirus infections. *J Virol* **80**, 8006-8018.

Tavalai, N. & Stamminger, T. (2008). New insights into the role of the subnuclear structure ND10 for viral infection. *Biochim Biophys Acta* **1783**, 2207-2221.

Temme, S., Eis-Hübinger, A. M., McLellan, A. D. & Koch, N. (2010). The herpes simplex virus-1 encoded glycoprotein B diverts HLA-DR into the exosome pathway. *J Immunol* **184**, 236-243.

Terry-Allison, T., Smith, C. A. & DeLuca, N. A. (2007). Relaxed repression of herpes simplex virus type 1 genomes in Murine trigeminal neurons. *J Virol* **81**, 12394-12405.

Thomas, D. L., Lock, M., Zabolotny, J. M., Mohan, B. R. & Fraser, N. W. (2002). The 2-kilobase intron of the herpes simplex virus type 1 latency-associated transcript has a half-life of approximately 24 hours in SY5Y and COS-1 cells. *J Virol* **76**, 532-540.

Thompson, R. L., Preston, C. M. & Sawtell, N. M. (2009). De novo synthesis of VP16 coordinates the exit from HSV latency in vivo. *PLoS Pathog* **5**, e1000352.

Thompson, R. L. & Sawtell, N. M. (2006). Evidence that the herpes simplex virus type 1 ICP0 protein does not initiate reactivation from latency in vivo. *J Virol* **80**, 10919-10930.

Thrower, J. S., Hoffman, L., Rechsteiner, M. & Pickart, C. M. (2000). Recognition of the polyubiquitin proteolytic signal. *EMBO J* **19**, 94-102.

Tsai, K., Thikmyanova, N., Wojcechowskyj, J. A., Delecluse, H.-J. & Lieberman, P. M. (2011). EBV tegument protein BNRF1 disrupts DAXX-ATRX to activate viral early gene transcription. *PLoS Pathog* **7**, e1002376.

van Lint, A. L., Murawski, M. R., Goodbody, R. E., Severa, M., Fitzgerald, K. A., Finberg, R. W., Knipe, D. M. & Kurt-Jones, E. A. (2010). Herpes simplex virus immediate-early ICP0 protein inhibits Toll-like receptor 2-dependent inflammatory responses and NF-kappaB signaling. *J Virol* **84**, 10802-10811.

Van Sant, C., Hagglund, R., Lopez, P. & Roizman, B. (2001). The infected cell protein 0 of herpes simplex virus 1 dynamically interacts with proteasomes, binds and activates the cdc34 E2 ubiquitin-conjugating enzyme, and possesses in vitro E3 ubiquitin ligase activity. *Proc Natl Acad Sci U S A* **98**, 8815-8820.

van Wijk, S. J. L., de Vries, S. J., Kemmeren, P., Huang, A., Boelens, R., Bonvin, A. M. J. J. & Timmers, H. T. M. (2009). A comprehensive framework of E2–RING E3 interactions of the human ubiquitin–proteasome system. *Mol Syst Biol* **5**, 295.

VanDemark, A. P., Hofmann, R. M., Tsui, C., Pickart, C. M. & Wolberger, C. (2001). Molecular insights into polyubiquitin chain assembly: crystal structure of the Mms2/Ubc13 heterodimer. *Cell* **105**, 711-720.

Vandevenne, P., Sadzot-Delvaux, C. & Piette, J. (2010). Innate immune response and viral interference strategies developed by human herpesviruses. *Biochem Pharmacol* **80**, 1955-1972.

Vanni, E., Gatherer, D., Tong, L., Everett, R. D. & Boutell, C. (2012). Functional characterization of residues required for the herpes simplex virus 1 E3 ubiquitin ligase ICP0 to interact with the cellular E2 ubiquitin-conjugating enzyme UBE2D1 (UbcH5a). *J Virol* **86**, 6323-6333.

VerPlank, L., Bouamr, F., LaGrassa, T. J., Agresta, B., Kikonyogo, A., Leis, J. & Carter, C. A. (2001). Tsg101, a homologue of ubiquitin-conjugating (E2) enzymes, binds the L domain in HIV type 1 Pr55Gag. *Proc Natl Acad Sci U S A* **98**, 7724-7729.

Verpooten, D., Ma, Y., Hou, S., Yan, Z. & He, B. (2009). Control of TANK-binding kinase 1-mediated signaling by the gamma(1)34.5 protein of herpes simplex virus 1. *J Biol Chem* **284**, 1097-1105.

Wagner, E. K. & Bloom, D. C. (1997). Experimental investigation of herpes simplex virus latency. *Clin Microbiol Rev* **10**, 419-443.

Ward, S. A. & Weller, S. K. (2011). HSV-1 DNA Replication. In *Alphaherpesviruses: Molecular Virology*, pp. 89-112. Edited by S. K. Weller. Norfolk, UK: Caister Academic Press.

Watson, R. J. & Clements, J. B. (1980). A herpes simplex virus type 1 function continuously required for early and late virus RNA synthesis. *Nature* **285**, 329-330.

Weir, J. P. (2001). Regulation of herpes simplex virus gene expression. *Gene* **271**, 117-130.

Weissman, A. M., Shabek, N. & Ciechanover, A. (2011). The predator becomes the prey: regulating the ubiquitin system by ubiquitylation and degradation. *Nat Rev Mol Cell Biol* **12**, 605-620.

Weitzman, M. D., Lilley, C. E. & Chaurushiya, M. S. (2010). Genomes in conflict: maintaining genome integrity during virus infection. *Annu Rev Microbiol* **64**, 61-81.

Weller, S. K. (2010). Herpes simplex virus reorganizes the cellular DNA repair and protein quality control machinery. *PLoS Pathog* **6**, e1001105.

Weller, S. K. & Coen, D. M. (2012). Herpes simplex viruses: mechanisms of DNA replication. *Cold Spring Harb Perspect Biol* **4** a013011.

Whitley, R., Kimberlin, D. W. & Prober, C. G. (2007). Pathogenesis and disease. In *Human Herpesviruses: Biology, Therapy, and Immunoprophylaxis*. Edited by A. Arvin, G. Campadelli-Fiume, E. Mocarski, P. S. Moore, B. Roizman, R. Whitley & K. Yamanishi. Cambridge: Cambridge University Press.

Wilkinson, D. E. & Weller, S. K. (2006). Herpes simplex virus type I disrupts the ATR-dependent DNA-damage response during lytic infection. *J Cell Sci* **119**, 2695-2703.

Windheim, M., Peggie, M. & Cohen, P. (2008). Two different classes of E2 ubiquitin-conjugating enzymes are required for the mono-ubiquitination of proteins and elongation by polyubiquitin chains with a specific topology. *Biochem J* **409**, 723-729.

Wolfstein, A., Nagel, C.-H., Radtke, K., Döhner, K., Allan, V. J. & Sodeik, B. (2006). The inner tegument promotes herpes simplex virus capsid motility along microtubules in vitro. *Traffic* **7**, 227-237.

Woodhall, D. L., Groves, I. J., Reeves, M. B., Wilkinson, G. & Sinclair, J. H. (2006). Human Daxx-mediated repression of human cytomegalovirus gene expression

correlates with a repressive chromatin structure around the major immediate early promoter. *J Biol Chem* **281**, 37652-37660.

Wysocka, J. & Herr, W. (2003). The herpes simplex virus VP16-induced complex: the makings of a regulatory switch. *Trends Biochem Sci* **28**, 294-304.

Xu, Z., Kohli, E., Devlin, K. I., Bold, M., Nix, J. C. & Misra, S. (2008). Interactions between the quality control ubiquitin ligase CHIP and ubiquitin conjugating enzymes. *BMC Struct Biol* **8**, 26.

Yao, F. & Schaffer, P. A. (1995). An activity specified by the osteosarcoma line U2OS can substitute functionally for ICP0, a major regulatory protein of herpes simplex virus type 1. *J Virol* **69**, 6249-6258.

Yasuda, J., Hunter, E., Nakao, M. & Shida, H. (2002). Functional involvement of a novel Nedd4-like ubiquitin ligase on retrovirus budding. *EMBO Rep* **3**, 636-640.

Yasuda, J., Nakao, M., Kawaoka, Y. & Shida, H. (2003). Nedd4 regulates egress of Ebola virus-like particles from host cells. *J Virol* **77**, 9987-9992.

You, A., Tong, J. K., Grozinger, C. M. & Schreiber, S. L. (2001). CoREST is an integral component of the CoREST- human histone deacetylase complex. *Proc Natl Acad Sci U S A* **98**, 1454-1458.

Zhang, S.-Y., Jouanguy, E., Ugolini, S., Smahi, A., Elain, G., Romero, P., Segal, D., Sancho-Shimizu, V., Lorenzo, L., Puel, A., Picard, C., Chapgier, A., Plancoulaine, S., Titeux, M., Cognet, C., von Bernuth, H., Ku, C.-L., Casrouge, A., Zhang, X.-X., Barreiro, L., Leonard, J., Hamilton, C., Lebon, P., Héron, B., Vallée, L., Quintana-Murci, L., Hovnanian, A., Rozenberg, F., Vivier, E., Geissmann, F., Tardieu, M., Abel, L. & Casanova, J.-L. (2007). TLR3 deficiency in patients with herpes simplex encephalitis. *Science* **317**, 1522-1527.

Zheng, N., Wang, P., Jeffrey, P. D. & Pavletich, N. P. (2000). Structure of a c-Cbl–UbcH7 complex: RING domain function in ubiquitin-protein ligases. *Cell* **102**, 533-539.

Zhong, S., Muller, S., Ronchetti, S., Freemont, P. S., Dejean, A. & Pandolfi, P. P. (2000). Role of SUMO-1-modified PML in nuclear body formation. *Blood* **95**, 2748-2752.

Zhou, Z. H., Dougherty, M., Jakana, J., He, J., Rixon, F. J. & Chiu, W. (2000). Seeing the herpesvirus capsid at 8.5 Å. *Science* **288**, 877-880.

Zhu, F. X., King, S. M., Smith, E. J., Levy, D. E. & Yuan, Y. (2002). A Kaposi's sarcoma-associated herpesviral protein inhibits virus-mediated induction of type I interferon by blocking IRF-7 phosphorylation and nuclear accumulation. *Proc Natl Acad Sci U S A* **99**, 5573-5578.

Zhu, F. X., Sathish, N. & Yuan, Y. (2010). Antagonism of host antiviral responses by Kaposi's sarcoma-associated herpesvirus tegument protein ORF45. *PLoS ONE* **5**, e10573.

Zweerink, H. J. & Stanton, L. W. (1981). Immune response to herpes simplex virus infections: virus-specific antibodies in sera from patients with recurrent facial infections. *Infect Immun* **31**, 624-630.